ANALYTICA CHIMICA ACTA

International monthly devoted to all branches of analytical chemistry
Revue mensuelle internationale consacrée à tous les domaines de la chimie analytique
Internationale Monatsschrift für alle Gebiete der analytischen Chemie

ELSEVIER PUBLISHING COMPANY
AMSTERDAM

Anal. Chim. Acta, Vol. 54, No. 3, 381–548, May 1971
Published monthly
Completing Volume 54

ANALYTICA CHIMICA ACTA

Publication Schedule for 1971

In the interests of rapid publication it has been found necessary to schedule 5 volumes for appearance in 1971. Since monthly publication will be maintained, this implies that 2 of the volumes will each consist of three issues, while 3 of the volumes will each consist of only 2 issues. The following provisional schedule applies:

Vol. **53**, No. **1**	January 1971	
Vol. **53**, No. **2**	February 1971	**(completing Vol. 53)**
Vol. **54**, No. **1**	March 1971	
Vol. **54**, No. **2**	April 1971	
Vol. **54**, No. **3**	May 1971	**(completing Vol. 54)**
Vol. **55**, No. **1**	June 1971	
Vol. **55**, No. **2**	July 1971	**(completing Vol. 55)**
Vol. **56**, No. **1**	August 1971	
Vol. **56**, No. **2**	September 1971	
Vol. **56**, No. **3**	October 1971	**(completing Vol. 56)**
Vol. **57**, No. **1**	November 1971	
Vol. **57**, No. **2**	December 1971	**(completing Vol. 57)**

Subscription price: $17.50 or Dfl. 63.— per volume plus postage. Total subscription price for 1971: $87.50 or Dfl. 315.— plus postage. Additional cost for copies by airmail available on request. For subscribers in the U.S.A. and Canada, 2nd class postage paid at New York, N.Y. For advertising rates apply to the publishers.

Subscriptions should be sent to:

ELSEVIER PUBLISHING COMPANY P.O. Box 211, Amsterdam, The Netherlands

---

GENERAL INFORMATION

Languages

Papers will be published in English, French or German.

Submission of papers

Papers should be sent to:

PROF. PHILIP W. WEST,
Coates Chemical Laboratories,
College of Chemistry and Physics,
Louisiana State University,
Baton Rouge 3,
La. 70803 (U.S.A.)

or to:

DR. A. M. G. MACDONALD,
Department of Chemistry,
The University,
P.O. Box 363
Birmingham B15 2TT (Great Britain)

Reprints

Fifty reprints will be supplied free of charge. Additional reprints (minimum 100) can be ordered at quoted prices. They must be ordered on order forms which are sent together with the proofs.

A New Elsevier Publication in Engineering

HEAT TRANSFER 1970

Papers presented at the Fourth International Heat Transfer Conference,
Paris – Versailles, 1970

Edited by U. GRIGULL and E. HAHNE, München, Germany

10 Volumes. 5102 pages, ISBN 0–444–999 39–6
Dfl. 650.00 (ca. $ 180.75) per set of 10 volumes.

These volumes contain the papers presented at the Fourth International Heat Transfer Conference held from August 31st to September 4th, 1970 at Paris-Versailles. The conference was sponsored by the General Assembly for Heat Transfer Conferences whose purpose it is to keep the sum total of knowledge in the field of heat transfer up to date and to provide a setting for reports and discussion on the subject within the framework of a four-yearly conference.

Approximately 350 contributions were selected to serve as a basis for thirty-six working sessions. The first eight volumes contain the papers presented at the conference, while volume nine covers the rapporteurs' critical review of them. A considerable portion of each working session was devoted to discussions and reports of these are published in volume ten.

CONTENTS:		
	Vol. I:	HEAT EXCHANGERS, 510 pages, 28 tables, 261 illus.
	Vol. II:	FORCED CONVECTION I, 522 pages, 20 tables, 376 illus.
	Vol. III:	FORCED CONVECTION II RADIATION, 590 pages, 15 tables, 399 illus.
	Vol. IV:	NATURAL CONVECTION RHEOLOGY, 550 pages, 23 tables, 273 illus., 4 plates, 4 photographs
	Vol. V:	BOILING I, 641 pages, 26 tables, 401 illus.
	Vol. VI:	BOILING II CONDENSATION, 534 pages, 22 tables, 336 illus.
	Vol. VII:	COMBINED HEAT TRANSFER, 500 pages, 21 tables, 222 illus.
	Vol. VIII:	ABSTRACTS OF THE PAPERS IN ENGLISH, FRENCH, GERMAN AND RUSSIAN LANGUAGE, 388 pages
	Vol. IX:	LECTURES OF THE RAPPORTEURS. 531 pages
	Vol. X:	DISCUSSIONS, 336 pages

Elsevier

Book Division, P.O. Box 211
Amsterdam - The Netherlands

133 E

MERCK

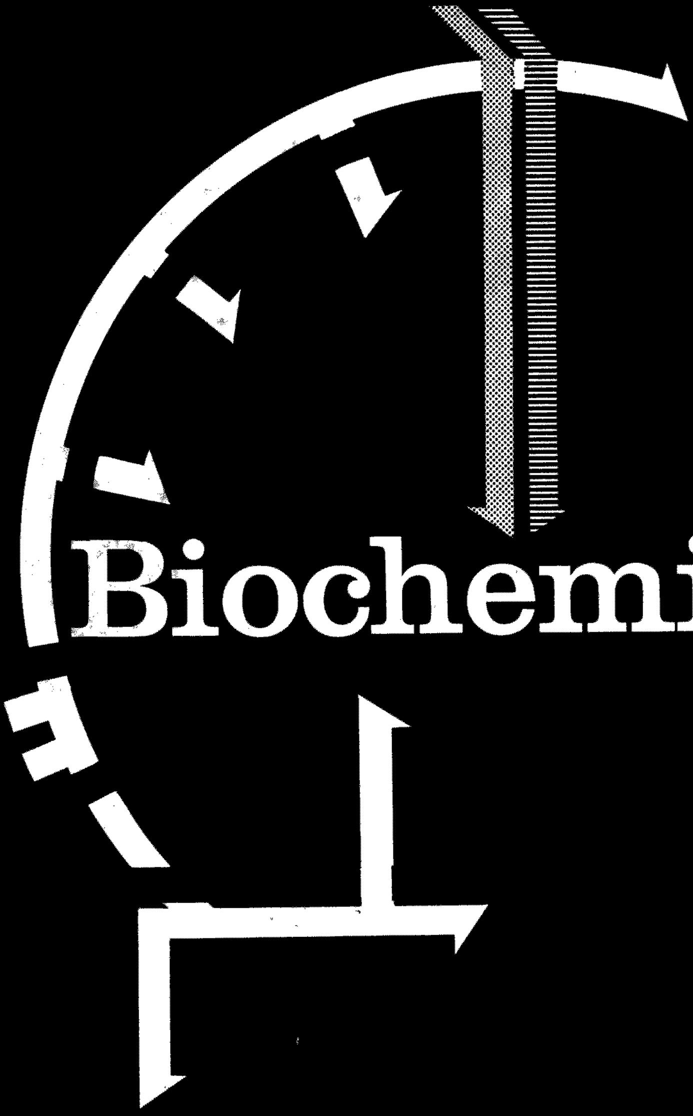

Biochemicals

Analytica Chimica Acta
Elsevier Publishing Company, Amsterdam
Printed in The Netherlands

OPTIMISATION OF SOME EXPERIMENTAL PARAMETERS IN THE PREPARATION AND OPERATION OF MICROWAVE-EXCITED ELECTRODELESS DISCHARGE LAMPS

D. O. COOKE, R. M. DAGNALL AND T. S. WEST
Chemistry Department, Imperial College of Science and Technology, London, S.W.7 (England)

(Received 6th December 1970)

Most workers now are aware of the existence of microwave-excited electrodeless discharge lamps and their use in atomic spectroscopy, as a result of several publications dealing with their advantages and limitations[1-3] and their use in routine analysis[4,5]. However, because of the difficulty of preparing lamps having identical or even similar characteristics, these sources have been regarded cautiously. For example, Fig. 1 shows the atomic fluorescence signal received at varying microwave powers from a random selection of three zinc electrodeless discharge lamps. As can be seen each source requires different operating conditions for optimum results. A similar situation can be observed with most series of sources for the same element. This effect prompted us to a further investigation of optimal preparation and operating conditions. It has

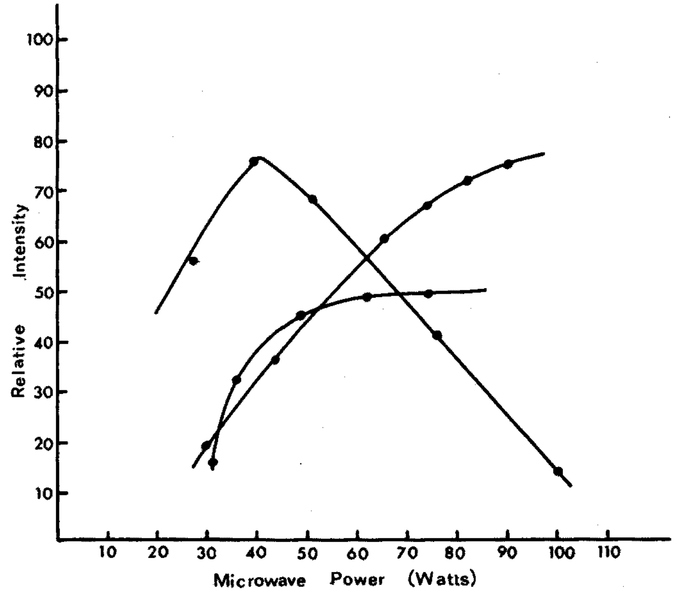

Fig. 1. Effect of microwave power ($P-R$) on a.f.s. of zinc for three randomly chosen zinc lamps.

been pointed out by Winefordner *et al.*[6] that there are several important parameters which must be controlled in the preparation and operation of these lamps, namely, lamp size (dimensions, etc.), nature and pressure of the inert fill gas used, type (metal alone, chloride or iodide) and amount of material used, microwave power applied, means of coupling microwave power into the lamp (type of resonant cavity or directional antennae used) and the position of the lamp within the microwave field. The present work examines some of the more important of these variables and more especially their effect on the analytical atomic absorption and fluorescence signal obtained. In addition, a new and more reproducible method of preparation is proposed which has the advantage of offering improved source stability.

EXPERIMENTAL

Apparatus

The electrodeless discharge lamps were prepared by the same general method as described previously[1] and any modifications are described in the relevant sections below. Microwave power for the sources was provided by a "Microtron 200" (Electro-Medical Supplies; Wantage, U.K.) microwave (2450±25 MHz) generator coupled with a reflected power meter (Electro-Medical Supplies). The Broida three-quarter wave cavity (Electro-Medical Supplies, No. 210L) was used except where stated and initiation was achieved with a "Tesla" high-frequency vacuum tester.

Spectroscopic evaluation was made with a modified[7] Hilger and Watts "Uvispek" (H700) spectrophotometer with an atomic absorption attachment. A premixed air–propane flame (perforated plate burner head with *ca.* 10-cm flame for atomic absorption and a Meker-type burner head for atomic fluorescence) was used and the analytical signal was displayed on a Servoscribe recorder used on the 0–20 mV range. Atomic fluorescence measurements were carried out with the lamps situated as close as practicable to the flame (*i.e. ca.* 4 cm). Modulation at 100 Hz was provided electronically by a modulation unit MK 11 (Electro-Medical Supplies) which was arbitrarily calibrated and set at position 5. No problems from overmodulation of the lamps were experienced at any of the power settings used. For some of the atomic absorption measurements mechanical modulation was utilised, but no change in the shape of the analytical signal *versus* applied power curves was observed on switching between the two methods.

EXAMINATION OF PARAMETERS INVOLVED IN THE PREPARATION OF ELECTRODELESS DISCHARGE LAMPS

In order to examine any one variable it was necessary to keep all other possible variables constant. For this reason the lamp length (8 mm internal diameter quartz tubing was used except where stated) was held constant at *ca.* 3 cm such that the entire bulb was within the microwave field. This bulb size in conjunction with the three-quarter wave cavity ensured good thermal stability and hence a more stable output[9]. The slight decrease in bulb size over that normally recommended[1] was not thought to be a disadvantage because it has been previously pointed out that short lamps tend to show higher brightness and to have increased lifetime owing to less clean-up[10]. The pressure of fill gas (argon was used except where stated) was standardised at 3 torr because previous experience had indicated this to be the best compromise between maximum intensity and long life.

Amount of material used

The effect of various amounts of material on the lamp intensity (*i.e.* integrated line intensity) has been investigated by several workers, but a complete evaluation does not appear to have been reported. Winefordner *et al.*[6] stated, on the basis of a statistical treatment, that there was no correlation between the weight of material used within the range 0.23–10 mg. Silvester and McCarthy[11] observed greater line intensities from lamps containing 5 mg of cadmium than from those containing 35 or 50 mg; lower quantities were not examined. Worden *et al.*[10] noted in spectral studies of curium that self-reversal was not observed with long lamps containing 100 μg of compound, but was readily observed with those containing 1 mg. Tomkins and Fred[12] have pointed out that lamps may be prepared from as little as 0.1 μg of metal halide. However, intensity was not a prime requirement in this work and it is considered unlikely that quantities as low as this would produce a sufficiently intense source for use in analytical atomic spectroscopy. The lack of any systematic examination of the effect of introducing small quantities of material in the past may have been due to the difficulties involved in accurately introducing microgram amounts into the lamp. In an endeavour to solve this problem the possibility of introducing the compound in the form of a solution was examined. Lamps were prepared from 5- or 10-μl aliquots of aqueous solutions of zinc or cadmium chloride. The water was removed under vacuum and the compound gently sublimed onto the walls of the lamp. The base of the lamp was cooled in water during the sealing procedure to minimise losses of material. A series of zinc lamps containing between 1 and 5000 μg (above 5000 μg a discharge could not be maintained) of zinc chloride were prepared and evaluated for use in atomic fluorescence and absorption spectroscopy. A similar series of lamps was prepared for cadmium with the exception that in the case of lamps containing more than 500 μg of cadmium chloride the discharge could not be maintained because of a pressure build-up within the lamp (presumably due to chlorine) which quenched the discharge.

Intensity and spectral characteristics

For all the zinc and cadmium sources prepared the integrated resonance line intensity (Zn at 213.8 and Cd at 228.8 nm) increased with increasing amount of material used.

The maximum integrated resonance line intensity of zinc lamps containing 1000 μg of zinc chloride was approximately twice that of a lamp containing 20 μg of zinc chloride. The increase in intensity was generally linear with applied power (taken as power indicated on microwave generator minus power reflected $(P-R)$) up to an applied power of about 75 W and then began to level off. In the case of lamps containing 1 mg or more of material the intensity began to fall at very high values of applied power (>100 W). As might be expected under these conditions, owing to unduly high vapour pressure, the integrated line intensity of the intercombination lines (Zn at 307.6 and Cd at 326.1 nm) increased more rapidly than the corresponding resonance lines and showed no sign of levelling off with increased values of applied power up to 125 W.

The spectral characteristics of lamps containing zinc or cadmium chloride were

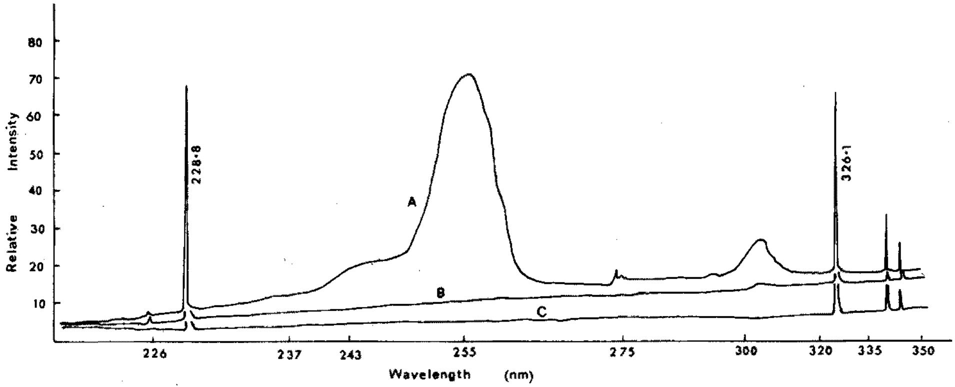

Fig. 2. Spectral characteristics of cadmium lamps. (A) 20 μg $CdCl_2$, $P-R=28$ W; (B) 20 μg $CdCl_2$, $P-R=60$ W; (C) cadmium metal, $P-R=30$ W.

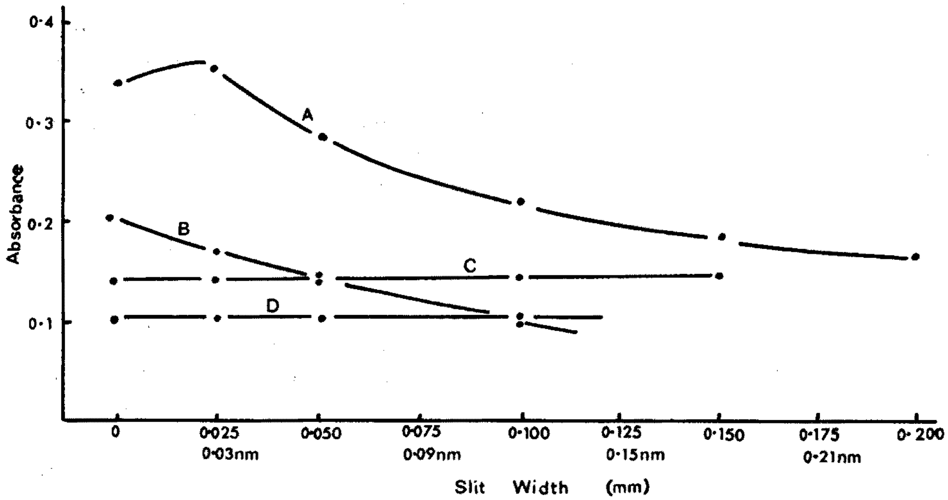

Fig. 3. Effects of variation of slit width on a.a.s. of cadmium (5 p.p.m.) at various power levels for 10 μg of cadmium chloride in the lamp. (A) $P-R=25$ W; (B) $P-R=38$ W; (C) $P-R=48$ W; (D) $P-R=59$ W.

not as clean as those containing the metal alone (Fig. 2). The band observed between 250.0–265.0 nm was much more pronounced in the cadmium lamp than in the zinc lamps and was attributed to the presence of chlorine. In both cases the band emission could be removed by over-running the lamps, although this of course results in a considerably decreased analytical signal. The appearance of this particular band is unlikely to cause any problems even with very low resolution monochromators. However, there is also a low intensity continuum in the region of the cadmium resonance line at 228.8 nm which results in a decrease in the analytical atomic absorption signal with increasing slit width. This problem does not arise with zinc chloride lamps. Operating the cadmium lamps at higher microwave powers removes the low intensity continuum and removes the slit width effect (Fig. 3), but under these circumstances the resonance line is considerably broadened and this generally results in an appreciably lower absorbance. Lamps containing very low quantities (< 5 μg) of zinc or cadmium chloride exhibited considerable fill gas background.

EVALUATION OF SOURCES FOR USE IN ATOMIC FLUORESCENCE SPECTROSCOPY

Zinc

For each lamp the effect of applied power ($P-R$) on the atomic fluorescence signal (obtained on nebulising 1 p.p.m. zinc solution) was investigated (Fig. 4). From this data an indication of the variation of the atomic fluorescence signal with the amount of material used in the lamp at fixed values of the applied microwave power was obtained (Figs. 5 and 6). From Fig. 5 it can be seen that the effect of power is much

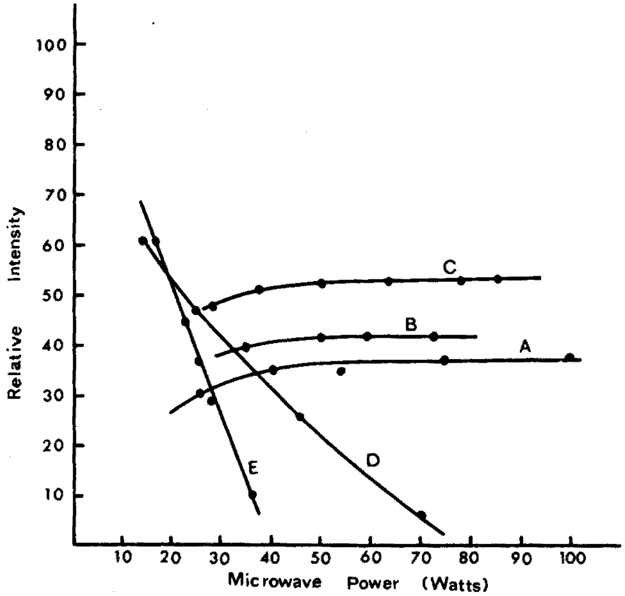

Fig. 4. Effect of microwave power ($P-R$) on a.f.s. of zinc for various zinc lamps. (A) 1 μg $ZnCl_2$; (B) 5 μg $ZnCl_2$; (C) 10 μg $ZnCl_2$; (D) 100 μg $ZnCl_2$; (E) 1000 μg $ZnCl_2$.

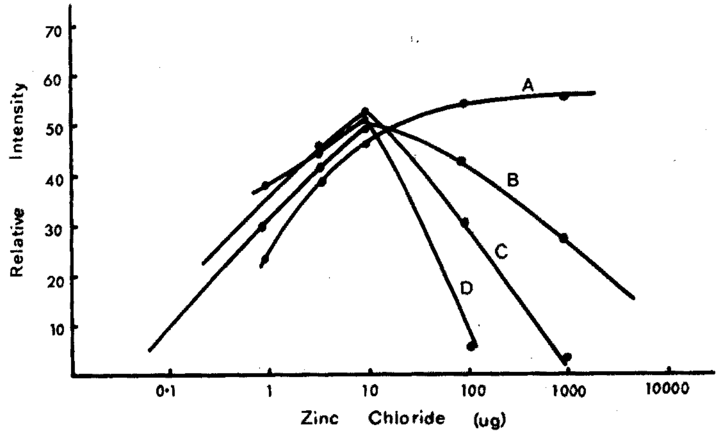

Fig. 5. Effect of amount of zinc chloride in zinc lamps on a.f.s. signal. (A) $P-R=20$ W; (B) $P-R=30$ W; (C) $P-R=50$ W; (D) $P-R=70$ W.

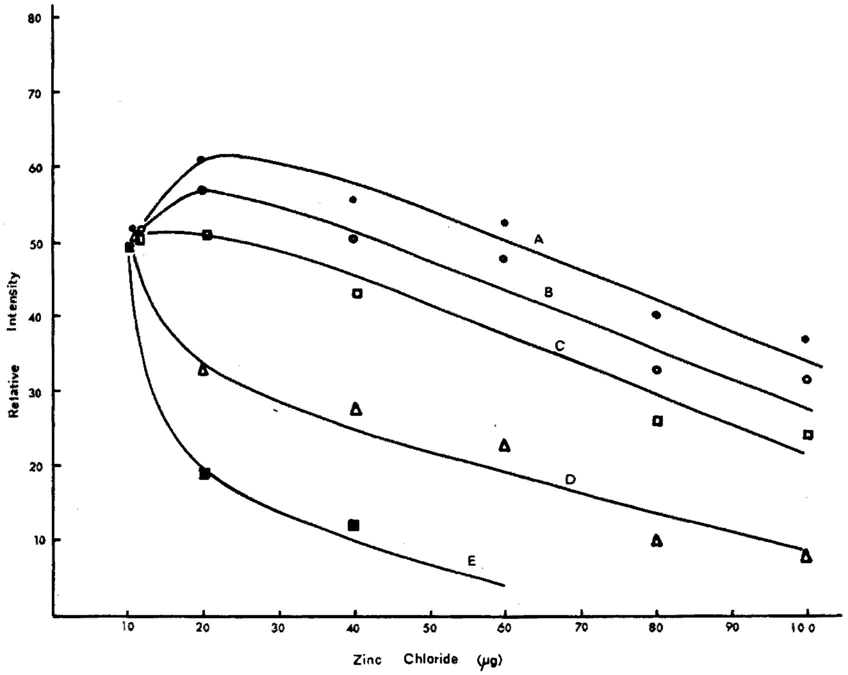

Fig. 6. Effect of amount of zinc chloride in zinc lamps on a.f.s. signal. (A) $P-R=30$ W; (B) $P-R=32.5$ W; (C) $P-R=35$ W; (D) $P-R=45$ W; (E) $P-R=55$ W.

less critical on the lamps containing low amounts of zinc chloride. This may be an advantage in that the analytical signal will be unaffected by any fluctuations in the microwave power supply. The rapid decrease in the atomic fluorescence signal with increase in applied power exhibited by lamps containing more than 10^{-4} g of zinc chloride (presumably owing to self-reversal of the resonance line concerned or quenching of the discharge by chlorine) may be reduced somewhat by strongly cooling the lamp. However, a decrease in signal with applied power is still observed and the use of cooling tends to result in a less stable output. A marked maximum in the atomic fluorescence signal was observed for lamps containing in the region of 20 µg of zinc chloride at all operating powers below about 35 W. At 20 W the atomic fluorescence signal increased up to 100 µg of zinc chloride. Five lamps containing 20 µg of zinc chloride all gave the same atomic fluorescence signal within ±5% when operated at 30 W. This indicated that the method of preparation is quite reproducible.

Cadmium

A similar evaluation was carried out on the cadmium lamps with the exception that the range was more limited for the reasons outlined above (Fig. 7). The results here are less conclusive; the largest atomic fluorescence signal which was unaffected by variations in the applied microwave power was obtained with lamps containing 10 µg of cadmium chloride or less. However, at this level the results were less reproducible because of the increased importance of the clean-up process. Consequently, a more

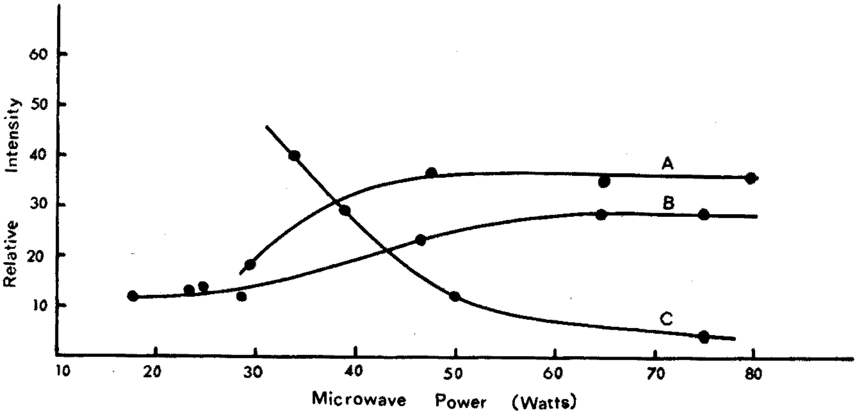

Fig. 7. Effect of microwave power ($P-R$) on a.f.s. of cadmium for various cadmium lamps. (A) 10 μg $CdCl_2$; (B) 5 μg $CdCl_2$; (C) 40 μg $CdCl_2$.

accurate assessment was not possible. In order to obtain long-lived lamps (>100 h) it is considered advisable to use at least 5 μg of cadmium chloride.

EVALUATION OF SOURCES FOR USE IN ATOMIC ABSORPTION SPECTROSCOPY

Choice of slit width

For both elements a slit width of 0.025 mm was used. For zinc sources this provided the optimal atomic absorbance for all the lamps tested and all microwave powers used. With cadmium, however, the relatively high background, which varied sometimes non-uniformly with increasing power, resulted in the maximum absorb-

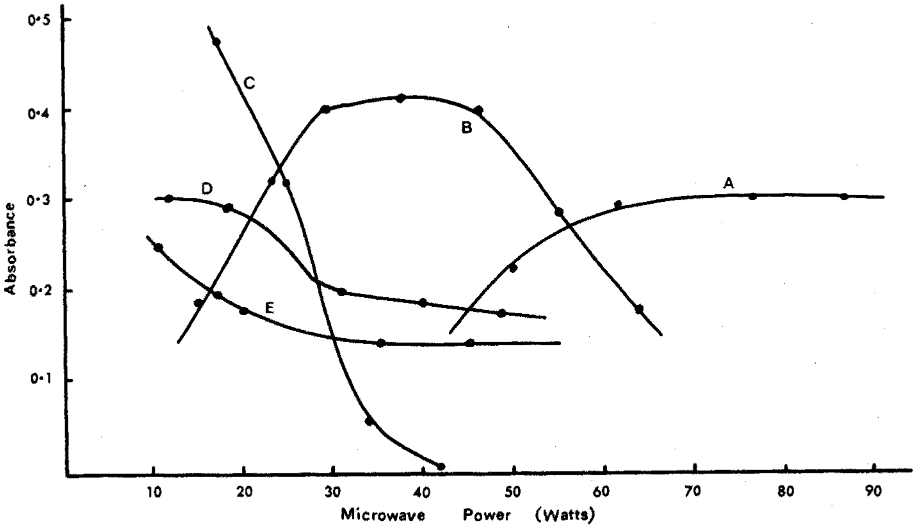

Fig. 8. Effect of microwave power ($P-R$) on a.a.s. of zinc for various zinc lamps. (A) 5 μg $ZnCl_2$; (B) 20 μg $ZnCl_2$; (C) 100 μg $ZnCl_2$; (D) <100 μg Zn metal; (E) >2000 μg Zn metal.

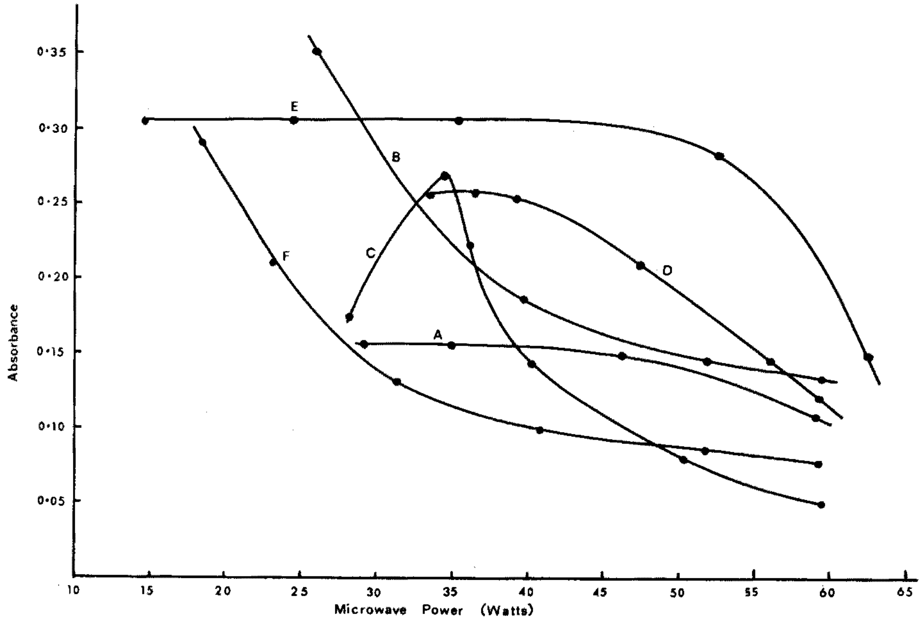

Fig. 9. Effect of microwave power ($P-R$) on a.a.s. of cadmium for various cadmium lamps. (A) 5 μg $CdCl_2$; (B) 10 μg $CdCl_2$; (C) 20 μg $CdCl_2$; (D) 40 μg $CdCl_2$; (E) <100 μg Cd metal; (F) >2000 μg Cd metal.

ance occurring at varying values of slit width from a minimum up to 0.025 mm. A slit width of 0.025 mm was chosen in order to compare the cadmium lamps because this value generally provided the highest atomic absorbance for all the lamps when run at their respective optimal microwave powers.

For each lamp the effect of applied microwave power on the atomic absorbance signal whilst nebulising a 5-p.p.m. solution was investigated. Lamps prepared from the metal alone were also examined in the same way and a selection of the results is shown in Figs. 8 and 9. In both cases it may be seen that the lower quantities of the element or compound are to be preferred; with zinc a distinct advantage was again obtained with lamps containing 20 μg of zinc chloride. For cadmium lamps low quantities of the metal offer a distinct advantage over the use of cadmium chloride, whilst for zinc there is no apparent advantage.

The remaining variables, *viz.* lamp dimensions, fill gas and type of cavity used were evaluated for zinc chloride (20 μg) and selenium metal (*ca.* 0.1 mg) lamps. Selenium was chosen because some problems (see below) were encountered in obtaining a complete evaluation with zinc or zinc chloride lamps. In addition, selenium unlike zinc metal does not plate out on the inner walls of the lamp.

Effect of lamp size (dimensions)

A discharge could not be maintained with small-bore zinc chloride lamps because of the unduly high vapour pressure prevailing. Hence this variable was examined by atomic fluorescence spectroscopy with selenium lamps prepared from 2-mm, 5-mm and 8-mm internal diameter quartz tubing. In all cases, the atomic fluorescence signal obtained was greatest for the 8-mm tubing and least for the 2-mm

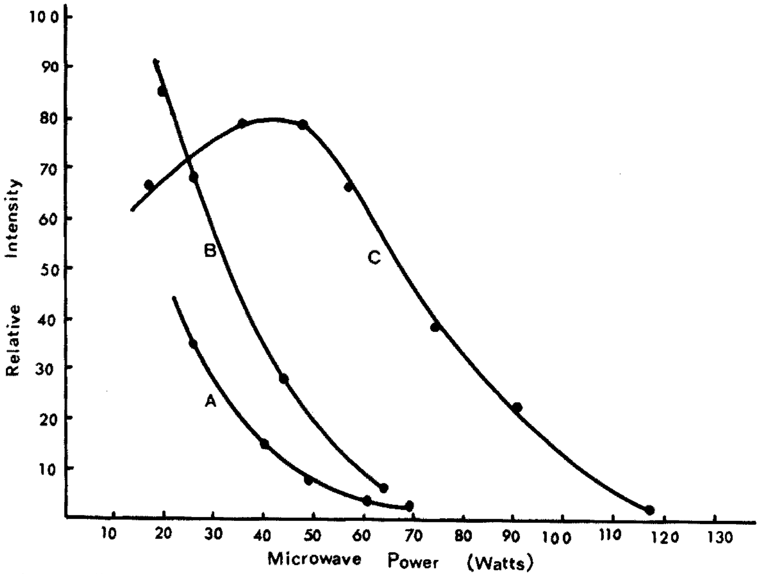

Fig. 10. Effect of microwave power ($P-R$) on a.f.s. of selenium with lamps prepared from various diameter quartz tubing. (A) 2 mm i.d.; (B) 5 mm i.d.; (C) 8 mm i.d.

tubing. The variation of the atomic fluorescence signal with applied microwave power for a typical set of lamps is shown in Fig. 10. These observations are in agreement with those of other workers[6,13]. The maximum diameter tubing which may be used with the Broida cavity used in this study is 13 mm outer diameter (*ca.* 11 mm internal diameter).

An attempt was made to examine the effect of bulb length, but with lamps greater than 4 cm in length and less than 2 cm, the discharge failed to fill the lamp at normal operating powers (*i.e.* $P-R=50$ W). Consequently, a sufficiently wide and accurate range of bulb sizes enabling predictions and conclusions to be made could not be obtained. With lamps shorter than 2 cm in length it is possible that the use of smaller quantities of material and a lower fill-gas pressure would enable this problem to be overcome. However, this is considered unlikely to be of any value in view of the reduced lifetime obtained under such conditions. The optimal conditions regarding lamp dimensions for operation in the Broida three-quarterwave cavity are therefore 8 mm internal diameter with a bulb length of between 2.5 and 3.5 cm. For a very volatile element or compound such as mercury some advantage may be gained by using lamps of much larger dimensions. The use of smaller dimensions may have some advantage when less volatile elements or compounds are used because such lamps can be run at a much higher temperature and can offer a higher integrated line intensity. However, the analytical signal is frequently reduced under these conditions because of excessive line broadening and/or self-reversal.

Choice of fill gas

Helium was examined as a possible alternative to argon as a fill gas. For zinc and selenium sources helium-filled lamps gave a lower analytical atomic absorption

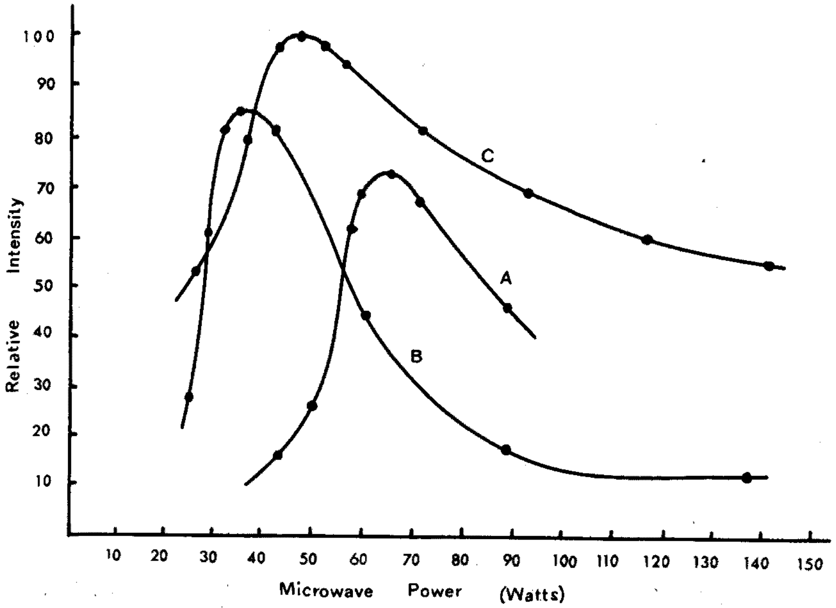

Fig. 11. Effect of microwave power ($P-R$) on selenium lamp intensity for different microwave cavities. The intensity of "A" has been reduced by a factor of two. (A) BKT; (B) BK-UT; (C) EMS 210L.

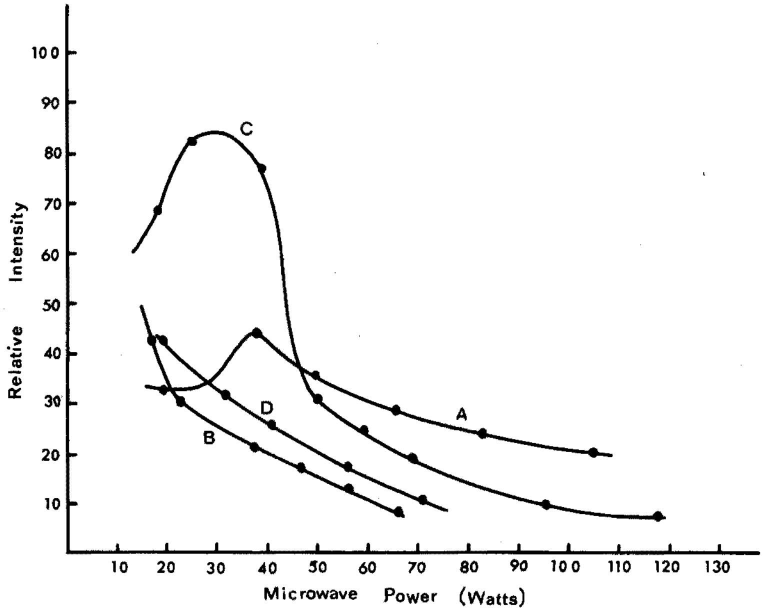

Fig. 12. Effect of microwave power ($P-R$) on a.f.s. of selenium for lamps with different cavities. (A) BK-T; (B) BK-UT; (C) EMS 210L; (D) BK-UT strongly cooled.

and fluorescence signal than argon-filled sources at all powers except the lowest used ($P-R=20$ W). However, under these low-powered conditions the discharge frequently was observed to oscillate between those of the inert gas and of the element spectrum required. Helium lamps also generally exhibited a much shorter life-time than their argon equivalent, particularly if they had been run at high microwave powers. This can no doubt be explained by the diffusion properties of helium through the red hot quartz walls of the lamp.

COUPLING OF THE MICROWAVE POWER

Three different types of three-quarterwave microwave resonant cavities were examined in this study, *viz.* the Electro-Medical Supplies No. 210L and two modifications of this (Beckman-RIIC, London, U.K.). The first of these modifications (designated hereafter as BK-UT) has provision for air-cooling the lamp and incorporates a solid base. Air flows through a pipe outside the cavity from the top into the base, up through the cavity and out via the viewing window or a series of holes in the upper portion of the cavity. The top is sealed by the use of a metal cap which also serves as a holder for the lamp in use. The second cavity (hereafter designated BK-T) is somewhat shorter than both the EMS 210L and BK-UT and has no built-in provision for air-cooling, but has two capacitative tuning stubs (calibrated in mm) of the type described by West *et al.*[3]. This cavity is open at the base and could if required be cooled by passing air up through the base of the cavity and out through the top, or, if the metal cap is used, through the viewing window. All cavities had approximately the same size of viewing apertures. Both the BK-UT and BK-T cavities have a built-in probe for initiation of the lamp and both are considerably more substantial than the EMS 210L (the BK-UT weighs 575.9 g, the BK-T 844.8 g and the EMS 210L 452.5 g).

Many lamps proved extremely difficult to initiate in the tuned cavity (BK-T) and indeed, it proved impossible to maintain a discharge with any of the zinc chloride lamps discussed above. Consequently, the cavities were evaluated with selenium lamps. The procedure adopted was to examine the performance of each cavity with regard to intensity of lamp and atomic fluorescence and atomic absorption signals obtained on nebulising a selenium solution. The same lamp was used throughout and each cavity was accurately located in the same position.

Intensity

The effect of applied power on the integrated line intensity at 196.1 nm was investigated for all three cavities (Fig. 11). The apparent high intensity using the BK-T cavity is caused by a considerable background in the region of 196.1 nm.

Atomic fluorescence measurements

Atomic fluorescence was measured at 196.1 nm by nebulising a 20-p.p.m. selenium solution. A slit width of 1 mm was used throughout these experiments because the flame background in this region is quite low. The BK-UT cavity was examined both with and without the use of air cooling. The effect of applied power on the atomic fluorescence signal is shown in Fig. 12.

Atomic absorption measurements

Atomic absorption was measured at 196.1 nm by nebulising a 1000-p.p.m. selenium solution. The effect of slit width was examined by operating the lamp at an applied power of 30–45 W (Fig. 13). Maximal atomic absorbance was obtained at a slit width of 0.05 mm in all instances, hence this value was used for all subsequent measurements. The effect of applied power on the atomic absorbance is shown in Fig. 14.

The dependence of the atomic fluorescence signal on the applied microwave power (Fig. 12) indicates that the coupling efficiencies of the three cavities are in the order BK-T, EMS 210L and BK-UT, the BK-T cavity being the least efficient. Consequently, it might be expected that the BK-T cavity could offer some advantages in atomic absorption spectroscopy, where spectral line intensity is not a prime requirement and the lower efficiency would probably result in a narrower line profile. How-

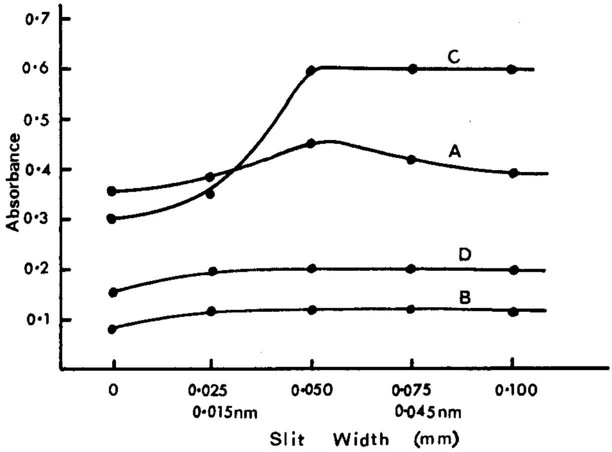

Fig. 13. Effect of variation of slit width on a.a.s. of selenium for lamps with various cavities. (A) BK-T, $P-R=44$ W; (B) BK-UT, $P-R=33$ W; (C) EMS 210L, $P-R=38$ W; (D) BK-UT (cooled), $P-R=33$ W.

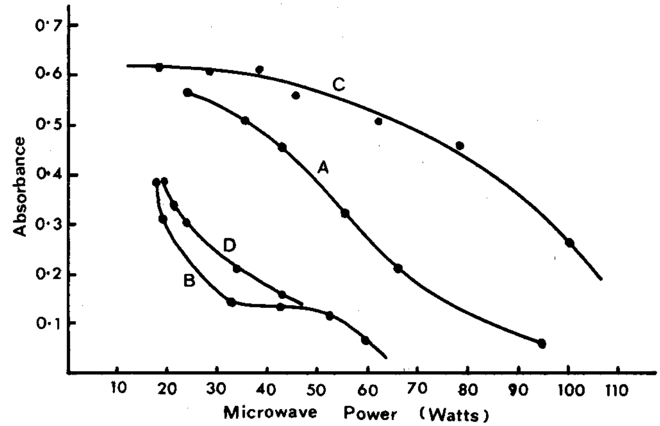

Fig. 14. Effect of microwave power ($P-R$) on a.a.s. of selenium for lamps with various cavities. (A) BK-T; (B) BK-UT; (C) EMS 210L; (D) BK-UT strongly cooled.

ever a similar pattern was observed in the atomic absorption measurements with the greatest absorbance resulting from the use of the EMS 210L cavity. The poor performance of the BK-T cavity compared to that which might be expected from consideration of the atomic fluorescence results was attributed to the high background radiation near 196.1 nm observed with this cavity (Fig. 11). However, even with this higher background the use of the BK-T cavity resulted in an atomic absorbance approaching that obtained when the lamp was operated in the EMS 210L cavity. Consequently, it is likely that this cavity might offer some advantages in atomic absorption spectroscopy for lamps prepared from volatile elements with resonance lines in a region of low background. The effect of background can be clearly seen in Fig. 13 which shows the effect of varying the slit width on the atomic absorbance of a 1000-p.p.m. selenium solution. Increasing the slit width from zero to 0.05 mm resulted in a sharp increase in atomic absorbance with the EMS 210L cavity, but only a slight increase with the BK-T cavity. The integrated line intensities follow the same pattern as the atomic fluorescence signal, with the exception that the BK-T cavity provides the highest intensity for the reasons discussed above. The peak integrated line intensity occurs at a slightly higher applied microwave power than the corresponding peak atomic fluorescence signal, as would be expected from line broadening and/of self-reversal considerations.

CONCLUSIONS

It has been shown that the optimal spectral performance of zinc and cadmium microwave-excited electrodeless discharge lamps is obtained when low quantities of the element or metal halide are used to prepare the lamp. The amount present has a marked effect on the analytical atomic absorption and fluorescence signals at all values of applied microwave power exceeding 25 W. This effect is almost certainly due to the fact that the compound used is completely volatilised at the operating temperature of the lamp. Under such conditions the partial pressure of the compound concerned within the lamp will be directly proportional to the amount of that compound used (provided of course that the lamp dimensions remain constant). It follows that above a certain quantity of material the pressure will be such that further increases in the amount used would not be volatilised and the amount present above this quantity would be without effect. It is to be expected that this would occur in the milligram region, which no doubt explains the results obtained by other workers[6]. The absence of a dependence of the atomic fluorescence signal on zinc chloride lamps with 10^{-4} g of material to prepare the lamp at operating powers of 20 W is in agreement with this because the low operating temperature afforded by the use of such a low operating power is insufficient to volatilise completely the material present. Clearly, the decrease in analytical signal with increasing amounts of compound used is due to an increase in pressure resulting in a gradual transition of light emission from the so-called "skin effect" (free from self-reversal and line broadening) to the formation of a central arc (exhibiting line-broadening and self-reversal effects).

Similar considerations explain the advantages of using 8-mm internal diameter tubing because the larger volume results in a reduced pressure when the element or compound is completely volatilised. The use of large lamps would at first seem attractive, but the lamp dimensions are to a very great extent controlled by the nature of the microwave field.

It is to be expected that the performance of lamps prepared from less volatile elements or compounds would show little or no dependence on the amount of compound used once present in amounts above the maximum which may be volatilised at the operating temperature of the lamp. The use of the minimum (microgram) amounts of material is to be preferred because this largely obviates the encountered problem of instability[14] caused by movement of material within the lamp during operation. The main improvement in the stability of the lamps used in this study was due to the elimination of unnecessary material and the production of an essentially gaseous discharge. In the case of zinc lamps containing *ca.* 20 μg of zinc chloride and operated under optimal conditions there was virtually zero long-term drift over a period of 1 h and a short-term drift of ±0.5% in emission intensity at 213.8 nm; these results are similar to the short- and long-term drifts associated with rare gas discharge lamps.

The optimal lamp dimensions for the particular experimental arrangement used in this study were found to be 8 mm internal diameter tubing with a bulb length of *ca.* 3 cm. Very small lamps or lamps prepared from narrow bore (< 5 mm i.d.) tubing appear to offer no advantage, except perhaps for elements or compounds of very low volatility.

The two new cavities examined were found to offer no advantages over the Electro-Medical Supplies three-quarter wave cavity for the operation of selenium lamps, although it might be expected that the BK-T cavity (the least efficient of the three examined) would offer some advantages for the operation of lamps prepared from very volatile elements or compounds. The most efficient, the BK-UT, might have some advantages for less volatile elements and compounds. This aspect is at present under investigation.

One of us (D.O.C.) would like to thank Beckman-RIIC Ltd. for financial support and loan of apparatus required to carry out this work.

SUMMARY

An attempt is made to prepare microwave-excited electrodeless discharge lamps exhibiting reproducible spectral characteristics. Some of the more important experimental parameters concerned with the preparation and operation of the sources are investigated with respect to spectral characteristics, resonance-line intensity and application of the lamps for atomic absorption and fluorescence purposes. A reproducible method of preparation is described for zinc and cadmium lamps giving improved spectral stability. Optimal results are obtained when microgram quantities of material are used to prepare the lamps. The use of a related series of three-quarter wave resonant cavities is compared.

RÉSUMÉ

On examine les possibilités de fabriquer des lampes à décharge, à onde courte, sans électrode, pouvant offrir des caractéristiques spectrales reproductibles. Parmi les paramètres expérimentaux les plus importants, on prend en considération les caractéristiques spectrales, l'intensité des lignes de résonance et l'application des lampes pour l'absorption atomique et la fluorescence. Une méthode de fabrication est décrite pour des lampes de zinc et de cadmium, présentant une meilleure stabilité spectrale.

ZUSAMMENFASSUNG

Es wird versucht, mikrowellenerregte elektrodenlose Entladungslampen mit reproduzierbaren Spektraleigenschäften herzustellen. Einige der wichtigeren experimentellen Parameter, die die Herstellung und den Betrieb der Lampen betreffen, werden in Hinblick auf Spektraleigenschaften, Resonanzlinienintensität und Anwendung der Lampen für Atomabsorption und -fluoreszenz untersucht. Es wird eine reproduzierbare Methode für die Herstellung von Zink- und Cadmiumlampen mit verbesserter spektraler Stabilität beschrieben. Optimale Ergebnisse werden erhalten, wenn Mikrogramm-Mengen des Elements für die Herstellung der Lampen verwendet werden. Die Anwendung einer entsprechenden Gruppe Dreiviertelwellen-Hohlraumresonatoren wird verglichen.

REFERENCES

1 R. M. Dagnall and T. S. West, *Appl. Opt.*, 7 (1968) 1287.
2 W. J. Price, in D. R. Browning, *Spectroscopy*, McGraw Hill, London, 1969.
3 K. M. Aldous, D. Alger, R. M. Dagnall and T. S. West, *Lab. Pract.*, (1970) 587.
4 C. J. Woodward, *Atomic Absorption Newsletter*, 8 (1969) 121.
5 G. F. Kirkbright, A. P. Rao and T. S. West, *Anal. Lett.*, 2 (1969) 465.
6 J. M. Mansfield, M. P. Bratzel, Jr., H. O. Norgordon, D. N. Knapp, K. E. Zacha and J. D. Winefordner, *Spectrochim. Acta*, 23B (1968) 389.
7 R. M. Dagnall, M. R. G. Taylor and T. S. West, *Spectrosc. Lett.*, 1 (1968) 397.
8 R. F. Browner, R. M. Dagnall and T. S. West, Paper presented at *XIth Eastern Analytical Symposium, New York, U.S.A., 1968.*
9 R. M. Dagnall, R. Pribil and T. S. West, *Analyst*, 93 (1969) 281.
10 E. F. Worden, R. G. Gutmacher and J. G. Conway, *Appl. Opt.*, 2 (1963) 707.
11 M. D. Silvester and W. J. McCarthy, *Anal. Lett.*, 2 (1969) 305.
12 F. C. Tomkins and M. Fred, *J. Opt. Soc. Amer.*, 47 (1967) 1087.
13 T. C. Rains, *N.B.S. Technical Note No. 454*, July 1967–June 1968.
14 J. C. O'Haver and J. D. Winefordner, *J. Chem. Educ.*, 46 (1969) 435.

Analytica Chimica Acta
Elsevier Publishing Company, Amsterdam
Printed in The Netherlands

EMISSION SPECTROSCOPY OF TRACE IMPURITIES IN POWDERED SAMPLES WITH A HIGH-FREQUENCY ARGON PLASMA TORCH

R. M. DAGNALL, D. J. SMITH, T. S. WEST
Chemistry Department, Imperial College, London, S.W.7
AND S. GREENFIELD
Research Department, Albright and Wilson Ltd., Oldbury, Warley, Worcs.(England)

(Received 22nd December 1970)

The inductively coupled high-frequency plasma torch has been recognised as a potentially useful spectroscopic analytical tool for some time[1-6]. Several of the previously published studies[1,3,5] have been concerned with the application of commercially available high-frequency plasma generators to the study of solution analysis. Only one publication has described a method for the analysis of powdered samples[3].

In the study described here, a system capable of exciting the major spectral lines of trace, refractory-oxide-forming elements present in a powdered matrix has been developed. All operating parameters have been carefully examined with respect to the use of powdered matrices.

The instrumental system used consisted of a Radyne model SC15 plasma generator (36 MHz) coupled to a Unicam SP900 flame spectrophotometer with a galvanometer and 0–1 mV chart recorder read-out. The spectrophotometer was carefully screened to eliminate strong high-frequency pick-up (see p. 403). The spectrographic box and trunking supplied with the generator were removed to give flexibility of operation and the torch unit was relocated on the generator casing so that both the torch and work coil could be adjusted independently. In addition "compoflex" flexible pressure leads were used to provide both high-frequency power and cooling water at 40 p.s.i. to the working coil.

INVESTIGATION OF OPERATING PARAMETERS

Coil design

Under the operating conditions only one direction of winding was found to be suitable, namely ascending anticlockwise when viewed from above. Coils wound in the opposite direction did not couple effectively with the gas flow. The preferred direction of winding is the reverse of the toroidal component of the gas flow in the standard torch cell which is ascending clockwise. It was found advantageous to earth the end of the coil nearest to the open end of the torch. This minimised overheating effects and consequent damage to the cell.

The working coil normally used with the Radyne SC15 generator consists of 2.5 turns of 0.25-in (outer diameter) cylindrical copper tubing. The overall height of such a coil is 22 mm and the coil separation is 1.5 mm. It was found that the use of 0.1875-in square-section tubing would allow the design of a more compact coil and still permit an adequate flow of cooling water. A coil made in this way gave an improved plasma formation, probably because of a higher electric field at the centre of the smaller coil. Coil separation was held at 1.5 mm (the minimum value before electrical breakdown occurred) and the overall height was 17 mm. The optimal internal diameter of the coil was found to be 32 mm which gave a 2-mm space between the coil and cell wall to prevent overheating effects.

Gas mixtures

The plasma torch has 3 separate gas flows, *viz.* plasma, coolant and injector flows, although all contribute to the plasma formation ultimately. Previous workers have mainly used argon for all three flows, but the addition of other gases such as nitrogen which has a higher heat content than argon has been shown to give a more controlled and compact plasma[7,8].

For the present studies, a facility was built into the gas-regulating system which enabled the coolant flow to be varied continuously from 100% argon to 100% nitrogen. The plasma could only be initiated with argon flowing, but once initiated

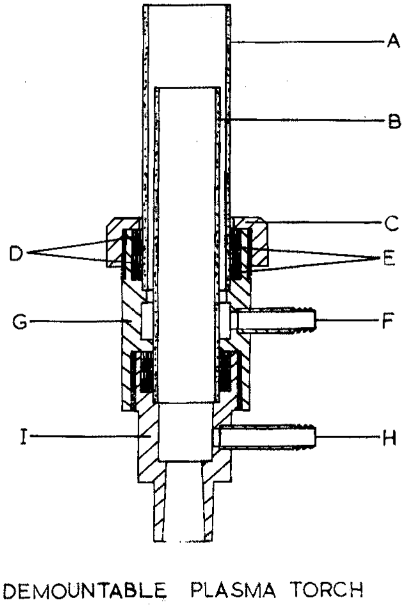

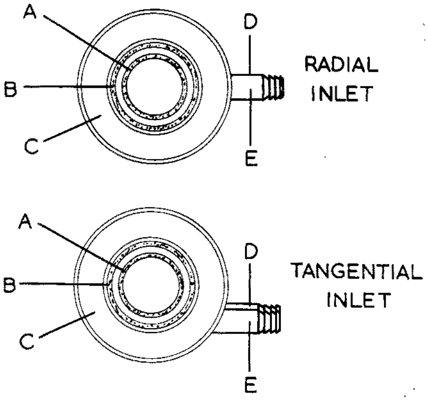

Fig. 1. Demountable plasma torch. (A) Outer silica tube; (B) inner silica tube; (C) locking cap; (D) spacer ring; (E) rubber "O" ring; (F) coolant gas inlet; (G) upper body; (H) plasma gas inlet; (I) lower body with B14 socket.

Fig. 2. Radial and tangential injection of plasma and cooling gases. (A) Inner silica tube; (B) outer silica tube; (C) torch body; (D) plasma gas inlet; (E) coolant gas inlet.

the coolant flow could be adjusted as required. The inductance and capacitance trimmers of the power supply were adjusted to give maximum power when the plasma was operated with nitrogen cooling[6,7].

Torch cell design

The standard torch cell[1] utilises a fused quartz design with tangential gas flow, hence repair is difficult if wall damage occurs. A demountable torch was constructed to obviate this; a brass base accommodated two concentric quartz tubes and a socket to accept the injector cone (Fig. 1). Two units were made, the first with coolant and plasma gases flowing tangentially as in the standard torch and the other with radial gas inlets (Fig. 2). The latter model was found easier to initiate although its position in the working coil was more critical. The plasma appearance was quite similar in both models except for the diminished size of the low-temperature hole formed with the radial inlet torch[1,6]. Laminar gas flow was ensured in the radial inlet by using corrugated strip between the outer and middle tubes and glass balls (3-mm diameter) between the injector and middle tubes. Schlieren photographs of the region immediately above the torch showed less turbulence with the radial inlet system than with the tangential inlet system. The brass base remained quite cool during operation even over periods of several hours and the possibility of excessive loading of this power into the base was discounted for this particular system.

Plasma modulation

It has been suggested that the high-frequency supply at 36 MHz has a 100-Hz ripple derived from the mains supply superimposed on it which causes a corresponding 100-Hz modulation of the plasma tail flame[8,9]. Such a modulation might be out of phase with the 50-Hz mains supply because of a phase shift in the generator; if this were the case, then only a fraction of the emission produced in the tail flame would be observed at the photomultiplier which receives radiation via a mechanical chopper rotating at 100 Hz and driven from the mains supply.

An estimate of the percentage modulation of the plasma discharge was obtained by viewing the plasma discharge through the blades of a mechanical 100-Hz chopper with a small photocell coupled to an oscilloscope. The waveform of the discharge intensity consisted of a high d.c. level with a 100-Hz sinusoidal wave superimposed on it. The sinusoidal shape arose from the power supply to the triode oscillator valve in the SC15 generator. The power supply has a full-wave rectified 50-Hz mains-derived waveform, subsequently smoothed with a choke-input filter. Whilst it is misleading to refer to a 100-Hz signal being in or out of the phase with a 50-Hz signal, it could be stated that the maxima of the 100-Hz modulated plasma waveform always occurred at the same instant in time as the maxima and minima of the 50-Hz mains waveform.

A comparison was made of the position of the plasma intensity trace on the oscilloscope with the controls first set to display d.c. and then to display a.c. This led to an estimate of the percentage modulation which when calculated as the amplitude of the modulated portion as a proportion of the mean d.c. level, was approximately 5%.

The internal chopper motor in the spectrophotometer used in these experiments was a shaded pole single-phase motor, which has a synchronous speed of 3000 r.p.m.

or 50 Hz and a fixed synchronisation axis. This ensures that the motor shaft has a constant phase relationship with the mains frequency. The chopper blade mounted on the motor shaft has two blades of 90°. At the synchronous speed of the motor, the radiation path to the photomultiplier is interrupted at a rate of 100 Hz. Radiation (d.c.) observed through this chopper appears as a 100-Hz square-waveform, indicating the times at which the radiation path is open or closed. It should be stressed that because the motor shaft bears a constant phase relationship to the mains waveform, so does the 100-Hz square-waveform, and because the plasma intensity has been shown to behave similarly, then the plasma intensity also bears a constant phase relationship to the 100-Hz square-waveform. By displaying the appropriate signals on the two traces of a double-beam oscilloscope, it was shown that the radiation path in the spectrophotometer always opens at a minimum point on the plasma intensity waveform and closes at a maximum. Exactly 180° of the 360° sinusoidal waveform is seen by the photomultiplier.

A marginal improvement could be obtained by adjusting the chopper blade position on the motor shaft, such that a 180° portion equally disposed around a maximum plasma intensity was observed. However, because this plasma was only 5% modulated, the signal improvement would be only about 3.2%. In instances where the plasma was modulated to a greater extent than 5%, this adjustment would become advisable. Evidence was obtained to indicate that not all Unicam SP 900A Spectrophotometer internal chopper motors have a fixed synchronisation axis. If a motor is used which does not bear a constant phase relationship to the mains frequency, then on different occasions, different portions of the plasma waveform will be observed by the photomultiplier. For a percentage modulation of 5%, the maximum possible discrepancy between the signals displayed would be 6.4% of the mean value. At higher amplitudes of modulation, the discrepancies become unacceptably large, and for the extreme case of 100% modulation, the discrepancy could amount to 127% of the mean value.

USE OF POWDERED SAMPLES

Two aspects of powder injection were studied (with particle sizes below 66 μm):

1. the means whereby a powder sample and a flow of argon could be mixed reproducibly to form a uniform particle cloud and
2. the optimum method of presenting the particle cloud to the plasma discharge.

Two quite distinct methods for producing a powder cloud were investigated, *viz.* the swirl cup and fluidized-bed chamber, and four different methods of introduction, *viz.* quartz, constricted pyrex, alumina and tantalum tubes.

Swirl cup

The swirl cup examined here is similar to the powder injection device used by previous workers[3] and involved downward injection of a flow of argon into a sample cup which also acted as a swirl chamber (Fig. 3). The cloud thus formed was led up to an offset outlet and thence to the torch cell.

There was a natural tendency for the centrally injected gas flow to blow the powder away from the base of the sample cup. The powder was then distributed up

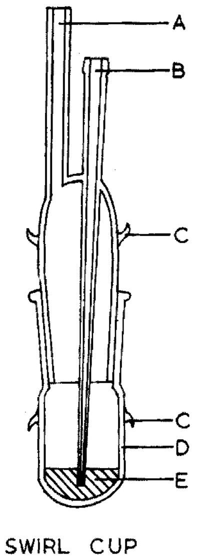

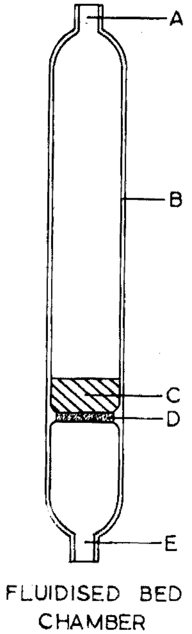

Fig. 3. Swirl cup chamber. (A) Gas/powder outlet; (B) gas inlet; (C) securing hook; (D) detachable powder cup; (E) powder.

Fig. 4. Fluidized-bed chamber. (A) Gas/powder outlet; (B) pyrex tube; (C) powder; (D) sintered glass disc; (E) gas inlet.

the walls of the cup and intermittently fell into the central area of the base. This resulted in powder surges whenever powder fell into the path of the gas-jet. The use of a mechanical vibrator to vibrate the sample cup reduced surging considerably. A multi-sample device was constructed along similar lines containing 4 swirl chambers each of which could be presented in turn to the single gas inlet position.

Fluidized-bed chamber

This system involved supporting the powder sample on a sintered glass disc of coarse porosity with an argon flow passing through the disc (Fig. 4). Mechanical vibration was found to stabilise the formation of the fluidized bed, above which a relatively surge-free cloud was produced.

Cyclone chambers

Attempts to remove the remaining small surges in both systems described were made by incorporating circular cyclone chambers between the cloud forming system and the tube leading into the plasma cell. These chambers ensured that any large particles or agglomerates were drawn from the main cloud by centrifugal force; however the possibility existed that some segregation of particles of varying density might occur giving erroneous analytical results. A further feature of the cyclone chambers was that they allowed a bleed-off valve to be incorporated. This allows a more flexible system in which it is possible to have a fast flow of gas to form the particle cloud, but a slower flow to carry the cloud into the plasma and hence provide plasma stability. However, stable emission intensities were only observed for *ca.* 60 sec after which excess of powder, deposited around the periphery of the cyclone chamber, was picked up by the circular flow of gas. Cyclone chambers were rejected at this stage as needing further work to eliminate the disadvantages mentioned.

Sample injector devices

Several systems were investigated in attempts to obtain a low powder flow rate with maximum plasma stability. The best results were achieved with a plain quartz tube (2-mm internal bore and 4 mm outside diameter) with the tip *ca.* 0.5 cm below the base of the plasma. Constricted pyrex tubes[6] were also investigated, but these were subject to overheating effects at their preferred height. Also, although they operated well enough with the swirl cup device, the superior fluidized-bed system induced powder build-up at the constriction with consequent fluctuations in delivery.

Thin-walled tantalum tubing (3-mm internal bore) was also investigated as a means of preheating the powder cloud before entry into the plasma region. When the lower end of the tube was earthed, the upper end which projected into the high-frequency field was heated to white heat by induction. The energy available for plasma production was decreased and a greater degree of plasma stability was obtained. Improved sample vaporisation was noted in comparison with the use of quartz or pyrex tubes, by the fact that higher gas flow rates could be tolerated before non-vaporised powder passed through the plasma. The disadvantage with this system was that slow degradation of the thin tantalum walls occurred at the hot tip which tended to alter the direction of the gas flow. It is possible that this could be alleviated with thicker walled tubing.

The optimal arrangement was found to be a combination of the fluidized-bed chamber and quartz tubing injector. The powder feed rate from the chamber was not quite constant, but decreased slowly in an inverse exponential manner. Thus, intensity readings also fell slowly with time. To overcome this problem a fixed weight of powder was introduced into the chamber, and the gas flow was started and adjusted to the correct value. After a selected delay time, the intensity reading was taken, and reproducible results were obtained. A suitable powder loading was 3.5 g of magnesium oxide, as this allowed the delay time before reading to be considerably extended whilst making adjustments. The mechanical vibrator was arranged to act against the chamber side at a point about 1 cm above the sintered disc. A short length of thin-walled rubber tubing connected the powder chamber to the quartz tube which passed through a "teflon" plug fitted into a B14 socket in the base of the torch cell. The injection gas flow rate could be varied from zero to 1 l min^{-1} without extinguishing the plasma. Higher flow rates caused plasma instability.

SELECTION OF MATRIX

A number of materials were examined, *viz.* $CaCO_3$, SiO_2, Al_2O_3 and MgO, with respect to their ability to produce a non-sticking powder cloud with a low background spectrum. All materials were passed through a 240-mesh sieve before use (*i.e.* particle sizes were less than 66 μm), although the calcium carbonate and magnesium oxide were more finely divided than this. Only silica appeared to suffer aggregation effects in the fluidized bed and was therefore considered undesirable.

Spectral examination under the above optimised experimental conditions, showed that calcium carbonate was unsuitable because it exhibited widespread high background emission from calcium atoms and ions and some impurity spectral lines (*e.g.* magnesium) and bands.

A lower background spectrum was given by alumina, but even the purest grade of alumina available here contained upwards of 100 p.p.m. of many elements, *e.g.* magnesium, silicon and boron.

Very intense radiation was observed from magnesium oxide at 285.2, 280.3 and 279.6 nm, but below *ca.* 255.0 nm the background level was quite low with only minor peaks at *ca.* 246 and 236 nm. The matrix was considered to be experimentally suitable for testing for the analysis of elements with major resonance lines in the low ultra violet region. Methods were, therefore, examined for the analysis of beryllium and boron in magnesium oxide at 234.9 and 249.7 nm.

EXPERIMENTAL

Apparatus

Plasma generator. Radyne Ltd. (Wokingham, Berks, U.K.). Model SC15 generator; frequency 36 MHz. Maximum power output 2.5 kW.

Plasma torch. Brass base with two double O-ring seals and B14 socket, all concentric. Tangential gas injection for cooling and plasma flows via two quartz tubes (outer 25 mm and inner 21 mm internal diameter respectively with 1.5 mm nominal wall thickness). The outer quartz tube extends 30 mm above the inner tube and the overall torch height is 18 cm.

Gas flow rates used are: plasma flow (argon) 7.5 $\mathrm{l\,min^{-1}}$, cooling flow (nitrogen) 7.5 $\mathrm{l\,min^{-1}}$ and injector flow (argon) 0.5 $\mathrm{l\,min^{-1}}$.

Working coil. 2.5 turns of a 0.1875-in square section of 20 gauge copper tubing with its ends silver-soldered to 0.25-in BSP fittings for connection to cooling water and high-frequency power supply. The coil separation is 1.5 mm with an internal diameter of 32 mm and an outside diameter of 41 mm. Coil winding ascends anticlockwise when viewed from above (*i.e.* from the open end of torch). The coil is located concentrically 4 mm above the upper end of the inner quartz tube.

Fluidized-bed chamber. Sintered glass disc (2 cm diameter, porosity 1) fused inside a borosilicate glass tube which is drawn out, 10 cm above and 2 cm below the disc, to 0.25-in outside diameter tubing. The required aliquot of powder is placed above the disc and gas is injected from below.

Spectrophotometer. Unicam SP900A spectrophotometer suitably high-frequency screened with the entrance slit reduced to 2 mm in height. Output from the amplifier is taken to a standard galvanometer attachment and a Honeywell 0–1 mV chart recorder equipped with a voltage dropping circuit. All component packs within the spectrophotometer were earthed and all external leads were provided with copper braid sleeves. The galvanometer and recorder leads were converted to coaxial cable and an auxiliary 6.3-V transformer was incorporated to feed the galvanometer bulb and exterior instrument lights. The detailed screening procedure for this instrument was established in the laboratory of one of the authors (S.G.) and is available from Pye-Unicam Ltd., Cambridge, U.K.

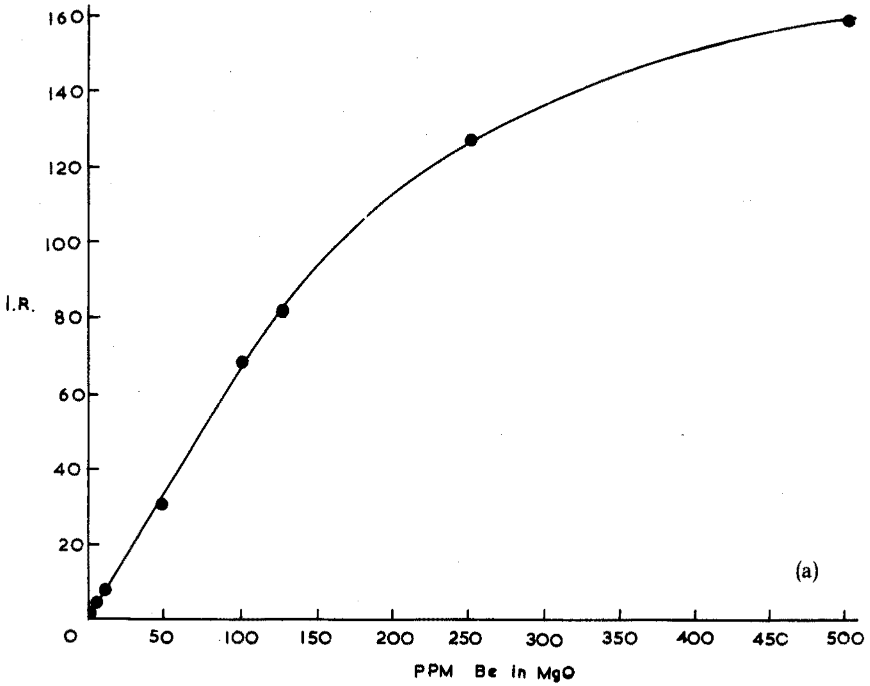

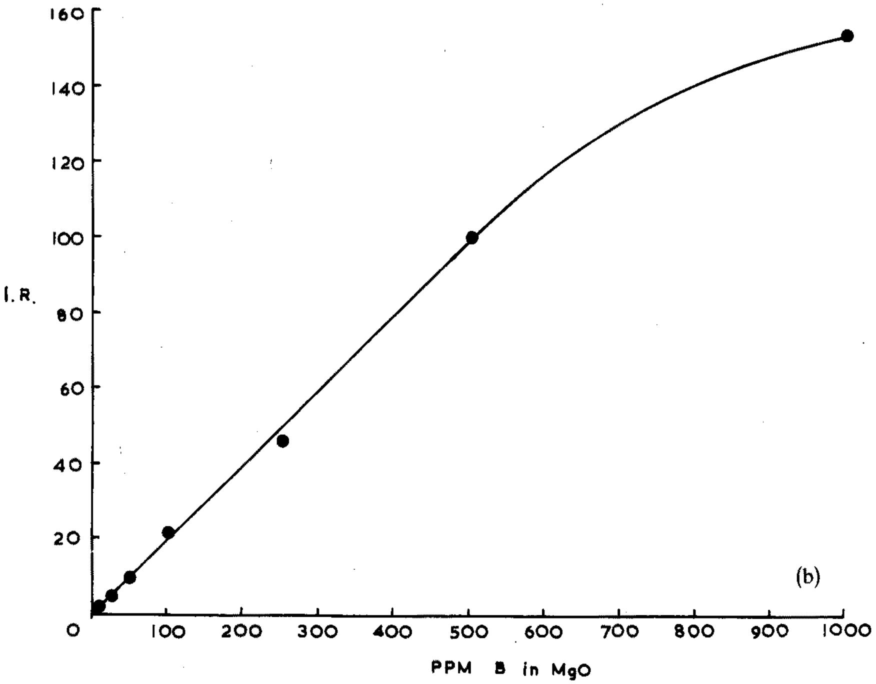

Fig. 5. (a) Calibration curve for beryllium in magnesium oxide; (b) calibration curve for boron in magnesium oxide.

Sample preparation

All substances were used in dry powder form and were ground in an agate mortar until they passed a 240-mesh sieve. The appropriate quantity of beryllium carbonate or boric acid was then added to a 10-g aliquot of magnesium oxide matrix to give a mixture containing 1000 p.p.m. of the desired element. This mixture was then thoroughly ground in the agate mortar to ensure homogeneity. Aliquots of the mixture were taken and further diluted with magnesium oxide to give a suitable concentration range. Care was taken to ensure thorough mixing at each stage.

Procedure

Introduce 3.5 g (±0.1 g) of powder into the clean fluidized-bed chamber via a filter funnel. Connect the quartz tube to the fluidized-bed chamber with a piece of rubber tubing, introduce the tube into the plasma torch and lock into position. Position the mechanical vibrator to give efficient chamber vibration.

Switch on water and mains power supply to the plasma generator and adjust the argon plasma and coolant flows to 7.5 l min^{-1}. Switch on the power to the working coil and insert a carbon rod into the torch mouth to initiate the plasma.

Gradually change the coolant flow from argon to nitrogen (7.5 l min^{-1}) and turn on the injector flow to *ca.* 0.5 l min^{-1}. Make fine adjustments to the injector flow rate to give a prearranged recorder reading with an emission line from the matrix as an internal standard; with the magnesium oxide used in this study the silicon line at 251.2 nm was found to be suitable for both beryllium and boron. Finally adjust the wavelength setting to the desired spectral line of the element of interest and record the emission intensity observed over a period of *ca.* 30 sec.

Extinguish the discharge, change the sample (either by cleaning the fluidized-bed chamber or by using a series of similar chambers) and repeat the above sequence of operations to record the emission signal from the next sample.

Calibration curves for boron and beryllium

Figure 5 shows the calibration curves obtained over the range 2–1000 p.p.m. for beryllium (at 234.9 nm) and boron (at 249.7 nm) in solid magnesium oxide. The limits of detection (signal = 2 × standard deviation of background) for beryllium and boron were 0.1 p.p.m. and 2.5 p.p.m. respectively.

DISCUSSION

The main purpose of the present study was primarily to develop a system for the direct introduction of powdered samples into the high-frequency plasma torch.

The analytical data which are discussed in the foregoing section are included chiefly to assist in the evaluation of the potential analytical utility of the system. The analytical parameters require to be investigated further and these will be reported at a later date when practical analytical samples have been analysed.

The relative standard deviations for 20 samples analysed by the technique as described above for 10 p.p.m. of impurities added to magnesium oxide were 6.5% for beryllium and 10% for boron; it must be appreciated that the 10 p.p.m. level for boron is rather close to its detection limit.

The effects of 10,000 p.p.m. of aluminium, calcium, lithium, tantalum and zinc were investigated on 10 p.p.m. of beryllium and boron in magnesium oxide, but in no instance was the variation in emission intensity significantly greater than that shown by the standard deviation for the beryllium or boron alone.

We are grateful to the Science Research Council for the provision of an S.R.C. research studentship to one of us (D.J.S.) under the Co-operative Award in Pure Science scheme. We also thank Albright and Wilson Ltd., Oldbury, Warley, Worcs, for the loan of apparatus and for technical assistance. The Radyne SC15 was purchased with a grant from the Courtauld Research Foundation.

SUMMARY

A commercial high-frequency plasma generator and torch have been modified for application to the analysis of powdered samples. Many of the operating parameters have been investigated and the optimised system has been tested for the analysis of beryllium and boron in magnesium oxide. Two possible methods of sample introduction have been developed.

RÉSUMÉ

On propose une modification du générateur à plasma, haute fréquence pour application à l'analyse d'échantillons en poudre, par spectroscopie d'émission. De nombreux paramètres sont examinés, en particulier en vue de l'analyse de traces de béryllium et de bore dans l'oxyde de magnésium. Deux méthodes possibles d'introduction de l'échantillon ont été développées.

ZUSAMMENFASSUNG

Ein handelsüblicher Hochfrequenzplasmagenerator und -brenner sind für die Anwendung auf die Analyse pulverförmiger Proben abgewandelt worden. Die Betriebsbedingungen wurden weitgehend untersucht und die Anordnung bei optimalen Bedingungen für die Analyse von Spuren Beryllium und Bor in Magnesiumoxid geprüft. Zwei mögliche Methoden der Probenzuführung sind entwickelt worden.

REFERENCES

1 S. Greenfield, I. L. Jones and C. T. Berry, *Analyst*, 89 (1964) 713.
2 R. H. Wendt and V. A. Fassel, *Anal. Chem.*, 37 (1965) 920.
3 H. C. Hoare and R. A. Mostyn, *Anal. Chem.*, 39 (1967) 1153.
4 C. Veillon and M. Margoshes, *Spectrochim. Acta*, 23B (1968) 503.
5 A. S. Bazhar, V. K. Zakharov, P. A. Koka and A. F. Malinorzkaya, *Zavodsk. Lab.*, 34 (1968) 294.
6 G. W. Dickinson and V. A. Fassel, *Anal. Chem.*, 41 (1969) 1021.
7 S. Greenfield, C. T. Berry and L. G. Bunch, *Spectroscopy with a High Frequency Plasma Torch*, Radyne International Inc., U.S.A.
8 S. Greenfield, I. L. Jones, C. T. Berry and L. G. Bunch, *Proc. Soc. Anal. Chem.*, 2, No. 7 (1965) 111.
9 S. Greenfield, P. B. Smith, A. E. Breeze and N. M. D. Chilton, *Anal. Chim. Acta*, 41 (1968) 385.

Analytica Chimica Acta
Elsevier Publishing Company, Amsterdam
Printed in The Netherlands

DETERMINATION OF OXYGEN IN GALLIUM PHOSPHIDE AND SILICON BY HELIUM-3 ACTIVATION

C. K. KIM

Bell Telephone Laboratories, Inc., Murray Hill, N. J. 07974 (U.S.A.)

(Received 10th August 1970)

The increasing importance of small concentrations of light elements such as oxygen, nitrogen and carbon in semiconductor crystals, either as dopants or as trace impurities, underlines the need for reliable analytical procedures enabling these elements to be estimated at low levels. Various techniques are currently being used; they include vacuum fusion gas analysis, infrared spectrometry, mass spectrometry and fast neutron activation. In the case of oxygen in gallium phosphide, however, disturbing disagreements have been noted in these laboratories between results obtained by some of these methods.

By vacuum fusion gas analysis, oxygen levels ranging from $2 \cdot 10^{18}$ to $3 \cdot 10^{20}$ atoms cm^{-3} have been obtained for gallium phosphide crystals prepared in various ways[1], and fast neutron activation has given similar results. In these same crystals, mass spectrometric studies[2] indicated substantially lower oxygen levels in the range 10^{16}–10^{17} atoms cm^{-3}; these are in better agreement with published estimates[3] of about 10^{17} atoms cm^{-3}.

In an attempt to resolve these uncertainties, another analytical method for determining oxygen based on activation of oxygen-16 with ^{3}He particles has been applied. The purpose here is to describe this analytical technique and to compare results obtained with those mentioned above. Similar measurements are also reported for the determination of oxygen in silicon crystals; these measurements were carried out in order to check the reliability of the oxygen determination by ^{3}He activation by means of a system in which oxygen levels are believed to be known fairly accurately.

EXPERIMENTAL

Single crystals of gallium phosphide or of silicon were irradiated with a beam of ^{3}He particles obtained from a fixed energy cyclotron (CS-15 Cyclotron, The Cyclotron Corporation, Berkeley, Calif.). Particles emerging from the accelerator have an energy of 22.5 MeV but, in order to prevent undesired nuclear reactions, this was reduced to about 14 MeV by placing a thin tantalum foil in front of the samples. Some oxygen atoms in the irradiated crystals were converted to ^{18}F by the reaction $^{16}O + {}^{3}He \rightarrow {}^{18}F + p$. ^{18}F is positron emitter ($t_{\frac{1}{2}} = 110$ min), and its activity was measured by coincidence counting of γ-pairs produced by annihilation of emerging positrons. To obtain a quantitative estimate of oxygen initially present in the sample, this activity was compared with that of a standard material (pure quartz in these experiments)

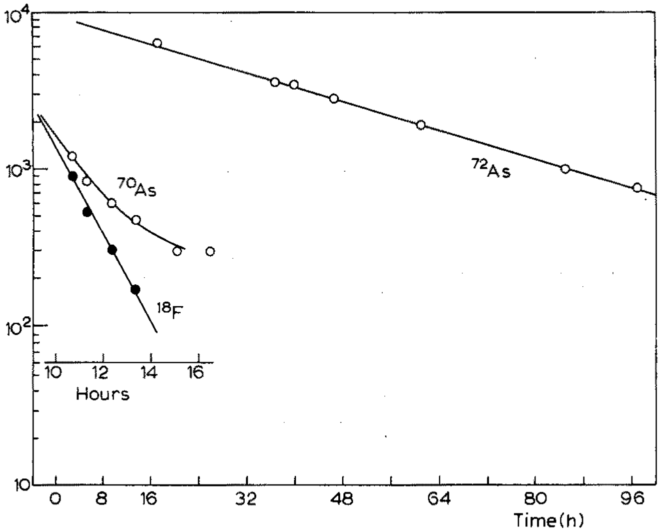

Fig. 1. Decay curves showing arsenic production from gallium phosphide.

whose oxygen content was known and which was irradiated under the same conditions as the sample. Precautions were taken to minimize errors which might arise from the irradiation of oxygen contained in surface impurities and of recoiled oxygen nuclei driven from the surface into the lattice during bombardment[4].

In the case of silicon, the irradiated single crystals were examined for activity with no treatment other than the removal of a thin surface layer. Irradiated single crystals of gallium phosphide, however, required careful chemical separation (after similar surface etching) in order to remove ^{70}As and ^{72}As nuclides formed by irradiation of the gallium in the material. These nuclides also are positron emitters ($t_{\frac{1}{2}} = 52$ min and 26 h, respectively) and their activities are generally higher than that of ^{18}F by many orders of magnitude. Figure 1 illustrates these activities and demonstrates the absolute necessity for chemical separation.

Sample mounting and ^{3}He activation

Samples in the form of crystalline wafers were mounted on a 1.5-in diameter brass disc, covered with 2 mil tantalum foil, and kept with fixed geometry during a 10-min bombardment by ^{3}He doubly charged ions at a beam intensity of 1 μA. The collimated beam size was of about 0.25 in diameter, and the target was water-cooled during the irradiation. The ^{3}He beam was monitored in each irradiation by a beam integrator and intensities for all of the samples were normalized. Irradiated samples were removed at the end of the bombardment, etched to remove surface contamination and, where necessary, subjected to chemical separation.

Etching

To ensure the removal of ^{18}F atoms produced from surface oxygen and from recoiled oxygen nuclei near the surface, a well-controlled method is required for removing thin surface layers from the irradiated crystals before activities are measured. For this purpose, chemical etches were used as follows.

Gallium phosphide was etched after bombardment in chlorine-saturated methanol–water (20 ml of methanol + 5 ml of water) for 3 min to remove what was estimated gravimetrically to be a 10-μm layer from the surface. The samples were then washed with distilled water and absolute alcohol, and were ready for chemical separation.

Silicon crystals were etched in 50 ml of a 1 + 20 mixture of concentrated hydrofluoric and nitric acids for 10 min with rotation of the 250-ml Teflon beaker at about 15 r.p.m. This removed a *ca.* 10-μm thick layer from the surface. The sample was washed with distilled water, and was then ready for counting since no chemical separation was required.

It is convenient at this point to mention briefly a series of experiments carried out with silicon single crystals to determine how thick a layer should be removed before activities are measured. Figure 2 shows the activities of irradiated crystals measured after stepwise removal of surface layers by etching; clearly the activity attains an almost constant level after a 10-μm layer has been removed. Figure 3 shows the dependence of ^{18}F activity upon the penetration depth in a silicon crystal irradiated with a 10-MeV beam of ^{3}He particles. Successive layers of the crystals were removed by etching and activities were determined in the etch solutions. (The activities shown have been normalized to zero time.) From these results it is concluded that the apparent oxygen levels in the surface layer are indeed anomalously high, but attain "normal" values at depths below 10 μm. According to Steward's calculation[4], the maximum recoil energy of ^{18}F by 14-MeV ^{3}He ions is about 2.1 MeV, and the penetration depth in silicon is about 3 μm. Below the surface, the production of ^{18}F increases gradually to a maximum at a depth of 100 μm, falling off steeply thereafter. Removal of a 10-μm layer by the etching technique described above is clearly sufficient to overcome uncertainties caused by surface contamination while decreasing the overall activity of the

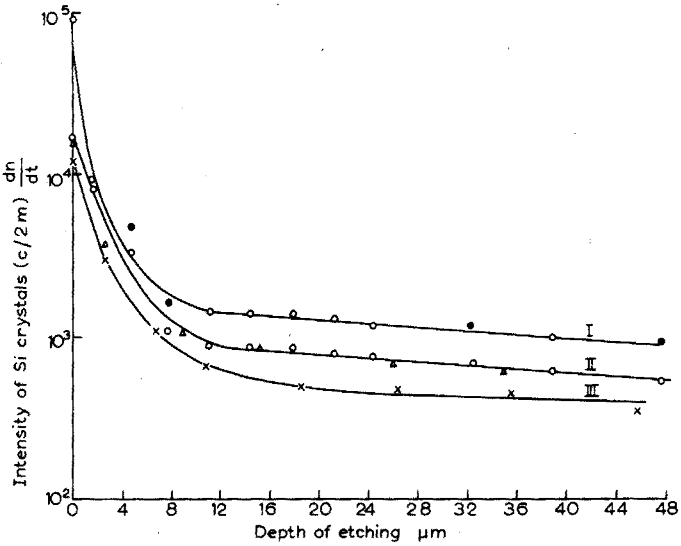

Fig. 2. Surface oxygen contamination and required depth of etch. (I) Silicon crystal #602830, (II) Texas Corp. (△: repeat measurements), (III) Dow Corning.

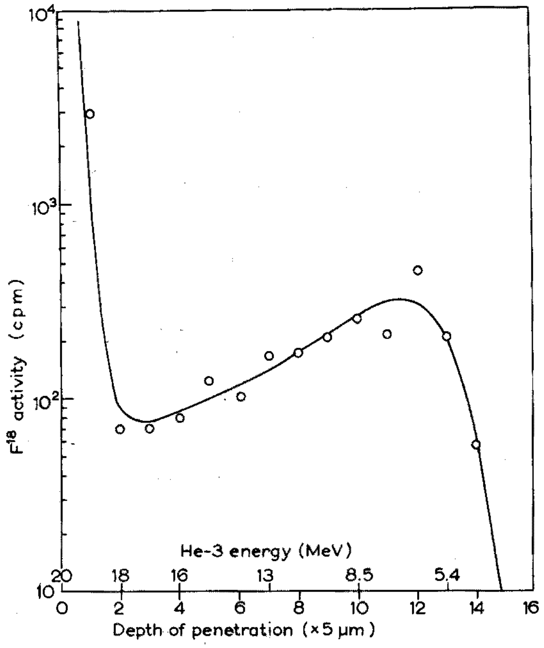

Fig. 3. Dependence of fluorine-18 production on penetration depth of ^3He in silicon.

sample by less than 10%. Similar considerations indicate that removal of a 10-μm layer from gallium phosphide crystal achieves the same result.

With either of the materials considered, errors caused by small variations in the thicknesses removed by the etchant are small, provided (*a*) that all effects caused by surface contamination are erased, and (*b*) that the etchant attacks the surface fairly uniformly. Examination of etched surfaces by optical microscopy and by scanning electron microscopy showed a moderate density of relatively shallow etch pits (< 1 μm deep). More important, it showed no indication of asperities corresponding to surface material resistant to the etch. (Figure 2 already suggests freedom from difficulties of this kind.)

It must be emphasized that, although the etching procedure introduces errors, these are *small* and are all in the direction of giving *underestimates* of oxygen content.

Chemical separation of ^{18}F from irradiated and etched gallium phosphide crystals

Etched crystals of gallium phosphide were each immersed with the irradiated side up in a 100-ml beaker containing a known amount of fluoride carrier (33.3 mg F^- ml^{-1}) and 25 ml of absolute methanol saturated with chlorine. Chlorine gas was then slowly bubbled through the solution until all the activated layer was removed from the crystal; about 15–20 min were required for this operation. (No activity was observed in the remaining crystals.) The methanol solution was then transferred to a 100-ml distilling flask containing 1 ml of arsenic hold-back carrier (*ca.* 10 mg As^{5+} ml^{-1}) and 20 ml of water. A few small pieces of quartz and 20 ml of concentrated phosphoric acid were added gently to the flask and the fluoride was then steam-distilled as fluorosilicic acid. About 50 ml of distillate was collected after distillation at a fixed temperature of 135–140° for 30 min*. The distillate was added to a flask containing an excess of 3% lead acetate solution (pH 4–5) to precipitate the fluoride as lead chlorofluoride[5]. The pH adjustment is critical both for better recovery and cleaner separation. The precipitate was quickly cooled and filtered through a Millipore filter (47 mm diameter, 0.8 μm porosity). It was then ready for the measurement of radioactivity.

In order to estimate the proportion of fluoride carried over in distillation, the lead chlorofluoride precipitate, after counting, was redissolved in 2 *M* nitric acid, and a known (excess) amount of silver nitrate was added to precipitate silver chloride. Excess of silver was then titrated with 0.1 *M* thiocyanate solution, with iron(III) alum as indicator.

Radioactivity measurement

The separated precipitate from gallium phosphide was sandwiched in 3 mil aluminum foil and positioned between two 3 × 3 in NaI (Tl) scintillation crystals equipped with an ORTEC overlap coincidence unit for the detection of pairs of 0.511-MeV annihilation γ-rays emitted in opposite directions by decaying ^{18}F nuclei. Two single-channel analyzers were used for energy discrimination and timing of the event. Etched specimens of irradiated silicon were similarly sandwiched between the scintillation crystals for the measurement of their activities.

The decay of ^{18}F was followed about every 30 min for three half-lives to make sure that all the activity was from this species.

Calculation of results

The measured radioactivity of a given sample was compared with that of a pure quartz standard which had been irradiated under the same conditions. Since the specimens were always thicker than the penetration depth of the activating ^{3}He particles these activities are related by the equation[6]

$$\frac{A_x}{A_s} = \frac{N_x I_x R_x}{N_s I_s R_s}$$

where *A* denotes measured activity at a given time after irradiation, *N* the number of ^{16}O nuclei per mg of sample, *I* the beam current during irradiation, and *R* the range of bombarding ^{3}He particles in the specimen; subscripts x and s refer throughout to sample and standard, respectively. The quantity N_s and the ranges R_x and R_s are all known[7], hence N_x may readily be computed.

RESULTS AND DISCUSSION

Results obtained from gallium phosphide crystals grown by a variety of methods are listed in Table I. The lowest oxygen content (*ca.* 10^{18} atoms cm^{-3}) was observed in undoped solution-grown crystals (polycrystalline gallium phosphide melted with gallium metal at 1300° under vacuum and cooled slowly). Oxygen contents were

---

* The distillation temperature should be kept lower than 140° and the steam generator requires a tall (18-in) air vent to prevent overflow of boiling water caused by abrupt and rapid heating.

TABLE I

OXYGEN CONTENTS OF GALLIUM PHOSPHIDE SINGLE CRYSTALS
(Duplicate determinations were made in each case)

Preparation of sample	*Count rate*[a] *(c.p.m.)*	*Chemical recovery (%)*	*Oxygen*[b] *(atoms cm^{-3})*
I. Halogen transport	150	68.0	$9 \cdot 10^{17}$
	160	71.0	$8 \cdot 10^{17}$
II. Solution growth	80	55.0	$5 \cdot 10^{17}$
	90	50.0	$6 \cdot 10^{17}$
III. Wet hydrogen transport, $P_{H_2O} = 1.9$ torr	1320	49.0	$5 \cdot 10^{18}$
	1020	48.0	$4 \cdot 10^{18}$
IV. Wet hydrogen transport, $P_{H_2O} = 1.6$ torr	1025	60.0	$4 \cdot 10^{18}$
	1600	57.0	$6 \cdot 10^{18}$
V. Solution growth (oxygen-doped)	4000	48.5	$2 \cdot 10^{19}$
	4800	53.4	$2 \cdot 10^{19}$

[a] Each irradiation was for 10 min with a beam current of 1 μA.

[b] Based upon $4.65 \cdot 10^{22}$ atoms cm^{-3} of oxygen in SiO_2, and upon a ratio of ranges of ^3He in SiO_2 and GaP of 0.748.

only slightly higher in crystals prepared by halogen transport. That these various crystals should contain relatively small proportions of oxygen is consistent with the exclusion of oxygen, except as a trace contaminant, during their growth. Crystals grown from the vapor with wet hydrogen transport according to the reaction scheme[8]:

$$2\ \text{GaP (polycrystalline)} + H_2O \xrightarrow{1100^\circ} Ga_2O(g) + H_2 + P_2$$

$$H_2 + Ga_2O + P_2(g) \xrightarrow{\text{cool}} 2\ \text{GaP (single crystal)} + H_2O$$

contain appreciably higher amounts of oxygen, which is not unexpected since oxygen is involved in the reaction. Finally, the largest oxygen contents ($2 \cdot 10^{19}$ atoms cm^{-3}) were observed in oxygen-doped solution-grown crystals.

The reproducibility of repeated measurements on the same crystals prepared in the same way is good, and suggests that the method is reliable. Indirect support for this view is provided by results obtained on crystals of silicon (Table II). Repeated determinations here indicate reproducibility to better than 20%, and measured oxygen contents agree reasonably well with the measurements by Baker[9] on the basis of infrared absorption analysis. ^3He activation experiments on silicon crystals by Aleksandrova *et al.* show similar agreement with infrared data[10].

The results reported in Table I may now be compared with representative data accumulated for gallium phosphide crystals by other methods of analysis. Comparison shows that in order of magnitude, the present oxygen contents are in fair agreement with those obtained by vacuum fusion gas analysis and by fast neutron activation. They are considerably higher, however, than the value of 10^{17} atoms cm^{-3} estimated from the solubility of oxygen in gallium phosphide as determined from electrical conductivities[3]. Disagreement is even more marked with results obtained by mass spectrometry. However, these disagreements may be more apparent than real, because the electrical measurements were sensitive only to substitutional oxygen, and because subsidiary mass spectrometric measurements of metal–oxygen ratios in Ga_2O_3 gave

TABLE II

OXYGEN CONTENTS OF SILICON SINGLE CRYSTALS

Sample	*Source*	*^{3}He activation (p.p.m. atomic)*					*Infrared absorption*[a] *(p.p.m. atomic)*
Texas (pulled)	Texas Instruments	11	12	12	10	12	—
605574	Dow Corning	—	16	—	16	20	22
602830	Dow Corning	26	—	—	27	30	35
699549	Dow Corning	—	13	—	15	16	17
89	Dow Corning	12	—	—	12	15	18
607058	Dow Corning	20	—	22	22	24	25
MONEX 24–21	Bell Labs						
#1	Bell Labs	7	8				
#2	Bell Labs	8	9				
#3	Bell Labs	5	4				
R–4	Bell Labs	31	32				
R–5	Bell Labs	36	35				
Dow 100137	Dow Corning					3	
NASA #3	NASA					18	
NASA #7	NASA					0.4	

[a] Results obtained by Baker[9].

strong indications of a troublesome and as yet unexplained interference which could result in underestimation of oxygen by up to two orders of magnitude[2]. The ^{3}He activation results are believed to be accurate and this implies that the total oxygen contents of gallium phosphide crystals examined exceeds by more than an order of magnitude the amount held substitutionally in the lattice. However, the identification and estimation of impurities in crystals of gallium phosphide is a difficult problem and further work is required.

The author thanks L. Luther for stimulating interest in this problem and for supplying the gallium phosphide crystals studied; J. S. Laughlin, Sloan Kettering Institute, for the use of the cyclotron; J. Mamacos, R. Tilbury and their associates for their kind help in sample irradiation; C. J. Frosch and D. L. Malm for permission to quote unpublished work; W. L. Brown and his associates for assistance in penetration depth studies of the helium beam; and F. A. Trumbore and H. D. Keith for critical readings of the manuscript.

SUMMARY

A method is described for determining small concentrations of oxygen in single crystals of gallium phosphide; 14-MeV ^{3}He particles were used to convert ^{16}O into ^{18}F, which was then separated from other radioactive nuclides produced by bombardment of gallium. Coincidence counting of γ-pairs produced by annihilation of emitted positrons was then used. Thin surface layers were removed from the crystals after irradiation to avoid interference from surface contamination and from recoiled oxygen nuclei driven into the lattice during bombardment. Results are reproducible and appear to be accurate to within 20%. Observed oxygen levels in gallium phosphide single crystals varied from about $5 \cdot 10^{17}$ atoms cm^{-3} in specimens prepared by solution growth or halogen transport, to about $5 \cdot 10^{18}$ atoms cm^{-3} in specimens prepared by wet hydrogen transport, $2 \cdot 10^{-19}$ atoms cm^{-3} in oxygen-doped solution-grown crystals.

RÉSUMÉ

On décrit une méthode pour le dosage de faibles concentrations d'oxygène dans des cristaux simples de phosphure de gallium. Les particules 14-MeV ^{3}He sont utilisées pour transformer ^{16}O en ^{18}F; ce dernier est ensuite séparé d'autres nuclides radioactifs produits par bombardement du gallium. On mesure sa radioactivité par comptage des paires produites par annihilation des positrons émis. Les résultats sont reproductibles et précis.

ZUSAMMENFASSUNG

Es wird eine Methode für die Bestimmung kleiner Konzentrationen Sauerstoff in Galliumphosphid-Einkristallen beschrieben. Mittels ^{3}He-Teilchen von 14 MeV wurde ^{16}O in ^{18}F umgewandelt, welches dann von anderen, aus Gallium entstandenen radioaktiven Nukliden abgetrennt wurde. Dann wurde eine Koinzidenzzählung der durch Vernichtung der emittierten Positronen erzeugten γ-Paare durchgeführt. Dünne Oberflächenschichten wurden nach der Bestrahlung von den Kristallen entfernt, um eine Störung durch Oberflächenkontamination durch zurückgestossene Sauerstoffkerne, die während der Bestrahlung in das Gitter gelangten, zu vermeiden. Die Ergebnisse sind reproduzierbar und scheinen innerhalb 20% richtig zu sein. Die beobachteten Sauerstoffgehalte in Galliumphosphid-Einkristallen betrugen etwa $5 \cdot 10^{17}$ Atome cm^{-3} in Proben, die in Lösung gewachsen waren oder durch Transport mit Halogen erhalten worden waren, etwa $5 \cdot 10^{18}$ Atome cm^{-3} in durch Wasserstofftransport erhaltenen Proben und $2 \cdot 10^{19}$ Atome cm^{-3} in sauerstoffdotierten, in Lösung gewachsenen Kristallen.

REFERENCES

1 C. J. Frosch, Bell Telephone Laboratories, Murray Hill, N. J., personal communication, 1968.
2 D. L. Malm, Bell Telephone Laboratories, Murray Hill, N. J., personal communication, 1968.
3 L. M. Foster and J. Scardefield, *J. Electrochem. Soc.*, 116 (1969) 494.
4 P. G. Steward, *Lawrence Radiation Laboratory Report UCRL-18121* (Ph.D. Thesis), 1965.
5 I. M. Kolthoff and P. J. Elving, *Treatise on Analytical Chemistry*, Part II, Vol. 7, John Wiley, 1961, p. 257.
6 E. Ricci and R. L. Hahn, *Anal. Chem.*, 37 (1965) 742.
7 C. F. Williamson, J. P. Boujot and J. Picard, *Rapport CEA-R 3042*, 1966.
8 L. Luther, Bell Telephone Laboratories, Murray Hill, N. J., personal communication, 1968.
9 J. Baker, Dow Corning Corp., Hemlock, Mich., personal communication, 1968.
10 G. I. Aleksandrova *et al.*, *At. Energ. U.S.S.R.*, 23 (1967) 106.

Analytica Chimica Acta
Elsevier Publishing Company, Amsterdam
Printed in The Netherlands

A NEW TYPE OF LEAD(II) ION-SELECTIVE CERAMIC MEMBRANE ELECTRODE

HIROSHI HIRATA AND KENJI HIGASHIYAMA
Wireless Research Laboratory, Matsushita Electric Industrial Co., Ltd., Kadoma, Osaka (Japan)

(Received 29th December 1970)

Many studies have recently been made of ion-selective electrodes[1]. A lead(II)-sensitive solid-state electrode has been developed by Orion Research Inc., where the membrane is a compacted disc of active material consisting of lead sulfide with silver sulfide[1]; its method of preparation is, however, not apparent from the literature.

Only one electrode membrane based on insoluble metal sulfide or a mixture of metal sulfides, seems so far to have been prepared by a sintering method, although halide ion-selective electrode membranes have been made by casting silver halides[1] and also by hot-pressing a mixture of silver halide and powdered thermoplastic polymer[2]. Recently, a ceramic copper(I) sulfide electrode membrane was introduced for copper(II)[3]; this electrode has been found to have several excellent properties, such as short response time, reproducible potential stability and very long life-time.

The present study was undertaken in order to produce a lead-sensitive ceramic electrode membrane by sintering a mixture of lead, silver and copper(I) sulfides. These electrodes yielded a Nernstian response to lead ion activity in the absence of interferences, and their sensitivities, their response rates to different concentrations, their life-times and their behavior in the presence of other ions were also entirely satisfactory.

The performance of these electrodes when different proportions of the metal sulfides were used, is described below.

EXPERIMENTAL

Apparatus

An Orion Model 801 digital pH meter was used to make the potentiometric measurements. A Horiba Seisakusho 2530-05T calomel reference electrode was used.

An electric furnace, made in the laboratory, served for the preparation of raw materials and sintered tablets in a quartz tube of 1 m length and 100 mm diameter, at a constant flow rate of a gas stream adjusted by a flow meter (0–1 l min^{-1}). The hot-press apparatus consisted of a small electric furnace with an oil-damped press (compression power, *ca.* 14 ton cm^{-2}); this was also made in the laboratory, and made it possible to sinter tablets of 30 mm diameter and 10 mm thickness in a silicon carbide mold at a maximum temperature of 800°.

Chemicals

All chemicals were analytical reagent-grade and were used without further purification. Stock solutions of lead nitrate were prepared by dissolving lead nitrate in distilled water, and were stored in polyethylene reagent bottles. A series of standard solutions for lead ion was prepared by suitable dilution of the stock solution, keeping the ionic strength at 0.1 *M* by addition of appropriate volumes of 1 *M* sodium nitrate solution. All solutions were prepared from water which had been both deionized and distilled.

Preparation of raw materials for making membrane

Preparation of raw materials can be divided roughly into the following two methods. The *precipitation method* depended on bubbling hydrogen sulfide through an aqueous solution of lead, silver or copper(I) nitrate to precipitate PbS, Ag_2S or Cu_2S, respectively. The *direct reaction method* involved the reaction of the corresponding metal powder with sulfur to produce the metal sulfide; lead sulfide was obtained by heating a mixture of lead powder and sulfur in the molar ratio 1:1, at 500° for 1 h in an atmosphere of hydrogen sulfide, whereas silver sulfide or copper(I) sulfide was prepared by solid reaction of silver or copper with sulfur in the molar ratio 2:1 at 500° for 1 h in a nitrogen stream. Each sulfide produced was ground to give a particle size of less than 10 μm, and was analysed by means of emission spectroscopy and X-ray diffractometry.

Preparation of membrane

The desired amounts of lead, silver and copper(I) sulfides were mixed thoroughly and compressed at a pressure of 10 ton cm^{-2} so as to form a tablet with a diameter of 15 mm and a thickness of 2–3 mm (compressed membrane). Then, the tablet was sintered at 350–500° for 3 h in a stream of hydrogen sulfide at 50–100 ml min^{-1} (sintered membrane). Other tablets containing the same components as the compressed membrane (20 mm in diameter and 5–7 mm in thickness) were prepared by hot-pressing at 350–450° for 2 h in a silicon carbide mold under a pressure of 3–7 ton cm^{-2} (hot-pressed membrane). After the tablets had been set in the electrode bodies, their surfaces were polished with diamond paste and washed with an ultrasonic cleaner.

Measurement of potentials

The cross-section of the lead ion-sensitive membrane electrode was quite similar to that of the copper(I) sulfide ceramic electrode previously described. A leading wire could be fastened directly to the inside surface of the ceramic membrane to yield a completely solid-state electrode and the membrane was sealed in the bottom of a plastic tube, so that an internal electrode and an internal reference solution were eliminated.

The potentials developed by the membrane electrode in the test solution were measured with a saturated calomel electrode as the reference electrode at 25.0±0.1°. The construction of the experimental cell can be represented as

Ion-selective electrode	Test solution $\mu = 0.1$ *M* ($NaNO_3$)	0.1 *M* $NaNO_3$	Saturated calomel electrode

The potential of the cell *E* is given by

$$E = \text{constant} + 2.303 \frac{RT}{2F} \log a_{Pb^{2+}}$$

where the "constant" is the sum of the potentials at the leading wire–membrane contact interface, at the liquid junction between the reference electrode and the test solution, and in the saturated calomel electrode, and the potential across the membrane when the lead ion activity in the test solution is unity. By the slope of the straight line of E *vs.* $\log a_{Pb^{2+}}$ and the concentration range for obedience to Nernst's law, the validity of the electrode membrane was evaluated.

All samples and standardizing solutions were stirred at a fixed rate to insure good reproducibility. Electrode potentials were attained rapidly, and in every case the equilibrium potentials were read within about 1 min after immersion of the electrode into the test solution.

RESULTS AND DISCUSSION

Comparison of methods for preparation of membrane

From the above methods used for the preparation of raw materials and electrode membranes, except the hot-pressing method, four methods for making membranes were considered:

1. a mixture of sulfides obtained by the precipitation method was compressed;
2. a mixture of sulfides prepared by the direct reaction method was compressed;
3. a tablet prepared as in (1) was heated at 400° for 3 h in an atmosphere of hydrogen sulfide;
4. a tablet prepared as in (2) was sintered under the same conditions as method (3).

Initially, membranes prepared by these methods from 30% lead sulfide and 70%

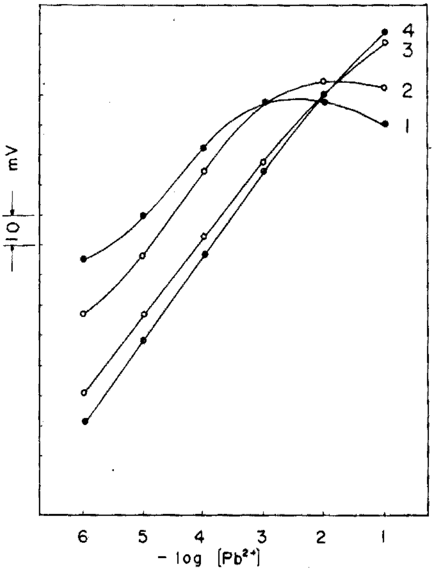

Fig. 1. Potential *vs.* concentration curves for membranes prepared by different methods. The numbers correspond to the preparative method (1), (2), (3), or (4) in the text.

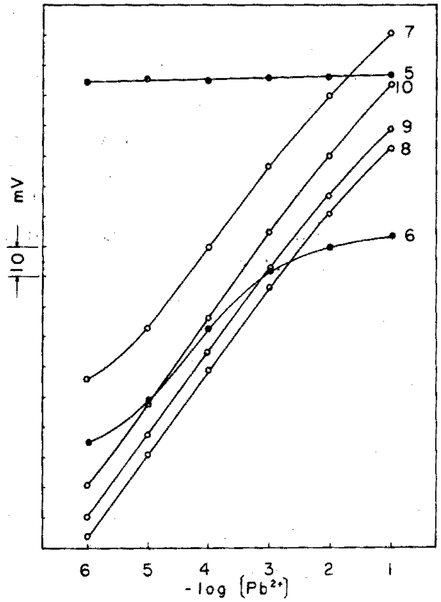

Fig. 2. Effect of addition of silver sulfide. Content of Ag_2S: (5) none, (6) less than 0.01%, (7) 1%, (8) 20%, (9) 50%, (10) 83%.

silver sulfide by weight were compared with each other, because the addition of copper(I) sulfide was supposed not to be essential for the functioning of the electrode, as will be described later. The potential *vs.* concentration curves for these membranes are given in Fig. 1. It can be seen that the potential change for each log $[Pb^{2+}]$ unit with the membranes obtained by the direct reaction method was greater than that by the precipitation method whether the membranes were compressed or sintered. However, the compressed membranes gave smaller potential changes than the sintered ones and also gaves erratic results in solutions stronger than 10^{-3} mol l^{-1}. The sintered membrane prepared by method (4) seemed quite suitable for analytical utilization; it exhibited about a 29.5-mV change in potential per log $[Pb^{2+}]$ unit at 25° and a Nernstian slope was obtained over a concentration range of 10^{-1}–10^{-6} mol l^{-1}. Lead(II) could be determined from 10^{-1} to 10^{-7} mol l^{-1}. The sintered membrane electrode responded more rapidly than the compressed one.

Effect of incorporation of silver sulfide

In an attempt to study the mechanism of the electrode membrane, various kinds of sintered membranes containing lead sulfide alone and mixed with the other metal sulfides were examined.

Ceramic membranes proved inert to lead ion unless silver sulfide was added. For example, a lead sulfide membrane containing copper(I) sulfide was not responsive to lead ion at all, despite the high-density ceramic.

A pure lead sulfide membrane, in which no trace of silver could be detected by emission spectroscopy, did not respond to lead ion, but an impure lead sulfide membrane containing less than 0.01% (w/w) of silver was rather more sensitive than a pure one (Fig. 2). Figure 2 also shows that a membrane containing 1% of silver sulfide showed a potential change of 27 mV for each tenfold change in the lead ion activity, and is satisfactory over the range 10^{-1}–10^{-5} mol l^{-1} of lead(II). When more than 1% of silver sulfide was added, the Nernstian formula was strictly applicable to the electrode membrane down to lower levels than 10^{-5} mol l^{-1} of lead(II).

These results suggest that this membrane is an ionic conductor in which charge is transferred by the movement of silver ions, but the potential is determined indirectly by the availability of sulfide ions. This availability is fixed by the activity of the divalent metal in contact with the membrane as suggested for a silver sulfide–copper(II) sulfide solid-state membrane electrode[1]. Nevertheless, a silicone rubber-membrane electrode impregnated with very pure lead sulfide is readily sensitive to lead ion without any trace of silver sulfide[4]. Silicone rubber is regarded as an inactive binder and the behavior of both the compacted and silicone rubber-impregnated types of electrode, as described by Pungor, can be interpreted in the same way, thus it may be undesirable to discriminate between solid-state and silicone rubber-membrane electrodes theoretically[5]. However, from the above results, any preconceived notions of mechanism of their functions should not be included in discussing the difference between the ceramic and the silicone rubber-impregnated membrane electrodes. Further investigations were not carried out in the present study.

Effect of addition of copper(I) sulfide to the lead sulfide–silver sulfide system

Some pores on the membrane surface caused a slow response to changes in ion concentration. In order to prepare a more compacted ceramic membrane without any pores, copper(I) sulfide was added to a mixture of lead and silver sulfides and the hot-press method was applied; the required amount of lead, silver and copper(I) sulfides was mixed, compressed, and hot-pressed at 300 ~500° under a pressure of 3–7 ton cm^{-2} for 2 h, and then left to cool. With these membranes potentiometric measurements were also made. Potential *vs.* concentration curves for the various ratios of lead sulfide–silver sulfide–copper(I) sulfide membranes prepared under the same conditions were obtained (Fig. 3). The membrane containing more than 30% of copper(I) sulfide did not obey the Nernstian law, while addition of less than 30% of copper(I) sulfide brought about responses similar to those of lead sulfide membranes containing only silver sulfide; however, the response time of the membranes containing 5–20% of copper(I) sulfide was 2/3–1/2 that of the PbS–Ag_2S membranes.

The density of a hot-pressed membrane was much greater than that of a membrane sintered at atmospheric pressure and no pores in the hot-pressed membranes could be observed by the naked eye. As the microscope photographs in Fig.4 show, black spots, which are produced by pores of a membrane surface on the photo-

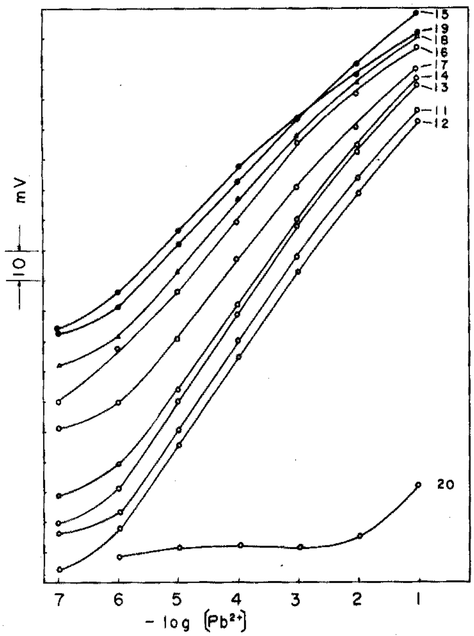

Fig. 3. Potential *vs.* concentration curves for various ratios of the lead sulfide–silver sulfide–copper(I) sulfide system.

No. of curve	*PbS* (%*w*/*w*)	Ag_2S (%*w*/*w*)	Cu_2S (%*w*/*w*)
11	30	70	0
12	30	65	5
	30	60	10
14	30	50	20
15	30	40	30
16	30	30	40
17	30	20	50
18	30	10	60
19	30	5	65
20	30	0	70

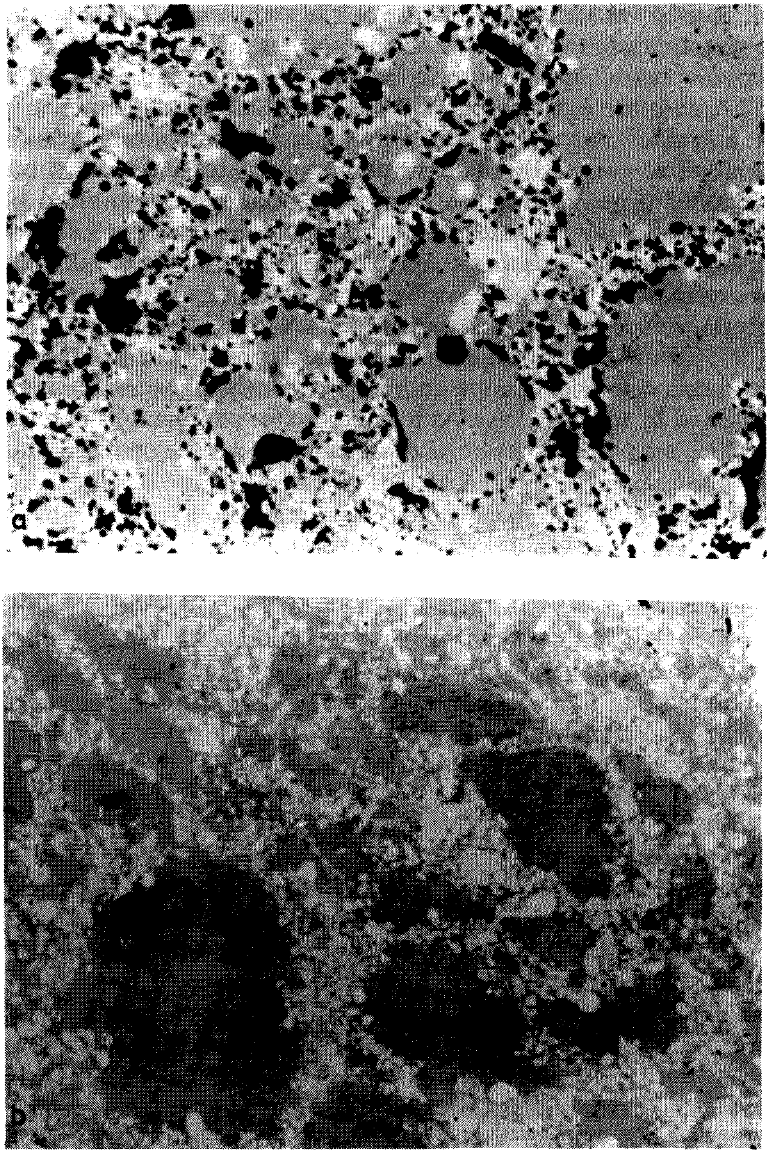

Fig. 4. Microscope photographs of sintered membrane surface. (a) Sintered at atmospheric pressure; (b) hot-pressed.

graph of a hot-pressed membrane, are much fewer than those found in membranes sintered at 760 mm Hg.

It was also shown by X-ray diffraction patterns that lead sulfide in a ceramic membrane did not produce a solid solution with silver sulfide or copper(I) sulfide. From these results, the fine structure of a sintered membrane sensitive to lead ion seems to have a number of lead sulfide grains dispersed in a solid solution of silver sulfide or silver and copper(I) sulfides. However, the operation of these electrodes is by no means fully understood. A mechanism involving adsorption and ion exchange at the interface between a lead sulfide grain and a test solution is usually invoked, but the transportation of charges from a lead ion to a silver ion in the ceramic membrane is not clear.

When the membranes contain 30, 50, and 80% of lead sulfide, the slopes of the corresponding calibration curves, as depicted in Fig. 5, are similar to each other; calibration curves for membranes containing less than 1% of lead sulfide show marked deviations from the Nernstian slope. The less the lead sulfide content, the longer the response time; the response of electrode membranes containing less than 5% of lead sulfide was extremely slowed down.

The authors thank Dr. S. Kisaka and Dr. K. Sugihara for their encouragement in this work. Thanks are also due to Mr. T. Miyazawa and Mr. H. Yamao for X-ray analysis and microscope photographs of the electrode membrane.

SUMMARY

A new type of lead ion-selective membrane electrode has been developed by a sintering method, and a hot-pressing method. These ceramic membranes consist of PbS–Ag_2S–Cu_2S systems. Nernstian response to lead ion activity was obtained over a concentration range of 10^{-1}–10^{-6} *M* and the analytical range was 10^{-1}–10^{-7} *M*,

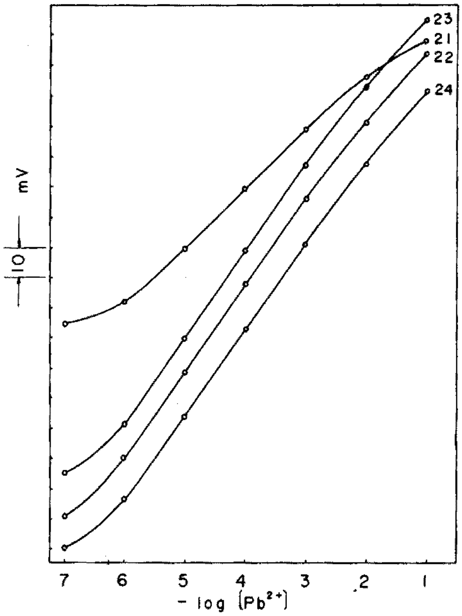

Fig. 5. Calibration curves of membranes containing 1, 30, 50 and 80% (w/w) of lead sulfide.

No.	*PbS*	*Ag_2S*	*Cu_2S*
21	1	94	5
22	30	65	5
23	50	40	10
24	80	16	4

when the membrane contained less than 30% of copper(I) sulfide and more than 1% of lead sulfide. The response time of the membrane containing 5–20% of copper(I) sulfide was 2/3–1/2 of that of PbS–Ag_2S membrane.

RÉSUMÉ

Un nouveau type d'électrode de plomb, à membrane, est proposé. Ces membranes céramiques sont constituées par le système PbS–Ag_2S. La réponse nernistienne à l'activité ionique du plomb est possible de 10^{-1} à environ $10^{-6}M$; le domaine analytique va de 10^{-1} à $10^{-7}M$ avec une membrane contenant moins de 30% de sulfure de cuivre(I) et plus de 1% de sulfure de plomb. Le temps de réponse de la membrane contenant 5 à 20% de sulfure de cuivre(I) est de $\frac{2}{3}$–$\frac{1}{2}$ de celui de la membrane PbS–Ag_2S.

ZUSAMMENFASSUNG

Es wurde ein neuer Typ einer bleiionenselektiven Membranelektrode nach einer Sintermethode und einer Pressmethode unter Anwendung von Wärme hergestellt. Diese keramischen Membranen bestehen aus PbS–Ag_2S–Cu_2S-Systemen. Die Elektrode zeigte Nernstsches Verhalten gegenüber der Bleiionenaktivität im Konzentrationsbereich 10^{-1}–10^{-6} M; der analytische Bereich war 10^{-1}–10^{-7} M, wenn die Membran weniger als 30% Kupfer(I)-sulfid und mehr als 1% Bleisulfid enthielt. Die Ansprechzeit der Membran mit 5–20% Kupfer(I)-sulfid betrug $\frac{2}{3}$–$\frac{1}{2}$ derjenigen der PbS–Ag_2S-Membran.

REFERENCES

1 R. A. DURST (Editor), *Ion-selective Electrodes*, N.B.S. Spec. Publ. 348, U.S. Printing Office, Washington, 1970.
2 M. MASCINI AND A. LIBERTI, *Anal. Chim. Acta*, 47 (1969) 399.
3 H. HIRATA, K. HIGASHIYAMA AND K. DATE, *Anal. Chim. Acta*, 51 (1970) 209.
4 H. HIRATA AND K. DATE, *Anal. Chem.*, 43 (1971) 279.
5 E. PUNGOR AND K. TÓTH, *Anal. Chim. Acta*, 47 (1969) 291.

Analytica Chimica Acta
Elsevier Publishing Company, Amsterdam
Printed in The Netherlands

ETUDE DE L'EXTRACTION DE L'ACIDE CHLORHYDRIQUE ET DU TRICHLORURE D'ANTIMOINE EN SOLUTION CHLORHYDRIQUE PAR LE TRIBUTYLPHOSPHATE EN SOLUTION DILUEE DANS LE SULFURE DE CARBONE

G. ROLAND ET G. DUYCKAERTS
Laboratoire de Chimie Analytique, Université de Liège au Sart Tilman, B-4000 Liège (Belgique)

(Reçu le 31 décembre 1970)

Dans un travail antérieur[1], nous avons étudié par spectrométrie infra-rouge les associations dans le sulfure de carbone entre le tributylphosphate (TBP) et le trichlorure d'antimoine, en l'absence d'eau et d'acide, et nous avons mis en évidence l'existence simultanée de deux complexes de stoechiométries respectives 1:1 ($TBP \cdot SbCl_3$) et 2:1 ($(TBP)_2SbCl_3$). La stabilité relativement élevée des entités dans ce solvant nous a amenés à penser que ce milieu pouvait présenter des propriétés intéressantes pour l'extraction du trichlorure d'antimoine.

La possibilité d'extraire le trichlorure d'antimoine par le TBP est connue depuis quelques années[2-7] mais peu de travaux ont été consacrés à l'extraction de ce sel. D'après Khorasani[6], la stoechiométrie du complexe extrait lors du traitement d'une phase aqueuse chlorhydrique contenant $SbCl_3$ en dose traceur par le TBP pur ou par une solution diluée de TBP dans l'éther de pétrole serait 2:1, ce rapport TBP: $SbCl_3$ étant confirmé dans un travail ultérieur par Khorasani et Hakim[7]. Selon Khorasani[6], il n'y aurait aucune interaction entre l'acide chlorhydrique et l'antimoine trivalent qui serait extrait sous forme de $SbCl_3$ et le coefficient de distribution serait maximum pour une concentration en acide chlorhydrique en phase aqueuse de 3.69 M.

Avant d'aborder l'étude de l'extraction de $SbCl_3$, il était nécessaire d'étudier l'extraction de l'acide chlorhydrique dont la présence s'avère indispensable pour éviter l'hydrolyse de $SbCl_3$ en phase aqueuse.

De très nombreux travaux ont déjà été consacrés à l'étude de l'extraction des acides "forts" en solution aqueuse par le TBP pur ou en solution et s'il existe actuellement de nombreuses données thermodynamiques et physico-chimiques très précises, la stoechiométrie, la structure et les constantes d'équilibre des complexes formés entre le TBP et les acides minéraux demeurent très mal connues.

Plusieurs formules ont déjà été proposées pour caractériser les entités formées en phase organique mais elles ne peuvent être acceptées que sous certaines réserves: ces formules sont souvent déduites de l'analyse chimique ou physico-chimique de la phase organique et la composition de la solution déterminée par ces méthodes ne peut nous renseigner sur la nature des composés formés que s'il n'y a qu'un seul composé en solution. En réalité, il est fort probable, surtout pour les fortes concentrations en TBP, qu'il y ait plusieurs complexes présents simultanément en solution et la stoechiométrie proposé ne représenterait, dans ce cas, que la stoechiométrie moyenne des différents complexes.

L'extraction de l'acide chlorhydrique par le TBP a été étudiée par plusieurs auteurs[8-24] mais, à notre connaissance, les constantes d'équilibre des complexes formés en phase organique n'ont été déterminées que pour le système TBP–H_2O–HCl dans le CCl_4. Dans ce solvant, Mitamura *et al.*[21] ont établi que le complexe extrait en phase organique se formait suivant la réaction:

$$H^+_{aq} + Cl^-_{aq} + y\,H_2O_{aq} + TBP_{org} \overset{K}{\rightleftharpoons} TBPH^+ \cdot y\,H_2O \ldots Cl^-_{org}$$

la valeur de y variant entre 0.2 et 0.5 suivant la concentration en TBP; la constante de stabilité de ce complexe serait $\log K = -4.65 \pm 0.04$.

Il nous est apparu intéressant d'entreprendre une étude quantitative de l'extraction de $SbCl_3$ en tenant compte des principales réactions en phase organique susceptibles de modifier le coefficient de distribution.

PARTIE EXPÉRIMENTALE

Le sulfure de carbone (p.a.) a été distillé avant l'emploi.

Le TBP commercial a été traité par une solution de Na_2CO_3 à 10% puis lavé à l'eau distillée plusieurs fois avant d'être séché et distillé sous vide (pression de 1 mm de mercure environ).

$SbCl_3$ (p.a.) a été distillé deux fois sous vide partiel (environ 20 mm de mercure) dans un tube en U chauffé extérieurement par une résistance électrique.

Les concentrations des solutions initiales de TBP et de $SbCl_3$ on été déterminées soit par pesée directe en ballon jaugé, soit par dilutions des solutions stocks.

L'équilibrage des solutions a été réalisé en agitant 20.0 ml de la phase organique et 10.0 ml de la phase aqueuse pendant trois heures à une température de $25 \pm 0.1°$.

La concentration en acide chlorhydrique a été déterminée par titrage potentiométrique au moyen d'une solution de NaOH étalonnée par le biiodate potassique.

Le dosage de l'antimoine en phase organique a été effectué de la manière suivante: on pipette un volume compris entre 2 et 10 ml de phase organique qu'on introduit dans une ampoule à décanter contenant 20 à 30 ml de CCl_4 et 50 ml d'une solution environ 3 *M* en HCl. L'antimoine trivalent réextrait en phase aqueuse après agitation vigoureuse des deux phases est ensuite dosé par polarographie à impulsion (Southern Harwell MKII Pulse Polarograph), la concentration en antimoine(III) étant déterminée par la méthode de l'ajout dosé.

La concentration en antimoine(III) en phase aqueuse a été calculée par différence en tenant compte des volumes respectifs des phases en présence.

Les concentrations en chlorure ont été déterminées par titrage potentiométrique au moyen d'une solution 0.02 *M* en $AgNO_3$ après extraction des ions chlorure de la phase organique par une solution 0.1 *M* en NaF.

Les valeurs de l'activité de l'acide chlorhydrique en phase aqueuse ($a_{HCl} = [H^+]_{aq} \cdot [Cl^-]_{aq}\, y^2 \pm HCl$) ont été exprimées en fonction de la molarité de l'acide et calculées d'après *Electrolyte Solutions* de R.A. Robinson et R. H. Stokes (2nd Edn., Butterworth, London, 1959).

RÉSULTATS EXPÉRIMENTAUX ET DISCUSSION

Extraction de l'acide chlorhydrique

Pour chaque série d'expériences, nous avons maintenu la concentration en HCl constante dans la phase aqueuse et nous avons fait varier la concentration en TBP total ($[TBP]_t$) de 0.04 à 0.1 *M*. Les résultats expérimentaux obtenus en travaillant à trois activités différentes en acide dans la phase aqueuse sont rassemblés dans le Tableau I.

LEAU I

ACTION DE L'ACIDE CHLORHYDRIQUE

$]_{aq} = 6.55\ M$		$[HCl]_{aq} = 7.06\ M$		$[HCl]_{aq} = 7.43\ M$	
$^{P}]_t \cdot 10^2 (M)$	$[HCl]_t \cdot 10^3 (M)$	$[TBP]_t \cdot 10^2 (M)$	$[HCl]_t \cdot 10^3 (M)$	$[TBP]_t \cdot 10^2 (M)$	$[HCl]_t \cdot 10^3 (M)$
	1.09	4.39	1.90	4.39	2.66
	1.22	5.01	2.20	5.02	2.99
	1.34	5.64	2.47	5.65	3.34
	1.50	6.27	2.83	6.28	3.69
	1.62_5	6.89	2.94	6.91	4.14
	1.82	7.52	3.30	7.53	4.39
	1.93_5	8.15	3.42	8.16	4.97
	2.06	8.77	3.73	8.79	5.16
		9.40	4.06	9.15	5.65
				10.00	6.03

Si nous portons en graphique les concentrations en HCl total ($[HCl]_t$) en phase organique en fonction de la concentration en TBP total, nous obtenons des droites (Fig. 1) dont les pentes et les origines obtenues par la méthode des moindres carrés sont les suivantes :

$[HCl]_{aq}$ (*M*)	*Pente*	*Origine* ($[HCl]_s$)
6.55	$(2.12 \pm 0.14) \cdot 10^{-2}$	$(9.0 \pm 9) \cdot 10^{-5}$
7.06	$(4.22 \pm 0.11) \cdot 10^{-2}$	$(8.1 \pm 8.3) \cdot 10^{-5}$
7.43	$(6.00 \pm 0.12) \cdot 10^{-2}$	$(-3.1 \pm 8.8) \cdot 10^{-5}$

Le graphique obtenu en portant, pour une concentration en $[TBP]_t$ constante, la concentration en HCl engagé dans le complexe en fonction du logarithme des activités de l'acide chlorhydrique en phase aqueuse (Fig. 2) est une droite de pente unitaire. Ce comportement très simple peut s'interpréter par la formation en phase organique d'un complexe non dissocié renfermant une molécule d'acide chlorhydrique et une molécule de TBP.

En présence d'acide chlorhydrique, le TBP en solution diluée dans le sulfure de carbone ($[TBP]_t < 0.1\ M$) se trouve essentiellement sous trois formes : le TBP libre (non engagé dans les différents complexes et réprésenté par $[TBP]_1$), le monohydrate de TBP ($TBP \cdot H_2O$) que nous avions mis en évidence dans un travail antérieur[25] et enfin le complexe entre le TBP et l'acide que nous représenterons par (TBP–HCl)

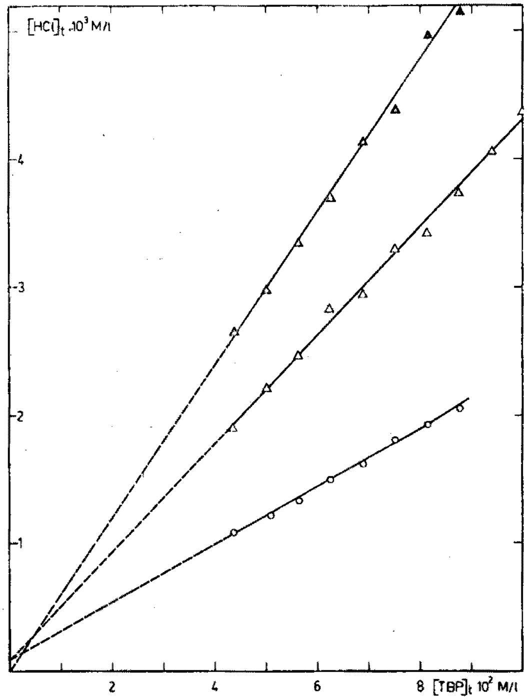

Fig. 1. Extraction de l'acide chlorhydrique par le TBP en solution diluée dans le sulfure de carbone. (○) $[HCl]_{aq}=6.55$ *M*; (△) $[HCl]_{aq}=7.06$ *M*; (▲) $[HCl]_{aq}=7.43$ *M*.

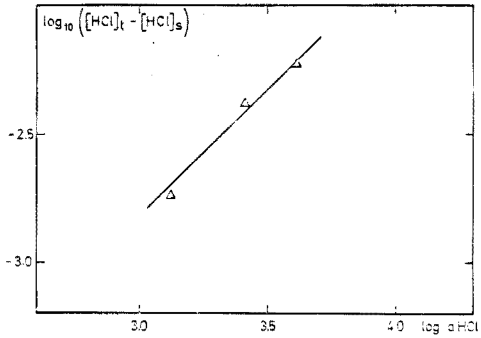

Fig. 2. Variation de la concentration en complexes TBP–HCl en fonction de l'activité de l'acide chlorhydrique en phase aqueuse. $[TBP]_t=0.10$ *M*.

dont la concentration en phase organique est égale à la concentration en HCl engagé dans le complexe ($[HCl]_c$). Les relations de bilan et d'équilibre s'écrivent alors:

$$[TBP]_t = [TBP]_l + [TBP \cdot H_2O] + [TBP\text{–}HCl]$$

$$[TBP\text{–}HCl] = [HCl]_c = [HCl]_t - [HCl]_s$$

$$[TBP \cdot H_2O]/[TBP]_l = 0.12 \cdot a_{H_2O}$$

où a_{H_2O} représente l'activité de l'eau en phase aqueuse.

Ces relations permettent d'obtenir directement les concentrations en $[\mathrm{TBP}]_l$ et $[\mathrm{TBP}\cdot \mathrm{H_2O}]$:

$$[\mathrm{TBP}]_l = \frac{[\mathrm{TBP}]_t - [\mathrm{HCl}]_c}{1+0.12\cdot a_{\mathrm{H_2O}}}$$

$$[\mathrm{TBP}\cdot \mathrm{H_2O}] = [\mathrm{TBP}]_l\cdot 0.12\cdot a_{\mathrm{H_2O}}$$

En soustrayant la concentration en monohydrate et la concentration en eau à saturation dans le solvant de la teneur en eau totale de la solution, on obtient la concentration en eau engagée dans le complexe TBP–HCl. On constate que le rapport $[\mathrm{H_2O}]/[\mathrm{HCl}]$ est nettement inférieur à l'unité, ce qui laisse supposer qu'il doit y avoir en solution au moins deux complexes constitués d'une molécule de TBP et de HCl mais se différenciant par leur degré d'hydratation.

Il serait cependent difficile de vouloir tirer des conclusions définitives basées essentiellement sur ces résultats car les dosages d'eau en très faibles teneurs dans le $\mathrm{CS_2}$ ($[\mathrm{H_2O}] < 0.01\ M$) ne sont guère aisés et risquent d'être affectés d'erreurs systématiques. Ces observations concordent néanmoins avec les résultats obtenus par plusieurs auteurs lors d'études similaires basées sur la résonance magnétique nucléaire[23] et sur l'analyse chimique de la phase organique[13,15,23].

Les spectres infra-rouges des solutions organiques confirment la présence d'eau associée à la molécule de HCl car on observe entre 3800 et 3000 cm^{-1}, en plus des bandes caractéristiques du monohydrate de TBP, une bande large située vers 3200 cm^{-1} attribuée à l'ion $\mathrm{H_3O^+}$[19] (Fig. 3), ce qui semble indiquer la présence en solution d'un complexe du type $\mathrm{TBP}\cdot\mathrm{H_3O^+Cl^-}$.

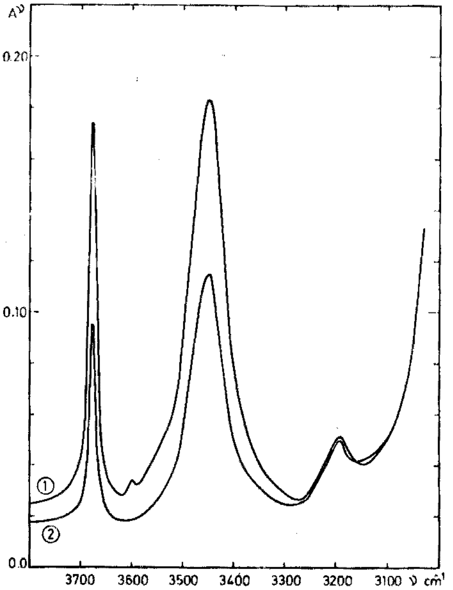

Fig. 3. Spectres infra-rouges des solutions organiques. $[\mathrm{TBP}]_t = 0.064\ M$ dans le $\mathrm{CS_2}$, cellule de 0.215 cm. (1) Solution équilibrée avec $\mathrm{H_2O}$; (2) solution équilibrée avec $[\mathrm{HCl}]_{\mathrm{aq}} = 7.86\ M$. $[\mathrm{HCl}]_c \simeq 0.008\ M$.

A priori, on peut imaginer que l'extraction de l'acide chlorhydrique s'effectue suivant les deux réactions:

$$H^+_{aq}+Cl^-_{aq}+TBP_{org} \overset{K_{1a}}{\rightleftharpoons} TBP\text{–}HCl_{org} \qquad (1)$$

avec

$$K_{1a}=[HCl]_c/[TBP]_l \cdot a_{HCl}$$

$$H^+_{aq}+Cl^-_{aq}+TBP_{org}+H_2O_{aq} \overset{K_{2a}}{\rightleftharpoons} TBP\cdot H_3O^+Cl^-_{org} \qquad (2)$$

avec

$$K_{2a}=[HCl]_c/[TBP]_l \cdot a_{HCl} \cdot a_{H_2O}$$

a_{HCl} désignant l'activité de l'acide chlorhydrique en phase aqueuse.

La réaction (1) conduit à un composé non hydraté tandis que la réaction (2) forme un composé hydraté. Il est évident qu'aucun de ces équilibres, pris séparément, ne permet d'interpréter complètement les résultats expérimentaux et il est fort probable que l'extraction de l'acide chlorhydrique résulte de la formation simultanée des deux complexes.

Le calcul des constantes d'équilibre, à partir des dosages d'acide en phase organique, ne permet pas d'éliminer une des deux possibilités envisagées: en portant en graphique $[HCl]_c$ en fonction des produits $[TBP]_l \cdot a_{HCl}$ ou $[TBP]_l \cdot a_{HCl} \cdot a_{H_2O}$ (Fig. 4), on obtient deux droites passant par l'origine dont les pentes nous donnent respectivement:

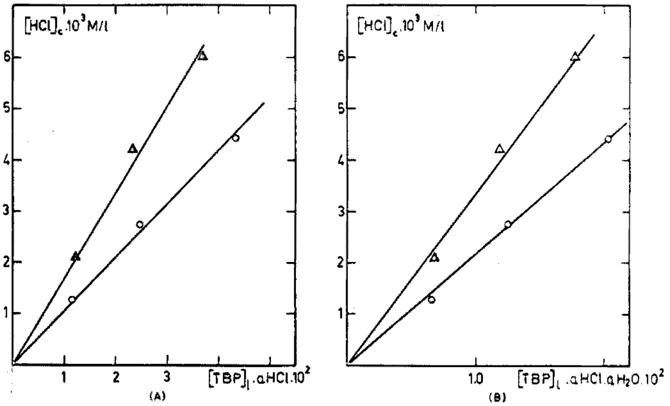

Fig. 4. Détermination des constantes de stabilité relatives aux équilibres:

$$H^+_{aq}+Cl^-_{aq}+TBP_{org} \overset{K_{1a}}{\rightleftharpoons} TBP\text{–}HCl_{org} \text{ (graphique A)}$$

et

$$H^+_{aq}+Cl^-_{aq}+H_2O_{aq}+TBP_{org} \overset{K_{2a}}{\rightleftharpoons} TBP\cdot H_3O^+ \ldots Cl^- \text{(graphique B)}$$

(△) Solvant CS_2, (○) solvant CCl_4.

$$K_{1a} = 1.67 \cdot 10^{-5}$$

$$K_{2a} = 3.32 \cdot 10^{-5}$$

Si ces deux relations d'équilibre ne reflètent pas exactement les phénomènes observés, elles permettent cependant de calculer la concentration en TBP engagé dans le complexe TBP–HCl et de déterminer la concentration en $[\mathrm{TBP}]_1$ à l'équilibre pour une activité donnée en HCl dans la phase aqueuse.

Extraction du trichlorure d'antimoine d'une phase aqueuse chlorhydrique

Pour chaque série d'expériences, nous avons maintenu la concentration initiale en HCl et en $SbCl_3$ constante dans la phase aqueuse et nous avons fait varier la concentration en TBP dans la phase organique. Les concentrations en $SbCl_3$ extrait en phase organique, pour des concentrations initiales en $SbCl_3$ en phase aqueuse égales à 0.1067 et 0.0452 *M* pour différentes activités en HCl, figurent au Tableau II et sont représentées graphiquement sur la Fig. 5.

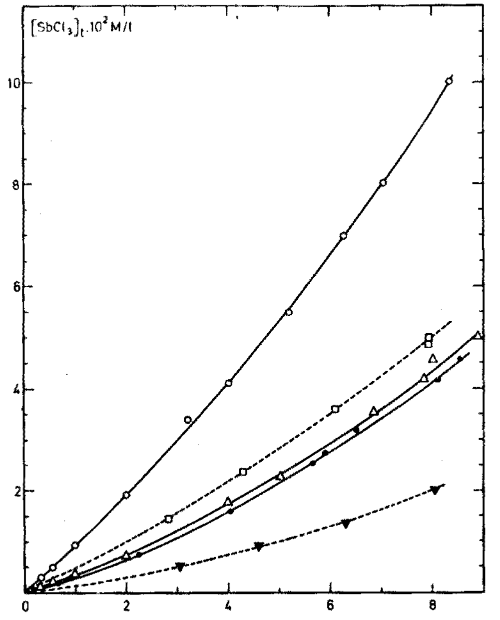

Fig. 5. Extraction du trichlorure d'antimoine en fonction de la concentration en $[\mathrm{TBP}]_t$. $[SbCl_3]_{aq\ initale} = 0.1067\ M$: (○) $[HCl]_{aq} = 3.48\ M$, (△) $[HCl]_{aq} = 7.40\ M$, (●) $[HCl]_{aq} = 7.86\ M$. $[SbCl_3]_{aq\ initiale} = 0.0452\ M$: (▼) $[HCl]_{aq} = 3.01\ M$, (□) $[HCl]_{aq} = 7.79\ M$.

En portant en graphique log *E* en fonction de log $[\mathrm{TBP}]_t$ (Fig. 6), on obtient des courbes dont la tangente vaut environ 1 pour des concentrations en TBP $\leqslant 0.02\ M$ et environ 1.5 pour le domaine de concentrations en TBP compris entre 0.02 et 0.1 *M*. L'allure des courbes suggère qu'il y a formation de deux complexes :

1. Un complexe 1:1 prédominant dans la zone de concentrations en TBP

TABLEAU II

EXTRACTION DU TRICHLORURE D'ANTIMOINE D'UNE PHASE AQUEUSE CHLORHYDRIQUE

$[TBP]_t(M)$	$[SbCl_3]_t$ (M)	$[Cl^-]_t$ (M)	$E \cdot 10^2$	$[TBP]_l(M)$	$\frac{E/E_0-1}{[TBP]_l}$	$[Cl^-]_t-[TBP \cdot HCl]+$ $-[Cl^-]_s$	$\frac{[Cl^-]_t-[TBP \cdot HCl]}{[Sb^{3+}]_t-[Sb^{3+}]_s}$
$[SbCl_3]_{aq\ initiale}=0.0452\ M$							
$[HCl]_{aq}=3.01\ M$							
0.0283_4	0.00145	0.0044_7	3.49	0.0238	2685	0.0044	3.03
0.0430	0.00238	0.0071_6	5.95	0.0359	3090	0.0071	2.98
0.0609	0.00360	0.0103_2	9.56	0.0506	3520	0.0102	2.85
0.0791	0.00485	0.0141_3	13.74	0.0656	3900	0.0141	2.90
0.0793	0.00498	0.0141_7	14.2	0.0656	4020	0.0141	2.83
0.0926	0.00567	0.0170	16.8	0.0768	4090	0.0169	2.98
0.101	0.00626	0.01865	19.2	0.0837	4275	0.0186	2.97
$[HCl]_{aq}=7.79\ M$							
0.0306	0.00054_2	0.00490	1.23	0.0260	3090	0.00196	3.61
0.0459	0.000940	0.00699	2.12	0.0389	3580	0.00286	3.05
0.0628	0.00138_6	0.0100	3.26	0.0530	4060	0.00444	3.20
0.0805	0.00204	0.0134	4.96	0.0677	4830	0.00642	3.15
0.0944	0.002525	0.0168	6.28	0.0793	5250	0.00900	3.56
0.0954	0.00251	0.0166	6.25	0.0802	5150	0.00872	3.47
$[SbCl_3]_{aq\ initiale}=0.1067\ M$							
$[HCl]_{aq}=7.86\ M$							
0.00329	0.000106	0.00124	0.10	0.0028	2210	—	—
0.00658	0.000203	0.00181	0.19	0.0055	2275	—	—
0.00911	0.000289	0.00228	0.27	0.0076	2415	0.00094	3.26
0.0224	0.000752	0.00486	0.72	0.0187	2680	0.00248	3.30
0.0405	0.00159	0.00916	1.52	0.0330	3245	0.00543	3.42
0.0566	0.00253	0.0137	2.46	0.0458	3810	0.00874	3.45
0.0592	0.00274	0.0142	2.70	0.0478	4020	0.00906	3.31
0.0651	0.00319	0.0161	3.18	0.0522	4330	0.0106	3.31
0.0809	0.00417	0.0215	4.24	0.0647	4670	0.0148	3.56
0.0855	0.00458	0.0230	4.70	0.0681	4920	0.0160	3.49

$[HCl]_{aq}=3.48$ *M*							
0.00328	0.000330	0.00092	0.31	0.0027	1990	0.00080	2.86
0.00554	0.000534	0.00154	0.51	0.0045	2250	0.00142	2.92
0.0101	0.000955	0.00291	0.91	0.0083	2320	0.00279	3.25
0.0202	0.00194	0.00608	1.89	0.0166	2475	0.00596	3.14
0.0322	0.00342	0.00991	3.43	0.0256	2985	0.00979	2.90
0.0403	0.00413	0.0131	4.19	0.0312	2990	0.0129	3.18
0.0519	0.00552	0.0170	5.77	0.0400	3210	0.0169	3.08
0.0627	0.00700	0.0212	7.55	0.0478	3520	0.0211	3.04
0.07065	0.00803	0.0243	8.86	0.0537	3675	0.0242	3.03
0.0836	0.0103	0.0296	11.90	0.0630	4200	0.0295	2.90
$[HCl]_{aq}=7.50$ *M*							
0.00314	0.000116	0.00089	0.11	0.0027	2320	—	—
0.00563	0.000205	—	0.19	0.0048	2460	—	—
0.0100	0.000374	0.00205	0.35	0.0086	2610	0.00105	2.81
0.0201	0.000743	0.00387	0.71	0.0172	2680	0.00226	3.04
0.0402	0.00180	0.00819	1.75	0.0337	3420	0.00555	3.08
0.0505	0.00228	0.0104	2.24	0.0422	3480	0.00723	3.17
0.0689	0.00356	0.0157	3.58	0.0563	4190	0.0116	3.25
0.0786	0.00419	0.0186	4.26	0.0637	4430	0.0140	3.35
0.0804	0.00460	0.0201	4.72	0.0647	4820	0.0155	3.36
0.0889	0.00502	0.0221	5.19	0.0716	4800	0.0170	3.38

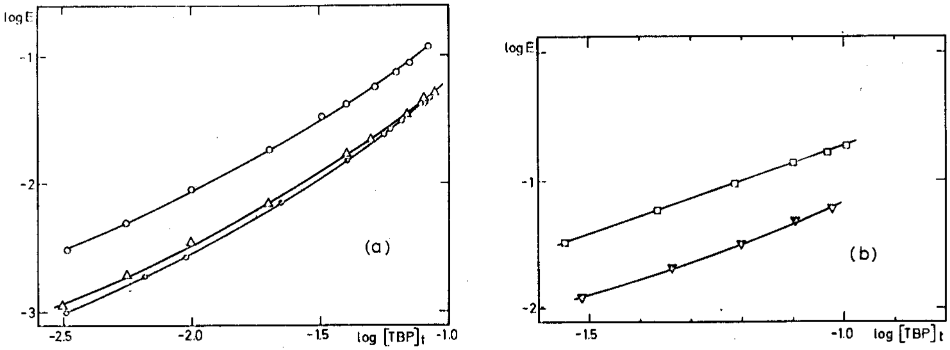

Fig. 6. Variation du coefficient de partage en fonction de la concentration en $[TBP]_t$. (a) $[SbCl_3]_{aq\ initiale} = 0.1067\ M$: (○) $[HCl]_{aq} = 3.47\ M$; (△) $[HCl]_{aq} = 7.48\ M$; (●) $[HCl]_{aq} = 7.86\ M$. (b) $[SbCl_3]_{aq\ initiale} = 0.04524\ M$: (□) $[HCl]_{aq} = 3.01\ M$; (△) $[HCl]_{aq} = 7.79\ M$.

comprise entre 0.003 et 0.2 M.

2. Un complexe 1:1 et 2:1 présents simultanément dans la zone de concentrations en $[TBP]_t$ comprise entre 0.03 et 0.1 M.

DÉTERMINATION DES CONSTANTES DE STABILITÉ

La détermination des constantes de stabilité des complexes extraits en phase organique nécessite la connaissance du coefficient de distribution E_0 de $SbCl_3$ entre la phase aqueuse chlorhydrique et le solvant seul. Le Tableau III donne les valeurs obtenues pour E_0 á différentes activités en HCl.

TABLEAU III

VALEURS DE COEFFICIENT DE DISTRIBUTION DE $SbCl_3$

$[SbCl_3]_{aq\ initiale} = 0.1067\ M$		$[SbCl_3]_{aq\ initiale} = 0.0452\ M$	
$[HCl]_{aq}(M)$	E_0	$[HCl]_{aq}(M)$	E_0
3.48	$4.49 \cdot 10^{-4}$	3.01	$5.37 \cdot 10^{-4}$
7.50	$1.50 \cdot 10^{-4}$	7.79	$1.51 \cdot 10^{-4}$
7.86	$1.40 \cdot 10^{-4}$		

Ce Tableau montre que le coefficient de partage diminue régulièrement quand la concentration en HCl en phase aqueuse augmente. Cette variation du coefficient de partage peut s'interpréter très simplement: en phase aqueuse chlorhydrique, l'antimoine trivalent se trouve sous différentes formes complexes[26] et la concentration de l'entité $SbCl_3$ diminue lorsque la concentration en HCl augmente, ce qui se traduit par une diminution de E_0. Signalons que la valeur du coefficient de partage de $SbCl_3$ entre une solution d'acide perchlorique et le CS_2 est de l'ordre de 0.17, ce qui semble indiquer que la complexation de l'antimoine(III) est déjà importante aux faibles activités en HCl.

La présence simultanée des complexes 1:1 et 2:1 conduit aux relations suivantes:

$$SbCl_{3\,org} \overset{E_0}{\leftrightarrows} SbCl_{3\,aq} \quad \text{avec} \quad E_0 = [SbCl_3]_{org}/[SbCl_3]_{aq}$$

$$SbCl_{3\,org} + TBP_l \overset{K_{1:1}}{\rightleftharpoons} SbCl_3 \cdot TBP \quad \text{avec} \quad K_{1:1} = \frac{[SbCl_3 \cdot TBP]}{[SbCl_3] \cdot [TBP]}$$

$$SbCl_{3\,org} + 2TBP_l \overset{K_{2:1}}{\rightleftharpoons} SbCl_3 \cdot 2TBP \quad \text{avec} \quad K_{2:1} = \frac{[SbCl_3 \cdot 2TBP]}{[SbCl_3] \cdot [TBP]^2}$$

Le coefficient de distribution E en présence des deux complexes s'écrit:

$$E = ([SnCl_3] + [SbCl_3 \cdot TBP] + [SbCl_3 \cdot 2TBP])_{org}/[SbCl_3]_{aq}$$

ou en remplaçant $[SbCl_3 \cdot TBP]$ et $[SbCl_3 \cdot 2\,TBP]$ par leur valeur tirée des constantes d'équilibre:

$$E = ([SbCl_3]_{org}/[SbCl_3]_{aq} \cdot \{1 + [TBP]_l \cdot K_{1:1} + [TBP]_l^2 \cdot K_{2:1}\}$$

Le rapport $[SbCl_3]_{org}/[SbCl_3]_{aq}$ étant par définition égal à E_0, la relation précédente se transforme en l'expression:

$$(E/E_0 - 1)/[TBP]_l = K_{1:1} + K_{2:1} \cdot [TBP]_l$$

qui n'est autre que l'éguation d'une droite $Y = K_{1:1} + K_{2:1} \cdot X$ avec

$$Y = (E/E_0 - 1)/[TBP]_l \quad \text{et} \quad X = [TBP]_l.$$

La pente de la droite obtenue en portant Y en fonction de X nous donne directement $K_{2:1}$ et l'ordonnée à l'origine $K_{1:1}$.

L'application de cette formule nécessite la concentration en $[TBP]_l$ à l'équilibre qui peut être obtenue aisément par la relation

$$[TBP]_l = \frac{[TBP]_t - n[SbCl_3]_{org}}{1 + a_{H_2O} \cdot 0.12 + 1.67 \cdot 10^{-5}\, a_{HCl}}$$

n étant la valeur de la tangente à la courbe $\log E = \log\, [TBP]_t$ à la concentration $[TBP]_t$.

Si nous portons en graphique (Fig. 7) les valeurs de Y et de X définies par les relations antérieures et figurant au Tableau II, nous obtenons, par les moindres carrés, les résultats dans le Tableau IV.

On peut constater qu'aux erreurs de mesures près, la constante $K_{1:1}$ est indépendante de la concentration en HCl en phase aqueuse tandis que la valeur de la constante $K_{2:1}$ croît lorsque l'acidité de la solution augmente.

DISCUSSION

Les valeurs des constantes d'équilibre que nous avons déterminées par spectrométrie infra-rouge dans un travail précédent[1] ($K_{1:1} = 1100$ mole^{-1} l et $K_{2:1} =$

9,030 mole^{-2} l^{2}) sont nettement différentes des valeurs obtenues par extraction liquide–liquide; en outre, le rapport $K_{2:1}/K_{1:1}$ est nettement différent et augmente lorsque la concentration en HCl dans la phase aqueuse croît. Cette anomalie a également été observée pour le système acétophénone–$SbCl_3$ dans le CCl_4[27]. Plusieurs hypothèses peuvent, à priori, être envisagées pour expliquer ces écarts:

TABLEAU IV

VALEURS DES CONSTANTES DE STABILITÉ

$[HCl]_{aq}$ (M)	$K_{1:1}$ $(M)^{-1}$	$K_{2:1}$ $(M)^{-2}$
$[SbCl_3]_{aq\ initiale} = 0.1067\ M$		
3.48	2,000 ± 60	32,750 ± 1630
7.50	2,200 ± 90	36,240 ± 1960
7.86	2,020 ± 65	41,440 ± 1570
3.01	2,130 ± 110	26,590 ± 1750
7.79	2,030 ± 100	39,950 ± 1660
$[SbCl_3]_{aq\ initiale} = 0.0452\ M$		
3.01	2,130 ± 110	26,590 ± 1750
7.79	2,030 ± 100	39,950 ± 1660

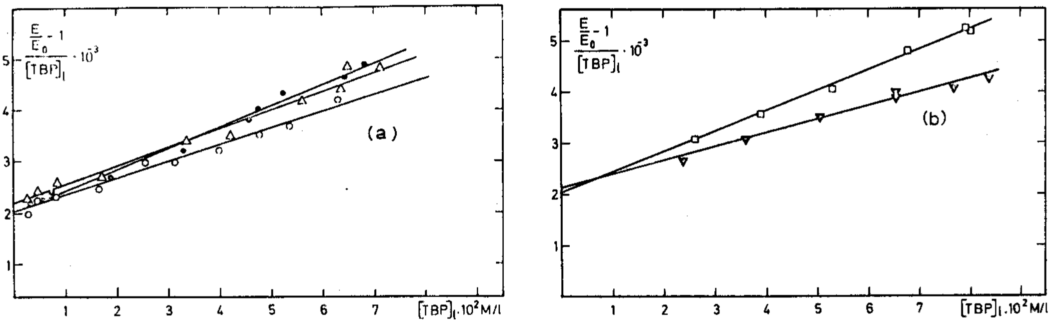

Fig. 7. Détermination graphique de $K_{1:1}$ et de $K_{2:1}$. (a) $[SbCl_3]_{aq\ initiale} = 0.1067\ M$: (○) $[HCl]_{aq} = 3.48\ M$; (△) $[HCl]_{aq} = 7.50\ M$; (●) $[HCl]_{aq} = 7.86\ M$. (b) $[SbCl_3]_{aq\ initiale} = 0.0452\ M$: (△) $[HCl]_{aq} = 3.01\ M$; (□) $[HCl]_{aq} = 7.79\ M$.

La répartition de l'antimoine(III) entre différentes entités dans le sulfure de carbone

La concentration en $SbCl_3$ que nous introduisons dans les relations d'équilibre est la concentration totale en Sb^{3+} à saturation dans le sulfure de carbone. Il n'est pas exclu qu'en présence d'eau ou d'acide en phase organique (la concentration en eau à saturation est environ 100 fois supérieure à la concentration totale en Sb^{3+}) qu'il y ait formation de différents complexes de l'antimoine trivalent avec et/ou l'acide. Dans ce cas, la concentration en $SbCl_3$ libre serait inférieure à la concentration totale en Sb^{3+} et les valeurs des constantes d'équilibre seraient encore plus élevées. Les valeurs de $K_{1:1}$, constantes aux erreurs de mesures près, semblent infirmer cette supposition car il est peu probable que le rapport $[SbCl_3]/[Sb^{3+}]_t$ reste constant pour une activité en HCl dans la phase aqueuse variant de 20 à 5600. Cette hypothèse, à elle seule, ne permet donc pas d'expliquer les écarts observés.

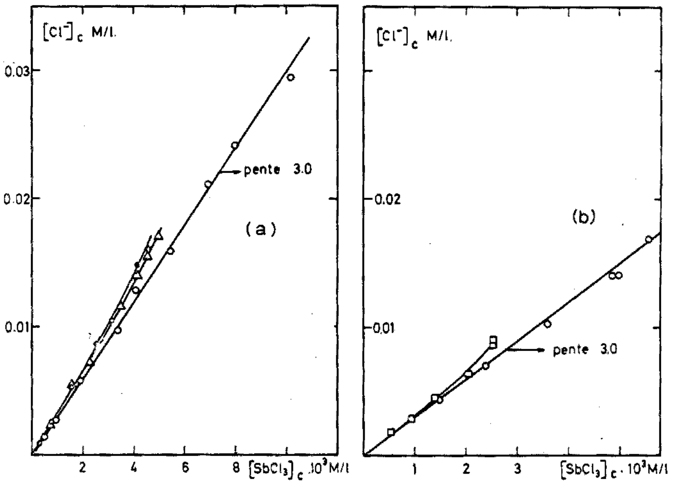

Fig. 8. Variation du rapport $[Cl^-]/[Sb^{3+}]$ dans les complexes TBP–$SbCl_3$. (a) $[SbCl_3]_{aq\ initiale} = 0.1067\ M$: (○) $[HCl]_{aq} = 3.47\ M$, (△) $[HCl]_{aq} = 7.50\ M$, (●) $[HCl]_{aq} = 7.86\ M$. (b) $[SbCl_3]_{aq\ initiale} = 0.045\ 2\ M$: (○) $[HCl]_{aq} = 3.01\ M$, (□) $[HCl]_{aq} = 7.79\ M$.

La présence de complexes en solution autres que $TBP \cdot SbCl_3$ *et* $(TBP)_2SbCl_3$

La présence de "nouveaux complexes" en phase organique a pu être établie pour des concentrations en HCl en phase aqueuse supérieures à 5 *M*. Si, pour ces concentrations en HCl, on dose l'antimoine et les chlorures extraits, on constate que le rapport $[Cl^-]/[Sb^{3+}]$, après soustraction de l'acide chlorhydrique extrait par le CS_2 et le TBP, est supérieur à 3.0 (Tableau II et Fig. 8). Il semble donc bien établi qu'en présence d'acide et d'eau, il puisse y avoir d'autres entités en solution que les complexes identifiés en milieu anhydre.

La présence de complexes chlorés pour lesquels le rapport $[Cl^-]/[Sb]^{3+}$ est supérieur à 3.0 pourrait donc expliquer, du moins en partie, les variations des constantes $K_{2:1}$ dont les valeurs augmentent lorsque l'activité de l'acide chlorhydrique dans la phase aqueuse croît. Il est très probable même que les hautes activités en HCl favorisent la formation en solution organique de complexes où les molécules de TBP seraient fixées non plus à $SbCl_3$, mais à H_3OSbCl_4 ou à $HSbCl_4$, par exemple. Signalons que la présence de complexes formés par paires d'ions entre le TBP, l'acide chlorhydrique et un acide de Lewis en phase organique a déjà été proposée par Startsev *et al.*[28] pour caractériser le complexe $TiCl_4$–HCl–TBP formé lors de l'extraction de $TiCl_4$ et par Hodiaumont[29] lors de l'étude par spectrométrie Raman de l'extraction de $SbCl_3$ par le TBP en solution dans le benzène.

Ces complexes ne peuvent cependant être responsables, à eux seuls, des variations des constantes d'équilibre les expériences réalisées en milieu acide ($[HCl]_{aq}$ 3.01 ou 3.48 *M*) ont montré qu'aux erreurs expérimentales près, le rapport $[Cl^-]/[Sb^{3+}]$ était égal à 3.0 (Fig. 8), ce qui semblerait indiquer que le TBP est lié à la molécule $SbCl_3$. Il faut cependant remarquer que la détermination du rapport $[Cl^-]/[Sb]^{3+}$ ne permet pas d'écarter la présence d'un complexe en phase organique où le TBP serait lié non plus à $SbCl_3$ mais à une autre molécule telle $SbCl_2H_2O^+Cl^-$ formée par hydrolyse partielle de $SbCl_3$ et dont le rapport $[Cl^-]/[Sb^{3+}]$ serait aussi égal à 3.0. La présence de molécules d'eau associées aux complexes formés entre le TBP et le trichlorure d'antimoine a déjà été envisagée par Khorasani et Hakim[7] et a été mise en évidence lors de l'extraction du $TiCl_4$[28] et du Co^{2+} [30] par le TBP.

Le profil des bandes d'absorption infra-rouge entre 4000 et 3300 cm^{-1} semble étayer cette hypothèse: si on compare le spectre des solutions organiques après équilibration de la phase organique avec l'acide seul puis avec l'acide et le trichlorure d'antimoine, on observe, en présence de $SbCl_3$, une absorption légèrement plus forte entre 3300 et 3000 cm^{-1} qui pourrait être attribuée à la présence d'ions hydroxonium en solution. La différence d'absorption nettement trop faible que pour en tirer des conclusions définitives, paraît cependant significative.

En conclusion, il semble donc que la présence d'eau et d'acide en phase organique influence fortement la nature et les constantes d'équilibre des complexes formés et que les relations établies en milieu anhydre ne peuvent pas toujours être appliquées à l'extraction liquide–liquide.

RÉSUMÉ

Nous avons étudié l'extraction de l'acide chlorhydrique et du trichlorure d'antimoine par le TBP en solution diluée dans le sulfure de carbone ($[TBP]_t < 0.1$ *M*); dans la phase aqueuse les concentrations en HCl variaient de 3.0 à 7.9 *M*, les concentrations en $SbCl_3$ étant 0.1067 et 0.0452 *M*. Les résultats expérimentaux montrent que l'acide chlorhydrique s'extrait dans la phase organique suivant la réaction:

$$TBP_{org} + H^+_{aq} + Cl^-_{aq} + yH_2O_{aq} \rightleftharpoons TBPH^+(H_2O)_y \ldots Cl^-{}_{org}$$

y étant inférieur à 1. Le trichlorure d'antimoine forme, en phase organique, des complexes de stoechiométrie 1:1 et 2:1 ($TBP/SbCl_3$); les dosages de chlorures montrent, en outre, la présence de complexes où le rapport $[Cl]/[Sb^{3+}]$ est supérieur à 3.0. Les constantes de stabilité des complexes $TBP–SbCl_3$ sont supérieures aux constantes mesurées en milieu anhydre; la valeur de la constante du complexe 1:1 est indépendante de l'activité en HCl dans la phase aqueuse tandis que celle du complexe 2:1 croît lorsque la concentration en acide augmente.

SUMMARY

The extraction of hydrochloric acid and of antimony trichloride by dilute solutions of TBP in carbon disulphide ($[TBP]_t < 0.1$ *M*) has been studied. In the aqueous phase the hydrochloric acid concentration ranged from 3 to 7.9 *M* and the $SbCl_3$ concentration was 0.1067 and 0.0452 *M*. The experimental results showed that hydrochloric acid is extracted into the organic phase according to the reaction:

$$TBP_{org} + H^+_{aq} + Cl^-_{aq} + yH_2O_{aq} \rightleftharpoons TBPH^+(H_2O)_y \ldots Cl^-{}_{org}$$

y being inferior to 1. Antimony trichloride forms, in the organic phase, complexes of 1:1 and 2:1 stoichiometry ($TBP/SbCl_3$); the chloride determinations show, moreover, the existence of complexes where the ratio $[Cl^-]/[Sb^{3+}]$ is higher than 3.0. The stability constants of $TBP–SbCl_3$ complexes are higher than those measured in anhydrous solutions; the value of the stability constant of the 1:1 complex is independent of the hydrochloric acid activity in the aqueous phase whereas that of the 2:1 complex increases with the acid concentration.

ZUSAMMENFASSUNG

Die Extraktion von Chlorwasserstoffsäure und Antimontrichlorid durch TBP in verdünnten Schwefelkohlenstofflösungen wurde untersucht ($[\mathrm{TBP}]_t < 0.1$ *M*). Die Salzsäurekonzentrationen in der wässrigen Phase schwankten zwischen 3.0 und 7.9 *M*, die SbCl$_3$ Konzentrationen waren 0.1067 und 0.0452 *M*. Die Ergebnisse zeigen das Chlorwasserstoffsäure nach folgender Gleichung in die organische Phase extrahiert:

$$\mathrm{TBP_{org}} + \mathrm{H_w^+} + \mathrm{Cl_w^-} + y\mathrm{H_2O_w} \rightleftharpoons \mathrm{TBPH^+(H_2O)_y \ldots Cl_{org}^-}$$
$$(y < 1).$$

Antimontrichlorid bildet in der organische Phase Komplexe der Stöchiometrie 1:1 und 1:2 (TBP/SbCl$_3$). Die Chloridbestimmungen zeigen ausserdem die Gegenwart von Komplexen, in denen das Verhältnis $[\mathrm{Cl^-}]/[\mathrm{Sb^{3+}}]$ grösser als 3.0 ist. Die Stabilitätskonstanten der Komplexe TBP.SbCl$_3$ sind grösser als die Konstanten, die in wasserfreiem Medium gemessen wurden. Der Wert der Konstanten des 1:1 Komplexes ist unabhängig von der HCl-Aktivität in der wässrigen Phase, während die Konstante des 2:1 Komplexes mit der Säurekonzentration wächst.

BIBLIOGRAPHIE

1 G. Roland, *Spectrochim. Acta*, 25A (1969) 1135.
2 M. M. Privalova et D. I. Ryabchikov, *Anal. Khim. Akad. Nauk SSSR*, 9 (1958) 301.
3 D. I. Ryabchikov et M. M. Privalova, *Zh. Neorgan. Khim.*, 3 (1958) 1964.
4 T. Ishimori, K. Watanabe et E. Nakamura, *Bull. Chem. Soc. Japan*, 33 (1960) 1443.
5 S. S. M. A. Khorasani, *Pakistan J. Sci. Ind. Res.*, 14 (1962) 80.
6 S. S. M. A. Khorasani, *Pakistan J. Sci. Ind. Res.*, 6 (1963) 233.
7 S. S. M. A. Khorasani et Q. A. Hakim, *Pakistan J. Sci. Ind. Res.*, 9 (1966) 220.
8 H. Irving et D. N. Eddington, *J. Inorg. Nucl. Chem.*, 10 (1959) 306.
9 E. Hesford et H. A. C. McKay, *J. Inorg. Nucl. Chem.*, 13 (1960) 156.
10 A. S. Kertes, *J. Inorg. Nucl. Chem.*, 14 (1960) 104.
11 A. S. Kertes, *J. Inorg. Nucl. Chem.*, 12 (1960) 377.
12 A. S. Kertes et N. Kertes, *Can. J. Chem.*, 38 (1960) 612.
13 E. Foa, N. Rosintal et Y. Marcus, *J. Inorg. Nucl. Chem.*, 23 (1961) 109.
14 D. G. Tuck et R. M. Diamond, *J. Phys. Chem.*, 65 (1961) 193.
15 K. Naito et T. Suzuki, *J. Phys. Chem.*, 66 (1962) 983.
16 H. A. C. McKay et J. H. Miles, *Nature*, 199 (1963) 65.
17 J. H. Miles, *J. Inorg. Nucl. Chem.*, 27 (1965) 711.
18 P. Biddle, A. Coe, H. A. C. McKay, J. H. Miles et M. J. Waterman, *J. Inorg. Nucl. Chem.*, 29 (1967) 2615.
19 E. V. Komarov, M. E. Obukhova et M. F. Pushlenkov, *Russ. J. Inorg. Chem.*, 12 (1967) 116.
20 S. S. Korovin, A. M. Reznik, E. N. Lebedeva et N. A. Spasskaya, *Russ. J. Inorg. Chem.*, 12 (1967) 1137.
21 R. Mitamura, I. Tokura, S. Nishimura, Y. Kondo et N. C. Li, *J. Inorg. Nucl. Chem.*, 30 (1968) 1019.
22 C. Hanson et A. N. Patel, *J. Appl. Chem.*, 18 (1968) 209.
23 Yu. M. Klubokov, V. V. Yostrobov et S. S. Korovin, *Zh. Neorgan. Khim.*, 14 (1969) 4, 1082.

24 L. K. Cucalin, Z. A. Grankina, S. P. Chramenko, B. I. Peščevickij et I. A. Kuzin, *Zh. Neorgan. Khim.*, 15 (1970) 1, 170.
25 G. Roland et G. Duyckaerts, *Spectrochim. Acta*, 24A (1968) 529.
26 F. Pantini et P. G. Desideri, *Gazz. Chim. Ital.*, 89 (1959) 1360.
27 G. Leclère-zur Nedden, *Thèse de doctorat en Sciences Chimiques*, Université de Liège, 1970.
28 N. N. Startsev, Yu. I. Sannikov, G. B. Ben Yosk et E. I. Krylov, *Zh. Neorgan. Khim.*, 13 (4) (1968) 1122.
29 A. Hodiaumont, *Thèse de licence en Sciences Chimiques*, Université de Liège, 1969.
30 B. Jerowska-Trzebiatowska, A. Bartecki et S. Kopacs, *Zh. Neorgan. Khim.*, 13 (3) (1968) 864.

Analytica Chimica Acta
Elsevier Publishing Company, Amsterdam
Printed in The Netherlands

THE EXTRACTION OF ZIRCONIUM(IV) FROM HYDROCHLORIC ACID SOLUTIONS BY HIGH-MOLECULAR-WEIGHT AMINES

TAICHI SATO AND HIROSHI WATANABE
Department of Applied Chemistry, Faculty of Engineering, Shizuoka University, Hamahatsu (Japan)

(Received 28th September 1970)

The extraction of zirconium(IV) from hydrochloric acid solutions with a high-molecular-weight quaternary ammonium chloride has been reported in a previous paper[1]. The extraction of uranium(VI) and cobalt(II) from hydrochloric acid solutions by long-chain aliphatic amines[2,3] and cyclohexylalkyl- and benzylalkyl-amines[4] has also been examined. The present paper extends this work to the extraction of zirconium(IV) from hydrochloric acid solutions by such high-molecular-weight amines.

EXPERIMENTAL

Reagents

The amines listed in Table I were of high purity, and were used without further purification. They were diluted with benzene, and were not preequilibrated with

TABLE I

Amine	Abbreviation	Molecular weight	Structure
Di-n-octyl	DOA	241	$[CH_3(CH_2)_6CH]_2NH$
Benzyl-2-ethylhexyl	BEHA	214	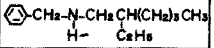
Cyclohexyl-2-ethylhexyl	CEHA	211	
Tri-n-octyl	TOA	354	$[CH_3(CH_2)_6CH_2]_3N$
Tri-n-dodecyl	TDA	522	$[CH_3(CH_2)_{10}CH_2]_3N$
Tris-2-ethylhexyl	TEHA	354	 $[CH_3(CH_2)_3CH(C_2H_5)CH_2]_3N$
Benzyl-di-n-dodecyl	BDDA	439	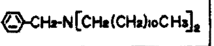
Benzyl-di-2-ethylhexyl	BDEHA	327	
Cyclohexyl di-n-dodecyl	CDDA	436	
Cyclohexyl di-2-ethylhexyl	CDEHA	324.	

hydrochloric acid solutions. The zirconium chloride solution was prepared by dissolving zirconium chloride in hydrochloric acid solution of the required concentration. The other chemicals were of analytical-reagent grade.

Extraction and analytical procedures

The procedure for obtaining partition coefficients (the ratio of the equilibrium concentration of zirconium in the organic phase to that in the aqueous phase) was as described previously[1]: equal volumes (15 ml) of amines in benzene and the aqueous solution containing hydrochloric acid were shaken for 10 min, and then zirconium was stripped from the organic phase with 0.5 *M* nitric acid solution.

Zirconium concentrations were determined by titration with EDTA with xylenol orange as indicator[1,5]. The chloride concentration of the organic phase was determined by Vòlhard's method, and the water content of the organic phase by Karl Fischer titration.

Infrared and n.m.r. spectral measurements

Infrared and nuclear magnetic resonance (n.m.r.) spectral measurements were carried out as described previously[1]: the infrared spectra were determined on a Japan Spectroscopic Co., Ltd. Model IR-S recording spectrophotometer, and n.m.r. spectra were obtained by using tetramethylsilane as an internal reference in carbon tetra-

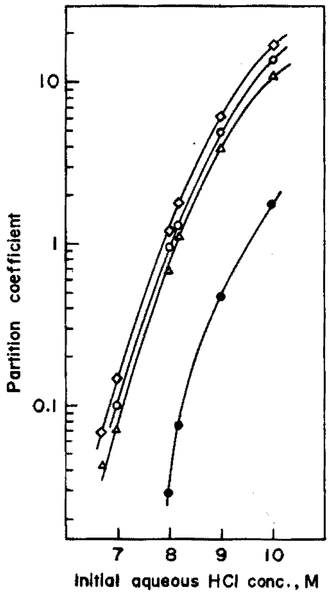

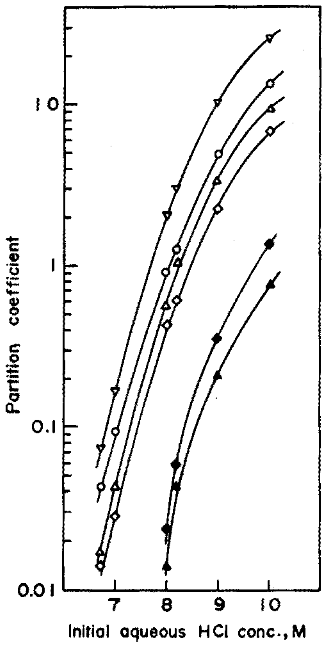

Fig. 1. Extraction of zirconium(IV) from hydrochloric acid solutions with 0.1 *M* solutions of long-chain aliphatic amines in benzene. (●) DOA, (△) TOA, (○) TDA, (◇) TEHA.

Fig. 2. Extraction of zirconium(IV) from hydrochloric acid solutions with 0.1 *M* solutions of cyclohexylalkyl- and benzylalkyl-amines in benzene. (▲) CEHA, (◇) CDDA, (△) CDEHA, (◆) BEHA, (○) BDDA, (▽) BDEHA.

chloride solution on a Hitachi Perkin-Elmer Model R-20 high-resolution n.m.r. spectrometer.

Thermogravimetric and differential thermal analyses (TGA and DTA)

TGA and DTA were carried out on an automatic recording thermobalance and DTA apparatus by using platinum–platinum/rhodium thermocouples. The heating rate was 5° min^{-1} in both cases.

RESULTS AND DISCUSSION

Extraction efficiency of various systems

The extraction of zirconium(IV) from aqueous solutions containing hydrochloric acid at an initial zirconium concentration of 0.0215 *M* with 0.1 *M* solutions of the various amines in benzene at 20° was examined at different acidities. Figures 1 and 2 show that for all amines the partition coefficient increases steeply with aqueous acidity at concentrations above about 6 *M*, in agreement with the extraction by the quaternary compound[1]. The partition coefficients for the extraction from 10 *M* hydrochloric acid solution with various amines are indicated in Table II. From these it can be seen that tertiary amines are more efficient extractants for zirconium than secondary amines; the efficiency is increased with the chain length of the alkyl group and is enhanced when the alkyl chain in tertiary amine is branched; a benzyl group is essential for promoting extraction efficiency. For the extraction of uranium(VI) and cobalt(II), however, the efficiency of cyclohexylalkyl and benzylalkyl tertiary amines is reduced when the alkyl chain is branched[4], and the order of the efficiency of long-chain aliphatic amine is TEHA > TDA > TOA > DOA for uranium(VI)[2] and TDA > TOA > TEHA > DOA for cobalt(II)[3].

Dependence on concentration of amine

If it is assumed that the increase in the partition coefficient with tertiary amines

TABLE II

Amine	Number of C.	Partition coefficient	Percentage extracted
DOA	16	1.78	64.0
BEHA	15	1.34	57.2
CEHA	14	0.76	43.3
TOA	24	11.0	91.7
TDA	36	13.9	93.3
TEHA	24	17.0	94.5
BDDA	31	13.4	93.1
BDEHA	23	25.0	96.2
CDDA	30	6.70	87.2
CDEHA	22	9.42	90.6

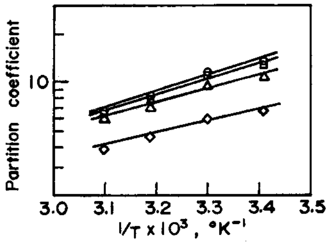

Fig. 3. Temperature dependence of partition coefficient for the extraction of zirconium from hydrochloric acid solutions with 0.1 *M* solutions of various amines in benzene. (△) TOA, (○) TDA, (◇) CDDA, (□) BDDA.

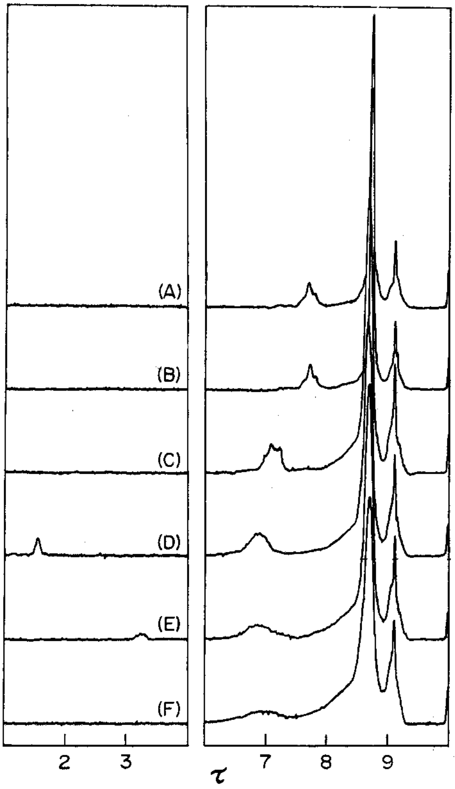

Fig. 4. N.m.r. spectra of the organic phases from the extractions of zirconium chloride solutions containing hydrochloric acid with 0.1 *M* TOA in carbon tetrachloride. (A) TOA; (B) TOA saturated with water; (C) and (D) 0.1 and 10 *M* HCl alone respectively; (E) zirconium chloride solution of 0.0215 *M*; (F) zirconium compound, freed from benzene, dispersed into carbon tetrachloride.

is governed by a solvating reaction similar to that in the extraction of uranium(VI) or cobalt(II)$^{2-4}$, *viz.*

$$\mathrm{ZrCl_4\,(a)} + n\mathrm{R_3NHCl\,(o)} \rightleftarrows \mathrm{(R_3NH)}_n\mathrm{ZrCl}_{n+4}\,\mathrm{(o)} \qquad (1)$$

and

$$\mathrm{ZrCl_4\,(a)} + n\mathrm{R_2R'NHCl\,(o)} \rightleftarrows \mathrm{(R_2R'NH)}_n\mathrm{ZrCl}_{n+4}\,\mathrm{(o)} \qquad (2)$$

where (a) and (o) represent aqueous and organic phases, respectively, R is the alkyl group, and R′ the cyclohexyl or benzyl group, the following reaction would be expected:

$$\log E_a^0 = \log \mathrm{K} + n \log (C_A - n\, C_{Zr}) \qquad (3)$$

in which E_a^0 is the partition coefficient, K the equilibrium constant, C_A the total amine concentration and C_{Zr} the zirconium concentration of the organic phase. From a log–log plot of E_a^0 *vs.* $(C_A - n\,C_{Zr})$ for the extraction of zirconium chloride solution (0.0215 *M*) containing 10 *M* hydrochloric acid, it was found that eqn. (3) is satisfied for $n=2$, the slopes of the lines being 2.2, 2.2, 2.0 and 2.2 for TOA, TDA, CDDA and BDDA, respectively. This suggests that each zirconium ion is associated with two amine molecules, eqns. (1) and (2) becoming:

$$ZrCl_4\,(a) + 2R_3NHCl\,(o) \rightleftarrows (R_3NH)_2ZrCl_6\,(o) \qquad (4)$$

and

$$ZrCl_4\,(a) \times 2R_2R'NHCl\,(o) \rightleftarrows (R_2R'NH)_2ZrCl_6\,(o) \qquad (5)$$

Temperature effect

The extraction of zirconium(IV) from aqueous solutions containing 10 *M* hydrochloric acid at initial zirconium concentration of 0.0215 *M* with 0.1 *M* solutions of TOA, TDA, CDDA and BDDA in benzene at temperatures between 20 and 50° gave the results shown in Fig. 3, which indicate that the partition coefficient decreases with rising temperature. This dependence on temperature is analogous to that for uranium(VI) and cobalt(II)[2-4], but is contrary to that for zirconium(IV) with quaternary amines[1]. The heats of reaction (change in enthalpy) (in kcal mol^{-1}) for eqns. (4) and (5) were estimated to be 4.0, 6.1, 3.9 and 4.8 for TOA, TDA, CDDA and BDDA, respectively.

N.m.r. spectra

The organic phase from the extraction of zirconium chloride solution (0.0215 *M*) containing 10 *M* hydrochloric acid with 0.1 *M* TOA in carbon tetrachloride at 20° was examined by n.m.r. spectroscopy. Similar experiments were carried out for the extraction of 0.1 and 10 *M* hydrochloric acid solutions alone. The spectra are given in Fig. 4.

The n.m.r. spectrum for TOA shows a peak at τ 9.15 in a triplet due to the methyl protons, a strong peak at 8.77, which arises from the methylene protons, and a doublet at 7.73, coming from the methylene protons attached immediately adjacent to the nitrogen atom. The spectrum for the TOA saturated with water closely resembles that for TOA, indicating that water is not accompanied by TOA. In the extraction of 0.1 *M* hydrochloric acid alone, the peak caused by the methylene protons appears at 8.68 and the resonance of the methylene protons attached to the nitrogen atom shifts to lower field as a broad signal at 7.15, because of the presence of a strong ion-pair. Simultaneously, the broad absorption from the formation of the compound $R_3NHCl \cdot H_2O$[6,7] appears at ~8.2 as a shoulder. The spectrum for the organic extract from 10 *M* hydrochloric acid solution without zirconium exhibits an absorption at 1.55, which is ascribed to proton-exchange between the extracted acid and the water associated with amine hydrochloride, and a shift of the signal, attributed to the methylene protons attached to the nitrogen atom, to lower field at 6.90.

In the spectrum for the organic solution from the extraction of zirconium chloride solution, the signal caused by proton exchange is shifted to a stronger field at 3.23 as a broad absorption. This signal almost disappears when the complex prepared by drying the organic phase is dispersed into carbon tetrachloride, demonstrating the absence of water in the complex. This corresponds to the fact that the water con-

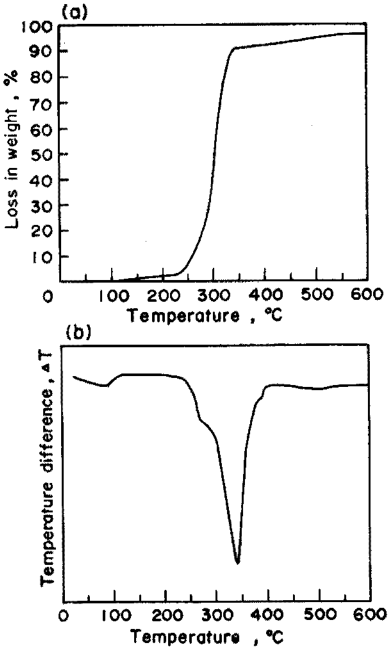

Fig. 5. TGA and DTA curves for TOA-zirconium chloro-complex. (a) TGA curve; (b) DTA curve.

tent of the organic phase is decreased by the extraction of zirconium.

Thermal analyses

TOA was chosen as a representative extractant and its complex with zirconium was investigated by thermal analysis. The TGA and DTA curves for the complex prepared by drying the organic phase are shown in Fig. 5.

The DTA curve exhibits three endothermic peaks at 275, 340 and 385°, and these peaks occur at the points near the change of the slope in the TGA curve. As already described[8], the DTA curve for TOA shows endothermic peaks at 275 and 380°, which arise from the formation of hydrocarbon by the cracking of amine and carbonization of its product, respectively, and the curve for amine hydrochloride shows peaks at 285 and 335°, which are due to the thermal decomposition of amine hydrochloride and the carbonization of its products, respectively. As the TGA and DTA curves for the zirconium complex resemble those for the TOA–copper(II) chloro-complex[8], the following interpretation is probably correct for the endothermic peaks in the DTA curve for the complex: at 275°, part of the coordinated chlorine is removed and the derived amine is coordinated immediately to zirconium through hydrogen bonding; at 340°, more chlorine is removed, and at the same time the derived amine is thermally decomposed and then the hydrocarbon formed is carbonized; at 385°, the retained chlorine is further removed. This explanation is supported by the data for the chlorine content in the thermally decomposed products of the complex.

The mole ratio of the components, zirconium:chlorine:TOA in the complex is 1:6:2, indicating the composition $(R_3NH)_2ZrCl_6$. The infrared spectrum of the amine hydrochloride shows the NH^+-stretching vibration[9,10] at 2350 cm^{-1}, indicating the presence of strong hydrogen-bonding, and the OH-stretching and OH-bending modes at 3360 and 1625 cm^{-1}, respectively, since one mole of water associates with each mole of amine hydrochloride[6,7]. For the complex, however, the NH^+-stretching vibration shifts to 2600 cm^{-1} and the OH-absorptions almost disappear. Hence the structure displaying a coordination number of 6 for zirconium may be proposed for the complex.

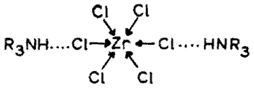

We wish to thank Messrs. F. Ozawa and M. Nishizaki for assistance with experimental work, and the Kao Soap Co. Ltd. and the Yoshitomi Pharmaceutical Industries Ltd. for samples of various amines.

SUMMARY

The extraction of zirconium(IV) from hydrochloric acid solutions with various amines in benzene was investigated under different conditions, in order to examine the effect of amine structure on the extraction. Tertiary amines are more efficient extractants for zirconium than secondary amines; the efficiency increases with the chain length of alkyl group and is enhanced when the alkyl chain in the tertiary amine is branched; a benzyl group is essential for promoting extraction efficiency. Organic solutions from the extraction were examined by infrared and high-resolution n.m.r. spectroscopy, and thermal analyses (TGA and DTA) were carried out for the complex prepared by drying the organic phase.

RÉSUMÉ

Les auteurs ont effectué une étude sur l'extraction du zirconium(IV), en solutions acide chlorhydrique, à l'aide de diverses amines dans le benzène, dans différentes conditions. Le but de ce travail est d'examiner l'influence de la structure des amines sur l'extraction. Les amines tertiaires constituent de meilleurs extractants pour le zirconium que les amines secondaires. L'extractibilité augmente avec la longeur de la chaîne du groupe alcoyle. Les solutions organiques d'extraction sont examinées par spectroscopie infra-rouge et de résonance nucléaire magnétique; des analyses thermiques (ATG et ADT) sont effectuées sur les complexes obtenus par évaporation de la phase organique.

ZUSAMMENFASSUNG

Es wurde die Extraktion von Zirkonium(IV) aus salzsauren Lösungen mit verschiedenen Aminen in Benzol unter verschiedenen Bedingungen untersucht und der Einfluss der Aminstruktur auf die Extraktion geprüft. Tertiäre Amine sind wirksamere Extraktionsmittel für Zirkonium als sekundäre Amine. Die Wirksamkeit

steigt mit der Kettenlänge der Alkylgruppe und wird erhöht, wenn die Alkylkette im tertiären Amin verzweigt ist; eine Benzylgruppe steigert die Extraktionswirksamkeit erheblich. Die organischen Lösungen der Extraktion wurden durch Infrarot- und hochauflösende K.m.r.-Spektroskopie untersucht; mit dem durch Trocknen der organischen Phase erhaltenen Komplex wurden thermische Analysen (TGA und DTA) ausgeführt.

REFERENCES

1 T. Sato and H. Watanabe, *Anal. Chim. Acta*, 49 (1970) 463.
2 T. Sato, *J. Appl. Chem.*, 16 (1966) 143.
3 T. Sato, *J. Appl. Chem.*, 16 (1966) 305.
4 T. Sato, *Anal. Chim. Acta*, 45 (1969) 71.
5 J. Kinnunen and B. Wennerstrand, *Chemist-Analyst*, 46 (1957) 92.
6 T. Sato, *J. Appl. Chem.*, 15 (1965) 10.
7 V. Bertocci and G. Rolandi, *J. Inorg. Nucl. Chem.*, 23 (1961) 323.
8 T. Sato and K. Adachi, *J. Inorg. Nucl. Chem.*, 31 (1969) 1395.
9 *E.g.*, R. C. Lord and R. E. Merrifield, *J. Chem. Phys.*, 21 (1963) 166; E. A. V. Ebsworth and N. Sheppard, *Spectrochim. Acta*, 13 (1959) 261; J. Bellanato, *Spectrochim. Acta*, 16 (1960) 1344.
10 L. J. Bellamy, *Infra-red Spectra of Complex Molecules*, 2nd Edn., John Wiley, New York, 1958, pp. 297–310.

Analytica Chimica Acta
Elsevier Publishing Company, Amsterdam
Printed in The Netherlands

DETERMINATION OF SMALL AMOUNTS OF WATER IN ORGANIC SOLVENTS BY SPECTROPHOTOMETRIC ANALYSIS

C. L. LUKE
Bell Telephone Laboratories, Incorporated, Murray Hill, N. J. 07974 (U.S.A.)

(Received 25th September 1970)

Small amounts of water in organic solvents are usually determined by the Karl Fischer method. The latter is based on the reaction between water, iodine, and the anhydride, sulfur dioxide. The method has proved to be very satisfactory. Nevertheless, the challenge of developing an alternative way of determining water was attractive and it seemed worth-while, as a starting point in the search for a new method, to try substituting the anhydride, chromium(VI) oxide, for the sulfur dioxide, with the hope that some means could be found for measuring the amount of chromic acid produced. Tests showed that, although the chromium oxide could not be used directly, a successful method for the determination of water could be had by taking advantage of the reaction

$$K_2Cr_2O_7+H_2O=K_2CrO_4+H_2CrO_4 \tag{1}$$

Thus, if a mixture of dichromate and wet 4-methyl-2-pentanone (MIBK) containing a little magnesium perchlorate dihydrate, is shaken, the chromic acid produced in the reaction between dichromate and water dissolves in the solvent and the reaction proceeds to the right by the law of mass action. The dichromate and chromate remain insoluble in the solvent. Some reaction of the solvent with the dichromate occurs to produce soluble $RHCrO_4$ but this side reaction is usually small. Thus, it is evident that if the amount of dissolved chromate in the solvent is measured and if correction for the $RHCrO_4$ is made, it should be possible to determine the water present. It was found that the dissolved chromate could be conveniently determined spectrophotometrically[1].

The reaction of water with dichromate is slow and long shaking is required to obtain complete reaction. As the reaction proceeds, the $RHCrO_4$ blank increases in proportion. Eventually, the chromate concentration becomes high enough to cause some oxidation of the solvent. In view of this, to limit the time of shaking and to make it possible to determine the water spectrophotometrically, it was necessary to use conditions where the reaction was only about 10% complete. Fortunately, adequate sensitivity in the analysis is assured.

Quantitative tests of the proposed method showed, as expected, that a plot of the weight of water added to dry MIBK *versus* the measured absorbance was linear. This confirms that the method will be suitable for the determination of water in MIBK. Attention was next focused on the problem of adapting the method to the analysis of a variety of other solvents. Organic solvents differ widely in their behavior and most of them cannot be analyzed directly. However, a large number of these solvents can be analyzed, provided that they are suitably diluted with 0.2% magnesium perchlorate dihydrate–MIBK solution before the reaction with dichromate. Data showed that, in such analyses, it is possible to determine as little as 0.002% of water, depending on the solvent being analyzed.

Since organic solvents vary in their reactivity and thus produce $RHCrO_4$ blanks of different magnitude, it is necessary, in the new method, to calibrate for each solvent being analyzed. However, only two points are required, one below and one above the water content of the sample being analyzed. The amount of water present in the sample can be obtained by simple interpolation, since the graphs are linear.

The method calls for considerable attention on the part of the analyst, but as he or she becomes familiar with the techniques required, the average time required for the calibration and analysis of a sample is about 10 min, which is not much more than that required to make an electrometric Karl Fischer analysis.

EXPERIMENTAL

Apparatus

Reciprocal shaker. A reciprocal shaker (Eberbach Corp, Ann Arbor, Mich.) was used. All solutions were shaken at a rate of 180 oscillations per min.

Spectrophotometer. A Beckman Model B unit with 1-cm absorption cells was used.

Reagents

Activated molecular sieve powder. Heat powdered 3A molecular sieve (Union Carbide Co.) at 175° for 24 h. Cool and protect from moist air.

Dry solvents. Transfer 100 ml of the solvents to be analyzed to 125-ml standard taper conical flasks. Add 5 g of the dry powdered 3 A molecular sieve, stopper and shake on the reciprocal shaker for 1 h. Allow the solutions to stand overnight to permit settling of the sieve. If the amount of solvent available is limited, add 10 ml of the solvent plus 1 g of 3A sieve to a glass stoppered 15-ml centrifuge tube, shake horizontally for 2 h and then centrifuge. Dispense the clear solutions by pipet, taking care not to disturb the powdered sieve on the bottom of the flasks or tubes. Discard any solution that becomes discolored on prolonged contact with the sieve.

Magnesium perchlorate–MIBK solution. Dissolve 1.5 g of magnesium perchlorate hexahydrate in 500 ml of MIBK and reserve. Dissolve 2 g of anhydrous magnesium perchlorate in 1 l of MIBK in a glass-stoppered bottle. Ignore any insoluble material. Add 10 g of powdered 3A sieve, shake for 1 h, or longer if necessary, on a reciprocal shaker, and filter through Whatman No. 40 filter paper supported on a large Millipore fritted glass filter with the aid of suction.

Add 50 mg of −400 mesh dichromate to a 10-ml portion of the filtered solution and then analyze, as directed in the *Procedure* described subsequently, using water as the reference solution. Then, if necessary, add small portions of the reserved wet MIBK solution, with intermittent analysis, until the blank reading is 35 to 45%T. If too much of the wet solution is added by accident, add more dry 0.2% magnesium perchlorate–MIBK solution. Store the adjusted solution under a blanket of dry nitrogen.

As needed, transfer a portion of the solution to a 300-ml standard taper flask and cap with a stopper unit through which a stream of dry nitrogen is flowing. If the nitrogen being used is not water-free, dry it by passage through a tower of 8-mesh anhydrous magnesium perchlorate. Dispense the solution through a hole in the stopper unit by means of a 10-ml pipet (Fig. 1).

Standard water solution. Transfer 1.0 ml of water to a dry 100-ml volumetric flask, fill to the mark with ethyl acetate dried with powdered 3A molecular sieve, and shake vigorously to assure complete mixing (1 ml = 10 mg H_2O). In the calibration, dispense this solution from a Gilmont Micrometer Syringe (Cole-Parmer Instrument Company, Chicago). The syringe has a capacity of 2 ml and can deliver as little as 0.002 ml through a stainless steel needle.

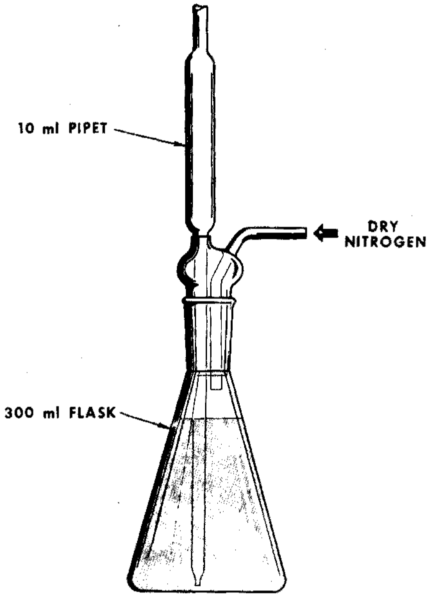

Fig. 1. Apparatus for dispensing prepared magnesium perchlorate–MIBK solution.

Fine-mesh potassium dichromate. Shake fine-mesh, crystalline potassium dichromate on a 100-mesh screen and reserve the −100 mesh salt that passes through the screen. Then pass a portion of the +100 mesh salt successively through 100-, 200- and 400-mesh screens by rubbing the salt on the appropriate screen with the bottom of a 250-ml beaker. Reserve a portion of each mesh-size salt. Dry the crystalline −100 and the crushed 100–200, 200–400 and −400 mesh salt in a 75° vacuum oven.

Reference solutions. Dissolve 0.1 g of potassium dichromate in 100 ml of water and mix. Dilute 1 and 5 ml of this solution to 100 ml with water and mix. Call these solutions 1 and 5% dichromate reference solutions.

Procedure

Sweep out two dozen or more dry, 50-ml, 19/38 standard taper conical flasks with dry nitrogen, stopper, and reserve for the analyses. Transfer 10.0 ml of adjusted 0.2% magnesium perchlorate–MIBK solution to 3 of the flasks. Add 1.0 ml of the dry solvent to be analyzed to flasks 1 and 2 and the same amount of the wet solvent to be analyzed to flask 3. Then add 0.1 ml of standard water solution (10 mg H_2O/ml) to flask 2 and analyze the 3 solutions consecutively in the order—flasks 1, 2 and 3.

Add 50.0 mg of −400 mesh potassium dichromate from a 30-ml beaker, through a small funnel to the flask, tapping the funnel vigorously with the inverted beaker to make sure that all the salt enters the flask. Stopper, grasp the flask, while holding the stopper in place with the index finger, invert the flask, extend the arm down in the normal resting position and then shake vigorously and almost vertically, so that the solution hits the top and bottom of the flask, for exactly 1 min.

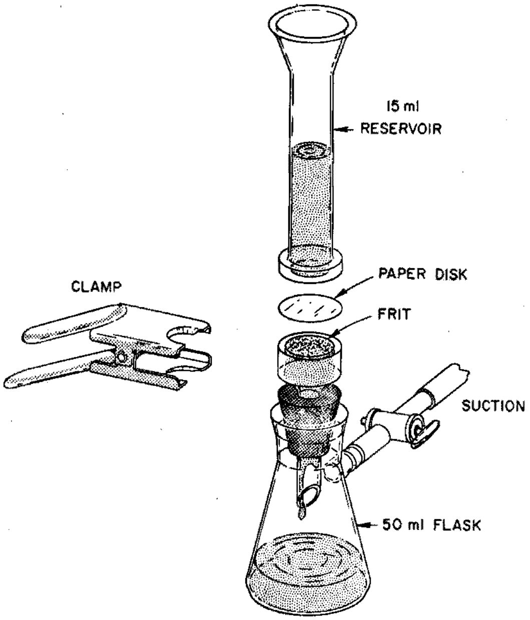

Fig. 2. Filtration apparatus.

Filter the solution immediately, with strong suction, using a small Millipore filter funnel (Fig. 2), through a dry 25-mm disk of Whatman No. 40 filter paper that has been cut out of a number of sheets of the paper with a die. Catch the filtrate in a 50-ml suction flask. Withough delay, fill a 1-cm absorption cell with the filtered solution and measure the percentage transmittance on a suitable spectrophotometer at 370 nm. Use water or the appropriate dichromate solution as the reference solution in order that a reading of not less than about 35%T for flask No. 1 is obtained. For ready accessibility, water and the two reference solutions should be contained in absorption cells placed in a multiple compartment holder in the spectrophotometer. Convert %T to absorbance (*A*) by referring to a suitable table that reads in units of 0.2%T, and then, for the sake of convenience, multiply *A* by 100 to obtain the values of 100*A*.

Calculations

If $100A$ for flask $3 - 100A$ for flask $1 = B$
$100A$ for flask $2 - 100A$ for flask $1 = C$
ml of solvent taken for analysis $= D$
density of the solvent being analyzed $= E$

then $$\frac{B}{C \cdot D \cdot E \cdot 10} = \%\text{ water in the solvent.}$$

Note

It is convenient to use a series of 6 filter units which can be loaded with paper disks and be ready for insertion into the neck of the 50-ml filter flask. After the spectrophotometric reading of the solution from flasks 1, discard the solutions and shake the filter flask and absorption cell to remove as much of the solvent as possible before proceeding to the next analysis. After completion of the third analysis, wash out the two vessels with a stream of acetone and dry them with a jet of compressed air. After all of the filter units have been used, demount them, loosen the dichromate on the rims of the reservoirs and then wash the reservoirs and the frit supports with acetone. Dry and reassemble. Wash the used 50-ml conical flasks with water and acetone. Wash the reservoirs and frit supports occasionally with hydrochloric acid to remove chromate ion.

DISCUSSION

When a drop of water is added to a small portion of fine-mesh potassium dichromate, MIBK is added and the mixture is shaken, little or no chromic acid appears in the MIBK. If the experiment is repeated but a small amount of an anhydrous hygroscopic alkali or alkaline earth chloride or perchlorate is present with the dichromate, the reaction of eqn. (1) occurs and the orange color of chromic acid can be seen in the MIBK. The role played by the hygroscopic salt is not understood. If the latter experiment is repeated but the water is dissolved in the MIBK before mixing with the dichromate plus hygroscopic salt, only magnesium perchlorate will induce the reaction of eqn. (1) to any appreciable extent. Apparently this strongly hygroscopic salt can break the bonding between the water and MIBK, and allow the reaction to proceed.

The concentration of the magnesium perchlorate in the MIBK influences the extent of reaction. This can be seen in the data in Fig. 3. To obtain these data, 0.02, 0.2 and 2.0% solutions of anhydrous magnesium perchlorate in MIBK were dried fairly well with 3A molecular sieve, and then 10-ml portions of the solutions were mixed with various amounts of standard water solution and analyzed by the *Procedure*, 100–200 or −400 mesh crushed dichromate being used. From curves 1 and 3 of the Fig. it is seen that a 0.2% solution is optimum for the analysis, since linearity between water added and net absorbance is obtained over an appreciable range of water content and the sensitivity is high. The graph for the 0.2% solution does not become linear until a $100A$ value of about 30 is obtained. The data plus other similar data obtained with completely dehydrated 0.2% magnesium perchlorate–MIBK solution suggests that, until approximately the dihydrate has been formed, the water that has been freed from the bonding of the MIBK cannot react normally with

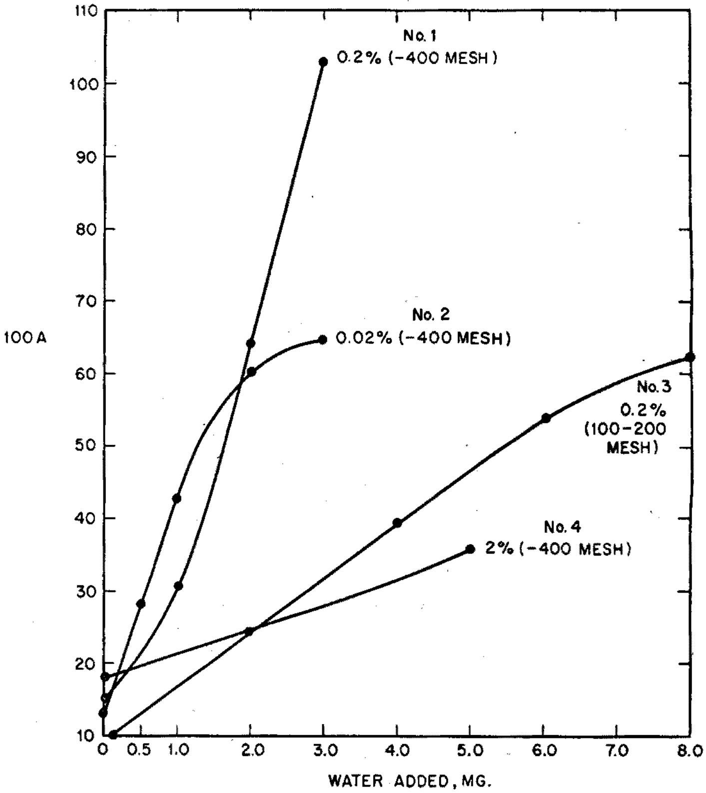

Fig. 3. Effect of magnesium perchlorate in the MIBK.

the dichromate[2]. From curve 3, which was obtained with adjusted 0.2% magnesium perchlorate–MIBK solution, it is seen that, as the amount of added water increases, linearity falls off just as it does in the graph for the 0.02% solution shown in the figure. This deviation from linearity starts when the salt has been converted to approximately the tetrahydrate, where its attraction for water is probably so weak that it cannot completely break the bonding between the water and the MIBK. The sensitivity in the analysis is low when 2% solution is used because the dihydrate has not been formed[2].

Choice of diluting solvent

The number of organic solvents that yield a small $RHCrO_4$ blank and a reasonably high net absorbance due to water, in the proposed method, is limited. The solvents which have proved to be useful, as diluting solvents, are MIBK, 5-methyl-2-hexanone, 2-octanone, 2-ethoxyethanol and the acetate esters from ethyl to octyl. Of these various solvents, MIBK has been found to be the best for use in the new method.

Choice of dichromate

Several alkali and alkaline earth dichromates were tried out but none proved to be superior to the potassium salt. Tests showed that the reaction of eqn. (1) is greater the more dichromate used, the smaller the mesh size of the dichromate, the longer the time of shaking and the greater the intensity of shaking.

In order to obtain reproducible analyses, the shaking of the dichromate–solvent mixtures must be reproducible. Attempts to use a wrist action or reciprocal action mechanical shaker failed, but it was shown that reasonably good reproducibility could be obtained by hand shaking. In order to reduce the labor involved, it is desirable to limit the time of shaking to 1 min. When this is done, it is necessary to use finely-divided dichromate in order to obtain a reasonably high net absorbance from the water. In the *Procedure*, −400 mesh salt is recommended but, in most cases, the more easily handled 200–400 mesh salt can be used instead.

A crushed salt has a greater surface area than a crystalline salt of similar mesh size, probably because of the presence of dust that cannot be removed in the sieving. The effect of the mesh size of the dichromate on the extent of reaction can be seen in Fig. 4 where calibration graphs, obtained with adjusted 0.2% magnesium perchlorate–MIBK solution and crushed dichromate of different mesh sizes, are given.

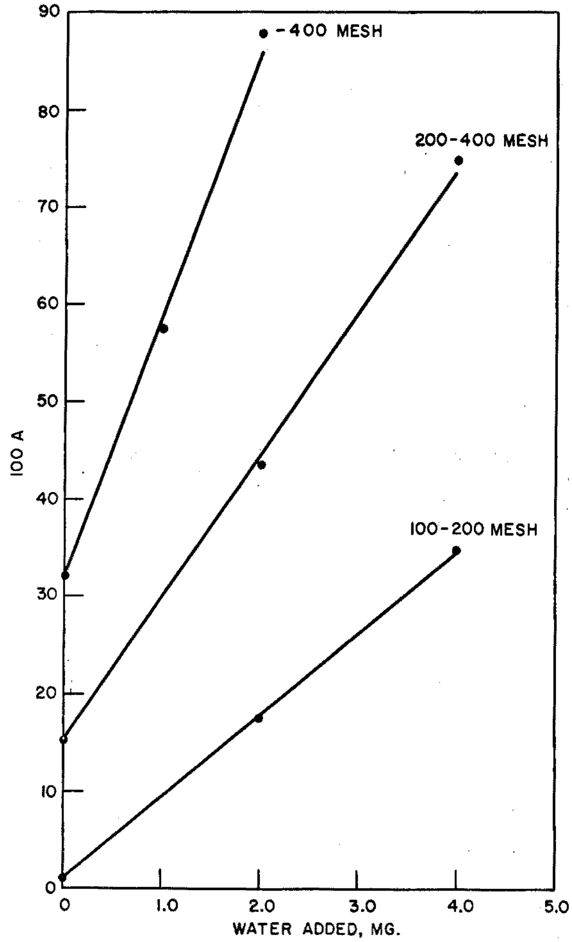

Fig. 4. Effect of mesh size of dichromate.

From the Fig., it is seen that linearity is obtained in all cases and that the $RHCrO_4$ blank and the net absorbance from a given amount of water are proportional to the surface area of the dichromate.

Because of the nature of the new method for water, which involves an incomplete reaction between a solid and a liquid, all variables must be closely controlled. If this is done, fairly good reproducibility and accuracy can be obtained. Data obtained with −400 mesh dichromate (Table I) showed that the reproducibility is reasonably good. The data in Fig. 4 and in Table I are different because they were obtained with different batches of adjusted magnesium perchlorate–MIBK solution.

TABLE I

DATA ON REPRODUCIBILITY

Water added (mg)	(100 *A*)	*Average*
0	43.7	42
	43.2	
	39.1	
0.5	61.3	61
	61.3	
	60.6	
1.0	82.4	79
	75.9	
	78.5	

Behavior of solvents

In the determination of a given amount of water in non-polar (non-reactive) solvents the total amount of chromate ion and the ratio of $RHCrO_4$ to H_2CrO_4 extracted by the MIBK varies from solvent to solvent because their reactivity and their ability to bond with water varies. The variation is not great and the extent of reaction approximates that obtained in MIBK alone. The great majority of organic solvents can be analyzed on a 1-ml sample, with −400 mesh dichromate. The *Procedure* above has been written to provide for these analyses. Whenever the solvent will permit, up to 5 ml of the sample should be used if the water content is less than 0.01%. On the other hand, if the water content of the sample is greater than 0.1% the sample size must be reduced so that no more than 1 mg of water is present, or the amount of water added to flask 2 must be increased so that it exceeds, by a small margin, the amount present in flask 3. In this latter case, if the transmittance for flask 2 is smaller than 10%, dichromate of coarser mesh should be used in the analysis. In any event, it is not advisable to take a sample for analysis that contains more than about 3 mg of water.

Small samples of reactive solvents can be analyzed with 200–400 or −400 mesh dichromate but, if larger samples are required to provide adequate sensitivity, dichromate of correspondingly coarser mesh must be used to control the size of the blank. Thus, as much as 5 ml of the reactive solvent acetonitrile can be analyzed provided that 100–200 mesh crystalline dichromate is used. Regardless of the reference solution used, the blank transmittance should not be lower than 35%T.

Solvents such as methanol, methyl acetate and 2-methoxyethanol cannot be analyzed because they readily react with dichromate and also form such a strong bond with water that the magnesium perchlorate is ineffective. Hence the blanks are high and the net absorbance caused by water is low or negative. The same is true, to a lesser extent, with solvents such as allyl alcohol, valeronitrile, ethanol and a few others. To analyze these latter solvents, it is necessary to limit the sample size.

A few solvents tend to reduce chromate and hence cause the color to fade in the spectrophotometric measurement. In most instances the fading is slow and can be compensated for in the calibration. However, when fading is more rapid, as it is in the analysis of 2-butoxyethanol, the sample size must not exceed 0.25 ml. The use of a coarser mesh dichromate is not as effective.

Solvents such as pyridine, tri-*n*-butylphosphate, the higher alcohols and acetate esters, propionic anhydride and, to a lesser extent, 1,4-dioxane, tend to suppress the reaction of water with dichromate. Hence, in the analysis of some of these solvents, 0.1 g of -400 mesh dichromate should be used and the solution should be shaken for 2 min in order to obtain an adequate reaction.

In the analysis of viscous solvents such as cyclohexanone or the higher alcohols, the mixed solvents in flask 3 should be allowed to stand for at least 10 min before adding the dichromate, to allow the solvent to become thoroughly dispersed in the MIBK.

The above discussion may suggest that the new method is not practical, but the fact remains that the number of solvents that require special handling is not great and experience with the method will make it possible to predict rather closely the sample size and mesh size of the dichromate that should be used for the analysis of a particular solvent.

It is obvious, from what has been said, that the various factors of reactivity of the solvent, sample size, and mesh size of the dichromate are interrelated. Moreover, it is clear why it is necessary to calibrate for each solvent being analyzed. Attempts to eliminate the need for this individual calibration by scavenging or sequestering the water from the solvents in a state where it could then be analyzed by the reaction of eqn. (1) were not successful. The sequestering agents used were molecular sieve 3A, silica gel, calcium sulfate and magnesium perchlorate.

Solvents which can be analyzed

The method has been tested qualitatively on more than 125 solvents that were chosen at random from those available in the laboratory. In most of this work, a 1-ml portion of the dry solvent plus 0 or 1 mg of water was analyzed, with -400 crushed dichromate. It was found that all of the alcohols and their acetate esters from ethanol to octanol, including their isomers, could be analyzed. Tert.-butanol had to be maintained at 30–35° during the drying and pipeting in order to keep it from solidifying. Other solvents tested that appear to be capable of being analyzed are listed in Table II. Future work will undoubtedly show that a great many others can also be analyzed.

The sensitivity of analysis of organic solvents depends on the sample size used. The permissible maximum sample size depends on the solvent being analyzed. It has been shown that 5-ml samples of many of the higher alcohols and acetate esters and a large number of the low or moderately reactive solvents listed in Table II can be analyzed. This means that these solvents can be analyzed for as little as 0.002% of

TABLE II

SOLVENTS WHICH CAN BE ANALYZED

Acetone
4-Methyl-2-pentanone
5-Methyl-2-hexanone
2-Pentanone
3-Heptanone
4-Heptanone
2-Octanone
Methyl ethyl ketone
Acetophenone
3,3-Dimethyl-2-butanone
2,4-Pentanedione
4-Hydroxy-4-methyl-pentanone[a]
Allyl acetate
Methyl bromoacetate
Methyl acetoacetate
Methyl sulfite
Methyl salicylate
Ethyl bromoacetate
Ethyl chloroacetate
Ethyl trichloroacetate
Ethyl cyanoacetate
Ethyl formate[a]
Ethyl sulfide
2-Methoxyethanol acetate
2-Ethoxyethanol acetate
2-Butoxyethanol acetate
Tri-*n*-butyl phosphate
Phenethyl alcohol
Allyl alcohol[a]
Benzyl alcohol
α,α-Dimethylbenzyl alcohol
2-Ethoxyethanol
2-Butoxyethanol[a]
2-Methyl-2-hexanol
p-Menth-1-en-8-ol
Acetic anhydride
Propionic anhydride[a]
Propionaldehyde[a]
Benzaldehyde
Butyraldehyde
Chloroform
Carbon tetrachloride
1,2-Dichloroethane
Trichloroethylene
Tetrachloroethane
Isoamyl chloride
Benzyl chloride
Bromobenzene
Fluorobenzene
o-Chlorophenol
3-Chloropentene
Bromotrichloromethane
Hexachloro-1,3-butadiene
α,α,α-Trichlorotoluene
Hexachloro-2-propanone
2-Bromobutane
1,4-Dioxane
Ethyl ether
Isopropyl ether
Bis(2-methoxyethyl)ether[a]
1,2-Bis(2-methoxyethoxy)ethane
Trimethyl orthoacetate[a]
Pyridine
2-Ethylpyridine[a]
4-Ethylpyridine
Tetrahydrofuran
Tetrahydro-2-methylfuran
Petroleum ether
Kerosene
Gasoline
Hexane
3-Heptane
3-Heptene
1-Hexene
n-Nonane
n-Octane
Cyclohexane
3-Methylpentane
1-Methyl-1-cyclopentene
Benzene
Toluene
Xylene
Tetrahydronaphthalene
Acetonitrile
Acrylonitrile
Propionitrile[a]
Valeronitrile[a]
Benzonitrile
Carbon disulfide
Acetone dimethylacetal
1,1-Dimethoxyethane
Nitromethane
Turpentine
tert-Butylbenzene

[a] 0.25-ml sample taken for analysis.

water. On the other hand, not much more than 0.5 ml of ethanol and nitromethane, or 0.25 ml of solvents which yield low net absorbance or which reduce chromic acid can be analyzed. In the analysis of 0.5 ml of ethanol and 1 ml of acetonitrile or acetone, it is necessary to use 200–400 mesh dichromate to control the size of the blank.

Solvents which cannot be analyzed

The only solvents encountered that could not be analyzed are listed in Table III. Some of these solvents form emulsions with the diluting solvent or precipitate the magnesium perchlorate. Acetylacetone forms such a strong chelate with chromium(III) that rapid reduction of chromate is induced. Nitrobenzene absorbs strongly at 370 nm. The method apparently will not be applicable to the analysis of acids, pyrrolidinones, amines, amides, glycols and a few other solvents.

Determination of water in soluble and insoluble organic and inorganic solids by the proposed method

It seems probable that it will be possible to determine water in various organic

TABLE III

SOLVENTS WHICH CANNOT BE ANALYZED

Methanol	Piperidine	*n*-Methylformamide
Methyl acetate	Dicyclohexamine	Dimethylformamide
Ethyl dichloroacetate	Diethanolamine	Ethyleneglycol
Acetic acid	Triethanolamine	2-Methoxyethanol
Acetyl acetone	Triethylamine	Dimethylsulfoxide
2-Pyrrolidinone	1,3-Propanediamine	Paraldehyde
1-Methyl-2-pyrrolidinone	Nitrobenzene	α-Methylstyrene

or inorganic solid compounds if they can be dissolved in a suitable solvent and if they do not interfere in the analysis. Moreover, in certain instances, it should be possible to extract water from various insoluble solids by refluxing with a suitable dry solvent and then determining the water in the solvent by the proposed method.

Other methods for determining the chromate in MIBK

The spectrophotometric method cannot be used for the analysis of colored solvents which absorb strongly at 370 nm. Fortunately, the number of such solvents is limited. Moreover, as long as such absorption is not excessive it can be compensated for in the calibration. In the present work, the only colored solvent tested that could not be analyzed was nitrobenzene. However, it was shown that this solvent could be analyzed by X-ray analysis. To do this, proceed as directed in the spectrophotometric method but use an adjusted 0.05% magnesium perchlorate–MIBK solution. Then add 0.5 ml of a 1% solution of anhydrous lead acetate in methanol to the solution after filtration to remove dichromate, allow the solution to stand for 1 min, filter through a dry 25-mm, 7-μm nylon Millipore disk, allow the disk to dry, using suction, and determine the lead in the precipitate by X-ray analysis[3]. The X-ray method is not as widely applicable as the spectrophotometric method because a few solvents (*e.g.* ethyl formate, methyl sulfite) precipitate lead and a few others cause the precipitate of lead chromate to be colloidal. Moreover, in the X-ray method, the total amount of chromate ion that can be handled is limited by the X-ray counter. The counts per second for the precipitate on a disk must not exceed about 20,000. In meeting this limit, it is not uncommon to find that the net count from water is low when very reactive solvents are analyzed. On the other hand, in the spectrophotometric method it is possible to compensate for large blanks by using a suitable reference solution. This makes it possible deliberately to use conditions which produce a large blank in order to obtain an adequate net absorbance due to water.

Another approach to the analysis of colored solvents that was tested, consisted of aspirating the filtered MIBK solution directly into the flame of an atomic absorption spectrometer for the analysis of chromium. This method has the advantage that there is no need to work quickly, since the reduction of chromate is of no consequence. On the other hand, it was found that most solvents, other than MIBK, tend to suppress the chromium radiation in the flame. For this reason the method has limited value.

Quantitative analysis of commercial solvents

In order to evaluate the new method for the quantitative determination of

TABLE IV

DETERMINATION OF WATER IN COMMERCIAL SOLVENTS

Solvent	*% Water found*	
	Karl Fischer	*Spectrophotometric*
1,2-Dichloroethane	0.007	0.007
Trichloroethylene	0.006	0.004
Ethyl ether	0.003	0.002
Ethyl acetate	0.019	0.018
Tetrahydrofuran	0.02	0.02
Acetonitrile	0.06	0.06
4-Methyl-2-pentanone	0.012	0.011
Benzene	0.014	0.013
Toluene	0.030	0.031
Xylene	0.02	0.02
Isopropanol	0.022	0.021
Octanol	0.065	0.07
1,4-Dioxane	0.09	0.09
Pyridine	0.07	0.06
Acetone	0.30	0.30
Cyclohexanone	0.23	0.21

water, several J. T. Baker Chemical Company solvents were analyzed. Samples of 5 ml were used in the analysis of the first three solvents, and 0.3-ml samples were used for the analysis of acetone and cyclohexanone. The data obtained are shown in Table IV. Included in this Table are Karl Fischer analyses supplied by J. T. Baker Chemical Company. It is seen that the agreement between the methods is very good.

The author wishes to thank Mr. John Killar of the J. T. Baker Chemical Co. for supplying the Karl Fischer analyses shown in Table IV, and Mr. L. Blitzer of these laboratories for performing the atomic absorption analyses.

SUMMARY

A new method has been developed for the determination of small amounts of water in a wide variety of organic solvents. The water in the solvent is made to react with potassium dichromate to produce potassium chromate and chromic acid. The latter is soluble in the solvent. By measuring its amount spectrophotometrically, the concentration of water present in the solvent can be determined.

RÉSUMÉ

Une nouvelle méthode est proposée pour le dosage de faibles quantités d'eau dans divers solvants organiques. L'eau dans le solvant réagit avec le dichromate de potassium pour donner chromate de potassium et acide chromique. Ce dernier est soluble dans le solvant. On peut ainsi déterminer la concentration en eau du solvant par spectrophotométrie.

ZUSAMMENFASSUNG

Es wurde eine neue Methode für die Bestimmung kleiner Mengen Wasser in verschiedenen organischen Lösungsmitteln entwickelt. Das Wasser im Lösungsmittel reagiert mit Kaliumdichromat unter Bildung von Kaliumchromat und Chromsäure. Diese ist im Lösungsmittel löslich; durch spektrophotometrische Bestimmung ihrer Menge kann die Konzentration von Wasser im Lösungsmittel ermittelt werden.

REFERENCES

1 E. B. Sandell, *Colorimetric Determination of Traces of Metals*, 2nd Edn., Interscience, New York, 1950, p. 390.
2 G. F. Smith, O. W. Rees and V. R. Hardy, *J. Amer. Chem. Soc.*, 54 (1932) 3513.
3 C. L. Luke, *Anal. Chim. Acta*, 41 (1968) 237.

Analytica Chimica Acta
Elsevier Publishing Company, Amsterdam
Printed in The Netherlands

SPECTROPHOTOMETRIC DETERMINATION OF TELLURIUM IN STEELS AND CAST IRONS

S. MANESCHI AND C. GALLAZZI
Centro Sperimentale Metallurgico Casella postale 10747, Roma Eur. (Italy)

(Received 20th November 1970)

The control of tellurium content as an additive in steels and cast irons[1] has developed a certain importance, because small quantities of tellurium markedly improve the workability of steels as well as increasing their ductility. In cast irons, even contents of the order of 0.06% are sufficient to increase their hardenability. Accordingly, it seemed opportune to make available an analytical method providing sufficient accuracy and reproducibility for the determination of relatively low tellurium contents in ferrous-based materials.

The analytical method proposed here comprises two fundamental steps: separation by reduction of the tellurium from the metallic matrix and spectrophotometric measurement.

Each of these two steps has been examined in detail, although they are subject to close interdependence owing to numerous factors, such as precipitation conditions, acidity, type and concentration of the reducing agents, presence of a colloidal protector, etc.

SEPARATION OF TELLURIUM FROM THE METALLIC MATRIX

The most commonly used method for the separation of tellurium involves precipitation as the element by suitable reducing agents[2-5]. However, yields may be very dependent on the precipitation conditions. Uzumasa *et al.*[6] state, for example, that for less than 100 μg of tellurium only 40% yields are obtained by reduction with solid tin(II) chloride in 3 *M* hydrochloric acid; they therefore recommended extraction of the iron with *n*-butyl acetate in presence of dichromate for steels, but a little tellurium was also extracted and the procedure for its recovery was tedious. The authors reported yields ranging from 94 to 115% for 33–330 μg of tellurium in 0.1–1 g of iron. However, trials of the method in this laboratory showed even less satisfactory results.

The classical method of precipitation with tin(II) chloride was therefore reconsidered. The literature data on this method disagree somewhat. According to Luke[7], not more than 93% yield is obtained for microgram amounts of tellurium, even when arsenic is used as coprecipitant. Goto and Kakita[2] made a detailed study of precipitation conditions (quantity of reducing agent, acidity, etc.), and obtained quantitative yields of *ca.* 100 μg of tellurium with a sufficient amount of tin(II) chloride over a wide range of acid concentrations (hydrochloric, perchloric or sulphuric). Burke *et al*[5] obtained similar results for 5–50 μg of tellurium in 1.6–8 *M* hydrochloric acid solutions.

In the work described here, the precipitation yield was found to be less than quantitative, although it was better than the 40% reported by Uzumasa *et al.*[6]. The principal difficulty was found in filtering the extremely finely divided tellurium These techniques were tested in attempts to avoid this problem. First, the reduction was done in the presence of a coprecipitant such as arsenic or selenium; however, this did not lead to a greatly improved yield, whereas it created problems in determining tellurium in the presence of large amounts of coprecipitant. Secondly, the reduction was done in the presence of filter pulp, which served as a mechanical collector of the precipitate; almost complete precipitation was thus achieved, and the clear filtrates obtained were free from tellurium, but it was difficult to eliminate the last traces of iron and the excess of tin(II) from the pulp. Furthermore, in the subsequent dissolution of the tellurium with nitric acid or hydrogen peroxide organic substances from the pulp passed into the solution and were very difficult to remove. As in the first modification, the final solution therefore contained, besides tellurium, various substances which interfered in the subsequent determination; for example, fuming with sulphuric or perchloric acid led to a permanent cloudiness through the insolubilization of tin. Finally, the filtration was done on cellulose membranes (Millipore BDWPO 4700) of 0.6-μm pore diameter. In this way, the filtrates were perfectly clear and the precipitate could be washed thoroughly in order to eliminate the iron and the excess of tin(II) chloride; a small amount of tin remains in the precipitate, as already noted by Burke *et al.*[5]. Redissolution of the precipitate was readily achieved by immersing the membrane in nitric acid, without interfering substances passing from it into the solution.

Various tests were made with this system to estimate the precipitation yield; the results are given in Table I. The yield is not quantitative but is sufficiently constant for different amounts; it is therefore possible to obtain valid results with a calibration curve obtained by means of the precipitation method, which takes account of the tellurium loss.

TABLE I

PRECIPITATION YIELD WITH TIN(II) AND FILTRATION ON MILLIPORE MEMBRANES

Te added (μg)	*Te found (μg)*	*Precipitation yield (%)*
40	36	90.0
80	71	88.7
140	125	89.3

SPECTROPHOTOMETRIC DETERMINATION

Few reagents for tellurium have been reported in the literature, and these are not particularly good with respect to selectivity, stability, etc. Sodium diethyldithiocarbonate (DDTC) was proposed by Bode[8], who recommended a pH around 8.5, and masked some of the many interferences with EDTA and cyanide. According to

Luke[7], and Goto and Kakita[2], tellurium can be extracted with DDTC in benzene or chloroform over a wide interval of acidity; Luke obtained satisfactory results in solutions of pH 8.5 up to 1–2 *M* acid, whereas Goto and Kakita used a sulphuric acid medium in concentrations varying from $5 \cdot 10^{-4}$ to 5 *M*. However, Nonova and Tuzsuzova[9] found the extraction to be strongly influenced by pH, being complete only in the limited pH range of 8.7–8.8. In the present work, the DDTC method was found to be unsatisfactory both in acid solution and in alkaline solution in the presence of complexing agents; the development of the colour was much influenced by the acidity, and was subject to numerous interferences. Moreover, the complex is unstable to light, particularly ultraviolet light. These difficulties led to the abandonment of the DDTC method.

The thiourea method[4] was then examined. Tellurium was separated by reduction with tin(II) chloride and dissolved in nitric acid, and the colour was developed by adding 1 g of thiourea. Maximum absorbance of the tellurium–thiourea complex occurs at *ca.* 320 nm, *i.e.* in a wavelength range at which interference from organic substances from the filter, or from minute amounts of iron or tin[10] left in the precipitate can readily happen. Though the Millipore membrane filtration reduced the first factor to a negligible level, the latter factor varied in an uncontrollable manner; spurious absorbance measurements were occasionally found, even though the solutions showed no visible colouration.

Finally, the spectrophotometric determination of tellurium precipitated in the colloidal state was examined. This method is less sensitive than the thiourea

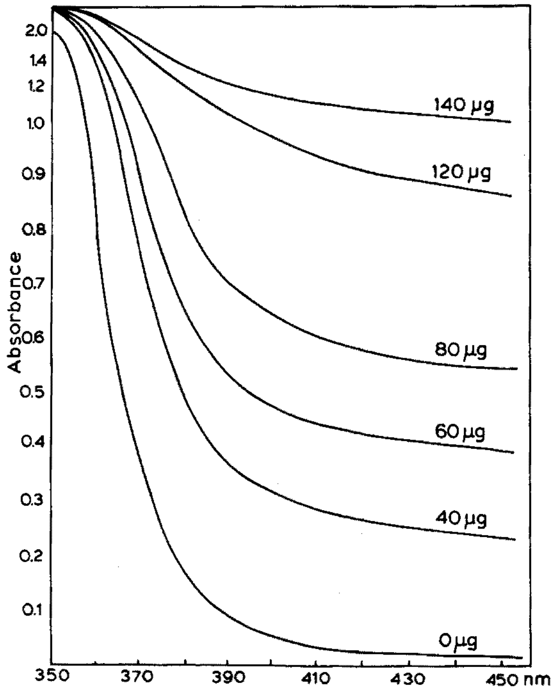

Fig. 1. Absorption curves of tellurium.

procedure but has the advantages that maximal absorbance occurs in the visible range, and that iron and tin do not interfere. Direct determination of tellurium in cast irons without previous separation from the matrix has been reported[11]. In order to increase the sensitivity for the present purpose, tellurium was separated by precipitation with tin(II) chloride and redissolved, and then a second precipitation was done in suitable conditions for the formation of a stable colloidal solution. The dimensions of the colloidal particles, and the absorption spectrum depend[12,13] on the precipitation conditions (acidity, type and concentration of the reducing agent, presence of a colloidal protector, etc.). In order to be able to conduct the measurements in the visible field, the operating conditions were those suggested by Schoeller[14]; a "red sol" whose absorbance is measured around 410 nm, was obtained.

Figure 1 shows the curves obtained for colloidal solutions with varying tellurium contents, after reaction with tin(II) chloride in a hydrochloric medium; absorbances were measured against water in 40-mm glass cells. When gum arabic was added, the absorbances were stable for more than 2 h. A wavelength of 410 nm was used for further measurements; at this wavelength the average molar absorptivity was 5,200, and the sensitivity was 0.0245 μg cm^{-2}, according to Sandell's definition[15].

The calibration curve prepared from 72 independent measurements in the presence of iron by the recommended method (see below) was found to be linear over the range 0–140 μg of tellurium. The correlation coefficient between the absorbance values and the amount of tellurium was 0.9963. Table II shows the values for the standard deviation and the coefficient of variation calculated for four series of calibration measurements.

TABLE II

VALUES OF THE ABSORBANCE MEASUREMENTS FOR FOUR LEVELS OF TELLURIUM

Te added (μg)	*No. of detns.*	*Absorbance, E*	*Standard deviation, σ*	*Coefficient of variation, $(\sigma/E)\cdot 100$*
0	12	0.040	0.0018	4.5
40	20	0.295	0.012	4.0
80	20	0.555	0.018	3.3
140	20	0.940	0.023	2.4

Interferences

There was a difference between the values obtained in the absence and in the presence of different quantities of iron, but this was not related to the amount of iron in the solution. It was shown that when the solution of tin(II) chloride used was previously filtered through a Millipore membrane, blank values were much more reproducible, and the results were practically independent of the presence of iron (Table III).

It was found that quantitative reduction was obtained even in the presence of large quantities of chromium(VI); 40 μg of tellurium in 1 g of iron was determined in the presence of 200 mg of chromium.

Of the other elements which may be present in the sample solution, the only

TABLE III

COMPARISON BETWEEN ABSORBANCE VALUES OBTAINED IN THE ABSENCE AND PRESENCE OF IRON

Te added (μg)	*Absorbance*	
	Without Fe	*With 0.5 g Fe*
20	0.165	0.172
60	0.408	0.415
100	0.650	0.647
140	0.940	0.940

ones which can interfere are those that can be precipitated by reduction with tin(II) in 3 *M* hydrochloric acid. Among elements which may be found in steel or cast iron, only arsenic causes interference, giving a brown precipitate. However, up to 500 μg of arsenic can be tolerated in the spectrophotometric determination of 100 μg of tellurium in 0.5 g of iron; 600 μg causes a positive error of 5%, whereas 1500 μg causes an error of +28%.

RECOMMENDED PROCEDURE

Dissolve in a 250-ml beaker a quantity of the sample containing between 10 and 150 μg of tellurium with 25 ml of a mixture prepared from 50 ml of perchloric acid ($d = 1.67$), 25 ml of concentrated nitric acid ($d = 1.40$) and 25 ml of water. Evaporate, fume with perchloric acid, cool and add a few millilitres of (1 + 1) hydrochloric acid. Boil for some minutes and filter if necessary to eliminate silica and any carbon. Dilute with (1 + 1) hydrochloric acid, bring almost to the boil, add 10 g of tin(II) chloride tetrahydrate and allow to boil until complete dissolution of the tin(II) chloride occurs. Allow to cool and leave for 1 h. Filter on a Millipore BDWPO 4700 membrane (pore diameter, 0.6 μm), washing three times with cold (1 + 1) hydrochloric acid and then with cold water. Put the membrane in the beaker in which precipitation was carried out and dissolve the tellurium with 15 ml of (1 + 1) nitric acid, heating on a sand bath. Remove the membrane, washing it with water, add 2 ml of sulphuric acid ($d = 1.83$) and evaporate the solution until it begins to fume. Transfer the solution to a 25-ml calibrated flask, washing the beaker with two 5-ml portions of hydrochloric acid ($d = 1.19$). Introduce 5 ml of a hydrochloric acid solution of tin(II) chloride (100 g of tin(II) chloride tetrahydrate in 100 ml of hydrochloric acid ($d = 1.19$) filtered on a Millipore membrane BDWPO 4700 and stored in the dark) and 2 ml of a 2% (w/v) solution of gum arabic, and finally dilute to volume with water. Measure the absorbance on a spectrophotometer at 410 nm in 40-mm cells against water.

Calibration curve

In a series of 250-ml beakers, place 1 g of pure "Merck" iron and 0, 2, 4, 6, 8 ml of a tellurium solution obtained by dissolving 0.01 g of metallic tellurium in 15 ml of (1 + 1) nitric acid and 10 ml of sulphuric acid ($d = 1.83$), fuming the sulphuric acid and diluting to 1 l (1 ml corresponds to 100 μg of tellurium). Then dissolve as for the samples and complete the procedure as described above.

RESULTS AND DISCUSSION

To check the method a series of determinations was carried out on the only two available commercial standard samples, NBS 1174 with certified 0.073% Te and NBS 1175 with certified 0.009% Te. The analysis certificates showed that laboratories of the National Bureau of Standards had standardized the samples by polarographic and radiochemical[16] methods.

Table IV shows the results obtained by the above recommended procedure. It can be seen that the values found are in excellent agreement with the certified values.

TABLE IV

TELLURIUM IN STANDARD SAMPLES OF WHITE CAST IRON

Sample	*Tellurium found (%)*		
	Polarographic method[a] *NBS*	*Activation method*[b] *NBS*	*Spectrophotometric method*[c] *CSM*
1174	0.071 0.071 0.071	0.071 0.079 0.073	0.070 0.074
			0.075 0.073
	0.070 0.072 0.071	0.075 0.068 0.080	0.076 0.072
	Mean 0.071	Mean 0.074	Mean 0.073
1175	0.0092 0.0094	0.0091 0.0092	0.0090 0.0094
	0.0086 0.0084	0.0092 0.0096	0.0095 0.0093
	0.0087 0.0089		0.0096 0.0092
	Mean 0.0089	Mean 0.0093	Mean 0.0093

[a] E. J. MAIENTHAL AND J. K. TAYLOR, Analytical Chemistry Division, NBS, Washington.
[b] D. A. BECKER AND G. W. SMITH, Radiochemical Analysis Section, NBS, Washington.
[c] C. GALLAZZI AND C. CATANO, Analytical Chemistry Group, CSM, Rome.

The method described appears to be applicable to cast irons and most types of steel. Copper and nickel do not interfere[11], and in the proposed method, the interference of chromium is avoided by the filtration procedure. Tests on a cast iron (NBS 342) containing 2.14% of graphitic carbon (2.45% of carbon) by the standard addition method showed that there was no interference from this source, and this was confirmed for other cast irons containing up to 2.63% of graphitic carbon.

The use of Millipore filters allows reasonably rapid yet quantitative filtration of the precipitated tellurium, without the introduction of interfering substances. The sensitivity obtained by measurement at 410 nm is sufficient for the present purpose. Greater sensitivity can be achieved by measuring at lower wavelengths but blank values then tend to be rather high.

SUMMARY

A method for the determination of tellurium in steels and cast irons is described. The conditions for separation of tellurium from the metallic matrix by precipitation as the element with tin(II) in hydrochloric acid medium and its subsequent filtration were examined. Tellurium is then dissolved and reprecipitated in a colloidal form for spectrophotometric determination. The method is free of interferences from elements commonly present in steels and cast irons, except for arsenic in amounts above 500 µg; chromium and graphitic carbon do not interfere. The procedure is suitable for tellurium in the range 0–140 µg.

RÉSUMÉ

On décrit une méthode de dosage du tellure dans les aciers et les fontes. Les conditions de séparation du tellure d'avec la matrice métallique sont examinées; elle consiste en une précipitation de l'élément avec l'étain(II) en milieu acide chlorhydrique et filtration. Le tellure est ensuite dissous, reprécipité sous forme colloïdale et dosé spectrophotométriquement. Cette méthode est exempte d'interférences d'éléments communément présents dans les aciers et les fontes, sauf pour l'arsenic en concentrations supérieures à 500 µg; le chrome et le carbone graphitique ne genent pas. Ce procédé convient pour des quantités de 0 à 140 µg de tellure.

ZUSAMMENFASSUNG

Es wird eine Methode für die Bestimmung von Tellur in Stählen und Gusseisen beschrieben. Die Bedingungen für die Abtrennung des Tellurs von der metallischen Matrix durch Fällung als Element mit Zinn(II) in salzsaurem Medium und seine anschliessende Filtration wurden untersucht. Das Tellur wird dann aufgelöst und in einer kolloiden Form für die spektrophotometrische Bestimmung erneut gefällt. Die Methode wird durch die in Stählen und Gusseisen vorliegenden Elemente nicht gestört, abgesehen von Arsen in Mengen grösser als 500 µg; Chrom und graphitischer Kohlenstoff stören nicht. Das Verfahren ist für Tellur im Bereich 0–140 µg geeignet.

REFERENCES

1 Centro Sperimentale Metallurgico, *Rapporto MES/P2, (re-1)*, 1966.
2 H. Goto and Y. Kakita, *Japan Analyst*, 3 (1954) 229.
3 H. Goto and Y. Kakita, *Sci. Rept. Res. Inst. Tohoku Univ., Ser. A*, 7 (1955) 365.
4 K. Ota, *Nippon Kinzoku Gakkaishi*, 23 (1959) 581.
5 K. E. Burke, M. M. Yanak and C. H. Albricht, *Anal. Chem.*, 39 (1967) 14.
6 Y. Uzumasa, K. Hayashi and S. Ito, *Bull. Chem. Soc. Japan*, 36 (1963) 301.
7 C. L. Luke, *Anal. Chem.*, 31 (1959) 572.
8 H. Z. Bode, *Z. Anal. Chem.*, 144 (1955) 90.
9 D. Nonova and A. Tuzsuzova, *Mikrochim. Acta*, 5 (1964) 784.
10 W. Nielsch and G. Boltz, *Z. Anal. Chem.*, 143 (1954) 161.
11 W. Westwood and A. Mayer, *Chemical Analysis of Cast Iron and Materials*, Allen and Unwin, London, 1960.
12 D. F. Boltz, *Colorimetric Determination of Nonmetals*, Interscience Publishers, New York, 1958, p. 315.
13 O. G. Koch and G. A. Koch-Dedic, *Handbuch der Spurenanalyse*, Springer Verlag, Berlin, 1964, p. 919.
14 W. R. Schoeller, *Analyst*, 64 (1939) 18.
15 E. B. Sandell, *Colorimetric Determination of Traces of Metals*, 3rd Edn., Interscience Publishers, New York, 1959, p. 75.
16 J. E. Maienthal and J. K. Taylor, *Anal. Chem.*, 37 (1965) 1516.

Analytica Chimica Acta
Elsevier Publishing Company, Amsterdam
Printed in The Netherlands

EXTRACTION-SPECTROPHOTOMETRIC STUDIES ON THE REACTIONS OF MANGANESE(II) WITH DITHIZONE

ZYGMUNT MARCZENKO AND MIROSŁAW MOJSKI
Department of Analytical Chemistry, Politechnika, Warsaw (Poland)

(Received 6th November 1970)

Dithizone (diphenylthiocarbazone) is a very important reagent for the colorimetric determination of metals, but its reaction with manganese(II) has not been fully studied. Akaiwa and Kawamoto[1] were the first to note the synergic effect of pyridine on the extraction of manganese by dithizone (H_2Dz) and to utilize this analytically. They showed that the extractable species had the composition $Mn(HDz)_2Py_n$, the value of n being unestablished. In the work described here, these results were extended, and practicable methods were developed for the determination of manganese(II).

EXPERIMENTAL

Apparatus

Several spectrophotometers were used, depending on the purpose of the measurement; unless otherwise stated, 1-cm glass cuvettes were used. pH values were measured with a Ridan compensation pH-meter, and a glass–saturated calomel electrode pair.

Reagents

Spectroscopically pure hydrochloric acid, nitric acid, and sulphuric acid, and an ammonia solution prepared by saturating twice-distilled water with gaseous ammonia were used. Twice-distilled water was used throughout.

Standard manganese solution, 0.1 *M*. Dissolve 7.5460 g of manganese(II) sulphate (dried at 150° and calcined at 400°) in water containing 1 ml of concentrated sulphuric acid and dilute to 500 ml with water.

Dithizone (H_2Dz), $5 \cdot 10^{-4}$ *M in* CCl_4 (*or in* $CHCl_3$). Dissolve 0.0320 g of purified dithizone[2] in carbon tetrachloride and dilute to 250 ml with the solvent. Dilute this stock solution suitably with the appropriate solvent to obtain working solutions.

Pyridine. Commercial (C.P.) pyridine was purified by distillation through a laboratory column to collect the fraction of b.p. 115.5°–115.6°.

Hydroxylamine, 2 *M solution*. Dissolve 14 g of hydroxylammonium chloride in 100 ml of water, neutralize with aqueous sodium hydroxide (pH *ca.* 7) and purify with dithizone.

Potassium sodium tartrate, 20% *solution*. Purify with dithizone at pH *ca.* 8.5.

Ammonia buffer, *pH* 9.8. Dissolve 21 g of ammonium chloride in water, purify the solution with dithizone, add 120 ml of concentrated ammonia, 1.4 g of potassium cyanide, and 200 ml of pyridine, and dilute to 1 l with water.

Distribution of manganese

Distribution coefficients were calculated from measurements of manganese in the aqueous and organic phases, manganese being stripped with 1 *M* hydrochloric acid from the organic phase. The manganese was determined either colorimetrically with formaldoxime[3] or spectrophotometrically by the procedure described below.

Direct determination of manganese

To less than 5 ml of a solution at pH 2–3 containing below 10 μg of manganese add 1 ml of the hydroxylamine solution. Shake the resulting solution (pH 6.5–7.0) with portions of 0.003% dithizone in carbon tetrachloride until the colour of dithizone does not change. To the aqueous solution, add 1 ml of the tartrate solution and 2.5 ml of the buffer. Dilute to *ca.* 10 ml with water and shake the mixture for 1 min with exactly 10 ml of 0.003% dithizone in carbon tetrachloride. Measure the absorbance at 510 nm against a blank solution.

Determination of manganese by reversion

Follow the direct method until the extract of the manganese complex in carbon tetrachloride is obtained. Halve the extract and shake one portion for 1 min with 10 ml of 1 *M* hydrochloric acid. Measure the absorbance of the carbon tetrachloride solution shaken with acid at 620 nm with the portion unshaken with hydrochloric acid in the reference cell.

RESULTS AND DISCUSSION

Manganese(II)–dithizone system

In chloroform solution dithizone reacts with manganese(II) at pH 9–11 to yield a violet complex which can be extracted into the organic phase. Hydroxylamine was added to keep manganese in the correct oxidation state.

The complex shows maximum absorbance at 515 nm; it decomposes on standing to regenerate dithizone. The composition of the complex was established by determining the manganese colorimetrically with formaldoxime, and the dithizone by its absorbance at 605 nm. Whether dithizone or manganese was in excess, the complex was found to be a primary dithizonate, $Mn(HDz)_2$.

Maximal extraction of manganese(II) occurs over the pH range 9.5–11, but the reaction is incomplete. For $[Mn]:[H_2Dz]$ ratios of 1:2.5, 1:12.5 and 1:50, the percentage extraction of manganese is 38, 45 and 58%, respectively. With a 1000-fold excess of manganese over dithizone, only about 60% of the latter is used.

When chloroform was replaced by the less polar solvent carbon tetrachloride, the primary manganese(II) dithizonate separated as a red-brownish solid at the interface. The composition of the complex was established by filtering off the solid and washing it before decomposition with 0.1 *M* sulphuric acid in the presence of silver ions and carbon tetrachloride; dithizone was determined by measuring the absorbance of silver dithizonate in carbon tetrachloride, and manganese with formaldoxime. With carbon tetrachloride, maximal extraction was obtained within the pH range 9.0–10.3, but as with chloroform percentage extraction was low, indicating the low stability of the complex.

Manganese(II)-dithizone–pyridine system

In the presence of pyridine, manganese(II) reacts with dithizone in carbon tetrachloride to yield an extractable complex $Mn(HDz)_2Py_n$ with maximal absorption at 510 nm[1]. Absorption curves for this complex and for dithizone in carbon tetrachloride solutions are presented in Fig. 1. The absorbance of the complex is stable for 10 min. Hydroxylamine was added to the aqueous phase to ensure the presence of manganese(II), and 0.005 *M* cyanide was added to mask heavy metal traces, without affecting the manganese-dithizone reaction.

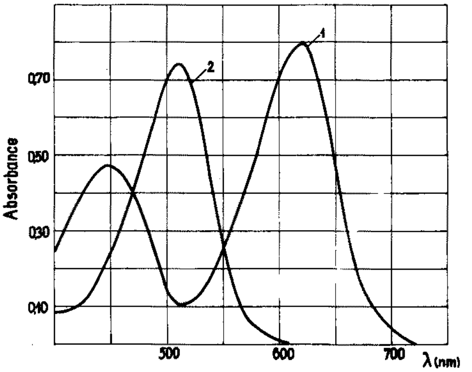

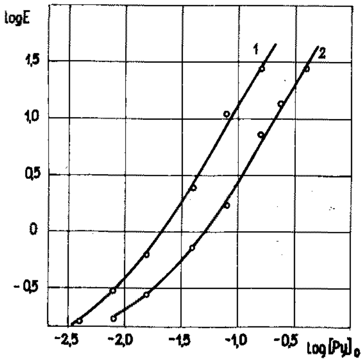

Fig. 1. Absorption spectra of a solution of $Mn(HDz)_2Py_2$ (2) and dithizone (1) in CCl_4. $[H_2Dz]=2.5\cdot10^{-5}$ *M*, $[Py]=0.62$ *M*, $[Mn]=1\cdot10^{-2}$ *M*, pH = 8.7.

Fig. 2. Coefficient of extraction (*E*) of manganese(II) in relation to concentration of pyridine in the organic phase. (1) $[H_2Dz]=2.5\cdot10^{-4}$ *M*, pH = 8.7; (2) $[H_2Dz]=8\cdot10^{-5}$ *M*, pH = 9.5.

The value of *n* was established by plotting the distribution ratio $E=\Sigma[Mn]_{org}$ $[Mn^{2+}]$, for different concentrations of pyridine. Plots of log *E* against log [Py] at a fixed concentration of dithizone and fixed pH were linear over the range 0.05–0.40 *M* pyridine (Fig. 2) and the slope of 2 indicates the composition $Mn(HDz)_2Py_2$ for the extracted complex. The equilibrium concentrations of pyridine were calculated from the known initial concentrations, taking into account the partition between the two phases, and using the value $P=[Py]_{CCl_4}/[Py]=1.7$, measured acidimetrically, for $0.1 \leqq [Py] \leqq 1.2$ *M*.

Linear plots (not reproduced) of slope 2 were also obtained for plots of log *E* against log $[H_2Dz]$ for $[Py]_{org}=0.39$ *M* and at pH 8.6 and 9.2, and for plots of log *E* against pH for $[Py]_{org}=0.39$ *M* and $[H_2Dz]_{tot}=8\cdot10^{-5}$ *M* and $[Py]_{org}=0.08$ *M* and $[H_2Dz]_{tot}=2\cdot10^{-4}$ *M*. These results establish conclusively the composition of the synergically extracted species.

Extraction of manganese can be represented by

$$Mn^2+2\,(H_2Dz)_{org}+2(Py)_{org} \rightleftharpoons (Mn(HDz)_2Py_2)_{org}+2\,H^+$$

hence,

$$K_{ex}=\frac{[Mn(HDz)_2Py_2]_{org}[H^+]^2}{[Mn^{2+}][H_2Dz]^2_{org}[Py]^2_{org}}=E\cdot\frac{[H^+]^2}{[H_2Dz]^2_{org}[Py]^2_{org}}$$

The extraction constant, K_{ex}, was measured at ionic strength $I = 0.2$ (NaCl) with $[CN^-]_{tot} = 0.005\ M$; the pH value lay in the range 7.2–8.7, where both protonation of pyridine (p$K = 5.22$) and hydrolysis of manganese(II) (p$K = 10.52$) are negligible. The complexing action of pyridine, chloride and ammonia on manganese(II) in the aqueous phase could be ignored; any error thus introduced would be lower than that inherent in measuring E, $[H_2Dz]_{org}$, and pH.

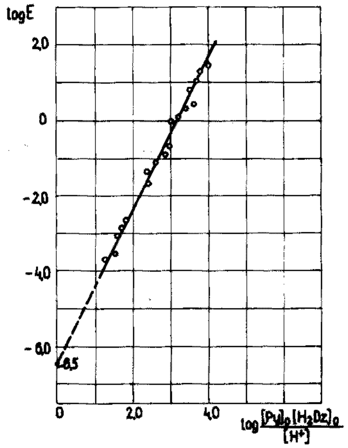

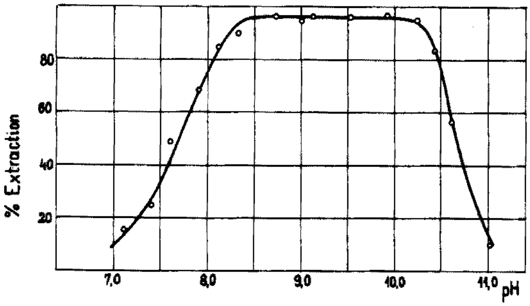

Fig. 3. Graphical determination of the extraction constant for $Mn(HDz)_2Py_2$ into carbon tetrachloride. $I = 0.2$ (NaCl), $[CN^-] = 0.005\ M$.

Fig. 4. Percentage extraction of manganese(II) in relation to pH. $[H_2Dz] = 1 \cdot 10^{-4}\ M$, $[Py] = 0.62\ M$, $[Mn] = 1 \cdot 10^{-5}\ M$.

The plot of log E *vs.* log $[H_2Dz]_{org}[Py]_{org}/[H^+]$ is linear and of the predicted slope of 2. Extrapolation gives log $K_{ex} = -6.5$ (Fig. 3).

The effects of concentrations of the reagents and of pH on the absorbance of the extracts were examined. Absorbances of carbon tetrachloride solutions of $Mn(HDz)_2Py_2$ were measured with reference to a blank, except when the effect of manganese concentration was studied, when carbon tetrachloride was used. Increase in the pyridine concentration increased the absorbance of the organic extract up to a concentration of 0.4 M, above which the absorbance remained constant, for $[H_2Dz] = 1 \cdot 10^{-4}\ M$, $[Mn^{2+}] = 1 \cdot 10^{-5}\ M$ and pH = 9.8. For $[Mn^{2+}] = 1 \cdot 10^{-5}\ M$ and $[Py] = 0.62\ M$ at pH 9.2 or 9.8, the percentage extraction of manganese(II) increased as the dithizone concentration increased, up to a molar excess of 10:1, after which it remained constant. Dithizone reacted completely with manganese when the concentration of the latter was at least 200 times as high as that of the former. With the adopted concentrations of dithizone and pyridine at pH 8.5–10.2, the percentage extraction of manganese was about 95% (Fig. 4). Above pH 10.2, the percentage extraction was reduced by hydrolysis of manganese and almost complete passage of dithizone from the organic into the aqueous phase.

Use of the complex $Mn(HDz)_2Py_2$ for the determination of manganese

The studies described above indicate that the ternary complex should be useful in providing a sensitive extraction–spectrophotometric method for the determination of manganese.

However, at the pH values necessary for almost quantitative extraction of manganese, a considerable portion of dithizone passes into the aqueous phase, and it is therefore essential to maintain a high concentration of dithizone in the organic phase. Unfortunately, this leads to an unfavourably high blank value. Free dithizone cannot be washed out of the carbon tetrachloride extract containing $Mn(HDz)_2Py_2$, because the complex is then partially decomposed. In Fig. 5, the blank absorbance value is plotted against the pH of the aqueous phase.

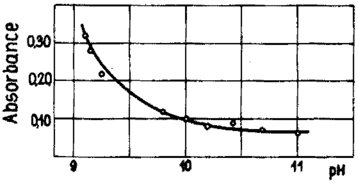

Fig. 5. Blank absorbance in relation to pH. $[H_2Dz]=1\cdot10^{-4}$ *M*, $[Py]=0.62$ *M*.

TABLE I

DETERMINATION OF MANGANESE IN SODIUM CHLORIDE P.A. AND IN HIGH-PURITY TIN METAL

Material	*Method*	*Mn found*[a] (%)	*Standard deviation, $\bar{s}$*	*Mn added* (%)	*Total Mn found* (%)
NaCl p.a.	Direct	$1.5\cdot10^{-5}$	$7\cdot10^{-7}$	$1\cdot10^{-5}$	$2.4\cdot10^{-5}$ $2.2\cdot10^{-5}$
	Reversion	$1.4\cdot10^{-5}$	$4\cdot10^{-7}$	$1\cdot10^{-5}$	$2.4\cdot10^{-5}$ $2.3\cdot10^{-5}$
High-purity tin	Direct	$7.4\cdot10^{-5}$	$3.4\cdot10^{-6}$	$1\cdot10^{-4}$	$1.6\cdot10^{-4}$ $1.6\cdot10^{-4}$
	Reversion	$7.5\cdot10^{-5}$	$2.8\cdot10^{-6}$	$1\cdot10^{-4}$	$1.7\cdot10^{-4}$ $1.6\cdot10^{-4}$

[a] The average of 6 determinations.

If it is assumed that the manganese concentrations are of the order of $1\cdot10^{-5}$ *M* (maximum 1 μg ml^{-1}), the following reagent concentrations are recommended: 0.003% (w/v) dithizone in carbon tetrachloride, 5% (v/v) pyridine in water, and a pH values of 9.8. Addition of hydroxylamine ensures the presence of only manganese(II), whereas addition of cyanide reduces the blank value.

Two procedures are suggested, the direct procedure and the reversion procedure[4]. In the latter, the absorbance of a dithizone solution obtained after the complex has been decomposed is measured, 1 *M* hydrochloric acid acting as the reversion agent.

In the direct procedure, the molar absorptivity (ε) is 57000 (specific absorptivity[5], $a=\varepsilon/(\text{at. wt.}\cdot1000)=1.02$) at 510 nm, and in the reversion procedure $\varepsilon=64000$ ($a=1.17$) at 620 nm.

The proposed method for the determination of manganese is highly selective.

Under the conditions adopted and with various metals removed by prior extraction with dithizone at pH 7, thallium is the only interference.

This dithizone–pyridine method was used to determine manganese in analytical reagent-grade sodium chloride and in high-purity tin. After the samples had been brought into solution, manganese was separated by using a lanthanum carrier[6]. The analytical data listed in Table I indicate the good precision and accuracy of the method employed; the reversion method affords the better precision.

SUMMARY

Manganese(II) can be extracted as the primary dithizonate $Mn(HDz)_2$ over the optimal pH ranges 9.5–11.0 ($CHCl_3$) or 9.0–10.3 (CCl_4). Even with the dithizone in large excess only 50–60% of manganese is extracted. Synergic enhancement in the presence of 0.6 *M* pyridine leads to extraction of the complex $Mn(HDz)_2Py_2$, over the pH range 8.5–10.2 provided that a 10-fold excess of dithizone is present. The extraction constant for CCl_4 is $3 \cdot 10^{-7}$. Direct and reversion procedures for the spectrophotometric determination of manganese(II) are described and applied to the determination of manganese in sodium chloride (p.a.) and high-purity tin. Only thallium(I) interferes.

RÉSUMÉ

Le manganèse(II) peut être extrait comme dithizonate primaire, $Mn(HDz)_2$, aux pH 9.5 à 11.0 ($CHCl_3$) ou 9.0 à 10.3 (CCl_4). On ne peut extraire que 50 à 60% de manganèse, même en présence d'un grand excès de dithizone. Une addition de pyridine 0.6 *M* conduit à une extraction du complexe $Mn(HDz)_2Py_2$ aux pH de 8.5 à 10.2, avec un excès de 10 fois de dithizone. La constante d'extraction pour CCl_4 est de $3 \cdot 10^{-7}$. Des méthodes sont proposées pour le dosage spectrophotométrique du manganèse(II) avec application dans le chlorure de sodium (p.a.) et l'étain très pur. Seul le thallium(I) gêne.

ZUSAMMENFASSUNG

Mangan(II) kann als primäres Dithizonat $Mn(HDz)_2$ in den optimalen pH-Bereichen 9.5–11.0 ($CHCl_3$) oder 9.0–10.3 (CCl_4) extrahiert werden. Auch mit Dithizon in grossem Überschuss werden nur 50–60% des Mangans extrahiert. Die synergetische Steigerung in Gegenwart von 0.6 *M* Pyridin führt zur Extraktion des Komplexes $Mn(HDz)_2Py_2$ im pH-Bereich 8.5–10.2, vorausgesetzt dass ein 10-facher Dithizonüberschuss vorhanden ist. Die Extraktionskonstante für CCl_4 ist $3 \cdot 10^{-7}$. Es werden unmittelbare und Umkehrverfahren für die spektrophotometrische Bestimmung von Mangan(II) beschrieben und auf die Bestimmung von Mangan in Natriumchlorid (p.a.) und hochreinem Zinn angewendet. Nur Thallium(I) stört.

REFERENCES

1 H. Akaiwa and H. Kawamoto, *Anal. Chim. Acta*, 40 (1968) 407.
2 O. B. Mathre and E. B. Sandell, *Talanta*, 11 (1964) 295.
3 Z. Marczenko, *Anal. Chim. Acta*, 31 (1964) 224.
4 H. M. Irving and E. J. Butler, *Analyst*, 78 (1953) 571.
5 G. H. Ayres and B. D. Narang, *Anal. Chim. Acta*, 24 (1961) 241.
6 Z. Marczenko and M. Mojski, *Chem. Anal. (Warsaw)*, 12 (1967) 1155.

Analytica Chimica Acta
Elsevier Publishing Company, Amsterdam
Printed in The Netherlands

DETERMINATION OF LEAD, CADMIUM, ZINC AND MANGANESE IN COPPER BY ANODIC STRIPPING VOLTAMMETRY

G. VAN DIJCK AND F. VERBEEK
Laboratory for Analytical Chemistry, Ghent University, Ghent (Belgium)

(Received 6th December 1970)

The determination of traces of four important impurities[1,2] in copper and copper compounds, *i.e.* lead, cadmium, zinc and manganese, by means of anodic stripping voltammetry on a hanging mercury drop electrode is discussed in this paper. The determination of bismuth in copper has already been described[3]; determinations of antimony and tin will be discussed later.

Because the half-wave potentials of the four elements studied are more negative than that of copper in all supporting electrolytes, separations are necessary. Classical polarography has already been used to determine these elements in copper and copper compounds[4-9]. After separation, the detection limit is between 1 and 40 p.p.m. which is sometimes insufficient for the determination of traces of these elements in high-purity copper. Anodic stripping voltammetry is a very versatile technique for trace analysis, because various metal ions in concentrations as low as 10^{-8}–10^{-10} M can be determined. The possibilities, sensitivity and the limitations of this technique have recently been reviewed in detail by Barendrecht[10] and Neeb[11].

EXPERIMENTAL

Apparatus and reagents

The equipment for stripping voltammetry and the working conditions were described earlier[3]. A Metrohm Polarecord 261R equipped with a Metrohm E410 hanging mercury drop electrode was used. The mercury drops had a weight of 4.52 mg.

A potentiostat, constructed as described by Lamphere and Rogers[12], was used for the electrolytic separation of copper at controlled potential.

Analytical-grade potassium chloride was purified by electrolysis of a concentrated solution in water for 24 h at a cathode potential of -1.5 V *vs.* S.C.E. The electrolysis was performed under a nitrogen atmosphere in separate electrode compartments. Ammonia solution was prepared by isopiestic distillation at room temperature. Other reagents were further purified as described previously[3]. High-purity nitrogen (< 1 p.p.m. of oxygen) was used to remove oxygen from the cell.

The mercury for the hanging drop electrode must be very pure. After oxidation of the impurities by an air current followed by filtration and distillation, the mercury was refined electrolytically by anodic oxidation and cathodic reduction in nitric acid (1 : 20)[13]. After washing thoroughly with water and drying, the mercury was ready for use.

Polarographic data

As already stated, the direct polarographic or voltammetric determination of traces of lead, cadmium, zinc and manganese in copper is not possible because the half-wave potentials of these elements are more negative than that of copper[14].

After preliminary separation of the copper matrix by electrolysis at controlled potential in 0.1 *M* hydrochloric acid (see below), lead ($E_{\frac{1}{2}} = -0.44$ V *vs.* S.C.E.) and cadmium ($E_{\frac{1}{2}} = -0.64$ V) can be determined directly in the remaining solution. Zinc is determined in 0.1 *M* ammonium chloride ($E_{\frac{1}{2}} = -1.0$ V) or in 0.1 *M* ammonium chloride – 0.3 *M* ammonia ($E_{\frac{1}{2}} = -1.35$ V), and manganese in 0.1 *M* potassium chloride ($E_{\frac{1}{2}} = -1.51$ V). The optimal pre-electrolysis potential and time, the influence of factors such as stirring, variation of temperature and scanning rate and also the dissolution potential of the four elements investigated, were established by a preliminary investigation.

When a mercury drop of 0.0233 cm^2 (weight 4.517 mg) and a scanning rate of 0.167 V min^{-1}, a volume of 25 ml and a pre-electrolysis time of 10 min are used, the quantitative limit of anodic stripping voltammetry, according to criteria given by Currie[15], is about 10^{-9} *M* for lead and zinc and $5 \cdot 10^{-10}$ *M* for cadmium. Under these conditions, the peak height is about 10 mm at an instrumental sensitivity of 10^{-10} A mm^{-1}. The limit for manganese is about 10^{-8} *M* for a preelectrolysis time of 25 min at an instrumental sensitivity of $5 \cdot 10^{-10}$ A mm^{-1}. This is less than for the other elements because of the sloping base line of the supporting electrolyte at the fairly negative potential where the oxidation of manganese occurs.

To verify the precision and the linearity between peak height and concentration, calibration curves were established over wide concentration ranges: for lead and cadmium in 0.1 *M* hydrochloric acid, for zinc in 0.1 *M* ammonium chloride and for manganese in 10^{-1} *M* potassium chloride. The observed values between 10^{-6} and

TABLE I

CALIBRATION CURVE VALUES

(Scanning rate, 0.167 V min^{-1}; sensitivity, 10^{-9} A mm^{-1}; temperature, 25.0°. Pre-electrolysis times: for lead in 0.1 *M* HCl, 3 min at −0.6 V *vs.* Ag/AgCl electrode; for cadmium in 0.1 *M* HCl, 2 min at −1.0 V; for zinc in 0.1 *M* NH_4Cl, 2 min at −1.5 V; for manganese in 0.1 *M* KCl, 5 min at −1.75 V)

Concentration (M)	*Peak height (mm)*			
	Pb[a]	*Cd*	*Zn*[a]	*Mn*
$1 \cdot 10^{-7}$	10	12	11	11
$2 \cdot 10^{-7}$	20.5	25	20.5	20
$3 \cdot 10^{-7}$	30.5	36	32.5	30.5
$4 \cdot 10^{-7}$	38.5	49.5	44	39.5
$6 \cdot 10^{-7}$	60	72	65	60
$8 \cdot 10^{-7}$	83	98	84	82
$1 \cdot 10^{-6}$	102.5	118	109	101

[a] Corrected for blank values.

10^{-7} *M* are given in Table I. The standard deviations for more than ten separate measurements of concentrations of about 10^{-7} *M*, were 2.8, 2.2, 2.8 and 4.4%, respectively, for lead, cadmium, zinc and manganese.

Separation technique

Electrolytic separation seems to be the most suitable method because the copper matrix can be separated in one step from lead, cadmium, zinc and manganese. After separation, or at least after reduction of the copper to a concentration of the same order as that of the investigated elements, these can be determined in the remaining solution. Electrolytic separation is also advantageous because no additional reagents are needed, so that further contamination of the analysed solution is excluded. The acids such as nitric and hydrochloric acids, which are necessary for dissolving the sample, can be easily purified by normal or isopiestic (HCl) distillation.

The electrolysis was performed in a cell with electrode compartments separated by a sintered glass filter (Jena type G4) with a large diameter. A platinum wire was used as anode and a rotating platinum gauze cylinder as cathode to obtain uniform metal deposition. The potential of the cathode was kept constant at −0.35 V *vs.* S.C.E. with the aid of a potentiostat. A preliminary investigation showed that at this potential none of the four elements to be determined was codeposited. At −0.4 V, 5.5% of the lead was lost after a 2-h electrolysis of a 0.1 *M* copper(II) solution, and at −0.5 V, 46.6% was lost after 1 h.

Procedure

Dissolve 0.5–2 g (depending on the concentration of the determined elements) of the copper sample in 5 or 10 ml of 14 *M* nitric acid. Evaporate to dryness, add 5 ml of 8 *M* hydrochloric acid and evaporate again. Dissolve the residue in 100 ml of 0.1

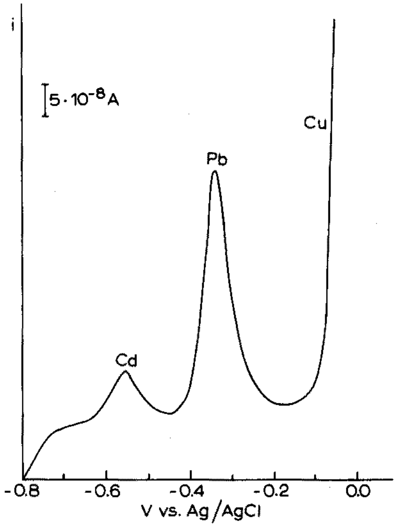

Fig. 1. Anodic stripping voltammogram of $4.84 \cdot 10^{-7}$ *M* cadmium(II) and $1.76 \cdot 10^{-6}$ *M* lead(II) in 0.1 *M* hydrochloric acid corresponding to 2.18 p.p.m. of cadmium and 17.6 p.p.m. of lead in $CuSO_4 \cdot 5H_2O$. Pre-electrolysis for 5 min at −0.8 V; scanning rate, 0.167 V min^{-1} at $5 \cdot 10^{-9}$ A mm^{-1}.

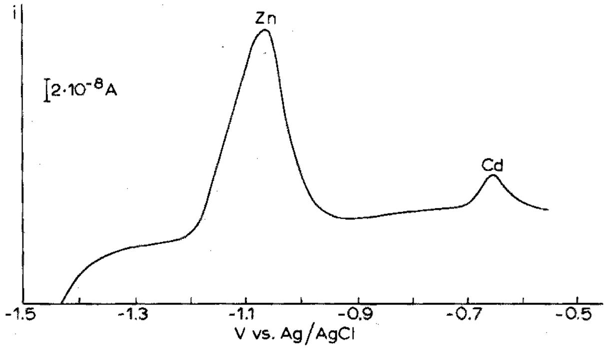

Fig. 2. Anodic stripping voltammogram of $7.02 \cdot 10^{-6}$ *M* zinc(II) and $1.99 \cdot 10^{-7}$ *M* cadmium(II) in 0.08 *M* ammonium chloride–0.3 *M* ammonia, corresponding to 33.6 p.p.m. of zinc and 1.65 p.p.m. of cadmium in $CuCl_2 \cdot 2H_2O$. Pre-electrolysis for 2 min at −1.5 V; scanning rate, 0.167 V min^{-1} at $2 \cdot 10^{-9}$ A mm^{-1}.

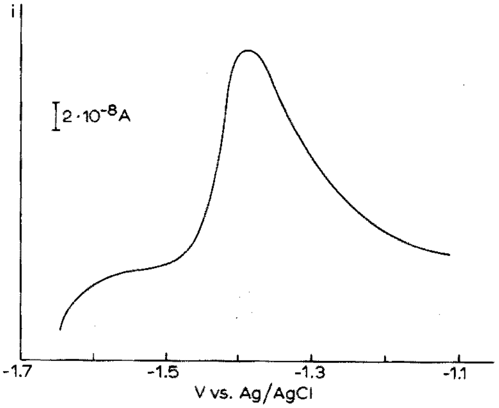

Fig. 3. Anodic stripping voltammogram of $2.85 \cdot 10^{-6}$ *M* manganese in 0.1 *M* potassium chloride corresponding to 9.18 p.p.m. of manganese in $CuCl_2 \cdot 2H_2O$. Pre-electrolysis for 2 min at −1.75 V; scanning rate, 0.167 V min^{-1} at $2 \cdot 10^{-9}$ A mm^{-1}.

M hydrochloric acid and transfer the solution to the cathode compartment of the electrolysis cell. Fill the anode compartment simultaneously with 0.1 *M* hydrochloric acid to the same height as the cathode compartment. Electrolyse the solution at −0.35 V *vs.* S.C.E. At the beginning of the electrolysis the potential must often be adjusted to a more positive value to prevent the current rising above 5 A.

Continue the electrolysis until the current has decreased to about 10 or 15 mA. This residual current is mainly due to the reduction of dissolved oxygen, because the current decreases to a small value after deaeration of the solution with nitrogen. Under these conditions, the remaining copper concentration is less than 10^{-6} *M*.

Transfer 20 ml of the electrolysed solution to the polarographic cell and deaerate for 10 min. Perform a pre-electrolysis at a potential of −0.9 V *vs.* the Ag/AgCl electrode ($E = -0.04$ V *vs.* S.C.E.) for 3–15 min while stirring. Stop stirring at the end of the timed electrolysis, and allow the solution to settle for 20 sec. Record the anodic stripping curve using a linearly varying potential of 0.167 V min^{-1}. Determine the concentration of the lead and the cadmium by the standard addition method.

Prepare a blank solution and record a current–voltage curve under the same conditions. A voltammogram is given in Fig. 1.

Add 5 ml of 1.9 *M* ammonia solution, perform a pre-electrolysis at a potential of −1.5 V *vs.* the Ag/AgCl electrode and determine the concentration of zinc by the standard addition method. Under these conditions cadmium can also be determined simultaneously with zinc (Fig. 2). Prepare a blank solution under the same conditions.

For the determination of manganese, evaporate 25 ml of the electrolysed solution under an infrared lamp. Dissolve the residue in 25 ml of 0.1 *M* potassium chloride and transfer 20 ml to the polarographic cell. Perform a pre-electrolysis at a potential of −1.75 V *vs.* the Ag/AgCl electrode and determine the concentration of the manganese by the standard addition method (Fig. 3). Record a voltammogram of a blank solution under the same conditions.

RESULTS

Various synthetic samples were analysed by means of the described procedure. Known quantities of lead, cadmium, zinc and manganese were added to copper chloride solutions, previously freed from the investigated elements by electrolysing

TABLE II

DETERMINATION OF LEAD, CADMIUM, ZINC AND MANGANESE IN SYNTHETIC SAMPLES

(0.5 g copper in 25 ml)

Element	*Weight added* (μg)	*Weight found* (μg)	*Weight recovered* (%)
Pb	0.063	0.068	107.9
	0.207	0.203	98.2
	0.517	0.498	96.5
	1.035	1.010	97.5
	2.071	2.123	102.5
	5.175	5.045	97.4
Cd	0.0092	0.0101	109.6
	0.045	0.043	96.6
	0.225	0.231	102.6
	0.450	0.432	96.2
	0.899	0.901	100.2
	2.248	2.242	99.75
Zn	0.653	0.683	104.4
	1.307	1.276	97.6
	2.615	2.516	96.2
	5.230	5.049	96.6
Mn	0.069	0.073	104.4
	0.137	0.143	103.0
	0.275	0.268	97.5
	0.549	0.558	101.5
	1.373	1.420	103.0

the copper at a potential of −0.35 V *vs.* S.C.E. The results are summarized in Table II; only for lead and zinc were blank values obtained.

Finally the procedure was applied to the analysis of some commercially available copper samples. Reproducible results (within 5%) were obtained for each element (Table III). Typical voltammograms of these analyses are given in Figs. 1–3.

TABLE III

DETERMINATION OF LEAD, CADMIUM, ZINC AND MANGANESE IN ANALYTICAL-GRADE COPPER AND COPPER COMPOUNDS

Product	*Lead (p.p.m.)*	*Cadmium (p.p.m.)*	*Zinc (p.p.m.)*	*Manganese (p.p.m.)*
Copper	43.3	0.391	11.8	0.118
	41.2	0.376	12.4	0.113
Copper	74.1	0.899	15.8	0.322
	77.3	0.945	16.3	0.309
$CuCl_2 \cdot 2H_2O$	48.6	1.72	35.7	9.19
	48.0	1.64	34.3	9.02
$CuSO_4 \cdot 5H_2O$	17.4	2.18	65.3	7.03
	17.9	2.25	64.2	7.18
	17.6	2.30	64.1	7.22

Anodic stripping voltammetry allows the determination of about 10^{-9} *M* lead(II) and zinc(II). This corresponds respectively to 0.01 and 0.003 p.p.m. for a 0.5-g sample in a final volume of 25 ml after separation. Nevertheless, in spite of careful purification of all reagents, the blank values obtained for lead and zinc reduced the determination limits to about 10^{-8} and 10^{-7} *M*, respectively. When these values are taken into account, it is possible to determine 0.1 p.p.m. lead and 0.3 p.p.m. zinc in copper by the procedure described. Cadmium and manganese can be determined in concentrations as low as $5 \cdot 10^{-10}$ *M* or 0.002 p.p.m., and 10^{-8} *M* or 0.03 p.p.m., respectively. Blank values for both elements were lower in all cases and could be neglected. The blank values for lead and zinc notwithstanding, these sensitivities are sufficient to allow the determination of lead, cadmium, zinc and manganese in the commercial copper samples investigated.

Thanks are due to the "Instituut voor Aanmoediging van het Wetenschappelijk Onderzoek in Nijverheid en Landbouw" for financial support to one of us (G.V.D.).

SUMMARY

Traces of lead, cadmium, zind and manganese in copper and copper compounds are determined, in some cases simultaneously, by anodic stripping voltammetry on a hanging mercury drop electrode. The four metals are separated from the bulk copper(II) by preliminary electrolysis of the copper matrix at a controlled potential on a platinum cathode. The method is applied to commercially available high-purity copper, showing satisfactory sensitivity and accuracy. The determination limits are about 10^{-9} *M* for lead, $5 \cdot 10^{-10}$ *M* for cadmium, 10^{-9} *M* for zinc and 10^{-8} *M* for manganese in solution; this corresponds, respectively, to 0.01, 0.002, 0.003 and 0.03 p.p.m. for a 0.5-g sample in a final volume of 25 ml after separation. However, because of blank values, the final determination limits are about 0.1 p.p.m. for lead and 0.3 p.p.m. for zinc.

RÉSUMÉ

Des traces de plomb, de cadmium, de zinc et de manganèse dans le cuivre et ses composés sont dosées, parfois simultanément, par voltammétrie anodique sur électrode à goutte pendante de mercure. Les quatre métaux sont séparés du cuivre(II) par électrolyse préliminaire de la matrice de cuivre, à potentiel contrôlé, sur cathode de platine. Les limites de dosage sont environ 10^{-9} *M* pour le plomb, $5 \cdot 10^{-10}$ *M* pour le cadmium, 10^{-9} *M* pour le zinc et 10^{-8} *M* pour le manganèse en solution; ce qui correspond respectivement à 0.01, 0.002, 0.003 et 0.03 p.p.m. pour un échantillon de 0.5 g, dans un volume final, après séparation, de 25 ml. Cependant, en raison des valeurs à blanc, les limites sont d'environ 0.1 p.p.m. pour le plomb et 0.3 p.p.m. pour le zinc.

ZUSAMMENFASSUNG

Spuren Blei, Cadmium, Zink und Mangan in Kupfer und Kupferverbindungen werden, in einigen Fällen simultan, durch Voltammetrie an einer hängenden Quecksilbertropfenelektrode nach dem anodischen "Stripping"-Verfahren bestimmt. Die vier Metalle werden von der Hauptmenge Kupfer(II) durch vorhergehende Elektrolyse der Kupfermatrix an einer Platinkathode bei gesteuertem Potential abgetrennt. Die Methode wird auf handelsübliches hochreines Kupfer angewendet; Empfindlichkeit und Genauigkeit sind zufriedenstellend. Die Bestimmungsgrenzen in der Lösung sind etwa 10^{-9} *M* für Blei, $5 \cdot 10^{-10}$ *M* für Cadmium, 10^{-9} *M* für Zink und 10^{-8} *M* für Mangan; dies entspricht 0.01, 0.002, 0.003 und 0.03 p.p.m. bei einer Probe von 0.5 g und einem Endvolumen von 25 ml nach der Abtrennung. Wegen der Blindwerte sind jedoch die schliesslichen Bestimmungsgrenzen etwa 0.1 p.p.m. für Blei und 0.3 p.p.m. für Zink.

REFERENCES

1 C. M. DOZINEL, *Modern Methods of Analysis of Copper and its Alloys*, Elsevier, Amsterdam, 1963.
2 W. T. ELWELL AND I. R. SCHOLES, *Analysis of Copper and its Alloys*, Pergamon Press, Oxford, 1967.
3 G. VAN DIJCK AND F. VERBEEK, *Z. Anal. Chem.*, 249 (1970) 89.
4 M. SPALENKA, *Chem. Anal. (Warsaw)*, 4 (1959) 393.
5 M. SATO, *Nippon Kagaku Zasshi*, 80 (1959) 1453.
6 P. N. KOVALENKO, *Uch. Zap. Rostovsk. Na Donu Gos. Univ.*, 60, no. 11 (1959) 65.
7 M. SIMEL, *Chem. Listy*, 50 (1966) 74.
8 A. J. EVE AND E. T. VERDIER, *Anal. Chem.*, 28 (1956) 537.
9 J. JANKOVSKY, *Chem. Listy*, 60 (1966) 1227.
10 E. BARENDRECHT, in A. J. BARD, *Electroanalytical Chemistry*, *Vol. 2*, M. Dekker, New York, 1967.
11 R. NEEB, *Inverse Polarographie und Voltammetrie*, Verlag Chemie, Weinheim, 1969.
12 T. W. LAMPHERE AND L. B. ROGERS, *Anal. Chem.*, 22 (1950) 463.
13 F. A. FER'YANCHICH, *Tr. Komis. po Analit. Khim., Otd. Khim. Nauk, Akad. Nauk SSSR*, 2 (1949) 87.
14 L. MEITES, *Handbook of Analytical Chemistry*, McGraw-Hill, New York, 1963.
15 L. A. CURRIE, *Anal. Chem.*, 40 (1968) 586.

Analytica Chimica Acta
Elsevier Publishing Company, Amsterdam
Printed in The Netherlands

ELECTROCHEMICAL DETERMINATIONS OF DIFFUSION COEFFICIENTS OF SOME POLYNUCLEAR COPPER(II) AND IRON(III) COMPLEXES

EDGAR N. DRAKE II* AND JERRY L. JONES**
Department of Chemistry, Texas A & M University, College Station, Texas (U.S.A.)

(Received 20th November 1970)

The Stokes–Einstein equation[1] has been shown to be a useful tool for estimating sizes of diffusing particles which are significantly larger than the solvent molecules in which they are dissolved. Use of the relationship does depend, however, on a knowledge of the diffusion coefficient of the particle. Electrochemical techniques afford one means of measuring diffusion coefficients provided that the diffusing species can be identified. Often, by adjustment of pH or ligand concentration, a single complex ion can be made to predominate in solution and a measured diffusion coefficient can be reliably attributed to a particular ion. While ligand substitution reactions seldom produce dramatic changes in the diffusion coefficient of a complex ion[2], dimerization (or more generally polymerization) reactions can change diffusion coefficients by 100% or more[3]. Changes of this magnitude can be observed easily by using chronopotentiometry or conventional d.c. polarography.

Recent studies of the citrate, malate, and tartrate complexes of copper(II) indicate that these ions polymerize in alkaline solutions[4]. The work of Timberlake[5] indicates that the monomeric iron(III) tartrate complex polymerizes in aqueous solution as the pH is increased. The four species reported to exist in acidic solutions with pH values less than 5.0 are: the monomer, $FeC_4H_4O_6^+$; the dimer, $Fe_2(OH)_4(C_4H_5O_6)_2$; the dimer, $Fe_2(OH)_4(C_4H_5O_6)(C_4H_4O_6)^-$; and the trimer, $Fe_3(OH)_6(C_4H_4O_6)_3^{3-}$. By adjustment of the pH, one of these species can be made to predominate in solution.

The present investigation was undertaken to measure the diffusion coefficients of some of the polynuclear copper(II) and iron(III) complexes and to estimate the sizes of the particles in solution.

EXPERIMENTAL

Apparatus

A conventional chronopotentiometric apparatus similar to that described previously[6] was employed. Chronopotentiograms were obtained with a Hewlett-

---

* Present address: Department of Chemistry, Angelo State College, San Angelo, Texas (U.S.A.).

** Present address: Department of Chemistry, Central Washington State College, Ellensburg, Wash. (U.S.A.). Correspondence should be sent to Dr. Jones.

Packard Model 130A oscilloscope equipped with a Hewlett-Packard Model 196B camera. Current values were obtained by measuring the voltage drop across a precision 200-ohm resistor (±0.01%). Conventional d.c. polarograms were obtained with a Sargent Model XXI polarograph. Mercury drops from a conventional dropping mercury electrode were caught in a glass spoon and transferred to a recessed, amalgamated platinum wire sealed in glass tubing to form a hanging mercury drop electrode. The resulting electrode surface area, calculated from the average weight of several drops, was 0.0280 ± 0.0003 cm^2.

Materials and methods

All chemicals were reagent grade with the exception of the primary standard-grade disodium (ethylenedinitrilo)tetraacetate dihydrate (EDTA). A 0.0100 *M* stock solution of copper(II) was prepared with copper sulfate pentahydrate. The solution was standardized by compleximetric titration with 0.01048 *M* EDTA and a 0.1% solution of 1-(2-pyridylazo)-2-naphthol (PAN) as indicator[7]. Solutions containing copper(II) and tartrate were prepared by adding 6.10 g of sodium perchlorate (anhydrous) and 1.50 g of D-tartaric acid to 50.00 ml of stock copper(II) solution and diluting to 500.0 ml with distilled water. The pH was adjusted to 9.1 with 6 *M* sodium hydroxide. Solutions containing copper(II) and citrate were prepared by adding 6.10 g of sodium perchlorate and 3.00 g of sodium citrate dihydrate to 50.00 ml of stock copper(II) solution and diluting to 500.0 ml. The pH was adjusted to 9.2 with 6 *M* sodium hydroxide. Solutions of yellow copper(II) salicylate, $CuC_7H_5O_3^+$, were prepared by adding 138 mg of salicylic acid and 6.1 g of sodium perchlorate to 50.00 ml of stock copper(II) solution and diluting to 500.0 with distilled water. The pH was adjusted to 5.5 with 6 *M* sodium hydroxide. Precipitation occurred above pH 6. Finally, solutions of green copper(II) 5-sulfosalicylate in the form of $Cu(C_7H_4O_3SO_3)_2^{2-}$ were prepared by adding 1.00 g of 5-sulfosalicylic acid to 6.1 g of sodium perchlorate and 50.00 ml of stock (0.0211 *M*) copper(II) solution and diluting to 500.0 ml with distilled water. The pH was adjusted to 6.4 with 6 *M* sodium hydroxide which assured solubility of the 5-sulfosalicylic acid.

Iron(III) tartrate solutions were prepared by adding 50.00 ml of stock iron(III) perchlorate solution to 6.1 g of anhydrous sodium perchlorate and 2.50 g of D-tartaric acid. The solution was diluted with distilled water and the pH was adjusted to 5.0 or 3.2 with 6 *M* sodium hydroxide. The stock solution was 0.0112 *M* iron(III) in 0.100 *M* perchloric acid and was standardized by direct titration with 0.01048 *M* EDTA and an aqueous 1% solution of N-(*p*-methoxyphenyl)-*p*-phenylenediamine hydrochloride (variamine blue) as indicator[8].

All solutions were purged with prepurified nitrogen (minimum purity 99.996%) prior to electrolysis.

Chronopotentiograms were obtained at current densities ranging from 0.98 to 7.40 mA cm^{-2} in the case of copper(II) solutions and from 0.36 to 3.8 mA cm^{-2} in the iron(III) solutions. With copper(II) 5-sulfosalicylate solutions, it was necessary to prepare a new hanging mercury drop electrode after each chronopotentiogram in order to obtain reproducible results. Although the currents remained constant for long periods of time, the current settings used were recalibrated daily.

Conventional d.c. polarographic reductions of all solutions were observed and all voltages were measured with respect to the saturated calomel electrode.

RESULTS AND DISCUSSION

Copper(II)

Only a single polarographic reduction corresponding to the transition Cu(II)–Cu(0) was exhibited. Half-wave potentials for the copper(II)–tartrate system at pH 9.1 and the copper (II)-citrate system at pH 9.2 were −0.29 and −0.40 V, respectively. For the copper(II) salicylate solution at pH 5.5 the half-wave potential was −0.05 V while the solution containing copper(II) and 5-sulfosalicylic acid at pH 6.4 exhibited a half-wave potential of −0.15 V. In the case of the last-mentioned solution, very large maxima rendered the polarographic limiting current unsuitable for use in calculating diffusion coefficients.

Meites[9] reports two reductions for the copper(II)–citrate system at pH 9.2 with the Cu(II)–Cu(I) transition at −0.20 V and the Cu(I)–Cu(0) transition at −0.40 V. The same author[10] reports a single reduction corresponding to Cu(II)–Cu(0) for the copper(II)–tartrate system at pH 9.0 with a half-wave potential of −0.285 V. In general, it appears that two reduction waves are observed for copper(II) in ammoniacal solutions while single waves are obtained in solutions made basic with sodium hydroxide[11].

The diffusion coefficients of several copper(II) complexes calculated from polarographic data are presented in Table I. These were obtained by the use of the Ilkovič equation and polarographic limiting currents which had been corrected by subtraction of the residual current.

Two one-electron reductions were observed for all copper(II) solutions studied chronopotentiometrically. The potentials corresponding to one-fourth of the transition time were −0.28 and −0.52 V for the copper(II)–tartrate, −0.20 and −0.60 V for the copper(II)–citrate, −0.16 and −0.44 V for the copper(II)–5-sulfosalicylate, and −0.10 and −0.38 V for the copper(II)–salicylate systems.

Before transition times may be used to calculate diffusion coefficients for complex species, the product $it^{\frac{1}{2}}$ must be shown to be independent of current density to establish that the complex species in question is not undergoing dissociation before reduction[12]. Such was the case for the copper(II) systems studied and typical chronopotentiometric data obtained for the copper(II)–5-sulfosalicylate complex are compiled in Table II. Transition times observed for all complexes studied were of the order of a fraction of a second. The chronopotentiogram of the copper(II)–tartrate complex shown in Fig. 1 illustrates the two reductions typically observed for the copper(II) complexes. Diffusion coefficients were calculated from chronopotentiometric data by means of the Sand equation[13] and these are presented in Table I.

TABLE 1

DIFFUSION COEFFICIENTS OF SOME COPPER(II) COMPLEXES[a]

Species	*Chronopotentiometric* (×10⁵)	*Polarographic* (×10⁵)
$Cu_2(OH)_2(C_6H_5O_7)_2^{2-}$	0.36 ± 0.03	0.38 ± 0.02
$Cu_3(OH)_3(C_4H_4O_6)_3^{3-}$	0.33 ± 0.03	0.33 ± 0.02
$CuC_7H_5O_3^+$	0.44 ± 0.03	0.47 ± 0.02
$Cu(C_7H_4O_3SO_3)_2^{2-}$	0.30 ± 0.03	

[a] All diffusion coefficients are expressed in $cm^2\ sec^{-1}$ and were measured at 25°.

TABLE II

CHRONOPOTENTIOMETRIC DATA FOR THE COPPER(II) COMPLEX OF 5-SULFOSALICYLIC ACID

Transition time (*sec*)	*Current* ($A \cdot 10^5$)	$it^{\frac{1}{2}}$ ($A\,sec^{\frac{1}{2}} \cdot 10^5$)
0.062	3.40	0.88
0.078	3.15	0.88
0.092	2.90	0.88
0.108	2.70	0.88

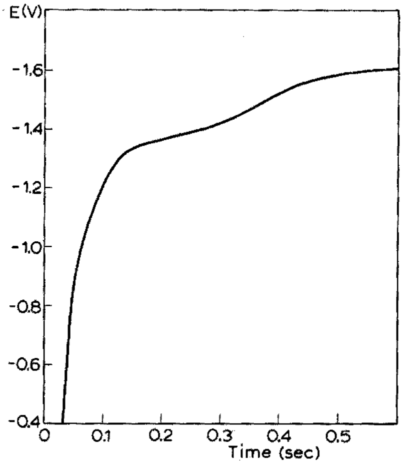

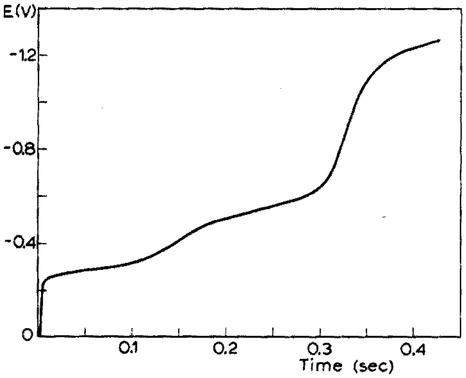

Fig. 1. Chronopotentiogram of $7.03 \cdot 10^{-4}$ *M* $Cu_3(OH)_3(C_4H_4O_6)_3^{3-}$ at pH 9.1.

Fig. 2. Chronopotentiogram of $3.7 \cdot 10^{-4}$ *M* $Fe_3(OH)_6(C_4H_4O_6)_3^{3-}$ in 0.100 *M* $NaClO_4$ at pH 5.0.

The Stokes–Einstein equation was used to compute approximate diameters of the electroactive species present in each solution. The viscosity of the solution was assumed to be the same as that for pure water or $8.94 \cdot 10^{-3}$ poise. The particle diameter calculated for the copper(II)–tartrate complex at pH 9.0 was 1.4 nm. $Cu(OH)(C_4H_4O_6)^-$ should be a component of this system at pH 9.1. However, Rajan and Martell[4] have demonstrated that dimerization can occur at considerably lower pH values and they imply that even further polymerization most likely occurs near pH 9. Scale models indicate that the diameter of the dimer, $Cu_2(OH)_2(C_4H_4O_6)_2^{2-}$, is 1.0 nm while that of the trimer, $Cu_3(OH)_3(C_4H_4O_6)_3^{3-}$, is 1.4 nm. It is therefore suggested that there exists a trimeric copper(II)–tartrate species at pH 9.1. Similar models constructed for the copper(II)–citrate complex indicate that the dimer, $Cu_2(OH)_2(C_6H_5O_7)_2^{2-}$, would be expected to have a diameter of 1.2 nm. The diameter calculated from the diffusion coefficient of this ion is 1.2 nm. Thus, the dimer appears to be the predominant species present in copper(II) solutions containing citrate at pH 9.2. Such a conclusion is compatible with the findings of Rajan and Martell.

The salicylate and 5-sulfosalicylate complexes of copper(II) were studied to determine the difference in size observed when first one, and then two, large organic ligands are attached to the metal ion. The copper(II)–salicylate complex containing copper(II) and salicylic acid in a mole ratio of 1 : 1 was prepared by reacting copper and salicylic acid in stoichiometric amounts at pH 5.5. The particle diameter, calculated from measured diffusion coefficients, was 1.0 nm. The complex containing copper and 5-sulfosalicylate in a ratio of 1:2 was prepared by reacting copper(II) with an approximately four-fold excess of 5-sulfosalicylic acid at pH 6.4. The particle diameter obtained from diffusion coefficient calculations for this complex was 1.6 nm. The observed increase of 0.6 nm is very near that expected for the addition of a second ligand to the copper(II) complex.

Iron(III)

Iron(III) tartrate solutions at pH 5.0 exhibited two reductions polarographically with half-wave potentials of −0.13 and −1.38 V. Reductions of iron(III) tartrate complexes in basic solutions have been reported[11] at −0.10 and −1.38 V. These reductions correspond to the transitions Fe(III)–Fe(II) and Fe(II)–Fe(0), respectively. At pH 3.2, the one-electron reduction was observed at −0.13 V but the two-electron reduction was obscured by hydrogen evolution which began at −1.3 V. The trimer is the only species present in appreciable amounts at pH 5.0. Its diffusion coefficient was calculated by means of the Ilkovič equation and the one- and two-electron reduction waves. Limiting currents were corrected by subtraction of the residual current. The resulting diffusion coefficients are shown in Table III.

A typical chronopotentiogram of the iron(III) tartrate system at pH 5.0 is shown in Fig. 2. The slight change of slope on the rising portion of the curve is attributed to the one-electron reduction, the transition time of which is small in comparison with that of the two-electron step.

Both the dimer (pH 3.2) and the trimer (pH 5.0) were found to have $it^{\frac{1}{2}}$ products which were independent of current, indicating that these complexes are reduced without undergoing dissociation. The Sand equation was used to calculate diffusion coefficients from measured transition times. In the case of the dimer at pH 3.2, no transition time was observed at −1.38 V, but the much shorter transition time at −0.13 V was used to compute the diffusion coefficient. The resulting diffusion coefficient appears in Table III.

The Stokes–Einstein equation was used to calculate the approximate sizes of the diffusing particles. The viscosity of the solution was taken to be the same as that for pure water. These calculations give approximate diameters for the dimer and for the trimer of 0.8 and 1.4 nm, respectively.

Timberlake[5] describes the iron(III) tartrate trimer as monomer units connected by hydroxyl bridges. For the ion to have a triple negative charge as has been proposed, six hydroxyl groups must be present. Construction of a model of the triply negatively charged trimer on a scale of 0.1 nm per inch shows that the ion approximates a sphere

TABLE III

DIFFUSION COEFFICIENTS OF IRON(III) TARTRATE COMPLEXES[a]

Species	*Chronopotentiometric*	*Polarographic*
Dimer	$(0.68 \pm 0.05) \cdot 10^{-5}$	
Trimer	$(0.35 \pm 0.05) \cdot 10^{-5}$	$(0.35 \pm 0.02) \cdot 10^{-5}$ (−0.13 V) $(0.36 \pm 0.02) \cdot 10^{-5}$ (−1.38 V)

[a] All diffusion coefficients are expressed in cm^2 sec^{-1} and were measured at 25°.

in shape which would give minimal viscous drag in solution. The model measures 1.5 nm in diameter which closely agrees with the 1.4-nm diameter calculated from measured diffusion coefficients. The model also indicates that quadridentate chelation by the tartrate, as suggested by Timberlake, is sufficiently difficult as virtually to preclude the possibility.

This work was conducted in partial fulfilment of the requirements for the Ph.D. degree at Texas A&M University (E.N.D. II).

SUMMARY

Electrochemical data obtained by simple techniques appear to provide a valid means of detecting polymerization of metal complexes in aqueous solutions. Diffusion coefficients have been determined for the dimeric and trimeric iron(III) tartrate complexes and for some tartrate, citrate, salicylate, and 5-sulfosalicylate complexes of copper(II) by means of chronopotentiometry and conventional d.c. polarography. Approximate particle diameters were calculated from measured diffusion coefficients by the Stokes–Einstein equation and these confirm the presence of polynuclear species reported by earlier investigators. Scale models of the complexes have diameters which agree closely with those obtained experimentally. Evidence for the existence of a trimeric copper(II) tartrate species at pH 9.1 is presented.

ZUSAMMENFASSUNG

Durch einfache Verfahren erhaltene elektrochemische Daten scheinen ein beweiskräftiges Mittel für den Nachweis einer Polymerisation von Metallkomplexen in wässrigen Lösungen zu sein. Durch Chronopotentiometrie und konventionelle Gleichstrompolarographie wurden Diffusionskoeffizienten für die dimeren und trimeren Eisen(III)-Tartrat-Komplexe und für einige Tartrat-, Citrat-, Salicylat- und 5-Sulfosalicylat-Komplexe von Kupfer(II) bestimmt. Aus den gemessenen Diffusionskoeffizienten wurden nach der Stokes–Einstein-Gleichung die ungefähren Teilchendurchmesser berechnet; sie bestätigen das Vorliegen mehrkerniger Spezies, über die von früheren Autoren berichtet worden ist. Schalenmodelle der Komplexe haben Durchmesser, die mit den experimentell erhaltenen gut übereinstimmen. Es wird der Beweis für die Existenz einer trimeren Kupfer(II)-tartrat-Spezies bei pH 9.1 vorgelegt.

REFERENCES

1 L. Meites, *Polarographic Techniques*, 2nd Edn., Interscience, New York, 1965, p. 141.
2 L. Meites, ref. 1, p. 144.
3 E. N. Drake, II and J. L. Jones, unpublished results.
4 K. S. Rajan and A. E. Martell, *J. Inorg. Nucl. Chem.*, 29 (1967) 463.
5 C. F. Timberlake, *J. Chem. Soc.*, (1964) 1229.
6 P. Delahay, *Discussions Faraday Soc.*, 17 (1954) 205.
7 H. Flaschka and H. Abdine, *Chemist-Analyst*, 45 (1956) 58.
8 G. Schwarzenbach, *Complexometric Titrations*, Interscience, New York, 1957, p. 78.
9 L. Meites, *J. Amer. Chem., Soc.*, 72 (1950) 180.
10 L. Meites, *J. Amer. Chem. Soc.*, 72 (1949) 3269.
11 Ref. 1, pp. 661–3.
12 P. Delahay and T. Berzins, *J. Amer. Chem. Soc.*, 75 (1953) 2486.
13 H. J. S. Sand, *Phil. Mag.*, 1 (1901) 45.

Analytica Chimica Acta
Elsevier Publishing Company, Amsterdam
Printed in The Netherlands

STUDIES WITH DITHIZONE

PART XXIII*. SOME OBSERVATIONS ON SECONDARY MERCURY(II) DITHIZONATE

TERESA NOWICKA-JANKOWSKA** AND H. M. N. H. IRVING
Department of Inorganic and Structural Chemistry, University of Leeds, Leeds 2 (England)

(Received 4th December 1970)

The chelate complexes M(HDz)$_n$ obtained by the interaction of a number of n-valent cations with dithizone (3-mercapto-1,5-diphenylformazan; H_2Dz) have found extensive use in analytical practice[1,2]. Originally and erroneously termed keto-complexes by Fischer[3] who formulated the mercury(II) complex as (I), the proof by one of us that the bonding involved sulphur[4] led to the suggested structure (II) with an inter-molecular hydrogen bond of the type well established in formazan chemistry. The structures of the solid complexes Hg(HDz)$_2$ (III), Cu(HDz)$_2$, Ni(HDz)$_2$ and Zn(HDz)$_2$ have been determined by single-crystal X-ray methods[5-8] and at least in the solid state, chelate rings with the metal bonded to sulphur and nitrogen (*cf.* III) appear to be general for these "normal" or "primary" dithizonates as they are now commonly called.

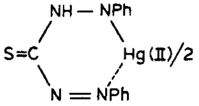
I

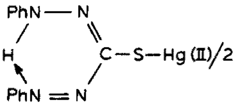
II

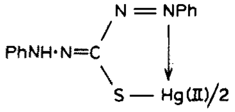
III

Much less is known about the secondary dithizonate complexes (formerly termed enol-complexes[3]) which have found no real applications in absorptiometry. Their stoicheiometry corresponds to the higher metal:ligand ratio of 2:n and it has generally been assumed that their formation involves the replacement by metal of the remaining proton in the anion HDz^{-}[1,2,9]. That a proton can be removed from some primary metal dithizonates can be demonstrated in various ways. Thus the acid dissociation constant of phenylmercury(II) dithizonate, Ph.Hg(HDz), has been measured absorptiometrically and found to have the value $pK = 11.46 \pm 0.01$ in a 52.75% (v/v) ethanol–water mixture[10]. We have recently shown that the remaining imino-protons in primary mercury(II) dithizonate, Hg(HDz)$_2$, can be replaced by silver ions to give the mixed secondary complex, Hg(AgDz)$_2$[11]. On the other hand, the source of the :N–H stretching frequencies at 1530 and 1528 cm^{-1} reported in the infrared absorption spectra of the secondary complexes Ag$_2$Dz and PdDz·2H$_2$O has not been explained[12] and on rather slender evidence Freiser and Freiser[13] have proposed that secondary copper(II) dithizonate is actually a primary dithizonate of

---

* *Anal. Chim. Acta*, (1970) is regarded as Part XXII of this series.

** Institute of Nuclear Research, Warszawa 31, nl. Dorodna 16, Poland.

copper(I), *viz.* Cu(HDz) in our nomenclature*. Indeed they suggest that the "keto–enol" equilibrium[9] is really a redox equilibrium between complexes of copper(II) and copper(I). This hypothesis can hardly be extended to the corresponding compounds of silver where the secondary complex Ag_2Dz would need to be interpreted as a complex of Ag(0) and it is clearly inapplicable to the mercury system where, as we show later, violet secondary mercury(II) dithizonate can readily be distinguished from the orange yellow primary mercury(I) dithizonate. Indeed their conclusion: "To attribute formation of the enol or secondary series of metal dithizonates to the formation of a doubly charged dithizonate ion is, therefore, no longer possible", is a premature and possibly too sweeping a generalisation to make at this stage.

In studies of the formation of the mixed mercury(II)–silver–dithizone complex[11] it was noted how much more reactive a solution of primary mercury(II) dithizonate in chloroform was to an aqueous solution of silver ions than to one of mercury(II) ions. Indeed, once formed, it is quite difficult to convert $Hg(HDz)_2$ into the secondary complex HgDz in the absence of excess of mercury(II). Whereas on the one hand the reactions

$$(\mathrm{HgDz})_{\mathrm{org}} + (\mathrm{H_2Dz})_{\mathrm{org}} \rightarrow (\mathrm{Hg(HDz)_2})_{\mathrm{org}} \qquad (1)$$

and

$$2(\mathrm{HgDz})_{\mathrm{org}} + 2\,\mathrm{H}^+ \xrightarrow[\mathrm{H_2SO_4}]{0.25\,M} (\mathrm{Hg(HDz)_2})_{\mathrm{org}} + \mathrm{Hg}^{2+} \qquad (2)$$

take place rapidly and quantitatively (the subscript org is used to distinguish species in the organic phase) the reverse reaction between primary mercury dithizonate and alkali is slow and often subordinated to the destruction of the primary dithizonate (Fig. 1). If a solution of dithizone in chloroform is shaken with an alkaline solution of mercury(II), a mixture of primary and secondary dithizonates is obtained with an absorption maximum between 505 and 520 nm. Studies of the equilibrium between primary and secondary mercury dithizonate as a function of pH and $[Hg^{2+}]$ led Kato *et al.*[17] to conclude that the secondary dithizonate "is much stabilised in the pH range 5–7" and that "there is a strong presumption for the association of the reactant in the organic layer". Their experimental procedure is not easily comprehended.

The best way of preparing pure secondary mercury dithizonate is by the reaction of mercury(II) ions with dithizonate ions in aqueous alkaline solution whereby the violet complex is first formed in the aqueous phase before its extraction into chloroform. The largest yield is obtained with 0.1 *M* potassium hydroxide (Fig. 2, curve 1) giving a complex with $\lambda_{\max}$ 530 nm. With less concentrated alkali (0.01 *M* potassium hydroxide) the yield is lower (Fig. 2, curve 2), though the difference may be due to a slower rate of reaction. With more concentrated alkali (1 *M* potassium hydroxide; Fig. 2, curve 3) there is a hypsochromic shift in $\lambda_{\max}$ and with 5 *M* potassium hydroxide a new species appears and there is a change in colour from violet to orange yellow,

---

* In their paper[13] Freiser and Freiser use the symbols HDz and Dz^- for dithizone and its uni-negative anion (H_2Dz and HDz^- in our nomenclature). They also use the terms enol- and keto-dithizonates and incorrectly apply the former to the complex Cl–Hg(HDz)[14], which like (aryl)Hg(HDz)[15] or $(C_2H_5)_3Sn(HDz)$, $(CH_3)_2Tl(HDz)$[16] and similar complexes are clearly primary ("normal") dithizonates derived from the cations $HgCl^+$, Aryl Hg^+, $(C_2H_5)_3Sn^+$ or $(CH_3)_2Tl^+$.

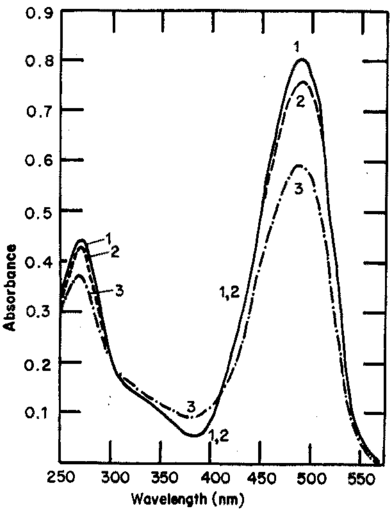

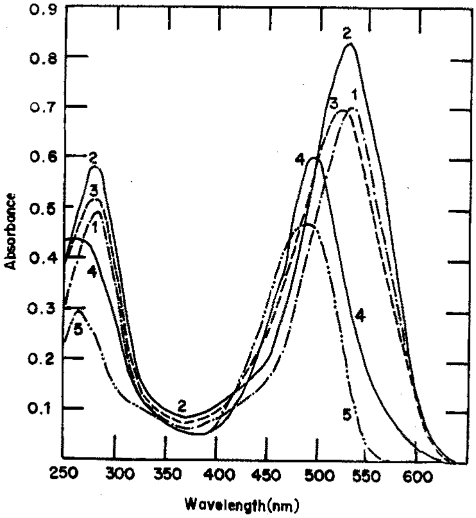

Fig. 1. The effect of alkali on the spectrum of primary mercury(II) dithizonate. A $1.225 \cdot 10^{-5}$ *M* solution of primary mercury dithizonate in chloroform (curve 1) was shaken in the dark for 5 min with equal volumes of 0.1 *M* or 1 *M* KOH (curve 1), 5 *M* KOH (curve 2) and 10 *M* KOH (curve 3).

Fig. 2. The preparation of secondary mercury(II) dithizonate and the spectrum of primary mercury(I) dithizonate. Curves 1, 2, 3 and 4 show the spectrum of the organic phase (see text) when 0.01, 0.1, 1.0 and 5 *M* KOH was used. Curve 5 shows the spectrum of a solution of primary mercury(I) dithizonate (ca. $1.56 \cdot 10^{-5}$ *M*) in chloroform.

λ_{max} 495 nm (Fig. 2, curve 4). It is possible that in the reactions which involve a large excess of hydroxyl ions, a mixed complex *e.g.* HO · Hg(HDz) is formed analogous to the mixed species Cl · Hg(HDz) formed with excess of chloride ions[14]. In each case dimerisation (with bridging –OH or –Cl) would give an acceptable coordination number to the mercury as in formula (IV).

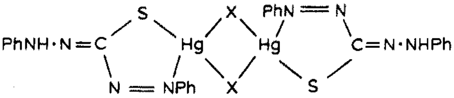

(IV)

Results precisely similar to those obtained with potassium hydroxide were obtained when this was replaced by the strong base tetra-*n*-butylammonium hydroxide, which was chosen because the cation cannot act as a donor. On the other hand, when potassium hydroxide was replaced by ammonium hydroxide, complete conversion of dithizone to secondary mercury dithizonate was never achieved. The best results were obtained when a solution of dithizone in chloroform was equilibrated with aqueous ammonium hydroxide at pH 10.5–11.0. After the organic layer (which still contained some dithizone) had been rejected, mercury(II) chloride was added, and a magenta-coloured solution (λ_{max} 518 nm) resulted on shaking. On equilibration with chloroform, the coloured species was transferred completely to the organic phase (λ_{max} 515 nm). With higher concentrations of ammonia the magenta colour certainly appears as before in the aqueous phase, but the chloroform extract has only an apricot colour (λ_{max} 495–500 nm). This originates from a mixture of species, for when the violet solution of secondary mercury(II) dithizonate (prepared from 0.1 *M* potassium hydroxide; Fig. 2, curve 2) is shaken with aqueous ammonia an apricot or orange-yellow colour appears depending on the concentration. This colour is not due to primary mercury(II) dithizonate, for it does not change to blue in sunlight[12]. Freiser and Freiser have recently reported similar observations[13] and note that the new yellow species, unlike primary mercury(II) dithizonate, is not reverted to dithizone by potassium iodide or sodium thiosulphate. They suggest the composition H_2NHgDz (*i.e.* $H_2N \cdot Hg(HDz)$ in our nomenclature) which represents it as a *primary* dithizonate of the complex cation $H_2N\text{–}Hg^+$. However we have found that similar yellow colours are given with piperidine, pyridine, trimethylamine and triethylamine. Like ammonia these are all donor ligands; but the two latter cannot form compounds analogous to $H_2N \cdot Hg(HDz)$ for lack of a replaceable hydrogen atom. An alternative possibility is that we are dealing with adducts, $B \rightarrow HgDz$, of secondary mercury dithizonate (where $B = NH_3$, $C_5H_{11}N$, C_5H_5N, $(CH_3)_3N$ or $(C_2H_5)_3N$). The situation was not clarified by the discovery that similar yellow colours develop when a large excess of any of these bases was added to a solution of primary mercury(II) dithizonate in chloroform. Sharp peaks develop at 293 (pyridine), 278 (piperidine), 291 (trimethylamine) or 290 nm (triethylamine) while that due to the mercury(II) dithizonate decreases (*cf.* Fig. 3, curves 1 and 2). On being kept for 24 h the absorption of the primary mercury dithizonate decreases to an extent which increases in the order pyridine < triethylamine < piperidine, whereas the absorption of the new species absorbing just below 300 nm remains essentially unchanged (Fig. 3, curve 3).

If the new yellow species are identical with those obtained directly from secondary mercury dithizonate, one would surmise that the equilibrium of eqn. (1) was displaced to the left by the formation of the salt $BH^+ \ HDz^-$ and that the secondary mercury dithizonate so formed then reacts with the base B to give a yellow adduct as described above. This is improbable, for the yellow dithizonate ion, HDz^-, absorbs most strongly at 465 nm in water or at 490 nm in chlorobenzene or 485 nm in a monophase consisting of 20% water, 30% chloroform and 50% ethanol[18]. As shown by comparable measurements in chloroform with triethylamine (Fig. 3, curves 4 and 5),

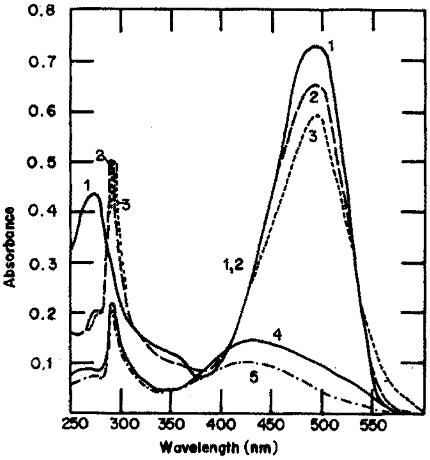

Fig. 3. The effect of triethylamine on the spectrum of solutions of primary mercury dithizonate and of dithizone in chloroform. (1) Mercury dithizonate alone; (2 and 3) the effect of triethylamine immediately and after 24 h; (4 and 5) the effect of triethylamine on dithizone alone, immediately and after 24 h.

the formation of dithizonate ions (or of the ion-pair $BH^+ HDz^-$ in the organic phase) should have been revealed by a hypsochromic shift of the band at 490 nm or at least by the development of a shoulder at *ca.* 450 nm. The constitution of the various new yellow species must await further work.

Freiser's suggestion[13] that secondary copper(II) dithizonate is actually a primary dithizonate derived from copper(I) raises the question whether secondary mercury(II) dithizonate is actually the primary dithizonate derived from mercury(I), a suggestion already made by Uzumasa and Miyasita[19] although the basis of their argument is not clear. Koroleff[20] prepared both primary and secondary mercury(I) dithizonates and reported λ_{max} 490 nm for the former in carbon tetrachloride; the latter was insoluble. We find the spectrum of yellow primary mercury(I) dithizonate to be extremely like that of primary mercury(II) dithizonate (λ_{max} 490 nm) but with a lower molecular extinction of 30,600. It is certainly entirely different to that of the violet secondary mercury(II) dithizonate. No oxidation product of dithizone can be detected when secondary mercury dithizonate is formed—as would be the case if a redox reaction had occurred—and no reduction product of dithizone was detected when primary mercury(II) dithizonate was obtained (*v.s.*) by mixing equivalent quantities of secondary mercury(II) dithizonate and dithizone, both dissolved in chloroform, according to eqn. (1).

EXPERIMENTAL

Spectra were measured with a Unicam Recording Spectrophotometer SP700. All reagents were of A.R. grade and the usual precautions for work with dithizone were taken[11].

Primary mercury dithizonate was prepared by shaking a $2.45 \cdot 10^{-5}$ *M* solution of dithizone in chloroform with a small excess of an aqueous $2 \cdot 10^{-4}$ *M* solution of mercury(II) nitrate in 0.1 *M* sulphuric acid. The organic phase was separated and washed once with 0.1 *M* sulphuric acid and twice with deionised water.

The preparation of secondary mercury(II) dithizonate

With potassium hydroxide. A $2.5 \cdot 10^{-5}$ *M* solution of dithizone in chloroform (15 ml) was shaken with 15 ml of 0.01 *M* potassium hydroxide; 5 ml of $2 \cdot 10^{-4}$ *M* mercury(II) nitrate (pH ~ 2) was added to the aqueous phase and the mixture was equilibrated in a separating funnel protected from light by being wrapped in aluminium foil (5 minutes). The aqueous phase (pH ~ 8) was slightly violet. The spectrum of the organic phase is shown in Fig. 2, curve 1. When the experiment was repeated with 0.1 *M* potassium hydroxide the aqueous phase was quite colourless; the spectrum of the chloroform extract is given in Fig. 2, curve 2. Similar results were obtained with 5 *M* potassium hydroxide (Fig. 2, curve 3), but with 10 *M* potassium hydroxide a violet colour appeared in the aqueous phase as previously, whereas the chloroform extract had an apricot colour (Fig. 2, curve 4).

*With tetra-*n*-butylammonium hydroxide.* An aqueous *ca.* 0.1 *M* tetrabutylammonium hydroxide solution (15 ml) was shaken with an equal volume of $1.56 \cdot 10^{-5}$ *M* dithizone in chloroform to remove any metallic impurities. The yellow organic phase was rejected. A further 15 ml of $1.56 \cdot 10^{-5}$ *M* dithizone was added and, after shaking, 5 ml of aqueous $2 \cdot 10^{-4}$ *M* mercury(II) nitrate solution was added; a violet colour then developed in the organic phase. The spectrum (λ_{max} 530,282; λ_{min} 375 nm) was recorded against a blank of chloroform that had been equilibrated with the quaternary ammonium base.

With ammonium hydroxide. Portions of $2 \cdot 10^{-5}$ *M* dithizone in chloroform were shaken with equal volumes of ammonium hydroxide of various concentrations. The organic layers which still contained some dithizone, were rejected (if this is not done the interaction of dithizone with secondary mercury dithizonate subsequently formed in the aqueous phase immediately gives primary dithizonate and a mixture of products must result). The aqueous solution of ammonium dithizonate $NH_4^+HDz^-$ was then treated with excess of aqueous mercury(II) nitrate solution and shaken in a separatory funnel avoiding exposure to strong light, especially direct sunlight. On extraction with chloroform, violet solutions of secondary mercury dithizonate were obtained starting from dilute ammonia, but as its concentration was increased, apricot and finally yellow coloured extracts resulted.

Reactions of primary mercury(II) dithizonate with various nitrogen bases.

Pyridine, piperidine or triethylamine (2 ml) were added severally to three 25-ml volumetric flasks and made up to volume with $1.225 \cdot 10^{-5}$ *M* primary mercury(II) dithizonate solution. In a further experiment, 2 ml of triethylamine was diluted to 25 ml with $2.45 \cdot 10^{-5}$ *M* dithizone solution. Spectra were run against blanks of the bases in chloroform. The results for triethylamine are shown in Fig. 3. Very similar results were obtained with the other nitrogen donor molecules.

The spectrum of primary mercury(I) dithizonate

A solution of mercury(I) nitrate was prepared by standard methods and diluted to $2 \cdot 10^{-4}$ *M* with 0.8 *M* nitric acid that had been freed from dissolved oxides of nitrogen. A $1.56 \cdot 10^{-5}$ *M* solution (15 ml) of dithizone in chloroform was shaken with 1.5 ml of $2 \cdot 10^{-4}$ *M* mercury(II) nitrate solution (30% excess), 2.5 ml of 0.8 *M* nitric acid and 12 ml of deionised water. The spectrum of the yellow complex is given in Fig. 2, curve 5.

Attempted preparation of solid secondary mercury(II) dithizonate

Dithizone (0.128 g) dissolved in chloroform was extracted into a 1:1 mixture of isopiestic ammonia solution and deionised water. The aqueous phase was poured into a solution of mercury(II) chloride (0.1358 g) in water (200 ml) and stirred vigorously. A dark precipitate separated overnight and was collected. On washing with water, part dissolved to give a violet solution (λ_{max} 530, broad shoulder at 590 nm); on exposure to sunlight the absorbance decreased but there was no other conspicuous change in the spectrum. The water-insoluble residue dissolved to a considerable extent in chloroform and the spectrum of the magenta coloured solution ($\lambda_{max} \sim 508$) suggested a mixture of primary and secondary dithizonates. A small residue of a violet precipitate (insoluble in both water and chloroform) gave an orange-yellow colour when treated with 1 *M* sulphuric acid and the spectrum in chloroform appeared to be that of primary mercury dithizonate.

SUMMARY

Optimum conditions are given for the preparation of violet solutions of secondary mercury(II) dithizonate by means of potassium hydroxide, tetra-*n*-

butylammonium hydroxide or ammonia solution. Concentrated potassium hydroxide or ammonia gives a yellow product which is not identical with primary mercury(II) dithizonate; similar yellow species obtained by the action of pyridine, piperidine, trimethylamine or triethylamine on both primary and secondary mercury(II) dithizonates are reported. Primary mercury(I) dithizonate has been prepared; it is not identical with secondary mercury(II) dithizonate. Various reactions of these dithizonates are discussed.

RÉSUMÉ

Des conditions optimales sont données pour la préparation de solutions violettes de dithizonate de mercure(II) secondaire, utilisant la potasse caustique, ou l'hydroxyde de tétra-*n*-butylammonium, ou d'hydroxyde d'ammonium. La potasse concentrée et l'ammoniaque donnent un produit jaune différent avec le dithizonate de mercure(II) primaire; des substances jaunes similaires sont obtenues par action de la pyridine, de la pipéridine, de la triméthylamine et de la triéthylamine, sur les dithizonates soit primaires soit secondaires.

ZUSAMMENFASSUNG

Es werden die optimalen Bedingungen angegeben für die Darstellung violetter Lösungen von sekundärem Quecksilber(II)-dithizonat unter Verwendung von Kaliumhydroxid oder Tetra-*n*-butylammoniumhydroxid oder Ammoniumhydroxid. Konzentriertes Kaliumhydroxid oder Ammoniak führen zu einem gelben Produkt, das nicht mit primärem Quecksilber(II)-dithizonat identisch ist. Über ähnliche gelbe Verbindungen wird berichtet, die durch Einwirkung von Pyridin, Piperidin, Trimethylamin und Triäthylamin auf sowohl primäres als auch sekundäres Quecksilber(II)-dithizonat erhalten werden.

Primäres Quecksilber(I)-dithizonat wurde dargestellt; es wird gezeigt, dass es mit sekundärem Quecksilber(II)-dithizonat nicht identisch ist. Es werden verschiedene Reaktionen dieser Dithizonate im Vergleich zu Arbeiten von Freiser und Freiser über die korrespondierenden Kupfersysteme erörtert.

REFERENCES

1 G. Iwantscheff, *Das Dithizon und seine Anwendung in der Mikro- und Spurenanalyse*, Verlag Chemie, Weinheim, 1958.
2 E. B. Sandell, *Colorimetric Metal Analysis*, 3rd Edn., Interscience, New York, 1959.
3 H. Fischer, *Wiss. Veröff. Siemens-Konzern*, 4 (1925) 158.
4 H. Irving and C. F. Bell, *J. Chem. Soc.*, (1954) 4253.
5 M. Harding, *J. Chem. Soc.*, (1958) 4136.
6 R. F. Ryan and P. M. Knopf, *Proc. Chem. Soc.*, (1961) 203.
7 P. Alsop and D. K. Laing, *Talanta*, 17 (1970) 242.
8 A. Mawby, *Anal. Chim. Acta*, in press.
9 R. W. Geiger and E. B. Sandell, *Anal. Chim. Acta*, 8 (1953) 197.
10 H. M. N. H. Irving and A. M. Kiwan, *Anal. Chim. Acta*, 45 (1969) 271.
11 H. M. N. H. Irving and T. Nowicka-Jankowska, *Anal. Chim. Acta*, 54 (1971) 55.
12 L. S. Meriwether, E. C. Breitner and C. L. Sloan, *J. Amer. Chem. Soc.*, 87 (1965) 4441.

13 B. S. Freiser and H. Freiser, *Anal. Chem.*, 42 (1970) 305.
14 G. B. Briscoe and B. G. Cooksey, *J. Chem. Soc.*, (1969A) 205.
15 H. M. N. H. Irving and A. M. Kiwan, *Anal. Chim. Acta*, 45 (1969) 255, 271 and refs. therein.
16 H. Irving and J. J. Cox, *J. Chem. Soc.*, (1961) 1470.
17 T. Kato, S. Takei and A. Okagami, *Tech. Rept. Tohoku Univ.*, 21 (1957) 291.
18 H. Irving, S. J. H. Cooke, S. C. Woodger and R. J. P. Williams, *J. Chem. Soc.*, (1949) 1847.
19 Uzamasa and Miyasita, *J. Chem. Soc. Japan, Pure Chem. Sect.*, 72 (1951) 38.
20 F. Koroleff, *Merentutkimuslaitoksen Julkaisu Havsforskningsinstitutets Skrift, Helsinki*, 145 (1950) 7.

Analytica Chimica Acta
Elsevier Publishing Company, Amsterdam
Printed in The Netherlands

DOSAGE DU MERCURE(II) EN PRÉSENCE D'ORGANOMERCURIELS
I. ÉTUDE PHYSICOCHIMIQUE DE DÉRIVÉS MERCURÉS DE LA 2-MÉTHOXYPROPYLURÉE
2-MÉTHOXYPROPYLURÉE

D. MONNIER ET A. GORGIA
Département de Chimie Analytique et Minérale, Université de Genève, Genève (Suisse)

(Reçu le 22 décembre 1970)

La mise au point d'une nouvelle méthode de dosage du mercure ionique en présence d'organomercuriels s'est avérée nécessaire du fait de l'emploi de plus en plus fréquent de certains de ces composés comme fungicides ou comme agents diurétiques, et de la toxicité du mercure ionique qui diffère fortement de celle du mercure lié à un reste organique. Récemment de nombreux cas de pollution et d'empoisonnements au mercure ont été signalés.

Un certain nombre de méthodes de dosage de mercure ionique en présence d'organomercuriels ont été décrites[1-3], mais elles se limitent en général à l'étude d'un seul organomercuriel, et sont le plus souvent semiquantitatives. D'autre part les études de la transformation biologique des organomercuriels a nécessité la mise au point de techniques de dosage du mercure ionique en présence d'organomercuriels[4,5]; ces techniques, par leur nature même, sont limitées à l'étude de la biotransformation des organomercuriels et de la rupture de la liaison carbone–mercure dans les tissus animaux.

L'objet de ce travail est une étude physicochimique préalable de quelques dérivés mercurés de la 2-méthoxypropylurée pour la mise au point d'une méthode de dosage du mercure ionique en évitant la libération du mercure de l'organomercuriel.

Afin de déterminer les conditions de stabilité de certains organomercuriels aliphatiques du type R–Hg–X, nous avons principalement utilisé la méthode des échanges isotopiques[6]: une solution contenant l'organomercuriel (R–Hg*–X) marqué au mercure-203 (Hg*) est agitée avec une goutte de mercure. La libération du mercure se traduit par une diminution de la radioactivité dans la phase aqueuse, elle se fait selon les équations:

$$\text{R–Hg*–X} \rightarrow \text{produit} + \text{Hg}^{*2+} \qquad (1)$$

$$\text{Hg}^{*2+} + \text{Hg(Hg)} \rightleftharpoons \text{Hg}^{2+} + \text{Hg*(Hg)} \text{ échange isotopique} \qquad (2)$$

PARTIE EXPÉRIMENTALE

Réactifs

Les organomercuriels utilisés ont été la 3-chloromercuri-2-méthoxypropylurée (Chlormérodrine), l'acide 3-(hydroxymercuri)-2-méthoxypropylcarbamoylsuccinamique (Meralluride) et l'acide *o*-3-(hydroxymercuri)-2-méthoxypropylcarbamoyl-phénoxyacétique (Mersalyl), qui sont des dérivés mercurés de la 2-méthoxypropylurée.

Dispositif expérimental

Le système utilisé est une modification de celui utilisé par Monnier et Loepfe[6]. Le vibreur est remplacé par un agitateur Hubsahl 275 comportant un support permettant l'agitation simultanée de 8 tubes gradués en polystyrène de 5 ml.

Mode opératoire

Dans les tubes on introduit 400 μl de mercure métallique et 4 ml de solution contenant l'organomercuriel ainsi que les réactifs. Les tubes sont fermés par des bouchons en polyéthylène. Après l'agitation 1 ml de la phase aqueuse est pipetté et introduit dans le puit de la sonde d'un scintillateur. Le rendement de réaction $Q\%$ est donné par le rapport entre l'activité initiale de la solution et l'activité finale de cette même solution, bruit de fond déduit:

$$Q\% = (A_0 - A_s)/A_0$$

où A_0 = activité initiale, et A_s = activité finale.

Ces activités sont mesurées par l'echelle de comptage Landys-Gyr.

Etude spectrophotométrique

Brown *et al.*[7] ont utilisé la bande d'absorption à 232 nm des chlorocomplexes du mercure(II) pour étudier la protodémercuration des organomercuriels aromatiques (chlorure de phénylmercure et ses dérivés substitués) par l'acide chlorhydrique dans l'éthanol à 90%. Une modification de cette méthode a été utilisée pour étudier la réaction des organomercuriels aliphatiques en présence d'acides halogènhydriques. Lors de ces expériences les organomercuriels utilisés ne sont pas marqués, car elles s'effectuent en évitant la présence de mercure métallique.

RÉSULTATS

Influence du pH

Les dérivés mercurés de la méthoxypropylurée sont stables en milieu neutre ou légèrement basique (pH 9) mais libèrent leur mercure en solution acide (par exemple HNO_3, H_2SO_4 $2.5 \cdot 10^{-2}$ *M*). Dans ces conditions il n'y a pas d'échange isotopique organomercuriel–mercure selon l'équation:

$$\text{R–Hg*–X} + \text{Hg(Hg)} \rightleftharpoons \text{R–Hg–X} + \text{Hg*(Hg)} \tag{3}$$

mais une démercuration de l'organomercuriel en reste organique et Hg^{*2+} selon l'éqn. (1). Par la suite il y a échange isotopique entre le Hg^{*2+} ainsi libéré et le mercure métallique.

La présence de protons est indispensable à la libération du mercure de l'organomercuriel mais en absence de tout ligand de l'ion mercure à caractère nucléophile la réaction de protodémercuration est très lente (Fig. 1).

Influence de la présence et de la nature d'un nucléophile X^-

L'acide nitrique seul ($2.5 \cdot 10^{-2}$ *M*) donne une réaction lente qui semble être

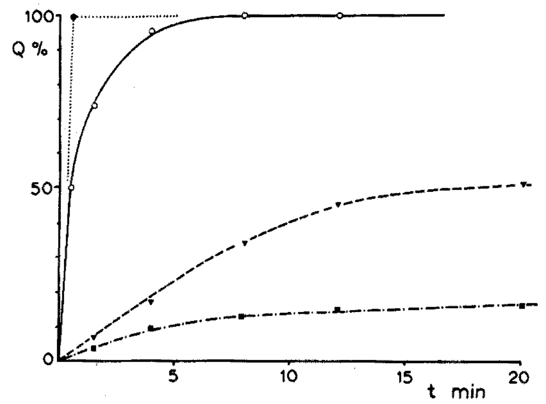

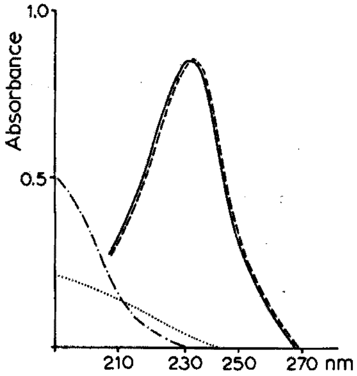

Fig. 1. Influence de la nature de l'halogénure sur la vitesse de protodémercuration. $[CME]=3.4\cdot10^{-7}\,M$, $[HNO_3]=5\cdot10^{-2}\,M$, pH = 1.2. (...●...) $[KJ]=2.5\cdot10^{-2}\,M$; (——○——) $[KBr]=2.5\cdot10^{-2}\,M$; (—▼—) $[KCl]=2.5\cdot10^{-2}\,M$; (-■-) $[KF]=2.5\cdot10^{-2}\,M$, identique à HNO_3 seul.

Fig. 2. Spectres d'absorption de la Chlormérodrine (CME) et des complexes $HgCl_3^-$ et $HgCl_4^{2-}$. (———) $[HgCl_2]=3.4\cdot10^{-5}\,M+[HCl]0.5\,M$; (......) $[HgCl_2]=3.4\cdot10^{-5}\,M$; (------) $[CME]=3.4\cdot10^{-5}\,M+$ $[HCl]$ 0.5 M; (-·-·-·-) $[CME]=3.4\cdot10^{-5}\,M$.

une simple hydrolyse acide au niveau de la liaison C–Hg. Dans ces conditions (pH 1.2) la vitesse de démercuration augmente en présence de nucléophiles complexants du mercure tels que les halogénures. L'influence des halogénures ($2.5\cdot10^{-1}\,M$) decroît dans l'ordre $I^- > Br^- > Cl^- > F^-$ (Fig. 1), l'ion fluor étant pratiquement sans influence sur la vitesse de réaction.

Etude spectrophotométrique: preuve de la protodémercuration

En présence d'ions chlorures le mercure(II) forme, contrairement aux organomercuriels, des complexes $HgCl_3^-$, $HgCl_4^{2-}$ dont le spectre d'absorption présente un maximum à 232 nm.

L'augmentation de la densité optique à 232 nm et le spectre d'absorption de la Chlormérodrine (CME) lors de la réaction en présence d'acide chlorhydrique (Fig. 2) et en absence de mercure métallique sont une preuve de la libération du mercure organique.

La cinétique de cette réaction, pour la Chlormérodrine, la Meralluride et le Mersalyl, est du pseudo-premier ordre, ceci est en accord avec l'excès de réactif ($[HCl]=0.5\,N$) par rapport à l'organomercuriel ($3.4\cdot10^{-5}\,M$).

Cinétique de la réaction de protodémercuration de R–Hg–X par HI

Pour déterminer l'ordre réel de la réaction de protodémercuration des dérivés de la 2-méthoxypropylurée, nous avons effectué une série d'expériences où les concentrations en Chlormérodrine et en HI étaient sensiblement égales. Tous les essais ont été effectués à 60°. Des solutions de 4 ml contenant de la Chlormérodrine marquée au mercure-203, de l'$HClO_4$ et du KI sont introduites dans des tubes en polystyrène et placés dans un thermostat. Les concentrations de la Chlormérodrine, du $HClO_4$ et du KI étudiées, ainsi que les temps de demi-réaction ($T_{\frac{1}{2}}$) obtenus sont représentés au Tableau I.

TABLEAU I

LES CONCENTRATIONS DES RÉACTIFS ET LES TEMPS DE DEMI-RÉACTION

$[CME]$ (M)	$[H^+]$ (M)	$[I^-]$ (M)	$T_{\frac{1}{2}}$ (min)
$3.4\cdot10^{-5}$	$2.5\cdot10^{-4}$	$5\cdot10^{-5}$	39
		$1.25\cdot10^{-4}$	33
		$2.5\cdot10^{-4}$	30
		$5\cdot10^{-4}$	25
$3.4\cdot10^{-5}$	$1.25\cdot10^{-4}$	$5\cdot10^{-4}$	74
	$2.5\cdot10^{-4}$		25
	$5\cdot10^{-4}$		15
$3.4\cdot10^{-4}$	$3.4\cdot10^{-4}$	$3.4\cdot10^{-4}$	90
$1.7\cdot10^{-4}$	$1.7\cdot10^{-4}$	$1.7\cdot10^{-4}$	47

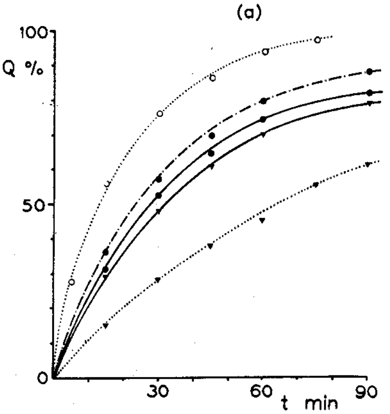

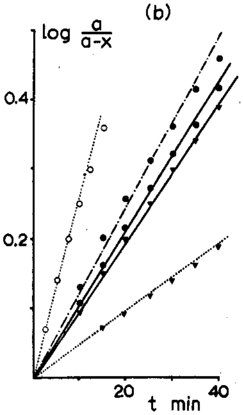

Fig. 3a. Augmentation du rendement de protodémercuration en fonction du temps.

Fig. 3b. Variation de log $a/(a-x)$ en fonction du temps. CME = $3.4\cdot10^{-5}$ M; température = 60°; (●-.-.-●) H^+ $2.5\cdot10^{-4}$ M, I^- $5\cdot10^{-4}$ M; (●———●) H^+ $2.5\cdot10^{-4}$ M, I^- $2.5\cdot10^{-4}$ M; (▼———▼) H^+ $2.5\cdot10^{-4}$ M, I^- $1.25\cdot10^{-4}$ M; (○......○) H^+ $5\cdot1\ ^{-4}$ M, I^- $5\cdot10^{-4}$ M; (●-.-.-●) H^+ $2.5\cdot10^{-4}$ M, I^- $5\cdot10^{-4}$ M; (▼......▼) H^+ $1.25\cdot10^{-4}$ M, I^- $5\cdot10^{-4}$ M.

Les tubes sont retirés du thermostat à intervalles réguliers et placés dans un bain de glace pendant 5 min, ce qui a pour effet d'arrêter la réaction. Puis on ajoute 400 μl de mercure métallique. Après agitation d'une minute, 1 ml de solution est pipetté, l'activité de la phase aqueuse est mesurée et le rendement de démercuration $Q\%$ est calculé. Quelques exemples de réaction sont représentés sur la Fig. 3a.

Pour une première estimation de l'ordre de réaction nous avons appliqué la méthode des pourcentages de réaction (rapports: $T_{\frac{1}{2}}/T_{\frac{1}{3}}$, etc.). Les résultats (Tableau II) sont en accord avec les valeurs théoriques obtenues pour une cinétique du premier ordre.

Sur la base de ces résultats, nous avons appliqué la formule de la cinétique du premier ordre: $K=2.303/t\cdot\log a/(a-x)$ à nos résultats expérimentaux. En portant log $a/(a-x)$ en fonction du temps nous avons obtenu pour les courbes expérimentales de la Fig. 3a, les droites de la Fig. 3b.

TABLEAU II

RAPPORTS DE TEMPS DE RÉACTION DE PROTODÉMERCURATION

	Rapport calculé moyen	*Rapport théorique*	
	± *écart type* ($n=8$)	*1er ordre*	*2e ordre*
$T_{\frac{1}{2}}/T_{\frac{1}{4}}$	2.451 ± 0.104	2.41	2
$T_{\frac{1}{2}}/T_{\frac{1}{3}}$	1.721 ± 0.055	1.71	3
$T_{\frac{1}{3}}/T_{\frac{1}{4}}$	1.482 ± 0.105	1.41	1.5

La protodémercuration des dérivés mercurés de la 2-méthoxypropylurée par les acides halogènhydriques est donc une réaction du premier ordre.

Démercuration de R–Hg–X en présence d'acides non halogènhydriques

Afin de compléter l'étude du comportement des organomercuriels aliphatiques dérivés mercurés de la 2-méthoxypropylurée et de leurs conditions de stabilité, nous avons étudié par la méthode des échanges isotopiques la démercuration de la Chlormérodrine marquée au mercure-203 en milieu aqueux, en présence d'un acide fort tel que l'HNO_3 et l'$HClO_4$ à de fortes concentrations (0.25 à 1 M). La vitesse de démercuration est relativement lente (suivant les conditions: entre 40 et 80% de rendement d'extraction dans la phase mercurielle après 30 min d'agitation) si l'on tient compte de la forte concentration de l'acide. Il est donc évident que les nucléophiles (iodure, chlorure, etc.) participent activement à la démercuration des dérivés mercurés de la 2-méthoxypropylurée en milieu acide.

Comportement de R–Hg–X en milieu éthanol

Reutov et Beletskaya[8], et Jensen et Rickborn[9] ont montré que le comportement des organomercuriels dépend entre autres de la nature du milieu, et que dans des milieux peu polaires (acétone, dioxane, éthanol) ces composés peuvent libérer leur mercure selon l'équations:

$$R\text{–}Hg\text{–}X + R\text{–}Hg\text{–}X \rightleftharpoons R\text{–}Hg\text{–}R + HgX_2 \qquad (4)$$

En milieu éthanol 98%, en l'absence de protons et d'halogénures, le 50% de mercure-203 de la Chlormérodrine ($3.4 \cdot 10^{-7}$ M) passe dans la phase mercurielle après 15 min d'agitation.

Dans les mêmes conditions en milieu éthanol 95%, le rendement d'extraction est de 40%, tandis qu'à partir de 80% et moins en éthanol la réaction n'a plus lieu.

Par contre, en milieu 1-pentanol (98%), on retrouve le 80% de mercure-203 de la Chlormérodrine dans la goutte de mercure après 15 min d'agitation.

Rappelons qu'en milieu aqueux le comportement de ce type d'organomercuriels est très différent puisqu'en l'absence de protons et d'halogénures, dans les mêmes conditions (soit 15 min d'agitation et plus, avec 400 μl de mercure métallique) le rendement d'extraction est nul.

En présence d'acides halogènhydriques la réaction de protodémercuration dans l'éthanol est plus rapide qu'en milieu aqueux. En effet, lorsque la Chlormérodrine marquée au ^{203}Hg ($3.4 \cdot 10^{-7}$ M) est agitée en présence de l'acide chlorhydrique 0.5 N en parallèle dans l'éthanol et dans le l'eau avec 400 μl de mercure métallique, 95 et

37% respectivement de la radioactivité initiale passe dans la phase métallique.

La protodémercuration subit donc des changements considérables lorsqu'on passe d'un milieu à un autre. L'interprétation de ces résultats est néanmoins difficile à cause du rôle important de phénomènes de surface. Ainsi les résultats obtenus en milieu éthanol diffèrent suivant les récipients utilisés (tubes en verre ou en polystyrène) et suivant la présence de substances actives en surface telle que la digitonine.

PROPOSITION D'UN MÉCANISME DE PROTODÉMERCURATION DE R–Hg–X

Pour résumer nous pouvons donc dire pour les dérivés mercurés de la 2-méthoxypropylurée:

1. La réaction de protodémercuration en milieu aqueux est du premier ordre.
2. Cette réaction a lieu en présence de protons. En l'absence de nucléophiles forts, elle est très lente; la présence d'anions (nucléophiles faibles) peut accélerer quelque peu la vitesse de réaction.
3. En présence des nucléophiles forts, la vitesse de réaction est considérablement augmentée (si les protons sont présents); l'influence du nucléophile va en diminuant de I^- à Cl^-.
4. En absence de protons, la vitesse de réaction est pratiquement nulle, même en présence de nucléophiles forts.
5. En milieu moins polaire que l'eau (éthanol) et en présence de HX (acide halogènhydrique), la vitesse de réaction est plus grande qu'en milieu aqueux.

Sur la base de ces résultats, nous proposons un mécanisme du type suivant:

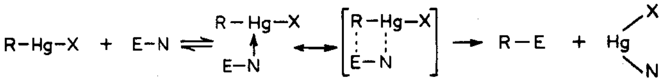

où E = partie électrophile du réactif, et N = partie nucléophile du réactif.

Ce mécanisme est classé comme Substitution électrophile avec "Catalyse" nucléophile interne[9], qui a pour intermédiaire instable une structure cyclique avec attaque électrophile et nucléophile sur la liaison C–Hg.

Ces "attaques" n'ont probablement pas lieu simultanément, "l'attaque" nucléophile ayant lieu dans une étape pré-cinétique avec formation d'un complexe intermédiaire peu stable. Ceci est d'autant plus vraisemblable qu'on connaît la forte tendance du mercure à la formation des complexes.

L'existence d'une telle liaison de coordination aurait pour effet de faciliter l'attaque électrophile, non seulement par l'augmentation de la nucléophilie de l'organomercuriel mais encore par l'augmentation de l'électrophilie du réactif, comme on le voit par le schéma suivant:

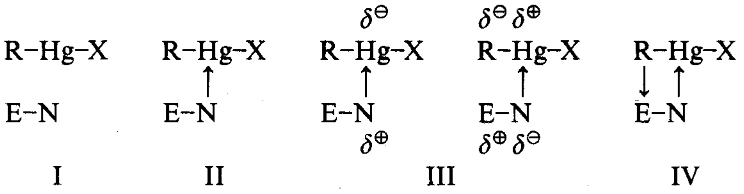

situation de départ — attaque nucléophile — stabilisation du complexe intermédiaire — attaque électrophile

Ce mécanisme expliquerait la réaction du premier ordre, car l'étape déterminant la vitesse de réaction est l'attaque électrophile et elle est donc dépendante de la concentration du complexe intermédiaire. Il est aussi en accord avec la stabilité des dérivés mercurés de la 2-méthoxypropylurée en présence des nucléophiles seuls et leur décomposition lente en présence d'électrophiles seuls. Enfin l'augmentation de la vitesse de réaction en milieu éthanol 95% par un acide halogènhydrique, est un argument supplémentaire en faveur de ce mécanisme puisque, dans ce cas, la concentration de HX dans sa forme moléculaire augmente par rapport au milieu aqueux, ce qui favoriserait la formation du complexe intermédiaire cyclique:

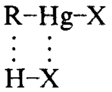

$$\begin{array}{l} R{-}Hg{-}X \\ \vdots \quad\;\; \vdots \\ H{-}X \end{array}$$

et augmentarait donc la vitesse de réaction.

Les complexants forts du mercure(II) tels que l'EDTA, l'acide diamino-1,2-cyclohexanetetracétique, la diphénylcarbazide, la thiourée, etc., attaquent la liaison C–Hg des organomercuriels même en milieu faiblement acide (pH 5).

Une étude comparative en milieu aqueux entre la Chlormérodrine, R–Hg–X aliphatique, et le sel sodique de l'acide *p*-chloromercuribenzoique, R'–Hg–X aromatique, a montré que la réactivité de la liaison C–Hg de ces deux types de composés est différente et plus grande chez l'organomercuriel aromatique, fait qu'on peut attribuer à la nature même de la liaison C–Hg.

CONCLUSION

Puisque le but de ce travail a été l'étude analytique du comportement de certains organomercuriels du type R–Hg–X afin de connaître leurs conditions de stabilité, les résultats obtenus nous ont permis par la suite le choix des conditions pour la mise au point d'une méthode de dosage du mercure(II) ionique en présence d'organomercuriels en évitant la démercuration de ces derniers.

RÉSUMÉ

La stabilité de la liaison C–Hg de 3 dérivés de la 2-méthoxypropylurée a été étudié par la méthode des échanges isotopiques. Les dérivés mercurés de la 2-méthoxypropylurée sont stables en milieu alcalin, neutre et faiblement acide; en présence de complexants du Hg^{2+} et en pH acide (pH 3) ces composés libèrent leur mercure sous forme de Hg^{2+}, cette réaction de protodémercuration a lieu selon une cinétique du premier ordre. Une réaction obéissant à des règles différentes, qui est une réaction d'échange, a lieu en milieu peu polaire (éthanol, 1-pentanol, etc.). Un mécanisme de réaction de protodémercuration est proposé et les conséquences pratiques pour le dosage de mercure ionique en présence d'organomercuriels sont tirées.

SUMMARY

The stability of the C–Hg bond of 3 derivatives of 2-methoxypropylurea was studied by the isotope exchange method. The mercury derivatives of 2-methoxypropylurea are stable in alkaline, neutral or weakly acidic media; in the presence of complexing agents for mercury (II) and at acidic pH (pH 3) these compounds liberated their mercury as mercury(II), the protodemercuration being a first order reaction. An exchange reaction of different order occurred in less polar media (ethanol, 1-pentanol, etc.). A mechanism for the protodemercuration reaction is proposed.

ZUSAMMENFASSUNG

Die Beständigkeit der C–Hg-Bindung von 3 Derivaten von 2-Methoxypropylharnstoff wurde nach der Isotopenaustauschmethode untersucht. Die Quecksilberderivate von 2-Methoxypropylharnstoff sind in alkalischem, neutralem und schwach saurem Medium beständig; in Gegenwart von Komplexbildnern für Quecksilber(II) und bei saurem pH (pH 3) gaben diese Verbindungen ihr Quecksilber in einer Reaktion erster Ordnung als Quecksilber(II) ab. Eine Austauschreaktion verschiedener Ordnung trat in weniger polarem Medium (Äthanol, 1-Pentanol, etc.) auf. Es wird ein Mechanismus für die Protodemercurisierungsreaktion vorgeschlagen.

BIBLIOGRAPHIE

1 L. J. Anghilieri, *Nucl. Med.*, 4 (1964) 193.
2 L. M. Burtseva, M. M. Mirkina, E. S. Sysoeva et V. T. Kharlamov, *Preparatov sp statei*, (1965) 121.
3 R. S. Mani, C. M. Desai et S. V. Raghanan, *Indian J. Chem.*, 3 (1965) 415.
4 V. L. Miller, D. Lillis et E. Csonka, *Anal. Chem.*, 30 (1958) 1705.
5 T. W. Clarkson et M. R. Greenwood, *Anal. Biochem.*, 37 (1970) 236.
6 D. Monnier et E. Loepfe, *Anal. Chim. Acta*, 37 (1967) 339.
7 R. D. Brown, A. S. Buchanan et A. A. Humfray, *Australian J. Chem.*, 18 (1965) 1507.
8 O. A. Reutov et I. P. Beletskaya, *Reaction Mechanisms of Organometallic Compounds*, North-Holland, Amsterdam, 1968.
9 F. Jensen et B. Rickborn, *Electrophilic Substitution of Organomercurials*, McGraw-Hill, 1968.

Anal. Chim. Acta, 54 (1971) 497–504

Analytica Chimica Acta
Elsevier Publishing Company, Amsterdam
Printed in The Netherlands

DOSAGE DU MERCURE(II) EN PRESENCE D'ORGANOMERCURIELS
II. MÉTHODE SPECTROPHOTOMÉTRIQUE OU FLUORIMÉTRIQUE PAR LE NICOTINAMIDE-ADÉNINE-DINUCLÉOTIDE RÉDUIT

A. GORGIA ET D. MONNIER
Département de Chimie Analytique et Minérale, Université de Genève, Genève (Suisse)

(Reçu le 22 décembre 1970)

Irving et Kiwan[1] ont montré que, dans certaines conditions, la dithizone forme avec les organomercuriels des complexes colorés, très proches, du moins en ce qui concerne leurs spectres, de celui fourni par le complexe du mercure(II) ionique avec la dithizone dans les mêmes conditions.

D'autre part, nous avons montré[2] que les réactifs habituels du mercure(II) attaquent la liaison C–Hg des organomercuriels avec libération d'ions Hg^{2+}. Par conséquent, pour doser le mercure(II) ionique en présence d'organomercuriels, il est nécessaire d'effectuer une séparation préalable, sauf si on dispose d'un complexant du mercure(II) sans effet sur la liaison C–Hg des organomercuriels.

Pour la recherche d'un tel réactif, nous avons étudié le comportement du nicotinamide–adénine–dinucléotide envers les ions mercure(II) car l'interaction de ce composé avec le mercure(II) est mesurable par spectrophotométrie[3] et la constante de stabilité du complexe formé est faible; on peut donc supposer que ce complexant n'attaquera pas la liaison C–Hg des organomercuriels.

PRINCIPE DE LA MÉTHODE

Le nicotinamide–adénine–dinucléotide réduit (NADH) présente une bande d'absorption à 340 nm; son coefficient d'extinction molaire est $6.22 \cdot 10^3$. Les solutions aqueuses du NADH ne sont pas stables car on observe une diminution lente de la densité optique à 340 nm au cours du temps. Les ions mercure(II) réagissent avec le NADH et on observe la disparition de la bande d'absorption à 340 nm caractéristique de ce composé (Fig. 1). Il s'agit de la formation d'un complexe NADH–Hg^{2+} comme l'ont prouvé McGarry *et al.*[3]; en effet l'adjonction d'un complexant fort du mercure(II) (*e.g.* EDTA) dans le milieu de réaction fait réapparaître la bande d'absorption à 340 nm ce qui nous a permis de montrer que nous sommes en présence d'un équilibre et non pas d'un processus d'oxydation du NADH (coenzyme réduit).

Sur cette base nous avons étudié la mise au point d'une méthode de dosage du mercure(II) en présence d'organomercuriels car pour des quantités équimolaires de Chlormérodrine (CME) et de NADH, le spectre d'absorption du NADH ne subit pas de modification, et aucune diminution de l'absorbance n'a été observé à 340 nm lorsque, pour une concentration constante en NADH (10^{-4} *M*) la concentration de CME varie de 10^{-5} à 10^{-4} *M*. C'est aussi le cas d'autres organomercuriels tels que l'acide *p*-chloromercuribenzoique, le borate de phénylmercure (Merfène), l'acide

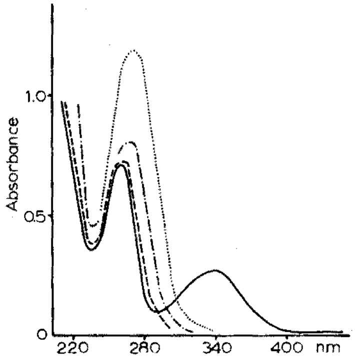

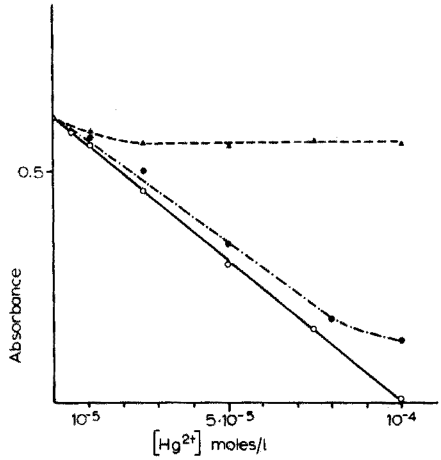

Fig. 1. Spectres d'absorption du NADH et du NAD^+ en présence et en absence de Hg^{2+}. (··········) $[NADH] = 5 \cdot 10^{-5}$ *M* + $[Hg(NO_3)_2] = 5 \cdot 10^{-5}$ *M*; (–·–·–) $[NAD^+] = 5 \cdot 10^{-5}$ *M* + $[Hg(NO_3)_2] = 5 \cdot 10^{-5}$ *M*; (————) $[NADH] = 5 \cdot 10^{-5}$ *M*; (— — —) $[NAD^+] = 5 \cdot 10^{-5}$ *M*.

Fig. 2. Courbes d'étalonnage NADH–Hg^{2+}. Influence du chlorure. (○————○) avec $Hg(NO_3)_2$; (●–·–·–●) avec $HgCl_2$; (▲- - - -▲) avec $Hg(NO_3)_2$ + NaCl 1%.

N-3-(hydroxymercuri)-2-méthoxypropylcarbamoylsuccinamique (Meralluride) et l'acide *o*-3(hydroxymercuri)-2-méthoxypropylcarbamoyl phénoxyacétique (Mersalyl).

Pour augmenter la sensibilité de la méthode nous avons utilisé la fluorescence native du NADH; en effet excité à une longueur d'onde voisine de 340 ou de 260 nm, il présente une bande d'émission dont le maximum se situe à 470 nm. La disparition de la bande d'absorption à 340 nm entraîne la disparition de la fluorescence à 470 nm, ce qui est le cas pour la forme oxydée du NADH, NAD^+, et pour le mélange Hg^{2+}–NADH.

PARTIE EXPÉRIMENTALE

Appareillage

Les mesures d'absorbances ont été effectuées sur le spectrophotomètre Beckman DB à double faisceau avec enregistreur Hitachi. Pour la première partie de l'étude fluorimétrique nous avons utilisé le spectrofluorimètre Zeiss avec deux monochromateurs (M4QIII) et une lampe à xenon (LX50) comme source lumineuse. Les conditions optimales déterminées à l'aide de cet appareil, il a été possible par la suite d'utiliser l'Eppendorf, appareil à filtres comportant comme source lumineuse une lampe à mercure, avec le filtre spécial pour fluorimétrie (313 nm + 366 nm), qui permet d'utiliser avec un maximum d'efficacité les raies du mercure les plus proches de 340 nm.

Dosage par spectrophotométrie d'absorption

Il existe une relation linéaire entre la concentration des ions mercure(II) (sous forme de $Hg(NO_3)_2$) et la diminution de l'absorbance à 340 nm (Fig. 2). Quelle que soit la concentration initiale du NADH, la pente des droites d'étalonnage (pH 5–6) reste constante et indique la formation d'un complexe NADH–Hg^{2+} 1:1, qui se manifeste par la disparition complète de la bande d'absorption à 340 nm lorsque $[Hg^{2+}] = [NADH]$. La quantité minimum dosée par la méthode spectrophotométrique est de $5 \cdot 10^{-6}$ moles l^{-1}, soit 1 μg $ml^{-1} \pm 17\%$ (écart type relatif).

Dosage par fluorimétrie

Comme en spectrophotométrie d'absorption, la relation entre la concentration des ions mercure(II) et l'intensité de fluorescence montre qu'il se forme un complexe NADH–Hg^{2+} correspondant à un rapport moléculaire 1:1 car lorsque $[Hg^{2+}] = [NADH]$ nous constatons une disparition totale de la fluorescence à 470 nm. Cependant, cette observation n'est valable que pour des concentrations en NADH supérieures à $5 \cdot 10^{-6}$ *M*. Aux concentrations plus faibles, on remarque une dissociation partielle du complexe qui devient importante pour des concentrations en NADH–Hg^{2+} inférieurs à $5 \cdot 10^{-7}$ *M* et qui rend le dosage du mercure(II) plus délicat. Ceci provient de la relativement faible constante de stabilité du complexe étudié.

Ce fait ne nous permet pas d'utiliser toutes les possibilités offertes par la forte fluorescence du NADH. Malgré cela, cette méthode est plus sensible que la spectrophotométrie d'absorption. En effet, il est possible de détecter $5 \cdot 10^{-8}$ moles l^{-1} de mercure(II), soit 10 ng ml^{-1}, et doser 30.8 ng ml^{-1} avec une fidélité de $\pm 15\%$. Ces résultats sont basés sur l'analyse statistique (droite de régression, limites de confiance[4]) d'un ensemble de 67 valeurs, et figurent au Tableau I.

TABLEAU I

L'ANALYSE STATISTIQUE DE 67 VALEURS

y (T%) arbitraire	*x (ng ml⁻¹) calculé*	*Limites de confiance (pour P = 0.05)*		*Limites de confiance en % de x calculé*	
60	30.8	26.3	34.8	−14.7	+13.1
50	72.5	68.8	76.0	− 5.2	+ 4.8
49.02	76.6	73.1	79.9	− 4.6	+ 3.5
40	114.3	110.2	118.3	− 3.6	+ 3.5
30	156.0	150.7	161.5	− 3.4	+ 3.5
20	197.7	197.9	205.1	− 0.09	+ 3.7

Influence du pH sur le complexe NADH–Hg^{2+}

L'étude de la formation du complexe NADH–Hg^{2+} en fonction du pH a montré que le dosage doit se faire a des pH compris entre 4 et 7. Aux pH supérieurs à 8, la formation des complexes hydroxylés du mercure(II) rend son dosage par le NADH impossible. D'autre part, lors de l'étude fluorimétrique, il est nécessaire de travailler à un pH d'environ 4.5 en milieu acide nitrique ($2.5 \cdot 10^{-5}$ *M*) car aux pH supérieurs, la complexation partielle du mercure(II) par les ions hydroxyles au dépens du NADH, se traduit par des déformations importantes de la droite d'étalonnage seulement aux très faibles concentrations en mercure(II) ($5 \cdot 10^{-8}$ à 10^{-6} *M*).

Pour des pH inférieurs à 3, le complexe est très rapidement détruit par hydrolyse acide.

A des pH supérieurs à 4.5 l'emploi d'un tampon phosphate (KH_2PO_4–Na_2HPO_4) 0.1 *M* pH 7 donne également des résultats satisfaisants pour ce dosage à condition que la concentration en mercure(II) soit supérieure à 10^{-6} *M*.

Le choix du tampon n'est pas sans importance car nous avons constaté que les ions phosphates ne gênent pas la formation du complexe. Par contre, un grand nombre d'anions tels que acétate, citrate, borate, etc. interférent avec la formation du complexe NADH–Hg^{2+} et la disparition de la bande d'absorption à 340 nm ainsi que la bande d'émission à 470 nm ne répondent plus à des rapports stoechiométriques.

Anions gênants. Effets d'anions complexants du mercure sur la formation du complexe

Le complexe NADH–Hg^{2+} est relativement peu stable et la présence de complexants forts du mercure(II) tels que les halogénures (I^-, Br^-, Cl^-), l'EDTA etc., empêche la formation quantitative du complexe selon l'équation:

$$\begin{tikzcd} Hg^{2+} + NADH \arrow[r, shift left] & NADH\text{–}Hg^{2+} \arrow[l, shift left] \arrow[d, shift left, "X^-"] \\ & HgX_n^{-n+2} + NADH \arrow[u, shift left] \end{tikzcd} \qquad (X^- = \text{anion complexant})$$

Cette réaction se traduit par la réapparition de la bande d'absorption à 340 nm (Fig. 2), ainsi que de la bande d'émission à 470 nm. Ainsi le dosage du mercure ionique en présence de chlorure nécessite l'introduction d'un facteur de correction lorsque $[Cl] > 5[NADH]$ et devient impossible lorsque le complexant est en grand excès par rapport au mercure(II).

Effets d'un excès d'organomercuriel sur la formation du complexe NADH–Hg^{2+}

La nature cationique des organomercuriels est la cause d'une certaine interaction entre ces composés et le NADH. Cette interaction n'est visible que pour des concentrations de 50 à 100 fois supérieures à celle du mercure ionique. Lorsque la

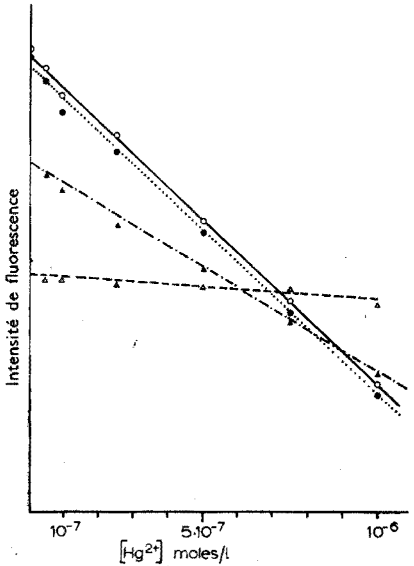

Fig. 3. Courbes d'étalonnage NADH–Hg^{2+} en présence de Chlormérodrine (CME) avec $[NADH] = 10^{-6}$ *M*. λ_{ex} 340 nm, λ_{em} 470 nm. (○———○) $[CME] = 0$ *M*; (●··········●) $[CME] = 10^{-5}$ *M*; (▲-·-·-▲) $[CME] = 10^{-4}$ *M*; (△----△) $[CME] = 10^{-3}$ *M*.

concentration d'organomercuriel augmente au delà de cette limite ($[R\text{–}Hg\text{–}X] \leq 100 [Hg^{2+}]$), le dosage du mercure ionique par cette méthode devient impossible (Fig. 3); ceci est valable pour la Chlormérodrine le Mersalyl, la Meralluride, le Merfène et l'acide *p*-chloromercuribenzoique.

CONCLUSION

Cette méthode de dosage malgré sa grande sensibilité et très bonne reproductibilité n'est pas toujours applicable au dosage du mercure(II) ionique en présence d'organomercuriel en excès, ou d'anions complexants forts du Hg^{2+}. Dans ce cas il est nécessaire de séparer ces deux constituants (mercure–organomercuriel) avant le dosage du mercure(II). C'est le problème que nous nous sommes efforcés de résoudre et qui fait l'objet de la suite de ce travail.

RÉSUMÉ

Une méthode de dosage de mercure(II) ionique en présence d'excès d'organomercuriel est décrite. Le mercure(II) ionique forme un complexe 1:1 avec le nicotinamide–adénine–dinucléotide réduit (NADH) avec disparition de la bande d'absorption à 340 nm caractéristique de ce composé. Cette propriété a été utilisée pour le dosage du mercure(II) ionique soit par spectrophotométrie d'absorption soit par fluorimétrie. Par la première méthode on peut doser 1 $\mu g\ ml^{-1}$ de mercure à $\pm 17\%$ près, et par la deuxième 30 ng ml^{-1} à $\pm 15\%$ près. L'influence de complexants du mercure et de grands excès d'organomercuriels sur la formation du complexe NADH–Hg^{2+} a été étudiée.

SUMMARY

A method is described for the determination of mercury(II) ions in the presence of excess of organomercurials. Mercury(II) forms a 1:1 complex with reduced nicotinamide–adenine–dinucleotide (NADH), and the characteristic absorption band of the reagent at 340 nm disappears. This can be utilized spectrophotometrically or fluorimetrically. In the former method, mercury(II) is determined at the 1 $\mu g\ ml^{-1}$ level with a precision of $\pm 17\%$; with the latter method, 30 ng ml^{-1} is determined with a precision of $\pm 15\%$. Strong complexing agents for mercury, and large excesses of organomercurials interfere with the formation of the NADH–Hg^{2+} complex.

ZUSAMMENFASSUNG

Es wird eine Methode für die Bestimmung von Quecksilber(II)-Ionen in Gegenwart eines Überschusses von Organoquecksilber verbindungen beschrieben. Quecksilber(II) bildet mit reduziertem Nicotinamid-adenin-dinucleotid (NADH) einen 1:1-Komplex, wobei die charakteristische Absorptionsbande des Reagenzes bei 340 nm verschwindet. Dies kann für eine spektrophotometrische oder fluorimetrische Bestimmung ausgenutzt werden. Im ersten Fall werden Quecksilber(II)-Gehalte von etwa 1 $\mu g\ ml^{-1}$ mit einer Reproduzierbarkeit von $\pm 17\%$ bestimmt; bei der zweiten Methode werden 30 ng ml^{-1} mit einer Reproduzierbarkeit von $\pm 15\%$ bestimmt. Starke Komplexbildner für Quecksilber und ein grosser Überschuss von Organoquecksilberverbindungen stören die Bildung des NADH-Hg^{2+}-Komplexes.

BIBLIOGRAPHIE

1 H. M. N. H. Irving et A. M. Kiwan, *Anal. Chim. Acta*, 45 (1969) 243.
2 D. Monnier et A. Gorgia, en voie de publication.
3 J. D. McGarry, P. Donkin et H. K. King, *Arch. Biochem. Biophys.*, 126 (1968) 973.
4 A. Linder, *Statistische Methoden*, Birkhauser Verlag, Basel, 1960.

Anal. Chim. Acta, 54 (1971) 505–510

Analytica Chimica Acta
Elsevier Publishing Company, Amsterdam
Printed in The Netherlands

UTILIZATION OF IONIC SURFACTANTS IN THE A.C. POLAROGRAPHIC DETERMINATION OF TITANIUM

H. K. HOFF AND E. JACOBSEN
Department of Chemistry, University of Oslo, Blindern, Oslo 3 (Norway)

(Received 22nd December 1970)

Well defined d.c. polarographic waves of titanium(IV) are obtained from strongly acidic solutions and from oxalate, citrate and tartrate buffers. Consequently, all these media have been recommended as supporting electrolytes for the polarographic determination of titanium[1-6]. In d.c. polarography excesses of easily reducible ions such as iron, copper and bismuth interfere seriously. Hence, Beevers and Breyer[7] recommend a.c. polarography for the determination of titanium in the presence of iron, and claim that a 75-fold amount of iron and a 2-fold amount of copper do not cause any interference when 0.2 *M* oxalate buffer is used as supporting electrolyte. According to Kowalski and Zarebski[8], titanium can be determined in the presence of a 40-fold amount of iron in 0.5 *M* citrate buffer by a.c. polarography. However, in this medium, copper, bismuth, cadmium and lead interfere.

By a.c. polarography it is difficult to determine less than a few p.p.m. of titanium in any of these electrolytes. Recent experiments indicate, however, that the presence of an ionic surfactant may result in an increase in the height of the wave and this phenomenon has been applied for increasing the sensitivity of the a.c. polarographic method[9-12]. Preliminary experiments showed that the height of the a.c. polarographic wave of titanium(IV) in citrate buffers increases in the presence of long-chain aliphatic amines. The present work was carried out in order to investigate the application of surfactants in the a.c. polarographic determination of small amounts of titanium in the presence of large amounts of other metal ions.

EXPERIMENTAL

Equipment

Polarograms were recorded with a Metrohm E 261 Polarecord connected to a Metrohm E 393 a.c. modulator. An external saturated calomel electrode (S.C.E.), connected to the cell by means of an agar bridge, served as reference electrode and a tungsten electrode was employed as auxiliary electrode. All a.c. polarograms were obtained with an a.c. amplitude of 10 mV r.m.s. The capillary characteristics of the dropping mercury electrode, measured in 0.1 *M* potassium nitrate (open circuit) at a mercury height of 62.6 cm, were $m = 2.421$ mg sec^{-1} and $t = 3.68$ sec. All experiments were performed at $25 \pm 0.1°$. Dissolved air was removed from the solutions by bubbling oxygen-free nitrogen through the cell for 10 min and passing it over the solution during the electrolysis.

Chemicals

All chemicals were reagent-grade and were used without further purification. A 0.1006 *M* titanium(IV) stock solution was prepared by diluting a 20% $TiCl_4$ solution (Riedel de Häen, Germany) with 2 *M* sulphuric acid, and was standardized by titration with EDTA[13]. Stock solutions of citric acid were prepared by dissolving the appropriate amount of the acid in distilled water. The following surfactants were used:

1. Decylamine (Koch-Light, Lab., England).
2. Dodecylamine (Armour Industrial Chemical Co., Chicago, Ill., U.S.A.).
3. Octadecyltrimethylammonium chloride, "Arquad 12/50" (Armour Hess Chemicals, Ltd., England).
4. Sodium dodecylsulphate (L. Light and Co., Ltd., England).
5. Sodium dodecyldiphenyletherdisulphonate, "Benax" (Dow Chemical Co., Midland, Mich., U.S.A.).

Stock solutions (1%) of the two amines were prepared by dissolving 1 g of the commercial product in 100 ml of perchloric acid containing an equivalent amount of the acid. Solutions of the remaining surfactants were prepared by dissolution of the product in distilled water.

RESULTS

Very few data for the polarographic reduction of titanium–citrate complexes are reported in the literature[2,8]. Hence, the polarography of titanium(IV) in citrate buffers was first studied in the absence of surfactants.

The effect of pH on the polarographic waves was investigated by recording a.c. and d.c. polarograms of 10^{-4} *M* titanium(IV) in 0.2 *M* citric acid. The pH of each solution was adjusted to the desired value by addition of sodium hydroxide or sulphuric acid. Well defined waves were obtained over a considerable pH range. The summit potential was shifted from −0.32 V at pH 1.0 to −1.0 V at pH 8.0. Above pH

TABLE I

EFFECT OF PRESSURE OF MERCURY ON THE POLAROGRAPHIC WAVES OF 10^{-4} *M* TITANIUM(IV) IN 0.2 *M* CITRATE BUFFER AT pH 6.1

h_{corr} (*cm*)	*d.c. current* (μA)	$i/\sqrt{h_{corr}}$ ($\mu A\ cm^{-\frac{1}{2}}$)	*a.c. current* (μA) (*r.m.s.*)
46.0	0.203	0.0300	0.280
51.0	0.215	0.0301	0.281
56.0	0.223	0.0298	0.285
61.0	0.237	0.0304	0.283
66.0	0.244	0.0301	0.282
71.0	0.252	0.0299	0.284
76.0	0.260	0.0299	0.284

8 the titanium started to hydrolyse and the polarographic wave disappeared. In the pH range 1.0–5.5 the height of the a.c. wave was very dependent on the pH of the electrolyte. Moreover, the slope of the log plot (log $i/(i_d - i)$ *vs.* E) and the width of the a.c. wave at half height showed an apparently irreversible reduction. However, in the pH range 5.5–6.8, the height of the a.c. wave was independent of pH (Fig. 4, curve A) and the slope of the log plot (−58 mV) for the d.c. wave and the width of the a.c. wave at half height (93 mV) indicated a reversible 1-electron reduction to a titanium(III) complex. Hence, the following experiments were performed with 0.2 *M* citrate buffer of pH 6.1 as supporting electrolyte. At this pH value the summit potential, E_s, was −0.93 V *vs.* S.C.E. and coincided with the half-wave potential.

The effect of droptime on the limiting current was determined by recording polarograms of 10^{-4} *M* titanium(IV) in 0.2 *M* citrate buffer at various heights of the mercury column. As indicated in Table I, the a.c. peak current, i_s, was practically constant, whereas the d.c. current increased with the height of the mercury column. The value $i/\sqrt{h}$, where h is the height of the column after correction for the "back pressure" was constant, which indicates that the current is diffusion-controlled.

The temperature coefficient (determined in the range 15–40°) of the d.c. current was +1.8%/degree, and of the a.c. peak current, +1.3%/degree; these values also indicate that the current is controlled essentially by diffusion. The temperature coefficient of the half-wave potential (−1.0 mV/degree) was of the proper sign and magnitude for a reversible process.

TABLE II

POLAROGRAPHIC DETERMINATION OF TITANIUM(IV) IN 0.2 *M* CITRATE BUFFER AT pH 6.1

Ti concn. (*mM*)	i_d (μA)	i_d/C ($\mu A\ mM^{-1}$)	i_s (μA) (*r.m.s.*)	i_s/C (μA (*r.m.s.*) mM^{-1})
1.00	2.44	2.44	2.40	2.40
0.80	2.00	2.50	2.04	2.55
0.60	1.50	2.50	1.60	2.67
0.40	0.99	2.47	1.16	2.90
0.10	0.240	2.40	0.281	2.81
0.08	0.200	2.50	0.218	2.73
0.06	0.145	2.42	0.165	2.75
0.04	0.098	2.45	0.110	2.75
0.02	0.050	2.50	0.051	2.55
	Mean:	2.46	Mean:	2.68

Polarograms recorded from 0.2 *M* citrate buffer of pH 6.1 with various amounts of titanium present, showed that the current increased proportionally to the concentration of titanium. The results (Table II) proved that titanium can be determined in the concentration range $2 \cdot 10^{-5}$–10^{-3} *M*. The a.c. current was hard to reproduce, and as shown in Table II, the relative deviation of i_s/C from the mean value 2.68 was about 9%. The a.c. polarograms exhibited a huge tensammetric wave with $E_{T+} = -0.4$ V *vs.* S.C.E. (Fig. 1) and at titanium concentrations below $2 \cdot 10^{-5}$ *M* this wave interfered with the titanium wave. The diffusion current constant, $i_d/Cm^{\frac{2}{3}}t^{\frac{1}{6}}$, calculated from the data in Table II was $I = 1.09$.

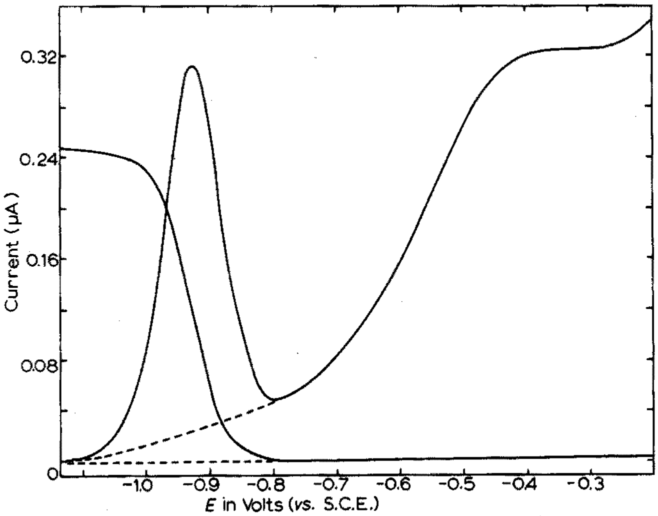

Fig. 1. A.c. and d.c. polarograms of 10^{-4} M titanium(IV) in 0.2 M citrate buffer at pH 6.1. Dashed lines represent the residual current.

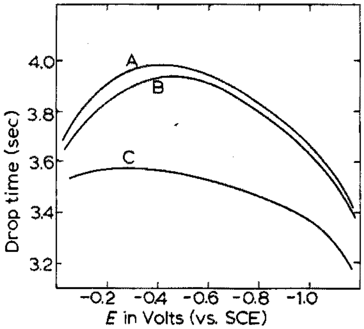

Fig. 2. Electrocapillary curves of 0.2 M citrate buffer pH 6.1 (curve A) containing $4 \cdot 10^{-5}$ M titanium(IV) (curve B) and 0.01% dodecylamine (curve C).

The appearance of a tensammetric wave (which is not followed by a d.c. polarographic step) implies that citrate is adsorbed on the electrode surface. Electrocapillary curves of the citrate buffer in the absence and in the presence of titanium (Fig. 2) indicated that the titanium citrate complex is also strongly adsorbed. The adsorption is probably very fast as the data in Table I clearly demonstrate that diffusion is the rate-controlling step in the overall electrode reaction.

Effect of surfactants

Experiments showed that the d.c. current of the titanium citrate complex was not affected by addition of cationic surfactants to the electrolyte. However, as indicated in Fig. 3, the a.c. polarographic peak height increased in the presence of such substances (dodecylamine and Arquad). The a.c. current increased also in the presence of decylamine but because the a.c. polarograms of decylamine exhibited a negative

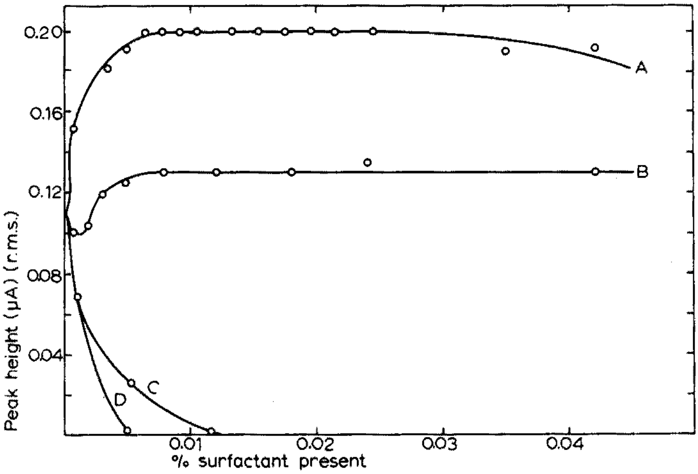

Fig. 3. Effect of various surfactants on the peak height of the a.c. polarographic wave of 4·10^{-5} *M* titanium(IV) in 0.2 *M* citrate buffer at pH 6.1. (A) Dodecylamine, (B) Arquad, (C) dodecylsulphate and (D) Benax.

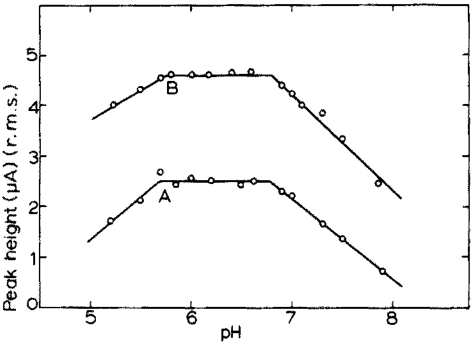

Fig. 4. Effect of pH on the peak height of 4·10^{-5} *M* titanium(IV) in 0.2 *M* citrate buffer in the absence (A) and in the presence of 0.01 % dodecylamine (B).

tensammetric wave which interfered with the titanium wave, these data are not included in the figure. In the presence of anionic surfactants (dodecylsulphate and Benax), the electrode reaction was inhibited and the a.c. wave disappeared.

In the presence of 0.005–0.025 % dodecylamine, the a.c. wave of titanium was independent of the amount of the surfactant present and the height of the peak was about 80 % greater than in the absence of surfactants. Hence, in the following experiments 0.01 % dodecylamine was added to each solution.

The effect of pH on the peak height of the a.c. polarographic wave of titanium in citrate buffers was the same both in the absence and in the presence of dodecylamine (Fig. 4) and citrate buffer of pH 6.1 appeared to be the best electrolyte also in the presence of dodecylamine. A.c. polarograms of titanium in this electrolyte are shown in Fig. 5. As indicated in the figure, the drop time was greatly decreased in the presence of dodecylamine and, hence, the precision of the peak height measurement was much

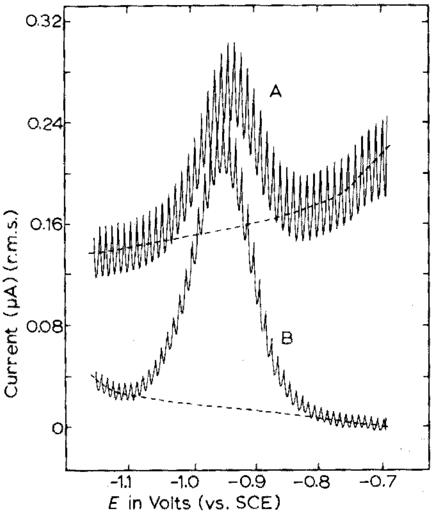

Fig. 5. A.c. polarograms of $4 \cdot 10^{-5}$ M titanium(IV) in 0.2 M citrate buffer, pH 6.1 in the absence (A) and in the presence of 0. 1% dodecylamine (B). Dashed lines represent the a.c. base currents.

TABLE III

A.C. POLAROGRAPHIC PEAK HEIGHT OF TITANIUM(IV) IN 0.2 M CITRATE BUFFER OF pH 6.1 WITH 0.01% DODECYLAMINE PRESENT

Ti concn. (*mM*)	*Current*, i_s (μA) (*r.m.s.*)	i_s/C (μA (*r.m.s.*) mM^{-1})
0.100	0.442	4.42
0.080	0.355	4.44
0.060	0.276	4.60
0.040	0.185	4.62
0.020	0.094	4.70
0.010	0.047	4.70
0.008	0.036	4.67
0.006	0.028	4.67
0.004	0.019	4.75
0.002	0.009	4.5

better. Moreover, the tensammetric citrate wave was depressed in the presence of the surfactant and did not interfere with the titanium wave.

A.c. polarograms recorded from 0.2 M citrate buffer of pH 6.1 with 0.01% dodecylamine and various amounts of titanium present showed that the peak height increased linearly with the concentration in the range $2 \cdot 10^{-6}$–$6 \cdot 10^{-5}$ M (Table III). At higher concentrations of titanium the value i_s/C decreased, but the peak height was still perfectly reproducible. Comparison of the data in Table II and III shows that the sensitivity of the method was increased ten times by the presence of dodecylamine and, besides, that the relative deviation was only about 2% compared to 9% in the absence of surfactants.

The effect of drop time and of temperature on the d.c. and a.c. polarographic waves of titanium(IV) in citrate buffer with 0.01 % dodecylamine present was investigated as described above. The d.c. current and the half-wave potential were not affected by addition of dodecylamine to the electrolyte, and the experiments showed that the current was also diffusion-controlled in the presence of dodecylamine. Exactly the same temperature coefficient was obtained in the presence as in the absence of dodecylamine. Hence, the electron-transfer reaction is fast even if the electrode surface is covered with dodecylamine and the diffusion of the complex must be the rate-determining step in the overall reaction.

Interfering elements

Experiments showed that although the peak height of the titanium wave increased about 80 % in the presence of dodecylamine, the peak height of other elements such as lead, copper, iron(III) and cadmium decreased from 25 to 50 % in the presence of the same surfactant. Consequently, there will be less interference from other elements when dodecylamine is incorporated in the supporting electrolyte.

TABLE IV

A.C. POLAROGRAPHIC DETERMINATION OF 0.06 m*M* TITANIUM(IV) IN SYNTHETIC MIXTURES

(Supporting electrolyte: 0.2 *M* citrate buffer of pH 6.1 with 0.01 % dodecylamine present)

Added species (*mM*)	*Ti found* (*mM*)	*Error* (%)
0.6 Fe^{3+}	0.0600	0.0
3.6 Fe^{3+}	0.0600	0.0
6.0 Fe^{3+}	0.0594	−1.0
0.6 Pb	0.0594	−1.0
0.9 Pb	0.0591	−1.5
0.6 Cu	0.0600	0.0
6.0 Cu	0.0608	+1.3
0.3 Cd	0.0596	−0.7
0.6 Cd	0.0594	−1.0
1.2 Tl^{+}	0.0586	−2.3
0.2 Bi	0.0592	−1.3
0.3 VO_3^-	0.0588	−2.0
0.6 VO_3^-	0.0582	
0.3 Sn	0.0594	−1.0
0.6 Sn	0.0586	−2.3
0.06 MoO_3^-	0.0617	+2.8
0.06 Sb^{3+}	0.0651	+8.5
60 SO_4^{2-}	0.0595	−0.8
60 NO_3^-	0.0601	+0.2

The alkali metals, magnesium, calcium, aluminium, cobalt and arsenic(V) were all polarographically inactive in the citrate buffer. The possible interference of other elements was investigated by recording a.c. polarograms of $6 \cdot 10^{-5}$ *M* titanium(IV) and various other elements in 0.2 *M* citrate buffer of pH 6.1 with 0.01 % dodecylamine present. The results are given in Table IV. It is interesting to note that when dodecylamine is added to the electrolyte, titanium could be determined in the presence of a

100-fold amount of iron and copper and at least a 10-fold amount of most other elements which normally interfere. Antimony(III) was reduced at almost the same potential as titanium and even a small amount of antimony caused significant interference. The relative deviation was less than 3 % in the presence of the other elements tested.

DISCUSSION

The most interesting result of this paper is that the peak height of the titanium wave increases about 80 % when dodecylamine is incorporated in the electrolyte. This effect is also observed in the presence of other cathionic surfactants, whereas the electrode reaction is inhibited in the presence of anionic surfactants.

As indicated in Fig. 2 the titanium–citrate complex is adsorbed on the electrode. At pH 6.1 the complex is probably negatively charged and the depolarizer is probably electrostatically repelled from the negatively charged adsorbed layer. However, as shown in Figs. 2 and 5 dodecylamine is more strongly adsorbed on the electrode and thus prevents the adsorption of the titanium complex. Moreover, the surfactant is positively charged and might facilitate the approach of the depolarizer to the electrode[9,14-16]. In order to confirm this assumption, the electrode reaction of the Ti^{4+}/Ti^{3+} couple will be investigated in the absence and presence of surfactants by cyclic voltammetry and chronopotentiometry.

The proposed method for the determination of titanium is very simple, selective and accurate. Furthermore, it is even more sensitive than the atomic absorption method. Because magnesium, calcium and aluminium are polarographically inactive in citrate buffer, the present method should be very suitable for the determination of small amounts of titanium in the presence of large amounts of these elements such as in clay, limestone, ores, etc.

SUMMARY

The height of the a.c. polarographic wave of titanium(IV) in citrate buffer increases by about 80 % on addition of the surfactant dodecylamine to the supporting electrolyte. At the same time the peak heights of most other elements decrease. Hence, citrate buffer of pH 6.1 with 0.01 % dodecylamine present is recommended as supporting electrolyte for the determination of 0.1–10 p.p.m. titanium in the presence of large amounts of other elements. Antimony(III) is the only element which causes significant interference. The relative deviation from the mean value is less than 3 %.

RÉSUMÉ

La hauteur de la vague polarographique du titane(IV) en milieu tampon citrique augmente d'environ 80% par addition de dodécylamine (agent tensio-actif) à l'électrolyte de base; par contre, on observe une diminution des hauteurs de pics de la plupart des autres éléments. On peut par conséquent recommander comme électrolyte de base un tampon citrique de pH 6.1 contenant 0.01% de dodécylamine, pour le dosage de 0.1 à 10 p.p.m. de titane, en présence d'un grand excès d'autres éléments. L'antimoine(III) est le seul élément présentant une interférence importante. La déviation relative de la valeur moyenne est inférieur à 3%.

ZUSAMMENFASSUNG

Die Stufenhöhe bei der Wechselstrompolarographie von Titan(IV) in Citratpuffer nimmt bei Zugabe von oberflächenaktivem Dodecylamin zum Trägerelektrolyten um etwa 80% zu. Gleichzeitig nehmen die Peakhöhen der meisten anderen Elemente ab. Deshalb wird ein Citratpuffer von pH 6.1 mit 0.01% Dodecylamin als Trägerelektrolyt für die Bestimmung von 0.1–10 p.p.m. Titan in Gegenwart grosser Mengen anderer Elemente empfohlen. Als einziges Element stört Antimon(III) erheblich. Die relative Abweichung vom Mittelwert ist kleiner als 3%.

REFERENCES

1 J. J. Lingane and J. H. Kennedy, *Anal. Chim. Acta,* 15 (1956) 294.
2 V. Vandenbosch, *Bull. Soc. Chim. Belg.,* 58 (1949) 532.
3 D. F. Adams, *Anal. Chem.,* 20 (1948) 891.
4 J. J. Lingane and V. Vandenbosch, *Anal. Chem.,* 21 (1949) 649.
5 R. L. Pecsok, *J. Amer. Chem. Soc.,* 73 (1951) 1304.
6 A. Blažek, *Anal. Chem.,* 24 (1952) 914.
7 J. R. Beevers and B. Breyer, *J. Electroanal. Chem.,* 1 (1959/60) 39.
8 Z. Kowalski and J. Zarebski, *Chem. Anal. (Warsaw),* 12 (1967) 1237; 13 (1968) 55.
9 N. Gundersen and E. Jacobsen, *J. Electroanal. Chem.,* 20 (1969) 13.
10 R. Kalvoda, W. Anstine and M. Heyrovský, *Anal. Chim. Acta,* 50 (1970) 93.
11 E. Jacobsen and G. Tandberg, *J. Electroanal. Chem.,* (1971) in press.
12 E. Jacobsen and T. Rojahn, *Anal. Chim. Acta,* (1971) in press.
13 B. Bieber and Z. Večeřa, *Collection Czech. Chem. Commun.,* 26 (1961) 2081.
14 A. N. Frumkin, *Trans. Faraday Soc.,* 55 (1969) 156.
15 A. N. Frumkin, N. Nikolajeva-Fedorovich and R. Ivanova, *Can. J. Chem.,* 37 (1959) 253.
16 E. Jacobsen and G. Kalland, *Anal. Chim. Acta,* 30 (1964) 240.

Analytica Chimica Acta
Elsevier Publishing Company, Amsterdam
Printed in The Netherlands

POLAROGRAPHY OF THE URANIUM(VI) CHELATE OF *trans*-1,2,-DIAMINOCYCLOHEXANE-N,N,N',N'-TETRAACETIC ACID

TSAI-TEH LAI AND CHEN-FENG KAO
Chemical Engineering Department, Cheng Kung University, Tainan, Taiwan (China)

(Received 8th October 1970)

The stability constant of the mercury(II)–1,2-diaminocyclohexane-N,N,N',N'-tetraacetic acid (CDTA) complex has been determined and the cathodic reduction of the complex at the dropping mercury electrode has been shown to be irreversible[1]. The metal–ligand ratio of the lead[2] and cadmium[3] complexes of CDTA has been determined to be 1:1 by amperometric titration. The polarographic behaviour of the antimony(III)[4] and thallium(I)[5] complexes with CDTA has been reported.

In this paper, the polarographic behaviour of the chelate formed between uranium(VI) and CDTA is described.

EXPERIMENTAL

Apparatus

All apparatus and experimental procedures were the same as reported previously[6]. The capillary characteristics were: $m = 1.75$ mg sec^{-1} and $t = 4.55$ sec at a mercury height of 70.0 cm in 1.0 mM $UO_2(ClO_4)_2$, 0.08 M CDTA and 0.2 M $NaClO_4$ at ionic strength 0.7 at closed circuit. All measurements were made at 30±0.1°.

Chemicals

The stock solution of 0.01 M uranyl perchlorate was prepared and analyzed as described previously[7].

A 0.4 M stock solution of CDTA was prepared by dissolving 36.436 g of *trans*-1,2-diaminocyclohexane-N,N,N',N'-tetraacetic acid monohydrate (Aldrich Co.) and 10 g of sodium hydroxide in distilled water and diluting to 250 ml. The ionic strength of the polarographic solution was adjusted to 0.7 by adding an appropriate volume of 2.0 M sodium perchlorate. Since no maxima were observed, a maximum suppressor was not used.

RESULTS AND DISCUSSION

The polarographic behaviour of the uranyl–CDTA complex was studied systematically over the pH range 2.48–11.00 with solutions containing 1.0 mM uranyl

TABLE I

POLAROGRAPHIC CHARACTERISTICS OF URANYL ION IN CDTA

[*CDTA*] (*M*)	*pH*	$-E_{\frac{1}{2}}$(*V vs. S.C.E.*)	i_d (*μA*)	$E_{\frac{1}{4}}-E_{\frac{3}{4}}$
0.02	2.50	0.230	3.36	0.080[a]
	3.50	0.252	2.46	0.077[a]
	4.00	0.260	2.25	0.074[a]
	4.98	0.305	1.38	0.074[a]
	6.02	0.348	0.81	0.045[b]
	6.82	0.382	0.36	0.035[b]
	7.98	0.562	0.31	0.080[a]
	9.02	0.930	1.14	0.225[a]
	10.00	0.970	1.35	0.100[a]
0.04	2.50	0.230	3.00	0.055
	3.50	0.250	2.22	0.055
	4.01	0.275	2.10	0.065
	4.98	0.302	2.10	0.062
	6.01	0.380	0.98	0.030[b]
	6.98	0.435	0.42	0.033[b]
	8.00	0.688	0.64	0.170[a]
	9.00	0.970	0.78	0.240[a]
	10.00	0.970	2.04	0.115[a]
0.08	2.48	0.250	3.30	0.050
	3.52	0.275	2.76	0.058
	4.02	0.295	2.52	0.057
	5.02	0.330	2.85	0.066
	6.01	0.406	3.30	0.060
	6.99	0.475	2.22	0.055
	8.02	0.810	3.60	0.320[a]
	9.01	0.960	3.60	0.200[a]
	9.98	1.005	3.60	0.107[a]
0.20	3.00	0.300	2.40	0.050
	3.98	0.320	2.85	0.050
	5.02	0.355	3.30	0.052
	6.02	0.406	3.54	0.050
	7.01	0.475	3.48	0.050
	8.00	0.730	4.74	0.325[a]
	9.00	1.020	3.54	0.155[a]
	9.98	1.020	2.25	0.090[a]
	11.00	1.015	2.31	0.090[a]

[a] Irreversible wave.
[b] Asymmetric wave.

perchlorate, varying concentrations (0.02–0.20 *M*) of CDTA and enough 2.0 *M* sodium perchlorate to give ionic strength 0.7 (Table I).

Owing to the weak buffer action of the ligand at lower concentrations, an irreversible reduction wave was observed for [CDTA] $<$ 0.04 *M*. However, for [CDTA] $>$ 0.04 *M*, a reversible reduction wave, corresponding to the reduction of the uranium(VI) complex to the uranium(V) complex, was obtained for pH values up to 7.0.

Near pH 6 for [CDTA] $\leqslant$ 0.04 *M*, the polarographic wave obtained was asym-

TABLE II

DETERMINATION OF THE DEGREE OF POLYMERIZATION OF URANIUM–CDTA CHELATES

[*CDTA*] (*M*)	*pH*	$\frac{E_{1/2}-E_{3/4}}{E_{1/4}-E_{1/2}}$	$E_{1/4}-E_{3/4}$	*a*	*b*
0.02	6.02	1.120	0.045	1.10	1.43
	6.82	1.040	0.035	1.54	1.68
0.04	6.01	1.000	0.032	1.75	1.75
	6.98	1.217	0.033	1.38	2.20

metric, indicating the formation of a polynuclear chelate, the polymerization degree of which was determined as described previously[7]. The results are shown in Table II, in which *a* and *b* denote the degree of polymerization of the oxidized and reduced forms of the uranium complex, respectively. It is obvious that partial dimerization occurred for the uranium(VI)– and uranium(V)–CDTA chelates.

Turbidity appeared above pH 10.0 for [CDTA] < 0.02 *M*, and above pH 12.0 for [CDTA] = 0.20 *M*. The greater the ligand concentration, the higher the pH at which turbidity appears.

The temperature coefficients of the half-wave potential for the polarographic solution containing 1.0 m*M* uranyl perchlorate, 0.08 *M* CDTA and sodium perchlorate at ionic strength 0.7 were 0.5 and 0.4 mV/° at pH 3.02 and pH 5.50, respectively, measured in the temperature range 20.0–40.0°. These results confirm that the reduction at the electrode is reversible under the conditions used.

The temperature coefficients of the limiting current under the above conditions were 2.12 and 1.62%/° at pH 3.02 and pH 5.50, respectively, indicating that the procedures are partially rate-controlled at pH 3.02 and diffusion-controlled at pH 5.50.

Effects of pH and ligand concentration on the half-wave potential

The dependence of the half-wave potential of the uranyl–CDTA chelate on the pH value in various concentrations of CDTA is shown in Fig. 1. Below pH 3.0, $\Delta E_{1/2}/\Delta$pH was -0.03 V, indicating that one hydrogen ion per two uranyl ions parti-

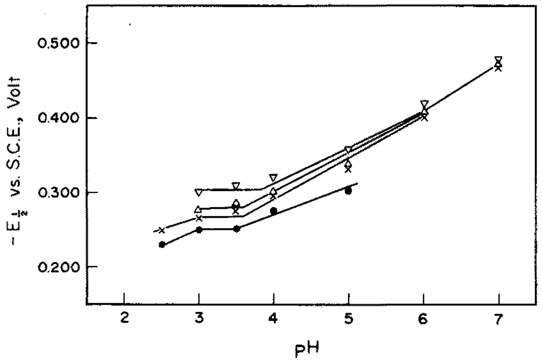

Fig. 1. Effect of pH on the half-wave potential of the uranyl–CDTA complex for various ligand concentrations. (●) 0.04 *M*; (×) 0.08 *M*; (Δ) 0.10 *M*; (∇) 0.20 *M*.

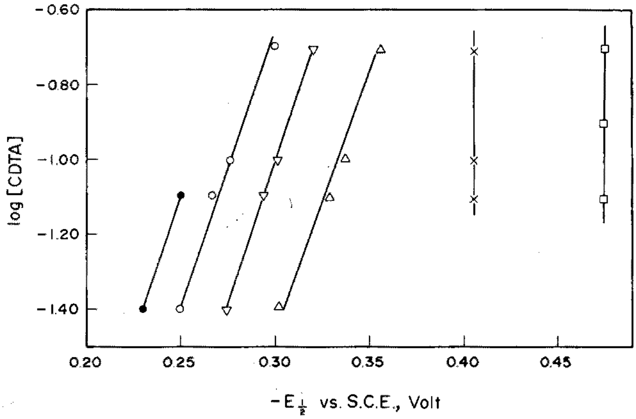

Fig. 2. Effect of ligand concentration on the half-wave potential of the uranyl–CDTA complex at various pH values. pH: (●) 2.50; (○) 3.00; (▽) 4.00; (△) 5.00; (×) 6.00; (□) 7.00.

cipated in the reduction. At pH 3.0–3.5, the half-wave potential was independent of pH, indicating that no hydrogen ion was involved. Above pH 3.5, except for [CDTA] = 0.04 *M*, the $\Delta E_{1/2}/\Delta\text{pH}$ was -0.06 V, showing that one hydrogen ion per one uranyl ion participated in the reaction.

It is obvious from Fig. 1 that the half-wave potential is independent of ligand concentration at pH 6.0–7.0; this proves that there is no change in the metal–ligand ratio in the reduction of uranium(VI)–CDTA chelate to uranium(V)–CDTA chelate.

Figure 2 shows the half-wave potential of the uranyl–CDTA chelate as a function of the logarithmic concentration of CDTA. For [CDTA] $\geqslant$ 0.04 *M*, straight lines with slopes of 0.066 and zero were obtained below pH 6.0 and for the pH range 6.0–7.0, respectively. These results show that the uranyl–CDTA chelate loses one ligand below pH 6.0, whereas there is no change in the ligand number in the pH range 6.0–7.0 after reduction at the electrode.

Electrochemical kinetic parameters

As shown in Table I, the reversibility of the electrode reduction is favored by higher ligand concentrations and lower pH values. For [CDTA] $\leqslant$ 0.02 *M*, an irreversible wave appeared at any pH value; however, it appeared only above pH 5.0 for [CDTA] = 0.04 *M*, and only above pH 7.0 for [CDTA] $\geqslant$ 0.08 *M*.

The electron-transfer coefficient α and rate constant K^0_{fh} at 30° for the irreversible wave were determined by applying the equation[8]:

$$E_{\text{d.e.}} = E' - \frac{0.0551}{\alpha n_a}\left[\log \frac{i}{i_d - i} - 0.546 \log t\right] \tag{1}$$

where
$$E' = \frac{0.06014}{\alpha n_a} \log \frac{1.349\, K^0_{\text{fh}}}{D_0^{\frac{1}{2}}} \tag{2}$$

and $n_a = 1$ is the number of electrons involved. The diffusion coefficient D_0 in eqn. (2) was determined from the maximum current reading by the formula[9]:

$$i_d = 706\, n D_0^{\frac{1}{2}} c m^{\frac{2}{3}} t^{\frac{1}{6}} \tag{3}$$

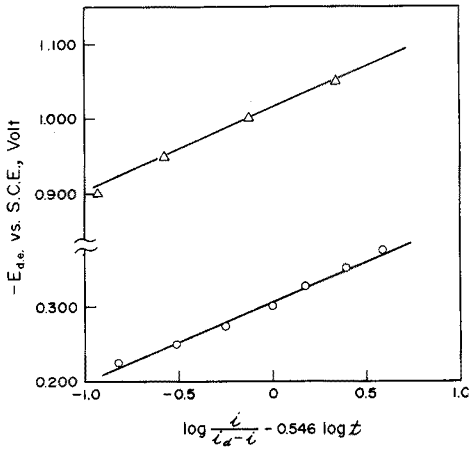

Fig. 3. Plot of $E_{d.e.}$ *vs.* [log $i/i_d - i$) − 0.546 log t]. 1.0 mM $UO_2(ClO_4)_2$, 0.02 M CDTA at ionic strength 0.7. pH: (○) 3.76; (△) 10.00

TABLE III

ELECTRON-TRANSFER COEFFICIENTS AND RATE CONSTANTS

[*CDTA*] (*M*)	*pH*	α	K_{fh}^0 (*cm sec*$^{-1}$)
0.02	2.50	0.599	$3.98 \cdot 10^{-6}$
	3.76	0.520	$2.94 \cdot 10^{-6}$
	9.02	0.250	$3.47 \cdot 10^{-8}$
	10.00	0.510	$2.03 \cdot 10^{-12}$
0.08	8.02	0.127	$2.11 \cdot 10^{-5}$
	9.01	0.270	$2.94 \cdot 10^{-8}$
	9.98	0.457	$2.64 \cdot 10^{-11}$
0.20	8.00	0.128	$3.76 \cdot 10^{-5}$
	9.00	0.296	$7.65 \cdot 10^{-9}$
	10.00	0.394	$8.50 \cdot 10^{-11}$
	11.00	0.487	$5.75 \cdot 10^{-12}$

Equation (1) shows that the plot of $E_{d.e.}$ *vs.* [log $i/(i_d - i)$ − 0.546 log t] should give a straight line and the value of α and K_{fh}^0 can be obtained from the slope and the intercept of the plot, respectively (Fig. 3). The data obtained at various pH values are listed in Table III.

The rate constants were found to be of the order of 10^{-5}–10^{-12} cm sec^{-1}. These results demonstrate that the electrode reductions are remarkably irreversible under the conditions used. Irrespective of the CDTA concentration, the rate constants decreased with increasing pH value, indicating that irreversibility increased with increasing pH value.

Nature of the limiting current

The equation for the limiting current controlled by the rate of reaction and by diffusion has been derived[10].

$$\bar{i} = r\,1255\, n m_0^{\frac{2}{3}} \tau_0^{\frac{2}{3}} c_0 K \left[1 - \Phi\left(K\sqrt{\frac{\tau_0}{HD}}\right)\right] \exp\left[\frac{K^2 \tau_0}{HD}\right] \tag{4}$$

TABLE IV

RATE CONSTANTS OF REACTION AND DIFFUSION COEFFICIENTS OF URANYL–CDTA CHELATE

pH	[*CDTA*] *M*	$KD^{-\frac{1}{2}}(sec^{-\frac{1}{2}})$	γ	$K\cdot 10^3(cm\ sec^{-1})$	$D\ (cm^2\ sec^{-1})$
3.00	0.02	0.01	0.600	0.82	$6.70\cdot 10^{-3}$
	0.04	0.65	0.735	2.21	$1.16\cdot 10^{-5}$
	0.08	0.65	0.735	2.43	$1.39\cdot 10^{-5}$
	0.10	0.30	0.681	1.55	$2.65\cdot 10^{-5}$
	0.20	0.01	0.600	0.80	$6.40\cdot 10^{-3}$
6.00	0.02	∞	0.857	∞	$5.10\cdot 10^{-7}$
	0.04	0.01	0.600	0.33	$1.06\cdot 10^{-3}$
	0.08	∞	0.857	∞	$8.35\cdot 10^{-6}$
	0.10	0.30	0.681	1.59	$2.80\cdot 10^{-5}$
	0.20	1.00	0.767	3.72	$1.38\cdot 10^{-5}$
9.00	0.02	0.01	0.600	0.38	$1.44\cdot 10^{-3}$
	0.04	2.00	0.816	1.46	$5.30\cdot 10^{-7}$
	0.08	2.00	0.816	6.80	$1.16\cdot 10^{-5}$
	0.10	2.00	0.816	6.60	$1.08\cdot 10^{-5}$
	0.20	∞	0.857	∞	$9.60\cdot 10^{-6}$

and

$$\frac{\bar{i}}{\bar{i}_0}=\frac{r}{r_0}\,\frac{\left[1-\Phi\left(K\sqrt{\dfrac{\tau_0}{HD}}\right)\right]}{\left[1-\Phi\left(K\sqrt{\dfrac{\tau_0}{H_0D}}\right)\right]}\exp\left[\frac{K^2\tau_0}{HD}-\frac{K^2\tau_0}{H_0D}\right] \tag{5}$$

where K is the rate constant, r is the ratio of the average limiting current to the maximum limiting current and other notations have their usual significance.

The rate constant of the reaction K and the diffusion coefficient D of the uranyl–CDTA chelate were determined by applying eqn. (4) in which $n=1$, $m_0=2.50\cdot 10^{-3}$ mg/sec-mm, and $\tau_0=3.19\cdot 10^3$ sec-mm/drop. The data listed in Table IV illustrate that for $KD^{-\frac{1}{2}}>1.0$, the limiting current was essentially diffusion-controlled. However, for $KD^{-\frac{1}{2}}\leqq 0.01$, the limiting current was exclusively rate-controlled. For $KD^{-\frac{1}{2}}$ values between 0.01 and 1.00, the limiting current was partly kinetic and partly diffusion-controlled.

The authors thank the National Science Council for financial support of this work.

SUMMARY

The chelate of uranium(VI) with CDTA was investigated polarographically over the pH range 2.48–11.00 and the ligand concentration range 0.02–0.20 *M*. A reversible one-electron reduction wave was obtained for [CDTA] >0.04 *M* below pH 7.0. The reversibility of the electrode reduction was favored by higher ligand concentrations and lower pH values. For [CDTA] ≦ 0.04 *M* at about pH 6, partial dimerization of the uranium(VI)- and uranium(V)-CDTA chelates was observed. The electron-transfer coefficient and rate constant at 30° for the irreversible waves were determined. The rate constants of the reaction and the diffusion coefficients of the chelate are given.

RÉSUMÉ

Le chélate de l'uranium(VI) avec CDTA est examiné au polarographe, à des pH compris entre 2.48 et 11.0 et des concentrations de ligand de 0.02 à 0.2 *M*. On obtient une réduction monoélectronique réversible pour [CDTA] > 0.04 *M*, à un pH inférieur à 7.0. La reversibilité de la réduction cathodique est favorisée par une concentration en ligand plus élevée et un pH plus bas. Les constantes de réaction et les coefficients de diffusion du chélate sont indiqués.

ZUSAMMENFASSUNG

Der Chelat von Uran(VI) mit CDTA wurde im pH-Bereich 2.48–11.0 und im Ligandkonzentrationsbereich 0.02–0.20 *M* polarographisch untersucht. Bei [CDTA] > 0.04 *M* und pH < 7.0 wurde die Stufe einer reversiblen Einelektronenreduktion erhalten. Die Reversibilität der Elektrodenreduktion wurde durch höhere Ligandkonzentrationen und niedrigere pH-Werte begünstigt. Bei [CDTA] ≦ 0.04 *M* und pH etwa 6 wurde eine teilweise Dimerisierung der Uran(VI)- und Uran(V)-CDTA-Chelate beobachtet. Der Elektronenübertragungskoeffizient und die Geschwindigkeitskonstante bei 30° wurden für die irreversiblen Stufen ermittelt. Die Geschwindigkeitskonstanten der Reaktion und die Diffusionskoeffizienten des Chelates werden angegeben.

REFERENCES

1 B. Matyska, J. Doležal and D. Roubalová, *Chem. Listy*, 49 (1955) 1012.
2 D. S. Jain and J. N. Gaur, *J. Indian Chem. Soc.*, 42 (1965) 753.
3 D. S. Jain and J. N. Gaur, *J. Indian Chem. Soc.*, 42 (1965) 759.
4 E. K. Wang and Z. X. Shang, *Acta Chim. Sinica*, 31 (1965) 463.
5 M. Kodama and Y. Tominaga, *Bull. Chem. Soc. Japan*, 42 (1969) 721.
6 T. T. Lai and C. S. Wen, *J. Electrochem. Soc.*, 117 (1970) 1122.
7 T. T. Lai and B. C. Wang, *Anal. Chem.*, 36 (1964) 26.
8 L. Meites and Y. Israel, *J. Amer. Chem. Soc.*, 83 (1961) 4903.
9 J. Heyrovský and J. Kůta, *Principle of Polarography*, Academic Press, New York, 1966, p. 82.
10 P. Delahay, *J. Amer. Chem. Soc.*, 73 (1951) 4944.

Anal. Chim. Acta, 54 (1971) 521–527

Analytica Chimica Acta
Elsevier Publishing Company, Amsterdam
Printed in The Netherlands

SHORT COMMUNICATIONS

The determination of formic acid by nuclear magnetic resonance spectroscopy

In work in this laboratory, there arose the need to determine quantitatively a small amount of formic acid in a system capable of generating an additional amount upon being heated. Therefore, the routine wet chemical method comprising refluxing of the sample with mercury(II) acetate to effect oxidation of formic acid to carbon dioxide[1] was not suitable; the formic acid generated during the analysis would invalidate the results. Nuclear magnetic resonance seemed likely to provide an expedient alternative, especially since other workers have shown that n.m.r. is ideally suited for specialized quantitative analysis[2].

As a result of the anisotropy of the carbonyl group, the formyl proton (H–C(=O)–) shows a sharp resonance signal in the n.m.r. spectrum at δ 8.0–9.0 p.p.m.—far removed from normal aliphatic resonances[3]. Since in the measurement of nuclear magnetic resonance, the magnetic field must be finely tuned at the resonance position to observe an effect, interference from other protons resonating at more distant field strengths is minimal, even though they may be present in much larger concentration. This makes n.m.r. spectroscopy useful for observing small amounts of a compound in a large volume of solvent.

Results and discussion

The sensitivity of the Varian A60 n.m.r. Spectrometer used in these experiments was determined by measuring standard solutions of formic acid in acetic acid. It was found that the formyl resonance could be distinguished from background noise down to a concentration of 0.05% (w/w).

The basic quantitative technique can be illustrated by a determination of formic acid in acetic acid. Quantitative results are obtained by comparing the peak areas of the unknown with standards run one after the other in the same n.m.r. tube, and under the same conditions. The sample tube was filled to a height of 10 cm with each solution and the same amount of tetramethylsilane internal standard was added to each sample. At low concentrations, 0.5% or less of formic acid, electronic integration of the peaks was not satisfactory. The relative areas of the unknown and the standards were measured by cutting the peaks out of the spectrum trace and weighing them. Actually, it was discovered that at these low concentrations, if the gap between the concentrations of the unknown and the standards is small, peak heights served as an accurate alternative to peak areas for interpolation.

Figure 1 shows an actual determination of formic acid in acetic acid. The peak heights measured in mm refer to the heights observed in the original spectrum. The unknown in this case contained 0.33% formic acid in acetic acid; exactly the same result was obtained by mercury(II) acetate oxidation of formic acid to carbon dioxide. Even at 0.06% formic acid there was agreement within 0.01% (w/w) by both methods. The larger the separation among the concentrations of the standards and the unknowns, the more inaccurate the results. For example, in Fig. 1, if the 0.30%

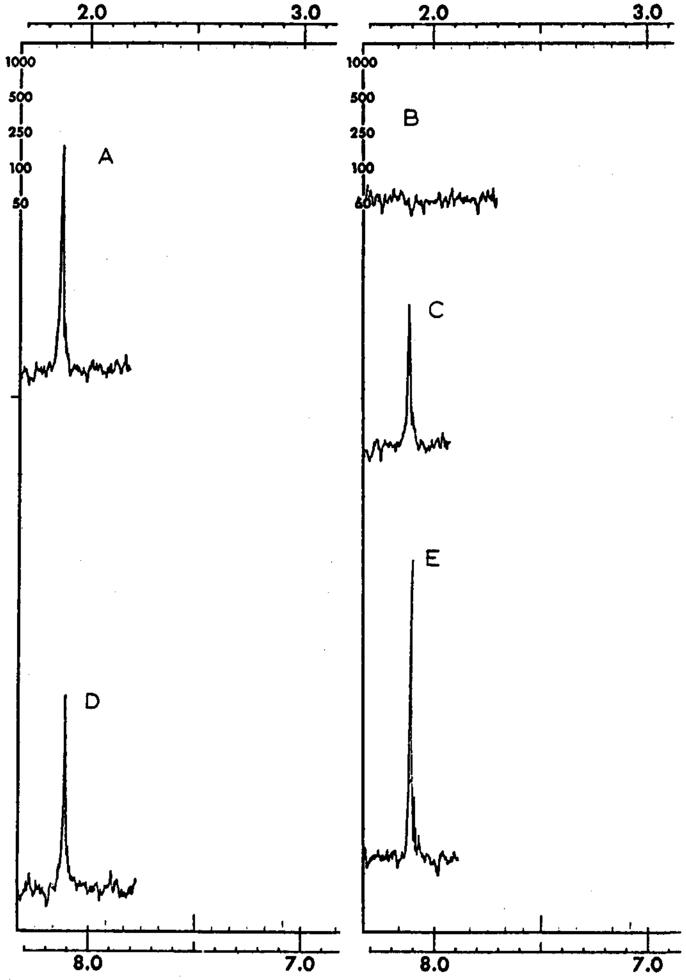

Fig. 1. N.m.r. analysis of an acetic acid sample containing an unknown amount of formic acid. (A) Unknown sample (63 mm = 0.325); (B) acetic acid blank; (C) standard solution of formic acid in acetic acid (0.20% = 40 mm); (D) as in C (0.30% = 56 mm); (E) as in C (0.40% = 84 mm).

Interpolation. 0.40% − 0.30% = 0.10%
(84 mm) (56 mm) (28 mm)
63 mm − 56 mm = 7 mm

$$\frac{7\ \text{mm}}{28\ \text{mm}} = \frac{X}{0.10\%}$$

$X = 0.025\%$

standard is considered as an unknown and the peak heights of the 0.20% and 0.40% standards are used for interpolation, one calculates a value of 0.27% formic acid.

If one does not have the exact composition of the mixture containing formic acid, the n.m.r. technique may still be used by employment of an internal standard. An accurately weighed amount of a compound with a one-proton resonance signal located near that of formic acid is introduced into the sample. Comparison of the peak areas then gives the molar concentration of formic acid from which one can calculate the percent concentration in the original sample. It must be ascertained that equal molar concentrations of the standard and formic acid give equal responses. Pure chloroform with its resonance signal at δ7.3–7.9 p.p.m. is a suitable standard.

The authors wish to thank Mr. A. J. Durbetaki for his helpful discussions, Mrs. C. B. Maksimow for taking the n.m.r. spectra, and Dr. J. J. Velenovsky, FMC Corporation, Organic Chemicals Division, Baltimore, for the analyses with mercury-(II).

Central Research Department,
FMC Corporation,
P.O. Box 8,
Princeton, N.J. 08540 (U.S.A.)

J. V. Burakevich
J. O'Neill, Jr.

1 J. D. Reid and H. D. Weihe, *Ind. Eng. Chem., Anal. Ed.*, 10 (1938) 271.
2 S. Barcza, *J. Org. Chem.*, 28 (1963) 1914 and reference therein.
3 L. M. Jackman and S. Sternhell, *Applications of Nuclear Magnetic Resonance Spectroscopy in Organic Chemistry*, 2nd Edn., Pergamon Press, Oxford, 1969, pp. 88–89.

(Received 18th November 1970)

Anal. Chim. Acta, 54 (1971) 528–530

Titrimetric determination of sulfate by ion exchange with homogeneously precipitated barium iodate 1-hydrate

There are few satisfactory methods for the determination of sulfate in the concentrations normally encountered in natural waters. Standard methods[1] involve gravimetric or turbidimetric determinations, based on precipitation of barium sulfate. Bertolacini and Barney[2] described barium chloranilate as a solid-phase reagent which exchanges colored chloranilate ion for sulfate. Webb[3] reported an iodometric method based on exchange of sulfate with solid barium iodate. This method is recommended by Barnes[4] for the determination of sulfate in sea water. A recent paper by Bowen[5] described a radiometric displacement method in which ^{131}I-labelled barium iodate is used.

The method of Webb can be improved in speed and convenience through the use of a column of very pure, granular barium iodate 1-hydrate, prepared by the method of Lambert and Yasuda[6]. In this preparation, iodate ion is produced in homogeneous solution in the presence of barium by the slow reduction of periodate with lactic acid at room temperature.

Reagent column

A large, compact plug of borosilicate glass wool is placed firmly in the lower end of an 8-mm outside diameter borosilicate glass tube that has been constricted to 1–2 mm inside diameter by heating and drawing. Sufficient barium iodate 1-hydrate (60–115 mesh or 125–250 μm) is added to the column to a depth of about 8 cm. The column is attached to a funnel by 75 cm of $\frac{1}{8}$-in inside diameter polyvinyl chloride tubing. The height of the funnel above the column is adjusted to provide a flow rate of 5 ml of solution every 4–5 min.

Determination of sulfate

Wash the column with deionized water to a constant low blank. Pass the solution containing sulfate through the column. Discard the first 10 ml of eluent, and collect an amount sufficient to provide a 25.00-ml sample. Add 1.0 g of solid potassium iodide and 10 ml of 0.8 *N* hydrochloric acid to the sample, and titrate with 0.0500 *N* sodium thiosulfate solution to the starch end-point.

Calibration curve and results

The calibration curve shown in Fig. 1 was prepared for use in the 0–1000 p.p.m. concentration range with 0.04824 *N* sodium thiosulfate as the titrant solution. The results are given in Table I. The curve consists of two straight lines which intersect at about 140 p.p.m. sulfate. No explanation for this break in the curve is offered, but the expanded portion of the calibration curve indicates non-linearity near the intersection of the two lines. For that reason, standard addition of sulfate to increase the concentration above 200 p.p.m. is recommended. The upper limit for good precision appears to be about 750 p.p.m.

No temperature control was attempted, but all solutions were stored and used in an air-conditioned laboratory maintained at 26 ± 2°. The useful life of the column appears to be limited by attrition of the crystals to a size sufficiently small to pass through the glass wool plug. This is indicated by an increase in the blank beginning after long usage. On one column, 30 determinations were made at the lower concentrations shown in Table I without an increase in blank, being noted. From other determinations, it is estimated that a total of 0.5–1.0 g of sulfate ion can be determined by

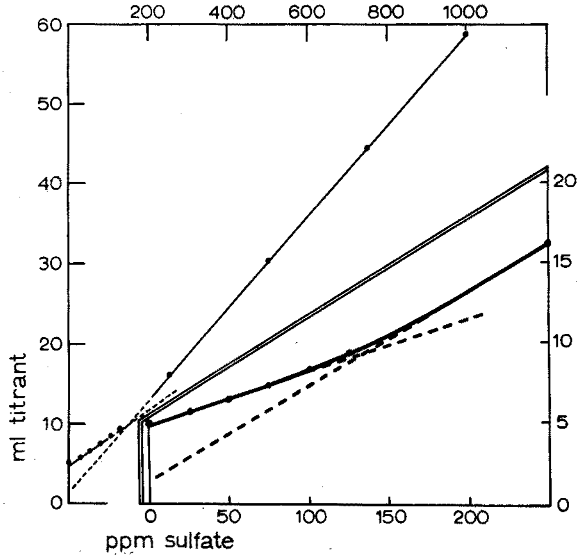

Fig. 1. Calibration curve for 0–1000 p.p.m. sulfate. The inset shows an expanded part of the curve at low concentrations.

one column. Column efficiency in terms of iodate exchange for sulfate was calculated to be 99.6% at 250 p.p.m. and 93.6% at 500 p.p.m. sulfate.

Interferences

pH has little effect between 5.8 and 9.5 on the results obtained with 250 p.p.m. sulfate. The following ions, when present in 250-p.p.m. concentration, did not interfere with the determination of 250 p.p.m. sulfate nor with a blank: sodium, potassium, calcium, chloride, and nitrate. Phosphate at 100 p.p.m. is a very slight negative interference in a blank (*i.e.*, causes less iodate to be released than does pure water), but produces a positive error of about 10% in the determination of 250 p.p.m. sulfate. Bicarbonate at 200 p.p.m. is a slight positive interference in a blank, but produces a positive error of about 10% in the determination of 250 p.p.m. sulfate.

TABLE I

EXPERIMENTAL RESULTS FOR CALIBRATION CURVE

Concn. SO_4^{2-} (p.p.m.)	*Volume of titrant (ml)*[a]		*Std. devn. ($\cdot 10^2$)*
	Average	*Range*	
0	5.06	5.04– 5.10	2.5
25	5.68	5.63– 5.73	4.4
50	6.51	6.45– 6.55	3.8
75	7.36	7.30– 7.40	4.0
100	8.22	8.19– 8.25	3.2
125	9.39	9.20– 9.60	18.2
250	16.08	15.85–16.28	17.6
500	30.24	30.10–30.40	14.7
750	44.34	44.10–44.50	16.7
1000	58.45	58.00–59.20	52.8

[a] Five determinations were made at each concentration.

This work was supported in part by National Science Foundation research grant GP-8629.

Department of Chemistry,
Kansas State University,
Manhattan, Kan. 66502 (U.S.A.)

Jack L. Lambert
David J. Manzo

1 *Standard Methods for the Examination of Water and Wastewater*, 12th Edn., Amer. Pub. Health Assoc., Inc., New York, 1965, p. 287.
2 R. J. Bertolacini and J. E. Barney II, *Anal. Chem.*, 30 (1958) 202.
3 D. A. Webb, *J. Exptl. Biol.*, 16 (1939) 438.
4 H. Barnes, *Apparatus and Methods of Oceanography. Part One. Chemical*, Interscience, New York, 1959, p. 219.
5 H. J. M. Bowen, *Analyst*, 95 (1970) 665.
6 J. L. Lambert and S. K. Yasuda, in J. Kleinberg, *Inorganic Syntheses*, Vol. VII, McGraw-Hill, New York, 1963, p. 13.

(Received 16th December 1970)

Analytica Chimica Acta
Elsevier Publishing Company, Amsterdam
Printed in The Netherlands

The halogen addition method in atomic absorption spectrophotometry of organometallic complexes

A serious problem in the analysis of gasolines for tetraalkyllead additives by atomic absorption spectrophotometry is that different lead compounds sometimes require different calibration curves. It has recently been shown[1] that this defect can be avoided by the addition of iodine to the gasoline solutions diluted with methyl isobutyl ketone (MIBK); under these conditions, a single calibration curve can be used for a wide variety of lead-containing additives, whether organic or inorganic.

Similar problems have arisen in the determination of other metals in petroleum products by atomic absorption spectrophotometry. The determination of metal-containing additives in oil blends was investigated by Mostyn and Cunningham[2], who diluted the samples with *n*-heptane and compared with standards prepared from an authentic additive and zinc naphthenate. The determination of nickel, iron and copper in crude petroleum oils was studied by Barras[3]; again, samples were diluted with *n*-heptane and compared with standards prepared from organometallic compounds.

In the work described below, calcium, barium, zinc, and copper compounds were examined. As in the case of lead, varying absorbance readings were obtained from the same concentration of metal when it was present in different inorganic and organic compounds. The effect of adding various halogens and halides was therefore examined. The addition of iodine proved to be the most efficient in ensuring equivalent absorbances from different types of metal compounds in MIBK solutions.

Experimental

A Perkin-Elmer Model 303 instrument fitted with a Perkin-Elmer premix-type burner with air–acetylene and nitrous oxide–acetylene burner heads, was employed. Automatic null recording was used with scale expansion and noise suppression. Hollow-cathode lamps for calcium, barium, zinc, copper and lead were obtained from Perkin-Elmer, Inc. The detailed examination was carried out with the acetylene–air and the acetylene–nitrous oxide flame under the conditions listed in Table I.

TABLE I

OPERATING CONDITIONS

	Ca	*Ba*	*Zn*	*Cu*	*Pb*
Wavelength (nm)	422.7	553.6	213.8	324.7	283.3
Lamp current (mA)	10	25	10	15	8
Oxidant flow (l $\min^{-1}$)	16.7(N_2O)	16.7(N_2O)	23.8(Air)	23.8(Air)	23.8(Air)
Acetylene flow (l $\min^{-1}$)	8.8	8.8	3.3	3.3	3.3
Burner height (mm)	10.0	10.0	8.0	8.0	8.0
Response time	1	1	1	1	1
Noise suppression	1	1	1	1	1
Scale expansion	1	10	3	1	1
Slit width (mm)	1.0	1.0	3.0	1.0	1.0

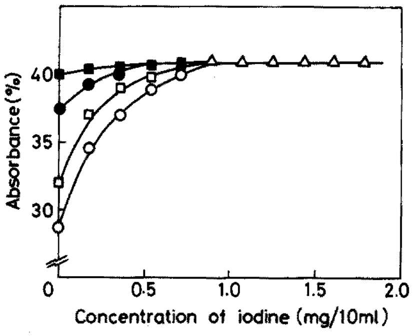

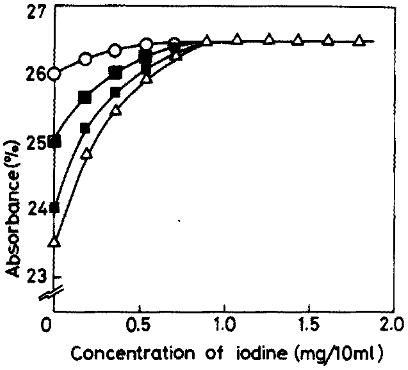

Fig. 1. Effect of iodine addition on calcium absorption. All solutions contained 2 p.p.m. calcium. (○) Calcium phenate, (●) calcium sulfonate, (□) calcium naphthenate, (■) calcium nitrate, (△) all calcium compounds.

Fig. 2. Effect of iodine addition on barium absorption. All solutions contained 5 p.p.m. barium. (○) Barium phenate, (●) barium sulfonate, (□) barium naphthenate, (■) barium phosphonate, (△) barium nitrate, (▲) all barium compounds.

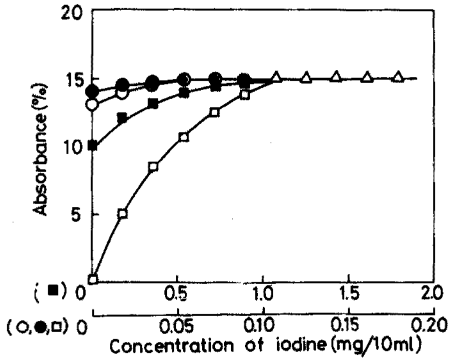

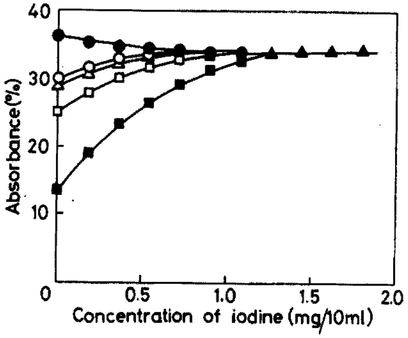

Fig. 3. Effect of iodine addition on zinc absorption. All solutions contained 2 p.p.m. zinc. (○) Zinc dialkyldithiophosphate, ● zinc dialkyldithiocarbamate, (□) zinc sulfate, (■) zinc nitrate, (△) all zinc compounds.

Fig. 4. Effect of iodine addition on copper absorption. All solutions contained 2 p.p.m. copper. (○) Copper naphthenate, (●) bis(1-phenyl-1,3-butanedione)copper(II), (□) copper cyclohexanebutyrate, (■) copper(II) sulfate, (▲) copper(II) nitrate, (△) all copper compounds.

Analytical-grade chemicals and pure additives were used throughout. All standards were prepared in analytical-grade methyl isobutyl ketone (MIBK). The inorganic compounds of each metal were prepared by dissolving the sulfate or nitrate in distilled water, then diluting with methanol, and finally diluting the solution to a known volume with MIBK. The compounds tested are listed in Table II.

TABLE II

EFFECT OF VARIOUS COMPOUNDS AND IODINE ADDITION

(Columns A show the results obtained with no addition of iodine. Columns B show the results with an addition of 2 mg of iodine per 10 ml of MIBK. The calcium, zinc and copper solutions contained 2 p.p.m., the barium solution contained 5 p.p.m. and the lead solution contained 16 p.p.m.)

	Wt.% metal in compound	*% Absorbances*									
		Calcium		*Barium*		*Zinc*		*Copper*		*Lead*	
		A	*B*	*A*	*B*	*A*	*B*	*A*	*B*	*A*	*B*
Calcium phenate	5.5	28.5	41.0	—		—		—		—	
Calcium sulfonate	9.5	37.5	41.0	—		—		—		—	
Calcium naphthenate	2.85	32.0	41.5	—		—		—		—	
Calcium nitrate	22.0	40.0	41.0	—		—		—		—	
Barium phenate	10.0	—		26.0	26.5	—		—		—	
Barium sulfonate	11.5	—		25.0	26.5	—		—		—	
Barium naphthenate	9.1	—		25.0	26.5	—		—		—	
Barium phosphonate	14.5	—		24.0	26.5	—		—		—	
Barium nitrate	55.5	—		23.0	26.5	—		—		—	
Zinc dialkyldithiophosphate	12.0	—		—		13.0	15.0	—		—	
Zinc dialkyldithiocarbamate	15.5	—		—		14.0	15.0	—		—	
Zinc sulfate	22.7	—		—		0.0	15.0	—		—	
Zinc nitrate	22.0	—		—		10.0	15.0	—		—	
Copper naphthenate	1.9	—		—		—		29.0	34.0	—	
Bis(1-phenyl-1,3-butanedione)copper-(II)	16.5	—		—		—		13.5	34.0	—	
Copper cyclohexane butyrate	15.8	—		—		—		30.0	34.0	—	
Copper(II) sulfate	25.45	—		—		—		36.0	34.0	—	
Copper (II) nitrate	26.3	—		—		—		25.0	34.5	—	
Tetramethyllead	0.715[a]	—		—		—		—		54.0	33.8
Tetraethyllead	0.79[a]	—		—		—		—		31.5	33.5
Lead nitrate	62.55	—		—		—		—		29.0	33.5

[a] $g\,l^{-1}$.

Difference of absorption in each metal in organic solutions

As can be seen in Table II, different organic and inorganic compounds in MIBK solutions containing the same concentration of the metal ion gave different absorbance readings. The effect was less marked for barium compounds than for the other metals tested, but would lead to significant error in almost all cases, if the calibration curves were prepared with compounds different from those present in the actual analysis. The addition of halogen or halogen compounds was found to have a remarkable effect on the results obtained for different organometallic and inorganic compounds; in the presence of 1.3 mg of iodine per 10 ml of MIBK solution, all the compounds of a particular metal showed the same absorbance for the same amount of metal (see Figs. 1–4 and Table II).

TABLE III

RELATIVE SENSITIVITIES FOR DIFFERENT CALCIUM COMPOUNDS IN PRESENCE OF HALOGENS AND HALOGEN COMPOUNDS
(% Absorbance)

Additive	*Phenate*	*Sulfonate*	*Naphthenate*	*Nitrate*
None	28.5	37.5	32.5	40.0
I_2	41.0	41.5	41.5	41.0
Br_2	37.0	37.0	37.5	37.0
Cl_2	30.5	30.5	31.0	31.5
KI	41.0	41.5	41.5	41.5
NaI	41.5	41.5	41.5	41.0
KBr	28.0	37.0	32.0	39.5
NaBr	28.5	36.5	32.0	39.0
CH_3I	28.5	37.5	32.0	40.0
$C_2H_4Br_2$	28.5	37.0	32.5	39.5
$C_2H_4Cl_2$	27.5	35.5	31.0	38.5

Effect of various halogens for absorption

To investigate the effects of various halogens and halogen compounds on the relative sensitivities for the determination of calcium phenate, calcium sulfonate, calcium naphthenate and calcium nitrate, the 10-cm slot burner for air–acetylene and the 7-cm slot burner for acetylene–nitrous oxide were used. Table III shows the relative sensitivities for calcium compounds when different halogens and halogen compounds were added to the solutions. Iodine, sodium iodide and potassium iodide not only produced similar sensitivities for the different calcium compounds tested but also provided improved sensitivity. The addition of sodium bromide, potassium bromide, methyl iodide, ethylene dibromide or ethylene dichloride had little effect on the results obtained. Chlorine or bromine provided a certain levelling effect for different organic compounds, but the sensitivity was less than that obtained with iodine.

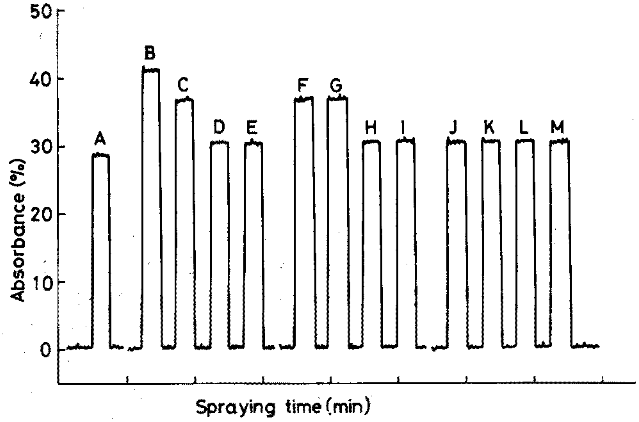

Fig. 5. Recorder traces from 2 p.p.m. of calcium as calcium phenate for various halogen additions. (A) No addition, (B) I_2 addition, (C) I_2+Br_2 addition, (D) $I_2+Br_2+Cl_2$ addition, (E) I_2+Cl_2 addition, (F) Br_2 addition, (G) Br_2+I_2 addition, (H) $Br_2+I_2+Cl_2$ addition, (I) Br_2+Cl_2 addition, (J) Cl_2 addition, (K) Cl_2+I_2 addition, (L) $Cl_2+I_2+Br_2$ addition, (M) Cl_2+Br_2 addition.

The simultaneous addition of two or three halogens was studied. The recorder trace for a solution of calcium phenate in MIBK is shown in Fig. 5. It can be seen that the effect of iodine was decreased by bromine or chlorine, and that of iodine and bromine was decreased by chlorine (iodine $<$ bromine$<$ chlorine). For example, when chlorine was added to the calcium sample followed by iodine or bromine, the absorbance of calcium was influenced by chlorine rather than by iodine.

The iodine addition method has proved remarkably effective for all the cases so far examined, and it should also be applicable to other organometallic and inorganic compounds.

The authors wish to thank Mr. T. Kozuma and Dr. T. Amemiya for their encouragement throughout the work, and Dr. H. Hasegawa for his kind guidance.

Maruzen Oil Company,
Research and Development Center,
P.O. Box 1, Satte,
Saltama 340-01 (Japan)

Masayuki Kashiki
Seigo Yamazoe
Shozo Oshima

1 M. KASHIKI, S. YAMAZOE AND S. OSHIMA, *Anal. Chim. Acta*, 53 (1971) 95.
2 R. A. MOSTYN AND A. F. CUNNINGHAM, *J. Inst. Petrol.*, 53 (1967) 101.
3 R. C. BARRAS, *Jarrell-Ash Newsletter*, June 1962, p. 13.

(Received 25th November 1970)

Anal. Chim. Acta, 54 (1971) 533–537

Atomic fluorescence spectroscopy of lead

In a recent article on the atomic fluorescence spectroscopy of lead[1] it is stated that, contrary to expectations, the fluorescence emission at 405.8 nm (direct line fluorescence) was more intense than that at 283.3 nm (resonance fluorescence).

It is stated further that the ratio $I_{405.8}$ nm/$I_{283.3}$ nm should increase with increasing flame temperature, which may partially account for the rise of the thermal population of the $6P^2\ {}^3P_2$ level and the resultant increase in resonance fluorescence at 405.8 nm.

Both these statements are questionable. The emission lines at 283.3, 364.0 and 405.8 nm occur as a result of transitions from the same electronic level ($7s\ {}^3P_1^0$). The mode of excitation to this level whether it be from the $6P^2\ {}^3P_0$, $6P^2\ {}^3P_1$ or $6P^2\ {}^3P_2$ level is immaterial to considerations of relative emission (fluorescence) intensities from this state. The intensity of emission from an energy level j to a lower level i is proportional to the Einstein transition probability for emission (A_{ji}) for such a transition. The relative intensities of a number of lines emanating from the same level will thus be in the ratio of their transition probabilities and would not be affected by temperature changes. The slight differences in the ratios of the relative fluorescence intensities (r.f.i.) observed by Browner *et al*[1]. in various flames could possibly be attributed to variations in the degree of absorption of the fluorescence radiation at various wavelengths by the molecular species present in the flames.

Anal. Chim. Acta, 54 (1971) 537–538

Since A_{ji} is proportional to $g_j f_{ji} \lambda_{ji}^{-3}$, where g_j is the statistical weight of level j and f_{ji} and λ_{ji}^{-3} are the oscillator strength and wavelength for the transition from j to i, the relative fluorescence intensities of lines emanating from the same level can be calculated as has been shown previously[2].

TABLE I

COMPARISON OF THEORETICAL AND EXPERIMENTAL ATOMIC FLUORESCENCE INTENSITIES OF LEAD

Wavelength (nm)	*Transition*	*Experimental r.f.i.*[a]	*Theoretical r.f.i.*
283.3	7s $^3P_1^0$–$6P^2\ ^3P_0$	52.5	30
364.0	7s $^3P_1^0$–$6P^2\ ^3P_1$	16.1	18
405.8	7s $^3P_1^0$–$6P^2\ ^3P_2$	100	100

[a] $A/O_2/N_2$ flame.

The theoretical r.f.i. of the lines arising from transitons from the 7s $^3P_1^0$ level obtained by the *gf* values of Corliss and Bozman[3] are shown in Table I together with the experimental results obtained by Browner *et al.*[1]. The agreement is within the limits of accuracy claimed for the *gf* values (±50%) and shows that the line at 405.8 nm should theoretically be the most sensitive.

Division of Laboratories and Research,
New York State Department of Health,
New Scotland Avenue,
Albany, N. Y. 12201 (U.S.A.)

Brian W. Bailey

1 R. F. Browner, R. M. Dagnall and T. S. West, *Anal. Chim. Acta*, 50 (1970) 375.
2 B. W. Bailey, *Spectroscopy Letters*, 2 (1969) 81.
3 C. H. Corliss and W. R. Bozman, *National Bureau of Standards Monograph 53*, U. S. Government Printing Office, Washington, D.C.

(Received 10th December 1970)

Anal. Chim. Acta, 54 (1971) 537–538

Adsorption of molybdophosphoric acid on dextran gel column

Gel chromatography is known as a technique for separating solute molecules according to their sizes. This technique has been applied increasingly for the investigation of inorganic polymers such as polyphosphates[1–7], polysilicates[8] and polymeric iron(III) hydroxides[9]. For example, when polyphosphates are chromatographed on a Sephadex column (cross-linked dextran) larger ions are eluted earlier than smaller ions. The gel-chromatographic behavior of molybdates[10] has also been investigated for Bio-Gel columns (cross-linked polyacrylamide) but insufficient data are available for Sephadex columns.

This work was undertaken to characterize the gel-chromatographic behavior of heteropoly molybdophosphoric acid. This compound[11,12], which has been extensively investigated from the view point of analytical chemistry, is known to be composed of polyanions such as $[PMo_{12}O_{40}]^{3-}$. An attempt was made to estimate the effective size of molybdophosphoric acid in solution and to compare it with the data for phosphates[6,7] and molybdates. However, contrary to expectation, no satisfactory results could be obtained because of the strong adsorption of molybdophosphoric acid on the Sephadex column. This feature is described below.

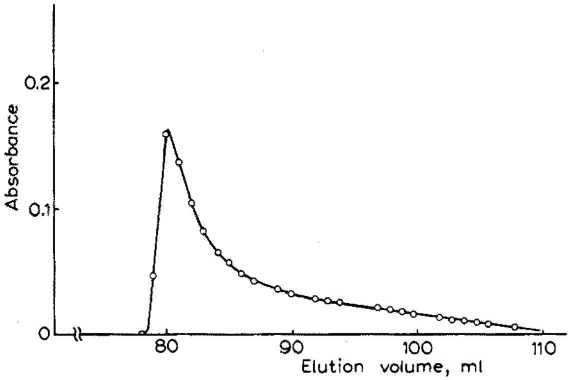

Fig. 1. Elution curve of molybdate on Sephadex G-25 column. Column, 1.5 ×57 cm; temperature, 20°; fraction volume, 1 ml; eluent 0.1 *M* $NaClO_4$; flow rate, 40 ml h^{-1}; sample, 0.01 *M* Na_2MoO_4.

The chromatographic behavior of molybdate was first examined. The elution curve of sodium molybdate from a Sephadex G-25 column (bed volume = 100 ml) with 0.1 *M* sodium perchlorate solution is shown in Fig. 1. Molybdate in the effluent was determined colorimetrically with thiocyanate. The elution peak position is smaller than the total liquid volume of the column. This suggests a considerable contribution of the sieving effect in the gel phase[14]. On the other hand, the shape of the elution curve is asymmetrical (tailing), and the elution peak position decreases with increasing sample concentration. These facts are in contrast with the elution behavior of phosphate[6,7] and suggest the contribution of a side effect such as adsorption[14]. A similar phenomenon was also observed when sodium molybdate was eluted with other acidic eluents, *i.e.*, 0.1 *M* solutions of sodium chloride, sodium sulfate or sodium perchlorate which had been adjusted to *ca.* pH 2 with the corresponding acids.

Since it was found by preliminary experiments that molybdophosphoric acid is strongly adsorbed on Sephadex columns, subsequent experiments were carried out with a smaller Sephadex G-25 column (bed volume = 18 ml) in order to observe the effect of acid concentration on the adsorption of molybdophosphoric acid. Perchloric acid of various concentrations and 0.1 *M* sodium hydroxide solution were used as eluents. Sample solutions of molybdophosphoric acid were prepared by dissolving both sodium phosphate ($NaH_2PO_4 \cdot 2H_2O$) and sodium molybdate ($Na_2MoO_4 \cdot 2H_2O$) in the perchloric acid which were to be used as eluents. The concentrations of phosphate and molybdate were adjusted to be 0.002 *M* and 0.04 *M*, respectively.

Column experiments were done in two successive steps. First, sample solution (2 ml) was applied to the Sephadex column and then the column was washed with 30 ml of perchloric acid. The amount of phosphate in the effluent (I) was determined colorimetrically. Secondly, the molybdophosphoric acid was eluted with 30 ml of 0.1 *M* sodium hydroxide solution and the amount of phosphate in the effluent (II) was also determined by the same method.

The relative amount (%) of phosphate in effluents I and II or recoveries I and II were calculated, respectively, on the basis of total phosphate applied and were plotted against the logarithms of the molar concentration of perchloric acid (Fig. 2).

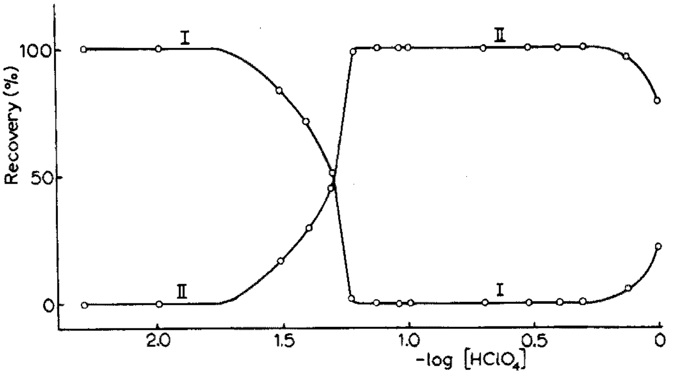

Fig. 2. Effect of acid concentration on adsorption of molybdophosphoric acid on Sephadex G-25 column. (I) Recovery I; (II) Recovery II.

It is well known[11-13] that orthophosphate reacts with molybdate to form a yellow product, molybdophosphoric acid, in acidic solution and its formation is greatly dependent on the acidity of the medium. Such a feature can be seen in Fig. 2. At lower acid concentrations where recovery I was 100%, no color development was observed either in the solution or on the column. With increasing acid concentrations, however, the yellow-colored species in the solution was retarded on the top of the column to form a distinct band. Such a band of the yellow complex migrated very slowly when the acidic eluents were used. At acid concentrations between 0.06 *M* and 0.5 *M* (pH 3.5–pH 0.3), no phosphate was detected in effluent I, which suggested the complete adsorption of phosphate on the Sephadex column as molybdophosphoric acid. On the other hand, recovery I tended to increase again at higher acid concentrations than 0.5 *M*. This may be attributed to the variation in the equilibrium of the formation of molybdophosphoric acid in the solution[11-13].

Figure 2 also shows that when the column was washed with 0.1 *M* sodium hydroxide solution, molybdophosphoric acid on the column was decomposed completely and all the phosphate thus produced appeared quantitatively in 30 ml of effluent II.

It is of interest that phosphate does not show any interaction with Sephadex gel[6], while molybdate and molybdophosphate are adsorbed. Adsorption of molybdophosphoric acid may be ascribed to the interaction of dextran gel with molybdate groups in the structure of molybdophosphoric acid. Similar discussion[14] has been reported concerning the adsorptive property of aromatic groups in organic compounds.

Department of Chemistry,
Faculty of Science,
Kyushu University,
Fukuoka (Japan)

Norimasa Yoza
Hiroyuki Matsumoto
Shigeru Ohashi

1 S. Ohashi, N. Yoza and Y. Ueno, *J. Chromatog.*, 24 (1966) 300.
2 P. A. Neddermeyer and L. B. Rogers, *Anal. Chem.*, 40 (1968) 755.
3 S. Felter, G. Dirheimer and L. P. Ebel, *J. Chromatog.*, 35 (1968) 208.
4 P. A. Neddermeyer and L. B. Rogers, *Anal. Chem.*, 41 (1969) 94.
5 J. H. Steward and M. E. Tate, *J. Chromatog.*, 45 (1969) 400.
6 Y. Ueno, N. Yoza and S. Ohashi, *J. Chromatog.*, 52 (1970) 469.
7 Y. Ueno, N. Yoza and S. Ohashi, *J. Chromatog.*, 52 (1970) 481.
8 T. Tarutani, *J. Chromatog.*, 50 (1970) 523.
9 R. A. Henry and L. B. Rogers, *Separation Sci.*, 3 (1968) 11.
10 C. A. Streuli and L. B. Rogers, *Anal. Chem.*, 40 (1968) 653.
11 S. R. Crouch and H. V. Malmstadt, *Anal. Chem.*, 39 (1967) 1084.
12 B. E. Reznik and L. P. Tsyganok, *Russ. J. Inorg. Chem.*, 10 (1965) 1042.
13 K. Murata and T. Kiba, *J. Inorg. Nucl. Chem.*, 32 (1970) 1667.
14 N. Yoza, T. Ogata and S. Ohashi, *J. Chromatog.*, 52 (1970) 329.
15 D. Eaker and J. Porath, *Separation Sci.*, 2 (1967) 507.

(Received 10th December 1970)

ANALYTICA CHIMICA ACTA, VOL. 54 (1971)

AUTHOR INDEX

ANALYTICA CHIMICA ACTA, VOL. 54 (1971)

SUBJECT INDEX

CONTENTS

(continued on page 4 of cover)

Continued from inside page of cover

Short Communications